

**DNA MISMATCH REPAIR AND CELLULAR RESPONSE TO
CYTARABINE: IMPLICATIONS FOR THE PATHOGENESIS
AND TREATMENT OF THERAPY-RELATED ACUTE
MYELOID LEUKAEMIA**

A thesis submitted in part requirement for the
degree of Doctor of Philosophy



Sarah Fordham

Northern Institute for Cancer Research,
Faculty of Medical Sciences,
Newcastle University

April 2011

ABSTRACT

The DNA mismatch repair (MMR) pathway is responsible for correction of replicative errors, hence is a key factor in maintenance of genomic stability. Paradoxically, functional DNA MMR also mediates the cytotoxicity of certain chemotherapeutic DNA damaging agents. Poor treatment response in therapy-related acute myeloid leukaemia (t-AML) is influenced by a number of factors, one of which might be chemoresistance due to acquired defects in DNA MMR.

Using a range of paired MMR proficient and deficient cell lines, investigations herein demonstrate that DNA MMR status mediates response to nucleoside analogues such as cytarabine (Ara-C) used in t-AML chemotherapy. Interestingly, defects of specific MMR components had different and opposing effects on the cytotoxicity of these agents. These findings implicate defects of MMR components as potential prognostic factors in t-AML and suggest assessment of DNA MMR status may be warranted in individual patients when selecting treatment.

Cytarabine was mutagenic to DNA at the *TK* and *HPRT* loci. Furthermore, the frequency of Ara-C-induced mutation was increased in an MMR-deficient cell line, supporting a role for MMR components in the cellular response to nucleoside analogues, and also suggesting that use of these agents themselves could contribute to the risk of t-AML development.

Defective DNA MMR might also contribute to development of relapsed AML, given that genomic instability is demonstrated in some patients at relapse. Genome-wide analysis of DNA copy number aberrations and loss of heterozygosity in a small cohort of matched presentation and relapsed AML samples demonstrated a potential MMR defect in one patient, and also provided some important insights into the clonal origins of relapsed AML.

The findings of these investigations together highlight several important considerations for the use of nucleoside analogues in the treatment of t-AML, as well as in other cancers in which dysfunction of the DNA MMR system is implicated.

ACKNOWLEDGEMENTS

Firstly, I would like to thank my supervisors, Dr Jim Allan and Dr Julie Irving for their valuable support, guidance and ideas throughout the project. I would also like to thank my colleagues in the Molecular Carcinogenesis group, Dr Nicola Sunter and Vicky Forster, for providing help, answering questions (many pointless) and supplying coffee! Thanks also to numerous members of staff within the Northern Institute for Cancer Research who have provided assistance during this project, especially Liz Matheson (the lab oracle), Lynne Minto, Marian Case and Dr Vikki Rand. I would also like to acknowledge Dr Nick Bown (Northern Genetics Service) and Dr Gail Jones (Royal Victoria Infirmary) for searching out archived clinical data.

I am grateful to my family and friends for support and understanding throughout my PhD, especially during the write up period when most of them probably forgot what I looked like! Special thanks go to my partner for providing motivation, chocolate and importantly, a shoulder to cry on when things were tough.

Finally, I would like to thank Leukaemia and Lymphoma Research for providing the funding which made this work possible. Grateful thanks are also given to the AML patients who volunteered material for inclusion in this work.

TABLE OF CONTENTS

Chapter 1. Introduction	1
1.1. The DNA Mismatch Repair Pathway	2
1.1.1. Overview of the DNA MMR pathway	2
1.1.1.1. MMR in <i>Escherichia coli</i>	2
1.1.1.2. MMR in Humans	3
1.1.2. MMR and Recombination	7
1.1.2.1. MMR and HRR	8
1.2. Mismatch Repair and Response to DNA Damaging Agents	11
1.2.1. Methylating Agents and 6-Thioguanine	12
1.2.1.1. DNA Damage Induced by Methylating Agents and 6-TG	12
1.2.1.2. <i>O</i> ⁶ -meG and me6-TG Cytotoxicity Mediated by DNA MMR	13
1.2.1.3. Methylation Tolerance in MMR-defective Cells	21
1.2.2. 5-Fluorouracil	22
1.2.2.1. MMR and 5-FU Cytotoxicity	22
1.2.3. Crosslinking Agents	24
1.2.3.1. MMR and Cisplatin Cytotoxicity	24
1.2.3.2. MMR and Repair of ICLs	25
1.2.4. Ionising Radiation	26
1.2.4.1. MMR and IR-Induced Cell Cycle Checkpoint Activation	26
1.2.4.2. MMR and Removal of 8-Oxoguanine	28
1.3. Acute Myeloid Leukaemia	29
1.3.1. Genetic Mutations in AML Leukaemogenesis	33
1.3.1.1. Class I Mutations	35
1.3.1.2. Class II Mutations	35
1.3.1.3. Class III Mutations	39
1.3.1.4. Other Genetic Abnormalities	39
1.3.2. Treatment Strategies for Acute Myeloid Leukaemia	40
1.3.2.1. Standard Chemotherapeutic Approaches in AML	40
1.3.2.2. Alternative Nucleoside Analogues for AML Treatment	41
1.3.2.3. Targeted Therapies for Treatment of AML	42

1.4. Therapy-Related Acute Myeloid Leukaemia	43
1.4.1. Methylating Agent-Related Acute Myeloid Leukaemia	44
1.4.1.1. <i>DNA MMR Dysfunction and t-AML Carcinogenesis – The ‘Genomic Instability’ Model</i>	44
1.4.1.2. <i>Cooperating Genetic Aberrations in t-AML Aetiology</i>	50
1.4.1.3. <i>Deregulation of Other DNA Repair Pathways</i>	50
1.4.2. DNA Topoisomerase Inhibitor-Related Acute Myeloid Leukaemia	51
1.4.3. Therapy-Related Acute Myeloid Leukaemia Following Radiotherapy	52
1.4.4. Therapy-Related Acute Myeloid Leukaemia Following Organ Transplantation	53
1.4.5. Atypical Therapy-Related Acute Myeloid Leukaemia	53
1.4.6. Genetic Predisposition to Therapy-Related Acute Myeloid Leukaemia	53
1.5. Cytarabine (Ara-C)	58
1.5.1. Structure of Ara-C	59
1.5.2. Cytotoxic Mechanisms of Ara-C	59
1.5.2.1. <i>Incorporation into Replicating DNA Leading to Chain Termination</i>	59
1.5.2.2. <i>Inhibition of DNA Repair</i>	63
1.5.2.3. <i>Inhibition of Topoisomerase Enzymes</i>	63
1.5.3. Mechanisms of Resistance to Ara-C	64
1.5.4. Other Therapeutic Nucleoside Analogues	65
1.6. Aims of Project	67

Chapter 2. Materials and Methods	69
2.1. Chemicals and Reagents _____	70
2.2. Cell Lines _____	70
2.3. General Cell Culture Methods _____	70
2.3.1. Routine Cell Culture	70
2.3.2. Cell Counting and Determination of Cell Density	71
2.3.3. Cryopreservation of Cell Stocks	71
2.3.4. Resuscitation of Frozen Cell Stocks	71
2.3.5. Preparation of Cell Pellets	73
2.4. Generation of Stable DNA MMR-Defective Cell Lines using Short Hairpin RNA-Mediated Gene Knockdown _____	73
2.4.1. shRNA Constructs, Controls and Reagents	73
2.4.2. Assessment of Puromycin Sensitivity	74
2.4.3. Assessment of Hexadimethrine Bromide Sensitivity	75
2.4.4. Assessment of Transduction Efficiency	75
2.4.4.1. <i>Assessment of GFP Expression by Flow Cytometry</i>	76
2.4.5. Lentiviral Transduction	78
2.4.6. Puromycin Selection of Transduced Cells	78
2.4.7. Selection of TK6 Knockdown Clones by Limiting Dilution	79
2.4.8. Expansion of HL-60 Knockdown Populations	80
2.4.9. Assessment of Knockdown Efficiency	80
2.4.10. Routine Culture of Knockdown Cell Lines for use in Cytotoxicity Assays	80
2.5. Generation of Drug Resistant Cell Lines by Escalating Dosage _____	81
2.5.1. Dose Finding Assay	81
2.5.2. Drug Dosing	83
2.5.3. Assessment of Resistance	83

2.6. Cytotoxicity Assays	84
2.6.1. Reagents and Exposures	84
2.6.2. 96-Well Clonogenic Assay	86
2.6.3. Growth Inhibition Assay	87
2.7. Western Immunoblotting	88
2.7.1. Cytosol Preparation	88
2.7.2. Estimation of Protein Concentration by Pierce BCA Assay	89
2.7.3. SDS PAGE and Electrophoretic Transfer	90
2.7.4. Antibody Detection and Visualisation of Bound Proteins	90
2.7.5. Stripping PVDF Membranes for Re-Probing	93
2.8. Gene Expression Analysis by Quantitative Real-Time PCR	93
2.8.1. RNA Extraction and Quantitation	93
2.8.2. Reverse Transcription of RNA into cDNA	94
2.8.3. Real-Time PCR Setup	96
2.8.4. Data Analysis	96
2.9. Genomic DNA Sequencing (For <i>N-RAS</i> and <i>K-RAS</i> Mutations)	97
2.9.1. DNA Extraction and Quantitation	97
2.9.2. PCR Amplification	99
2.9.3. Agarose Gel Electrophoresis	99
2.9.3.1. Gel Preparation	99
2.9.3.2. Electrophoresis	100
2.9.3.3. Visualisation of DNA	100
2.9.4. Cleanup of PCR Products for Sequencing	100
2.9.5. Sequence Analysis	101
2.10. <i>In Vitro</i> Mutation Assays	101
2.10.1. Removal of Spontaneous Mutants using CHAT Medium	101
2.10.2. Drug Exposure	103

2.10.3. Assessment of Cytotoxicity	103
2.10.4. Selection of TK Mutants	104
2.10.5. Selection of HPRT Mutants	104
2.10.6. Calculation of Mutation Frequency	105
2.10.7. Statistical Analysis	105
2.11. Molecular Analysis of <i>HPRT</i> Mutants	106
2.11.1. Expansion of Mutant Cell Populations	106
2.11.2. Multiplex PCR for <i>HPRT</i> Exon Deletions	106
2.11.2.1. <i>DNA Extraction</i>	106
2.11.2.2. <i>Multiplex PCR Setup</i>	108
2.11.2.3. <i>Analysis of PCR Products</i>	109
2.11.3. Sequencing of <i>HPRT</i> cDNA for Detection of Point Mutations	109
2.11.3.1. <i>RNA Extraction and cDNA Preparation</i>	109
2.11.3.2. <i>Amplification and Sequencing of <i>HPRT</i> cDNA</i>	109
2.11.4. Amplification of <i>HPRT</i> Exons for Sequencing of Putative Splice Mutants	110
2.11.5. Calculation of Absolute and Ara-C-Induced Mutant Fractions	111
2.11.6. Statistical Analysis	112
2.12. Leukaemic Blast Quantitation and Enrichment from AML Patient Samples	112
2.12.1. Immunophenotyping	112
2.12.1.1. <i>Antibody Labelling</i>	113
2.12.1.2. <i>Flow Cytometry</i>	115
2.12.2. Magnetic-Activated Cell Sorting	115
2.12.2.1. <i>MicroBead Labelling</i>	115
2.12.2.2. <i>Cell Separation</i>	116
2.12.3. Storage of Cell Populations	116
2.13. SNP Array Analysis	117
2.13.1. Preparation of DNA for SNP Array	117
2.13.2. Data Analysis	117

Chapter 3. Loss of DNA MMR Components Mediates Response to Chemotherapeutic Nucleoside Analogues <i>in vitro</i>	119
3.1. Introduction	120
3.1.1. Aims of Chapter 3	121
3.2. Results	123
3.2.1. Phenotypic Characterisation of the MMR-Defective Cell Line MT-1	123
3.2.1.1. Expression Levels of MMR Proteins Determined by Western Immunoblotting	123
3.2.1.2. Expression Levels of MMR Genes Determined by Quantitative RT-PCR	124
3.2.1.3. Cytotoxicity in Response to MNU and 6-TG	124
3.2.2. Cytotoxicity in TK6 and MT-1 Cells Following Treatment with Ara-C	128
3.2.3. Cytotoxicity in TK6 and MT-1 Cells Following Treatment with Fludarabine, Cladribine and Clofarabine	128
3.2.4. Assessment of RAS Mutation Status and Activity in TK6 and MT-1 Cells	130
3.2.4.1. Sequencing of N-RAS and K-RAS Exons	130
3.2.4.2. Quantification of Activated ERK via Western Immunoblotting	130
3.2.5. Assessment of MMR Status in shRNA Knockdown Cell Lines	132
3.2.5.1. Expression Levels of MutS Protein Components Determined by Western Immunoblotting	132
3.2.5.2. Cytotoxicity Following Treatment with MNU and 6-TG	134
3.2.6. Cytotoxicity in MMR Knockdown Cell Lines Following Treatment with Nucleoside Analogues	134
3.2.7. Cytotoxicity in MMR-Deficient Cell Lines Following Exposure to IR and UV Radiation	137
3.2.8. Summary of Relative Cytotoxic Responses in MMR-Deficient Cell Lines Following Exposure to DNA Damaging Agents	140
3.3. Discussion	140
3.3.1. Summary of Chapter	149

Chapter 4. Overexpression of <i>MSH3</i> Confers Resistance to Nucleoside Analogues <i>in vitro</i>	150
4.1. Introduction	151
4.1.1. Aims of Chapter 4	152
4.2. Results	154
4.2.1. Phenotypic Characterisation of MSH3-Overexpressing Cell Lines	154
4.2.1.1. <i>Expression Levels of MMR Proteins Determined by Western Immunoblotting</i>	154
4.2.1.2. <i>Expression Levels of MMR Genes Determined by Quantitative RT-PCR</i>	156
4.2.1.3. <i>Cytotoxicity in Response to MNU and 6-TG</i>	156
4.2.2. Cytotoxicity in MSH3-Overexpressing Cells Following Treatment with Nucleoside Analogues	159
4.2.3. Cytotoxicity in MSH3-Overexpressing Cells Following Exposure to IR and UV Radiation	159
4.3. Discussion	163
4.3.1. Summary of Chapter	165

Chapter 5. Development of *in vitro* Cellular Model Systems of Therapy-Related Acute Myeloid Leukaemia 167

5.1. Introduction	168
5.1.1. Aims of Chapter 5	170
5.2. Results	171
5.2.1. Cell Lines	171
5.2.2. Characterisation of Cell Lines Treated with MNU	171
5.2.2.1. Confirmation of Stable MNU Resistance in TK6, KG-1 and EoL-1	171
5.2.2.2. Cytotoxicity in MNU-Resistant Cell Lines Following Treatment with 6-TG	173
5.2.2.3. Expression Levels of MMR Proteins Determined by Western Immunoblotting	173
5.2.2.4. Assessment of Thiopurine Methyltransferase Status in KG-1 MNU ^R via Western Immunoblotting	176
5.2.2.5. Cytotoxicity in MNU-Resistant Cell Lines Following Treatment with Cytarabine	178
5.2.2.6. Cytotoxicity in KG-1 MNU ^R Following Treatment with Clofarabine and Fludarabine	178
5.2.3. Characterisation of Cell Lines Treated with 6-TG	181
5.2.3.1. Confirmation of 6-TG Resistance in HL-60 and TK6	181
5.2.3.2. Cytotoxicity in 6-TG-Resistant Cell Lines Following Treatment with MNU	181
5.2.3.3. Expression Levels of MMR Proteins Determined by Western Immunoblotting	184
5.2.3.4. Assessment of HPRT Status in 6-TG-Resistant Cell Lines	184
5.2.4. Characterisation of Cell Lines Treated with Ara-C	188
5.2.4.1. Confirmation of Ara-C Resistance in HL-60 and TK6	188
5.2.4.2. Cytotoxicity in Ara-C-Resistant Cell Lines Following Treatment with MNU and 6-TG	188
5.2.4.3. Expression Levels of MMR Proteins Determined by Western Immunoblotting	191
5.2.4.4. Cytotoxicity in Ara-C-Resistant Cell Lines Following Treatment with Clofarabine and Fludarabine	191
5.3. Discussion	194
5.3.1. Summary of Chapter	198

Chapter 6. <i>In vitro</i> Mutagenicity of Cytarabine in Mismatch Repair Proficient and Deficient Cell Lines	199
6.1. Introduction	200
6.1.1. Aims of Chapter 6	202
6.2. Results	203
6.2.1. Effect of MNU Exposure on Mutation Frequency at TK and HPRT Loci in MMR-Proficient TK6 and MMR-Deficient TK6 MSH2i Cells	203
6.2.2. Effect of Ara-C Exposure on Mutation Frequency at TK and HPRT Loci in MMR-Proficient TK6 and MMR-Deficient TK6 MSH2i Cell Lines	206
6.2.3. Molecular Analysis of Mutations at the HPRT Locus in TK6 Cells	210
6.2.3.1. <i>Analysis of large deletions</i>	210
6.2.3.2. <i>Analysis of Point Mutations in HPRT Coding Region</i>	216
6.2.3.3. <i>Analysis of Splice Site Mutations</i>	216
6.2.3.4. <i>Comparison of Spontaneous and Ara-C-Induced HPRT Mutational Spectra</i>	219
6.3. Discussion	221
6.3.1. Summary of Chapter	227

Chapter 7. The Clonal Origins of Relapse in Acute Myeloid Leukaemia	228
7.1. Introduction	229
7.1.1. Aims of Chapter 7	230
7.2. Results	232
7.2.1. Patients	232
7.2.2. Immunophenotypes of Leukaemic Blasts	232
7.2.3. Copy Number Abnormalities	235
7.2.3.1. Putative Focal CNAs	239
7.2.4. Copy-Neutral Loss of Heterozygosity	240
7.3. Discussion	243
7.3.1. Summary of Chapter	249
Chapter 8. Concluding Discussion	250
8.1. DNA MMR Dysfunction and Chemoresistance in t-AML	251
8.2. Exploitation of DNA MMR Dysfunction to Improve Therapeutic Outcome	252
8.3. Detection of DNA MMR Defects in t-AML Patients	253
8.4. Chemotherapy Involving Nucleoside Analogues and Risk of t-AML Development	255
8.5. Clonal Evolution and Clonal Heterogeneity in AML	257
8.6. Summary of Findings	258
8.7. Future Directions	259
References	261

LIST OF FIGURES

Figure 1.1. The human DNA MMR pathway.	4
Figure 1.2. Homologous recombination repair.	9
Figure 1.3. 6-thioguanine and its intracellular metabolism.	14
Figure 1.4. DNA mispair formation following exposure to methylating agents or 6-thioguanine.	16
Figure 1.5. Involvement of DNA MMR in signalling cell cycle arrest/apoptosis in response to methylating agent- or 6-thioguanine-induced DNA damage.	17
Figure 1.6. Pathways which may mediate MMR-dependent G ₂ cell cycle arrest and apoptosis in response to methylating agents or 6-thioguanine.	19
Figure 1.7. Simplified representation of human haematopoiesis.	30
Figure 1.8. Genetic pathways in t-AML pathogenesis.	45
Figure 1.9. Frequency of microsatellite instability in AML.	47
Figure 1.10. DNA MMR loss in methylating agent-related t-AML carcinogenesis.	49
Figure 1.11. Uptake and intracellular metabolism of cytarabine.	60
Figure 1.12. Replication fork stalling and S phase arrest in response to Ara-C.	62
Figure 1.13. Structures of the normal nucleoside, 2'-deoxyadenosine and its analogues fludarabine, cladribine and clofarabine.	66
Figure 2.1. Flow cytometric assessment of transduction efficiency of TK6 with Mission® TurboGFP™ Control Transduction Particles.	77
Figure 2.2. General workflow of mutation assays (TK and HPRT) in TK6 cells.	102
Figure 3.1. MMR protein expression in TK6 and MT-1 cell lines.	125
Figure 3.2. Relative expression of DNA MMR components in MMR-deficient MT-1 cells.	126
Figure 3.3. Cytotoxicity in response to MNU and 6-TG in TK6 and MT-1 cell lines.	127
Figure 3.4. Cytotoxicity in response to Ara-C in TK6 and MT-1 cell lines.	127
Figure 3.5. Cytotoxicity in response to adenosine nucleoside analogues in TK6 and MT-1 cell lines.	129
Figure 3.6. ERK-2 and pERK-2 protein expression in TK6 and MT-1 cell lines.	131

Figure 3.7. MutS protein expression in MMR knockdown cell lines.	133
Figure 3.8. Cytotoxicity in response to MNU and 6-TG in MMR knockdown cell lines.	135
Figure 3.9. Cytotoxicity in response to Ara-C, fludarabine and clofarabine in MMR knockdown cell lines.	136
Figure 3.10. Cytotoxicity in response to IR and UV exposure in MMR-deficient cell lines.	138
Figure 3.11. Ara-C lesions induce replication slippage in cell-free assays.	145
Figure 3.12. Possible roles for DNA MMR components in cellular response to nucleoside analogues.	148
Figure 4.1. Structural organisation of human <i>DHFR</i> and <i>MSH3</i> loci.	153
Figure 4.2. MMR protein expression in methotrexate-resistant cell lines.	155
Figure 4.3. Relative expression of DNA MMR components in methotrexate-resistant cell lines.	157
Figure 4.4. Cytotoxicity in response to MNU and 6-TG in <i>MSH3</i> -overexpressing cell lines.	158
Figure 4.5. Cytotoxicity in response to nucleoside analogues in <i>MSH3</i> -overexpressing cell lines.	160
Figure 4.6. Cytotoxicity following exposure to IR and UV in <i>MSH3</i> -overexpressing cell lines.	162
Figure 5.1. Stable acquired resistance to MNU in subcultures derived following escalating MNU exposure.	172
Figure 5.2. Cytotoxicity following treatment with 6-TG in MNU-resistant cell lines.	174
Figure 5.3. MMR protein expression in MNU-resistant cell lines.	175
Figure 5.4. TPMT protein expression in KG-1 and KG-1 MNU ^R .	177
Figure 5.5. Cytotoxicity following treatment with Ara-C in MNU-resistant lines.	179
Figure 5.6. Cytotoxicity in KG-1 MNU ^R following treatment with clofarabine and fludarabine.	180
Figure 5.7. Stable acquired resistance to 6-TG following prolonged 6-TG exposure.	182
Figure 5.8. Cytotoxicity following treatment with MNU in 6-TG-resistant cell lines.	183

Figure 5.9. MMR protein expression in 6-TG-resistant cell lines.	185
Figure 5.10. Multiplex amplification of the <i>HPRT</i> locus in 6-TG-resistant cell lines.	186
Figure 5.11. Sequencing of the <i>HPRT</i> coding region in TK6 6-TG ^R .	187
Figure 5.12. Stable acquired resistance to Ara-C following prolonged Ara-C exposure.	189
Figure 5.13. Cytotoxicity following treatment with MNU and 6-TG in Ara-C-resistant cell lines.	190
Figure 5.14. MMR protein expression in Ara-C-resistant cell lines.	192
Figure 5.15. Cytotoxicity following treatment with clofarabine and fludarabine in Ara-C-resistant cell lines.	193
Figure 6.1. Mutagenicity of MNU at <i>TK</i> and <i>HPRT</i> loci.	205
Figure 6.2. Mutagenicity of Ara-C at <i>TK</i> and <i>HPRT</i> loci.	208
Figure 6.3. Comparison of the mutagenicity of MNU and Ara-C at equivalent cytotoxicity.	209
Figure 6.4. Multiplex PCR amplification of the <i>HPRT</i> locus.	211
Figure 6.5. Extent of genomic deletions observed in spontaneous and Ara-C-treated <i>HPRT</i> mutants.	215
Figure 6.6. Distribution of point mutations within the <i>HPRT</i> coding region.	217
Figure 6.7. Splice site mutations in the <i>HPRT</i> gene, causing splicing of exon 8.	218
Figure 6.8. Spectra of spontaneous and Ara-C-induced <i>HPRT</i> mutations in TK6 cells.	220
Figure 7.1. Clonal evolution of leukaemia.	231
Figure 7.2. Immunophenotyping of leukaemic blasts in peripheral blood at presentation and relapse in patient 3.	234
Figure 7.3. Complex copy number abnormality of chromosome 17 (pter – p12) at second relapse in AML patient 3.	237
Figure 7.4. Clonal evolution of relapse in AML patients.	245

LIST OF TABLES

Table 1.1. Overview of the French-American-British (FAB) classification system of AML.	32
Table 1.2. Summary of genetic mutations observed in <i>de novo</i> and therapy-related AML.	34
Table 1.3. Genetic polymorphisms reported to modify risk of t-AML.	55
Table 2.1. Routine passage schedule of cell lines.	72
Table 2.2. Dosing Schedule for generation of drug-resistant sub-cultures from myeloid (HL-60, EoL-1 and KG-1) and lymphoblastoid (TK6) cell lines.	82
Table 2.3. Preparation of stock solutions of cytotoxic agents.	85
Table 2.4. Antibodies used in western immunoblotting.	92
Table 2.5. TaqMan® Gene Expression Assays used in RT-PCR assessment of DNA MMR gene expression.	95
Table 2.6. Sequences of oligonucleotide primers used for PCR amplification of RAS exons for sequencing.	98
Table 2.7. Sequences of oligonucleotide primers used for multiplex PCR amplification of <i>HPRT</i> exons.	107
Table 2.8. Fluorescence-conjugated antibodies used in flow cytometric assessment of blast immunophenotype.	114
Table 3.1. Summary of MMR protein expression, MMR status and drug response phenotypes in MMR-deficient cells (relative to MMR-proficient parental cells).	139
Table 6.1. Effect of MNU exposure on mutation frequency at <i>TK</i> and <i>HPRT</i> loci.	204
Table 6.2. Effect of Ara-C exposure on mutation frequency at <i>TK</i> and <i>HPRT</i> loci.	207
Table 6.3. Large deletions observed in spontaneous and Ara-C-treated <i>HPRT</i> mutants.	214
Table 6.4. Point mutations observed in spontaneous and Ara-C-treated <i>HPRT</i> mutants.	217
Table 6.5. Summary of spontaneous and Ara-C-treated <i>HPRT</i> mutants.	220
Table 7.1. Selected features of matched presentation and relapsed AML patient samples included in this study.	233

Table 7.2. Regions of detected copy number abnormality in AML patients at presentation and relapse.	236
Table 7.3. Regions of detected copy-neutral LOH in AML patients at presentation and relapse.	241

ABBREVIATIONS

5-FU	5-fluorouracil
6-TG	6-thioguanine
8-oxoG	8-oxoguanine
8-oxoGTP	8-oxoguanine triphosphate
A	Adenine
ALL	Acute lymphoblastic leukaemia
AML	Acute myeloid leukaemia
AML1	Acute myeloid leukaemia 1
ANOVA	Analysis of variance
APC	Adenomatous polyposis coli
APE1	Apurinic/aprimidinic endonuclease 1
APL	Acute promyelocytic leukaemia
Ara-C	Cytarabine
Ara-CMP	Cytarabine monophosphate
Ara-CTP	Cytarabine triphosphate
Arg	Arginine
ATCC	American Type Culture Collection
ATM	Ataxia telangiectasia mutated
ATP	Adenosine triphosphate
ATR	Ataxia telangiectasia and Rad3 related
ATRA	All-trans retinoic acid
ATRIP	ATR interacting protein
ATXN3	Ataxin 3
AZA	Azacytidine
BCA	Bicinchoninic acid
BER	Base excision repair
BLAST	Basic Local Alignment Search Tool
BLM	Bloom
bp	Base pair
BRAF	v-Raf murine sarcoma viral oncogene homologue B1

BRCA (1, 2)	Breast cancer, early onset
BSA	Bovine serum albumin
C	Cytosine
C/EBP α	CCAAT/enhancer binding protein alpha
CAPS	N-cyclohexyl-3-aminopropanesulphonic acid
CBF	Core binding factor
CCNU	N-(2-chloroethyl)-N'-cyclohexyl-N-nitrosourea
CD (33, 34, 45 etc)	Cluster of differentiation
CDC (2, 25A, 25C)	Cell division cycle
CDK2	Cyclin dependent kinase 2
cDNA	Complementary DNA
CDS	Coding domain sequence
CE	Cloning efficiency
CHAT	Cytidine hypoxanthine aminopterin thymidine
Chr	Chromosome
CI	Confidence interval
Clad	Cladribine
CLL	Chronic lymphocytic leukaemia
Clof	Clofarabine
CN	Copy number
CNA	Copy number abnormality
cn-LOH	copy neutral loss of heterozygosity
CR	Complete response
CSF	Colony stimulating factor
Ct	Cycle threshold
CTNNA1	Catenin alpha 1
CYP	Cytochrome P450
dCK	Deoxycytidine kinase
dCTP	Deoxycytidine triphosphate
DEC	Decitabine
del	Deletion
dFdCTP	Gemcitabine triphosphate

dGTP	Deoxyguanosine triphosphate
DHFR	Dihydrofolate reductase
DMSO	Dimethyl sulfoxide
DNA	Deoxyribonucleic acid
DNMT	DNA methyltransferase
dNTP	Deoxyribonucleotide triphosphate
DSB	Double strand break
ECL	Enhanced chemiluminescence
EDTA	Ethylenediaminetetraacetic acid
EGR1	Early growth response 1
EPO	Erythropoietin
ERCC (2, 5)	Excision repair cross-complementing rodent repair deficiency, complementation group
ERK (1, 2)	Extracellular signal-regulated kinase 2
ES	Embryonic stem
EVI1	Ecotropic virus integration site 1
EXO1	Exonuclease 1
FAB	French American British
FAM	Carboxyfluorescein
FANCD2	Fanconi anaemia, complementation group D2
FBS	Foetal bovine serum
FISH	Fluorescence in situ hybridisation
FITC	Fluorescein isothiocyanate
FLT3	Fms-related tyrosine kinase 3
Flud	Fludarabine
G	Guanine
GADD45 α	Growth arrest and DNA damage-inducible alpha
GATA- (1, 2, 3)	GATA binding protein
G-CSF	Granulocyte colony stimulating factor
GFP	Green fluorescent protein
Gln	Glutamine
GM-CSF	Granulocyte macrophage colony stimulating factor

GO	Gemtuzumab ozogamycin
GST (P1, T1)	Glutathione S-transferase
GTPase	Guanosine triphosphatase
Gy	Gray
hENT1	Human equilibrative nucleoside transporter 1
HIV	Human immunodeficiency virus
HL	Hodgkin lymphoma
HNPCC	Hereditary non-polyposis colorectal cancer
HPRT	Hypoxanthine-guanine phosphoribosyltransferase
H-RAS	v-Ha-ras Harvey rat sarcoma viral oncogene homolog
HRR	Homologous recombination repair
HSC	Haematopoietic stem cell
ICL	Intrastrand crosslink
IDL	Insertion/deletion loop
Ig (G ₁ , G _{2a} , M)	Immunoglobulin
IGF1	Insulin-like growth factor 1
IL (1, 3, 6 etc)	Interleukin
Ile	Isoleucine
inv	Inversion
IR	Ionising radiation
ITD	Internal tandem duplication
JNK	Jun N-terminal kinase
kb	Kilobase
kDa	KiloDalton
K-RAS	V-Ki-ras2 Kirsten rat sarcoma viral oncogene homolog
kV	Kilovolts
LIG4	Ligase 4
LOH	Loss of heterozygosity
Lys	Lysine
M	Molar
mA	Milliamp
MACS®	Magnetic activated cell sorting

MAPK	Mitogen activated protein kinase
Mb	Megabase
M-CSF	Macrophage colony stimulating factor
MDS	Myelodysplastic syndrome
Me6-TG	Methyl 6-thioguanine
MEF	Mouse embryonic fibroblast
MeTGMP	Methylthioguanine monophosphate
MF	Mutation frequency
mg	Milligram
MGMT	O6-methylguanine DNA methyltransferase
miRNA	Micro RNA
mJ	Millijoule
MLH (1, 3)	Mut L homologue
MLL	Myeloid/lymphoid or mixed-lineage leukaemia
mM	Millimolar
MMC	Mitomycin C
MMR	Mismatch repair
MNNG	N-methyl-N'-nitro-N-nitrosoguanidine
MNU	N-methyl-N-nitrosourea
MOI	Multiplicity of infection
MRE11	Meiotic recombination 11
MRN	MRE11-RAD50-NBS1
mRNA	Messenger RNA
MSH (2, 3, 6)	Mut S homologue
MSI	Microsatellite instability
MTH1	Mut T homologue 1
MTHFR	Methylenetetrahydrofolate reductase
MTX	Methotrexate
MYH	Mut Y homologue
MYH11	Myosin heavy chain 11
N	Nitrogen
NAD	Nicotinamide adenine dinucleotide

NAD(P)H	Nicotinamide adenine dinucleotide phosphate
NBS1	Nijmegen breakage syndrome protein 1
NER	Nucleotide excision repair
Nf1	Neurofibromin 1
NF-E2	Nuclear factor (erythroid-derived 2)
ng	Nanogram
NHEJ	Non-homologous end joining
NHL	Non-Hodgkin lymphoma
NICR	Northern Institute for Cancer Research
nM	Nanomolar
nm	Nanometre
NPM1	Nucleophosmin 1
NQO1	NAD(P)H: quinone oxidoreductase 1
N-RAS	Neuroblastoma RAS viral (v-ras) oncogene homolog
NRTI	Nucleoside reverse transcriptase inhibitor
O ⁶ -meG	O6 methylguanine
OGG1	8-oxoguanine DNA glycosylase
p (53, 21, 38 α , 73 α)	Protein
PAGE	Polyacrylamide gel electrophoresis
PARP-1	Poly (ADP-ribose) polymerase 1
PBS	Phosphate buffered saline
PBSA	Phosphate buffered saline albumin
PCNA	Proliferating cell nuclear antigen
PCR	Polymerase chain reaction
PE	Phycoerythrin
PerCP	Peridinin chlorophyll protein
PML	Promyelocytic leukaemia
pmol	Picomolar
PMS (1, 2)	Post meiotic segregation
pol (α , β , δ , ϵ , λ)	DNA polymerase
Pro	Proline
PTD	Partial tandem duplication

PVDF	Polyvinylidene fluoride
RAD (51, 52, 54 etc)	Radiation sensitivity abnormal
RAD51L1	RAD51-like 1
RAR α	Retinoic acid receptor alpha
RF10	RPMI, FBS 10%
RFC	Replication factor C
RISC	RNA-induced silencing complex
RNA	Ribonucleic acid
ROS	Reactive oxygen species
RPA	Replication protein A
RPMI	Roswell Park Memorial Institute
RT	Reverse transcriptase
RTK	Receptor tyrosine kinase
RT-PCR	Real-time polymerase chain reaction
RUNX1	Runt-related transcription factor 1
RUNX1T1	Runt-related transcription factor 1; translocated to, 1
SAM	S-adenosylmethionine
SCF	Stem cell factor
SCL	Stem cell leukaemia protein
SDS	Sodium dodecyl sulphate
SEM	Standard error of the mean
Ser	Serine
shRNA	Short hairpin RNA
siRNA	Small interfering RNA
SNP	Single nucleotide polymorphism
SSB	Single strand binding protein
t	Translocation
T	Thymine
t-AML	Therapy-related acute myeloid leukaemia
TBE	Tris-buffered EDTA
TBS	Tris-buffered saline
TdT	Terminal deoxynucleotidyl transferase

TE	Tris-EDTA
ter	Terminal
TFT	Trifluorothymidine
TGMP	Thioguanine monophosphate
THC	Thymidine hypoxanthine cytosine
thio-dGTP	Deoxythioguanine triphosphate
TK	Thymidine kinase
Topo (I, II)	Topoisomerase
TP53	Tumour protein 53 gene
TPMT	Thiopurine methyltransferase
Tris	Tris(hydroxymethyl)aminomethane
TSG	Tumour suppressor gene
TU	Transduction units
UPD	Uniparental disomy
UV	Ultraviolet
V	Volt
Val	Valine
v/v	Volume/volume
w/v	Weight/volume
x g	Gravity
XRCC (1, 3)	X-ray repair complementing defective repair in Chinese hamster cells
µg	Microgram
µM	Micromolar

Chapter 1. Introduction

1.1. The DNA Mismatch Repair Pathway

The DNA mismatch repair (MMR) pathway is one of a number of cellular mechanisms responsible for maintaining the stability of the genome, by ensuring DNA replication errors are corrected before they can result in mutation. There are two main types of error for which MMR is able to elicit repair. Simple base:base mismatches, which occur when a DNA polymerase enzyme inserts an incorrect base in the daughter strand which is subsequently missed by its proofreading activity. Secondly, insertion/deletion loops (IDLs) which are extrahelical loops of DNA arising either when DNA polymerase inserts an extra base during replication (single base IDLs) or when the template and primer strands in a repetitive sequence (microsatellite) misalign, resulting in a larger IDL. Dysfunction of the DNA MMR pathway gives rise to genomic instability and predisposition to the acquisition of mutations throughout the genome. This is referred to as a 'mutator phenotype' (Branch et al., 1993) which can contribute to the development of cancer (see Section 1.4.1.1), and exemplifies the importance of DNA MMR in maintaining replication fidelity.

In addition to repair of replication errors, DNA MMR components have been implicated in other cellular processes including regulation of recombination (see Section 1.1.2), and also play an important role in mediating cell cycle arrest and/or apoptosis in response to certain DNA damaging agents (described in Section 1.2).

1.1.1. Overview of the DNA MMR pathway

1.1.1.1. MMR in Escherichia coli

The *Escherichia coli* MMR pathway has been extensively studied and is well characterised both biochemically and genetically. The pathway is highly conserved from prokaryotes to eukaryotes, hence *E. coli* MMR has provided a useful framework for understanding DNA MMR in other organisms. Furthermore, a large number of proteins involved in MMR in humans, and in other species, have been identified based on their homology to *E. coli* MMR proteins.

Reconstitution of the *E. coli* DNA MMR pathway in a purified system demonstrated the biochemistry of the reactions involved in mismatch correction (Lahue et al., 1989). The initial step in the process involves recognition of replication

damage, which is mediated in *E. coli* by the homodimeric protein MutS. Upon recognition of damage, MutS physically interacts with a second homodimeric protein, MutL, forming a complex in an ATP-dependent manner (Spampinato and Modrich, 2000), which in turn activates a third protein, MutH. MutH is responsible for distinguishing the newly replicated daughter strand (which it does by recognition of a hemimethylated dGATC sequence either 5' or 3' to the mismatch), whereupon it generates a single strand nick. MutS and MutL then activate UvrD helicase, the role of which is to unwind the DNA duplex, generating single-strand DNA. This is rapidly bound by single-strand DNA binding protein (SSB) in order to protect it from nuclease attack and to allow one of several exonucleases to digest the mismatch-containing strand from the nicked site to the mismatched base. The resulting gap is refilled by the DNA polymerase III holoenzyme, which is probably recruited to the damage intermediate by physical interaction with MutL (Li et al., 2008a). Finally, DNA ligase functions to seal the remaining nick in the daughter strand.

1.1.1.2. MMR in Humans

A basic representation of the processes involved in DNA MMR in humans is shown in Figure 1.1. Detection of replication-related DNA damage is mediated by two MutS complexes, each with specific substrate specificities (Figure 1.1, top inset). Whereas *E. coli* MutS is a homodimer, the human MutS homologues form heterodimers in order to mediate damage recognition. MutS α is a heterodimer of the proteins MSH2 and MSH6 (Drummond et al., 1995; Acharya et al., 1996). It preferentially recognises base:base mispairs, and also has some activity towards small IDLs of 1 or 2 nucleotides (Genschel et al., 1998). MutS β on the other hand, consisting of MSH2 heterodimerised with MSH3 (Acharya et al., 1996) recognises both small and large IDLs but cannot mediate recognition of mispairs (Palombo et al., 1996; Genschel et al., 1998).

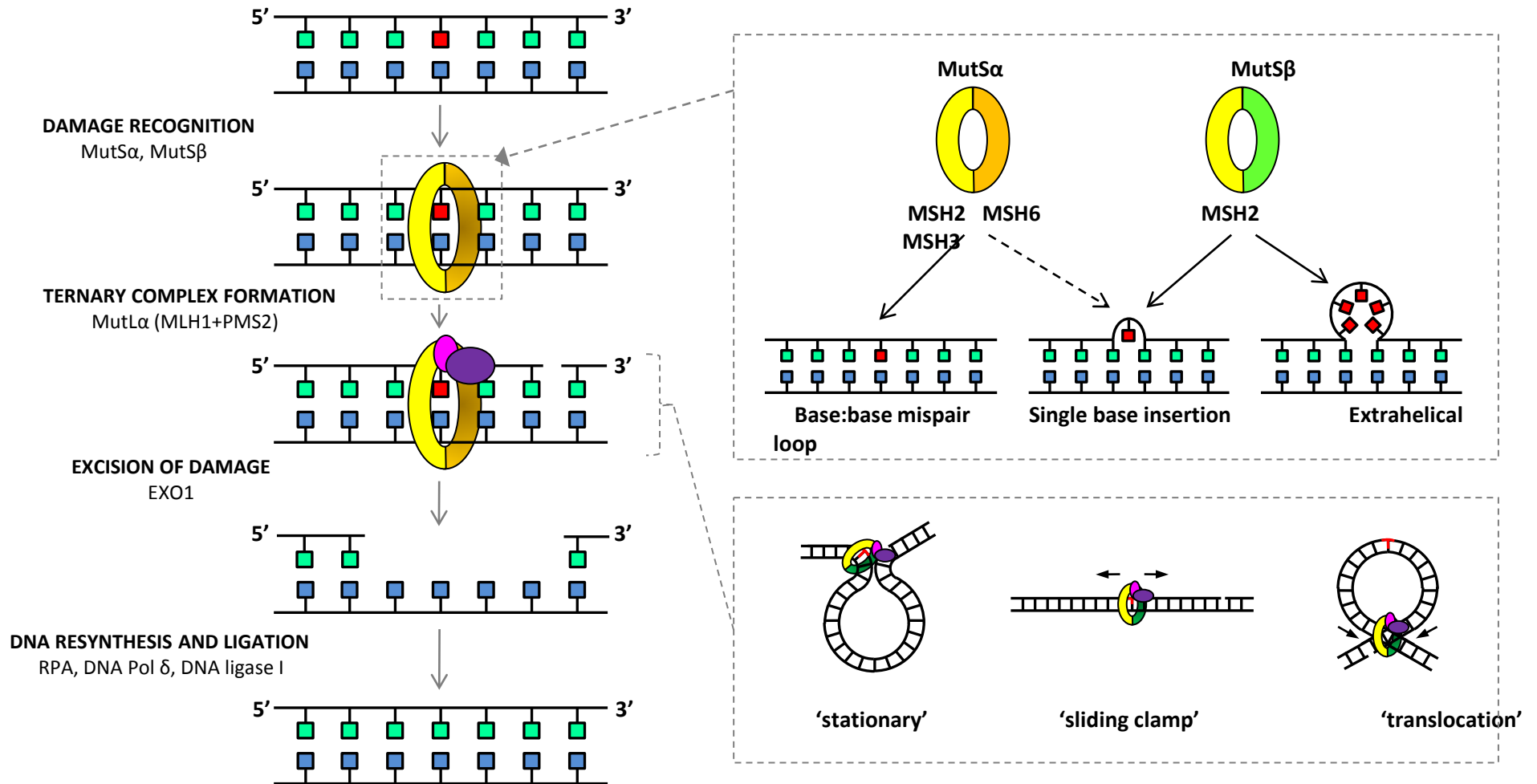


Figure 1.1. The human DNA MMR pathway.

See text for description of pathway. Top inset illustrates substrate specificities of MutS α and MutS β . Lower inset displays three alternative models by which MMR components might facilitate communication between the damage site (red) and the single strand nick from which excision is initiated (described in text).

Like *E. coli* MMR, MutS α and MutS β are ATPases which are activated following damage detection, and recruit MutL homologues to the damaged site (Blackwell et al., 1998). Recent investigations have shown that MutS complexes function as transient clamps that scan duplex DNA for mismatched nucleotides (Jeong et al., 2011). Mismatch identification provokes ATP binding, transforming MutS scanning clamps into highly stable signalling clamps which are speculated to be capable of chromatin remodelling, enabling interaction with MutL homologues, as well as other MMR components (Jeong et al., 2011).

At least four human MutL homologues (MLH1, MLH3, PMS1 and PMS2) have been identified. MutL α , a heterodimer of MLH1 and PMS2, is the major complex involved in replication-related MMR (Li and Modrich, 1995). Recruitment of MutL α to the damaged site results in formation of a ternary complex which promotes intracellular signalling to initiate excision and repair of the damage (Kadyrov et al., 2006). Alternative MutL complexes may have roles in other cellular processes, for example MutL γ (a heterodimer of MLH1 and MLH3) has been implicated in meiosis (Li, 2008).

As in *E. coli* MMR, excision of the damage-containing region appears to originate from a single strand nick in the daughter strand which can be either 3' or 5' to the damage (Li, 2008). A number of fundamental problems however remain to be resolved regarding the mechanisms associated with strand excision. Firstly, it is not clear in humans, how the daughter DNA strand is distinguished from the parental strand following DNA replication. In the case of lagging strand DNA replication, the presence of Okazaki fragments may serve to identify the daughter DNA strand, and the gaps between fragments could provide the origin for excision of the damaged region. Replication of the leading strand however, proceeds in a continuous manner and it remains undetermined how the daughter strand is identified and which protein is responsible for generating the single strand nick.

Whereas damaged strand excision in *E. coli* can be mediated by at least four exonucleases, in humans, only one DNA MMR-related exonuclease has as yet been identified. This exonuclease, exonuclease I (EXO1), is a 5'→3' exonuclease, yet has been shown to be involved in excision originating either 5' or 3' of the damaged site (Genschel et al., 2002). Hence another unsolved problem is how an exonuclease with

only 5'→3' activity can mediate excision in both directions. It was originally suggested that EXO1 may possess a cryptic 3'→5' exonuclease activity (Genschel et al., 2002), however this is not supported by current data. Recent investigations suggest that, following recognition of a nick 3' to the damage site, MutL α makes an incision 5' to the damage, via its endonuclease activity, allowing EXO1 to perform 5'→3' excision through the damage site to the 3' nick (Kadyrov et al., 2006).

A further unsolved problem in human DNA MMR, which also applies to MMR in *E. coli* and other organisms, is the key question of how MMR components facilitate communication between the site of the mismatch and the physically distant single strand nick, be it either 5' or 3' to the site of damage. A number of alternative models have been proposed for this process (Figure 1.1, lower inset). The 'stationary' model proposes that MutS α (or MutS β) is bound at the site of the mismatch, whereas MutL α and other MMR components are located at the nicked site. Activation of MutS α promotes physical interaction with MutL α , bringing the two distant sites together by bending or 'looping out' of the intervening DNA (Guarne et al., 2004). The 'moving' model, sometimes referred to as the 'sliding clamp' model, proposes that the MutS α -MutL α (or MutS β -MutL α) ternary complex forms at the site of the mismatch and undergoes an ATP-dependent conformational change which allows it to slide along the DNA in either direction. This leaves the damage site empty for formation of further MutS α -MutL α sliding clamps. Excision is initiated when one of the clamps encounters a nicked site (Gradia et al., 1997; Gradia et al., 1999). A variation of this model, referred to as the 'translocation' model, suggests that sliding clamps move in a unidirectional manner, scanning bidirectionally from the mispair (hence forming a looped DNA structure containing the mismatch) until a nicked site in either orientation is reached (Allen et al., 1997). Although a number of studies have attempted to elucidate which model is most likely to occur, the available evidence has not allowed firm conclusions to be made. For instance, recent studies demonstrated that a double strand break (DSB) or protein 'blockage' between the mismatch site and the nick inhibits MMR *in vitro* (Pluciennik and Modrich, 2007), arguing in favour of the 'moving' models. This however is at odds with a similar previous investigation supporting the 'stationary' model, in which mismatch-provoked excision could still occur despite the placement of a biotin-streptavidin blockade between the mismatch and nick (Wang and Hays, 2004).

Following excision, the single strand DNA-binding protein, replication protein A (RPA) is required to protect the nascent single stranded regions and recruit DNA polymerase δ and DNA ligase I to re-synthesise DNA (Longley et al., 1997; Ramilo et al., 2002). Other proteins which are essential in human DNA MMR, but have no identified homologue in *E. coli*, include proliferating cell nuclear antigen (PCNA) (Umar et al., 1996) and replication factor C (RFC) (Dzantiev et al., 2004). PCNA in particular has roles in almost every step of the pathway. It can interact with MSH2, MSH3 and MSH6 (Gu et al., 1998; Clark et al., 2000) and may help localise MutS α and MutS β to damage sites in newly replicated DNA (Kleczkowska et al., 2001; Lau and Kolodner, 2003). It can also interact with MLH1 and is essential, in combination with RFC, for the endonuclease function of MutL α (Kadyrov et al., 2006).

1.1.2. MMR and Recombination

In general terms, recombination provides a mechanism by which genetic information can be exchanged or transferred between homologous DNA sequences. In mammals, this occurs largely during meiosis and also forms the basis of the homologous recombination repair (HRR) pathway, a key mechanism for the repair of DSBs, as described below. To maintain genomic integrity, perfect homology is required, hence a system must exist to regulate recombination events. A significant body of evidence points to DNA MMR as a likely regulator of recombination.

It was initially demonstrated in prokaryotes that DNA MMR was able to provide a barrier against recombination between unrelated species, whose DNA differs significantly in sequence, by aborting or destabilising mismatched heteroduplex recombination intermediates (Rayssiguier et al., 1989). Subsequently, using gene targeting experiments in yeast (Selva et al., 1995), mouse (de Wind et al., 1995; Abuin et al., 2000) and human cells (Ciotta et al., 1998), it was found that the frequency of recombination events between imperfectly matched (homeologous) sequences was significantly elevated in MMR-defective cells. These studies demonstrated a role for MMR in suppression of recombination between diverged or homeologous sequences.

Studies in mice and yeast reveal an essential role for DNA MMR components in meiotic recombination processes. Notably, homozygous *Mlh1* or *Pms2* knockout mice are sterile (Baker et al., 1995; Baker et al., 1996; Edelman et al., 1996). Specific details

regarding the involvement of MMR components in meiosis are beyond the scope of this project, however Kolas and Cohen (2004) provide a comprehensive review on this subject.

1.1.2.1. MMR and HRR

HRR is one of two major DNA repair pathways responsible for repair of DSBs, a particularly genotoxic form of DNA damage occurring as a result of exogenous agents (e.g. ionising radiation (IR)), endogenous processes (e.g. collapsed replication forks) or during specialised recombination events (e.g. immunoglobulin class switching). HRR ensures accurate repair of DSBs because homologous sequences in the form of undamaged sister chromatids are used as repair templates, it is therefore only operational during late S and G₂ phases of the cell cycle when these are available (Hoeijmakers, 2001). The HRR pathway and the major components involved in DSB repair are shown in Figure 1.2A.

MSH2 and MSH6 have both been shown to co-localise with key HRR proteins in mammalian cells, including BRCA1 (Wang et al., 2000) and RAD51 (Rajesh et al., 2009), suggesting a role for MMR components in the HRR pathway. The specific involvement of MMR components in HRR remains unclear, however several lines of evidence suggest a role in ensuring that recombination intermediates formed as a result of strand exchange are true homologues, and in mediating abortion of recombination if this is not the case. In the yeast *Saccharomyces cerevisiae*, MSH2 interacts directly with recombination intermediates (Alani et al., 1997; Evans et al., 2000) and a model was proposed in which it interacts with a helicase enzyme to unwind heteroduplex regions containing mismatches (referred to as heteroduplex rejection) (Sugawara et al., 2004; Goldfarb and Alani, 2005). Similarly, in human cell lines, MSH2 and MSH6 have been shown to regulate the activity of the BLM helicase (Yang et al., 2004b), which is localised to recombination intermediates (Wu et al., 2001), also suggesting a role in mediating heteroduplex unwinding.

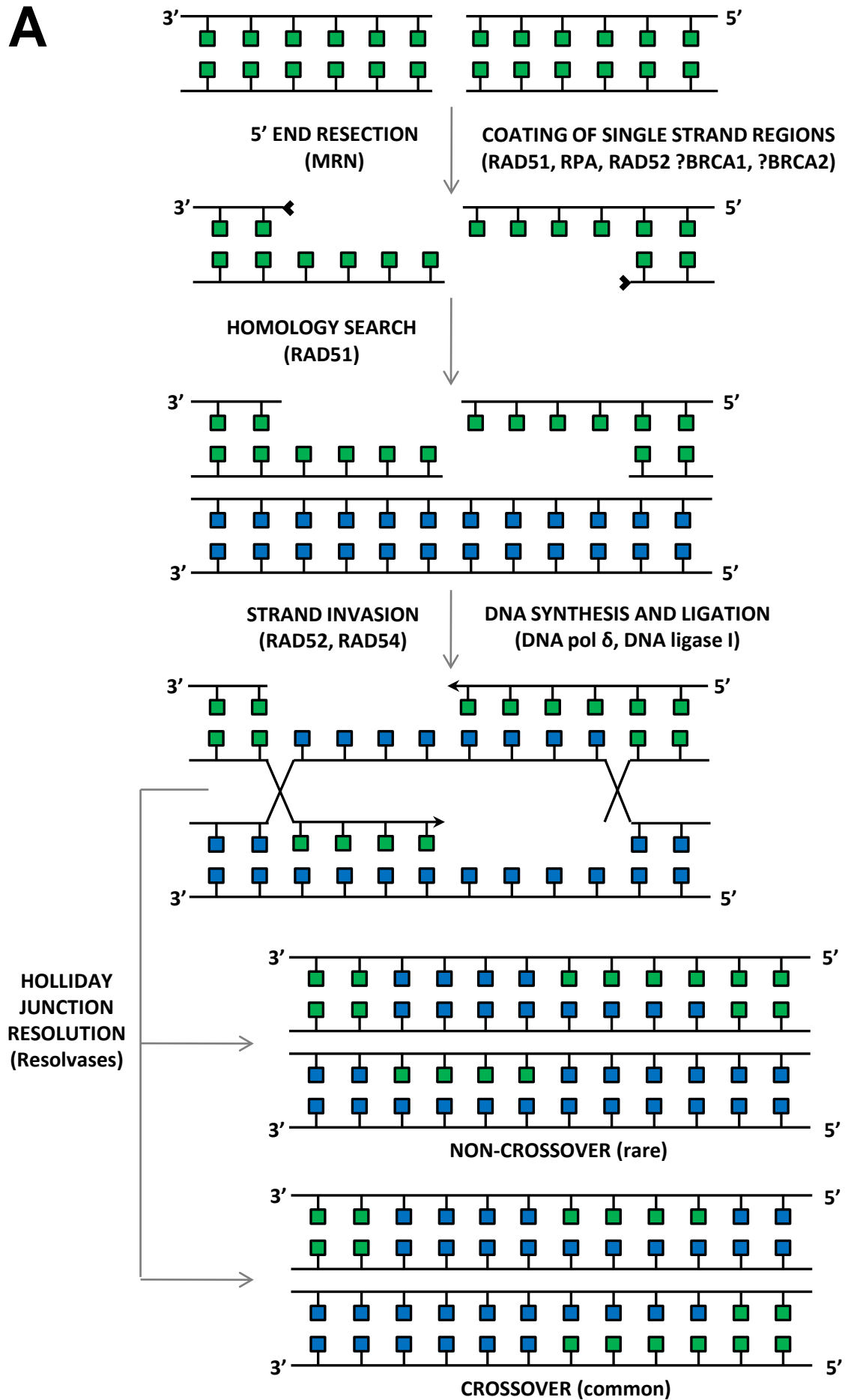
A

Figure 1.2. Homologous recombination repair (continued on next page).

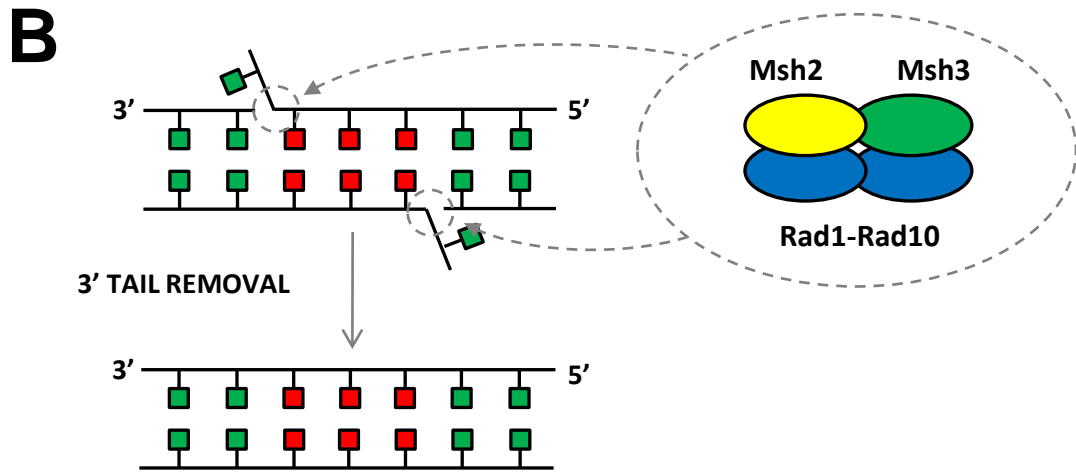


Figure 1.2. Homologous recombination repair (continued from previous page).

A. Following DSB formation, activation of ATM mediates cell cycle arrest via p53 (Morrison et al., 2000), as well as phosphorylation of the histone, H2AX, in the vicinity of the DSB, which may provide a local chromatin state necessary for repair (Paull et al., 2000) (not shown in figure). ATM also activates a complex consisting of MRE11, RAD50 and NBS1 (MRN) which exposes 3' DNA ends at the break via its 5'-3' exonuclease activity (Petrini, 2000). RAD51 polymerises onto the single-stranded DNA, assisted by RPA and RAD52, to form a nucleoprotein filament (Symington, 2002). In addition, BRCA1 and BRCA2 are also implicated in mediating a proper RAD51 response although their roles are not well understood (Gudmundsdottir and Ashworth, 2006). The RAD51 nucleoprotein filament searches for the homologous duplex DNA and, once located, DNA strand exchange generates a recombinant heteroduplex between the damaged molecule and its undamaged homologue (Baumann and West, 1998), a process stimulated by RAD52 and RAD54 (Symington, 2002). DNA synthesis by polymerase fills in the single stranded gaps using the intact homologue as a template, after which DNA ligase seals the nicks. Finally, the junctions between the DNA strands (termed Holliday junctions) are resolved. This can occur in either a horizontal or vertical fashion, giving rise to non-crossover or crossover events respectively.

B. Homologous recombination intermediates in *S. cerevisiae* require additional processing to remove 3' non-homologous ends resulting from heteroduplex formation. The DNA MMR proteins Msh2 and Msh3 are involved in this processing step to recruit the Rad1-Rad10 endonuclease (see text).

Cells deficient in MSH2 demonstrate aberrant RAD51 (and MRE11) foci formation and a higher level of chromosomal damage following exposure to low dose-rate IR (Franchitto et al., 2003; Barwell et al., 2007). Similarly, RAD51 levels decrease in response to low dose-rate IR, but only in cells with functional MLH1 protein (Yan et al., 2009). Loss of MLH1 also results in an increase in IR-induced mitotic recombination (Wang et al., 2006) and chromosome translocations (Zhang et al., 2008). Together these data indicate that MSH2 and MLH1 may regulate RAD51 to suppress HRR.

Inactivation of DNA MMR can result in deregulation of HRR by permitting the completion of imperfect recombinational exchanges. Repair of DSBs by HRR is deregulated in murine embryonic stem (ES) cells deficient in *Msh2* (*Msh2*^{-/-}) (Elliott and Jasin, 2001). Although *Msh2*^{-/-} mutants can efficiently repair DSBs, they cannot repair mismatches in the heteroduplex DNA formed adjacent to the DSB, resulting in gene conversion. Similar results have also been observed in human cell lines deficient in MSH2 (Villemure et al., 2003; Smith et al., 2007) and MLH1 (Siehler et al., 2009).

MMR proteins in *S. cerevisiae* are known to have an additional function in HRR which involves removal of non-homologous 3' ends which result following heteroduplex formation (Figure 1.2B). Both Msh2 and Msh3 are required to recruit the Rad1/Rad10 endonuclease to the sites of recombination (Sugawara et al., 1997), although Msh2 and Msh3 only appear to be required if the 3' ends are at least 30 nucleotides in length (Paques and Haber, 1997). More recent evidence suggests that binding of an Msh2/Msh3 complex alters the conformation of the junction between the heteroduplex and the 3' ends which may facilitate recognition by Rad1/Rad10 (Surtees and Alani, 2006; Lyndaker and Alani, 2009). A similar function of MSH2/MSH3 has yet to be demonstrated in mammalian cells.

1.2. Mismatch Repair and Response to DNA Damaging Agents

The finding that MMR-defective cells were more resistant to certain DNA damaging agents than MMR-proficient counterparts implicated DNA MMR as a mediator of drug cytotoxicity and furthermore highlighted defective MMR as a potential drug resistance mechanism. This was considered a somewhat paradoxical finding given that DNA MMR is a repair pathway. Careful molecular investigation has

since revealed that DNA MMR components have an important role in induction of cell cycle arrest and apoptosis in response to certain DNA damaging agents, as is described in this section.

1.2.1. Methylating Agents and 6-Thioguanine

Early studies showed that MMR-deficient cells demonstrated a high level of resistance to methylating agents, as well as cross-resistance to the base analogue 6-thioguanine (6-TG) (Goldmacher et al., 1986; Aquilina et al., 1989; Aquilina et al., 1990; Kat et al., 1993; Hawn et al., 1995; Shin et al., 1998; Humbert et al., 1999). Despite the apparent diversity of these agents, they were subsequently found to exert their cytotoxicity by a common mechanism, which is absolutely dependent on functional DNA MMR.

1.2.1.1. DNA Damage Induced by Methylating Agents and 6-TG

Methylating agents are a class of DNA damaging agents which can add a methyl group to nucleophilic sites on DNA bases. N-methyl-N-nitrosourea (MNU) and N-methyl-N'-nitro-N-nitrosoguanidine (MNNG) are examples of model unimolecular nucleophilic substitution-type methylating agents. Those in clinical use include procarbazine, dacarbazine, streptozocin and temozolomide. Of the numerous adducts produced in DNA by methylating agents, methylation at the O⁶ position of guanine (O⁶-meG) is the most cytotoxic, despite accounting for only 7% of the total adduct burden produced (Beranek, 1990). In mammals, O⁶-meG lesions can be directly repaired, both prior to and post DNA replication, by the protein O⁶-methylguanine DNA methyltransferase (MGMT) in a reaction which involves transfer of the methyl group from the base to a cysteine residue in the catalytic pocket of the protein (Margison and Santibanez-Koref, 2002) (see Figure 1.4). Cells deficient in MGMT are unable to repair O⁶-meG lesions (Goth-Goldstein, 1980) and demonstrate hypersensitivity to the cytotoxic effects of methylating agents compared to MGMT-proficient counterparts (Yarosh et al., 1983; Kaina et al., 1991; Kaina et al., 1997; Tominaga et al., 1997; Meikrantz et al., 1998). Studies demonstrating that loss of MMR activity counteracted the hypersensitivity to MNU observed in MGMT-deficient cells provided the initial suggestion that DNA MMR was responsible for the cytotoxicity of O⁶-meG in the absence of MGMT (Branch et al., 1993).

6-thioguanine (6-TG), as well as azathioprine and 6-mercaptopurine, belongs to a class of compounds known as thiopurine antimetabolites, which have widespread use as immunosuppressive, anti-cancer and anti-inflammatory agents. 6-TG is an analogue of the purine nucleobase, guanine. It is distinguished from guanine solely by the substitution of the oxygen atom with a thiol group at position 6 of the purine ring (Figure 1.3A). Following administration, 6-TG is readily transported into cells and metabolised via the purine salvage pathway, resulting in the active DNA precursor, deoxythioguanine triphosphate (thio-dGTP) (Figure 1.3B). Given its similarity to deoxyguanosine triphosphate, thio-dGTP is a good substrate for replicative DNA polymerases and is readily incorporated within DNA (Ling et al., 1991). The thiol group of 6-TG is highly reactive however, and renders the incorporated nucleotide susceptible to methylation *in situ* by S-adenosylmethionine (SAM), a cellular methyl donor (Swann et al., 1996). Unlike O⁶-meG, there have been no mechanisms discovered which can reverse methylation of 6-TG.

1.2.1.2. O⁶-meG and me6-TG Cytotoxicity Mediated by DNA MMR

In vitro, unrepaired O⁶-meG within DNA impedes the function of replicative polymerases, although the lesion can be replicated by low-fidelity translesion polymerases (Perrino et al., 2003; Choi et al., 2006). Under physiological conditions however, approximately one third of O⁶-meG lesions become mispaired by incorrect insertion of thymine opposite the lesion (Abbott and Saffhill, 1979; Toorchen and Topal, 1983; Snow et al., 1984). Replication of methylated 6-TG (me6-TG) lesions on the other hand occurs readily, as demonstrated by *in vitro* primer extension assays (Ling et al., 1991), however like O⁶-meG, mispairing with T often occurs (Swann et al., 1996). The subsequent mispairs can escape proofreading by polymerases due to the structural similarity to canonical base pairs (Warren et al., 2006). Functional MutS α and MutL α are essential for cell cycle arrest and subsequent cytotoxicity induced by O⁶-meG and me6-TG (Koi et al., 1994; Umar et al., 1997; Shin et al., 1998; Hickman and Samson, 1999; Cejka et al., 2003), however the exact mechanisms by which DNA MMR mediates these responses remain ill defined.

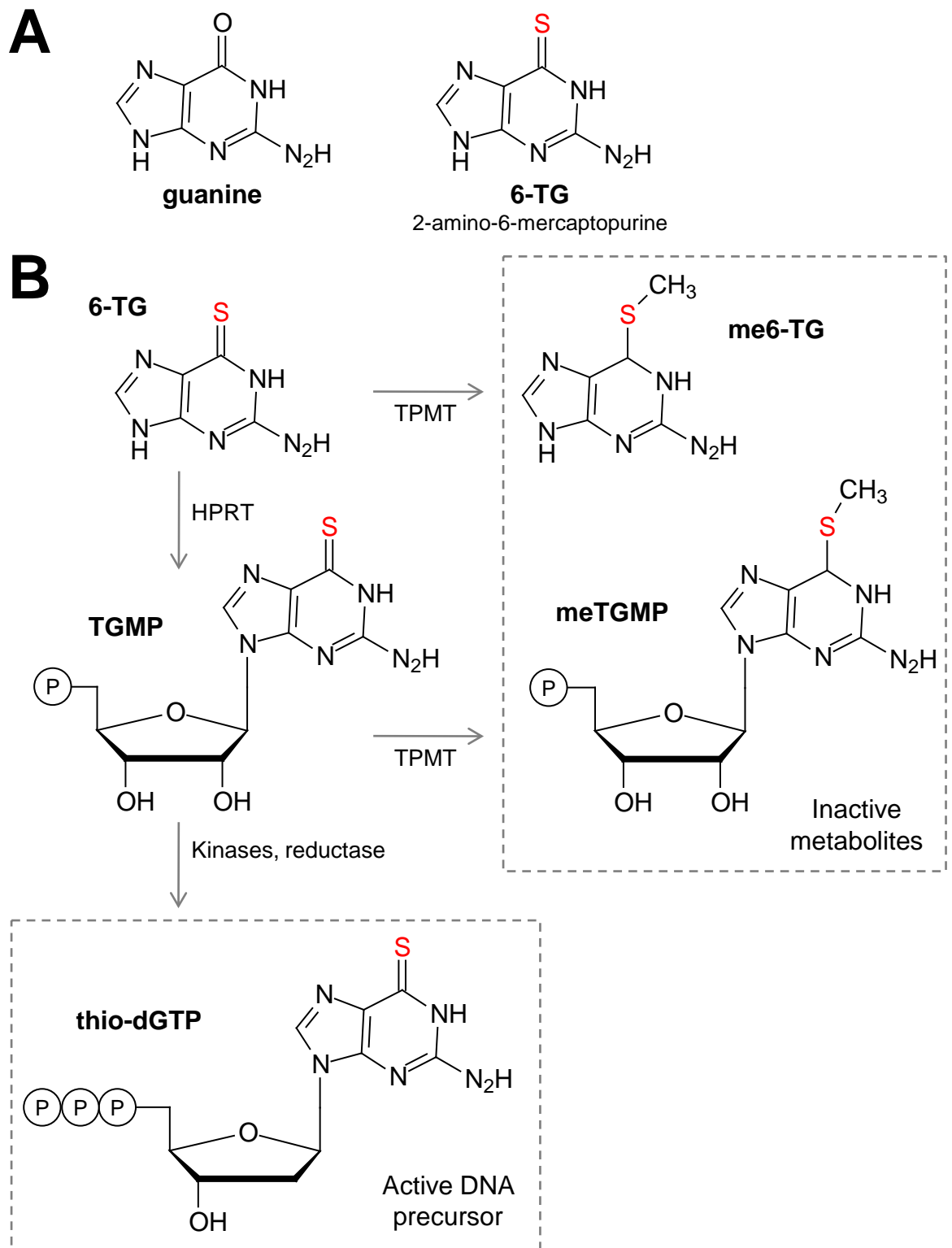


Figure 1.3. 6-thioguanine and its intracellular metabolism.

A. Structures of the normal nucleobase, guanine, and its analogue, 6-thioguanine (6-TG; 2-amino-6-mercaptapurine). The thiol group of 6-TG is shown in red. **B.** Metabolism of 6-TG occurs via purine salvage. Hypoxanthine-guanine phosphoribosyltransferase (HPRT) converts 6-TG to thioguanine monophosphate (TGMP) which is subsequently converted to the active DNA precursor, deoxythioguanine triphosphate (thio-dGTP) by deoxynucleoside kinases and reductase. Both 6-TG and TGMP are also substrates for thiopurine S-methyltransferase (TPMT), an enzyme which methylates the thiol groups resulting in the inactive metabolites, me6-TG and meTGMP. For a recent review, see Karran and Attard (2008).

Following treatment with methylating agents or 6-TG, MMR-proficient cell lines undergo cell cycle arrest in G₂ phase but this is delayed until the second cell cycle following treatment (Zhukovskaya et al., 1994; Hawn et al., 1995; Carethers et al., 1996; Cejka et al., 2003; Stojic et al., 2004a). Furthermore, only replicating cells undergo significant levels of cell death (Roos et al., 2004). These data suggest that replication of O⁶-meG and me6-TG must be a requirement for cell cycle arrest and cell death (Figure 1.4). Consistently, MutS α can recognise and bind to O⁶-meG or me6-TG mispaired with thymine with high efficiency, but not when paired with the canonical partner cytosine (Duckett et al., 1996; Swann et al., 1996; Waters and Swann, 1997; Berardini et al., 2000). What remains unclear is how detection of these mispairs by MutS α is linked to G₂ cell cycle arrest and what causes subsequent cell death.

Two models have been proposed to explain how DNA MMR might mediate cell cycle arrest in response to methylating agents and 6-TG (Figure 1.5A). In the model initially proposed, referred to as the 'futile repair' model, O⁶-meG:T or me6-TG:T mispairs detected by MutS α are subject to attempted MMR-mediated repair however, given that the methylated lesion would be in the template DNA strand and MMR can only be directed to the daughter strand, insertion of the incorrect base (thymine) opposite the lesion is predicted to recur. Repeated futile repair attempts are proposed to result in formation of aberrant repair intermediates which activate DNA damage signalling pathways to induce cell cycle arrest. Following unsuccessful resolution of these complex intermediates, attempted presumably by other repair pathways, cells die by apoptosis. The demonstration that O⁶-meG:T mispairs cannot be successfully repaired by MMR provided biochemical evidence for this model (York and Modrich, 2006). Furthermore, reports of persistent single strand DNA regions in cells treated with these agents (Yan et al., 2003; Mojas et al., 2007) also supports a futile processing model. Additional recent evidence that murine embryonic fibroblasts (MEFs) deficient in EXO1 demonstrate resistance to methylating agents also suggests that MMR-mediated excision and resynthesis is required for the cytotoxic effects of methylating agents, although EXO1 may have other functions in the induction of DNA damage responses that could also explain this observation (Klapacz et al., 2009).

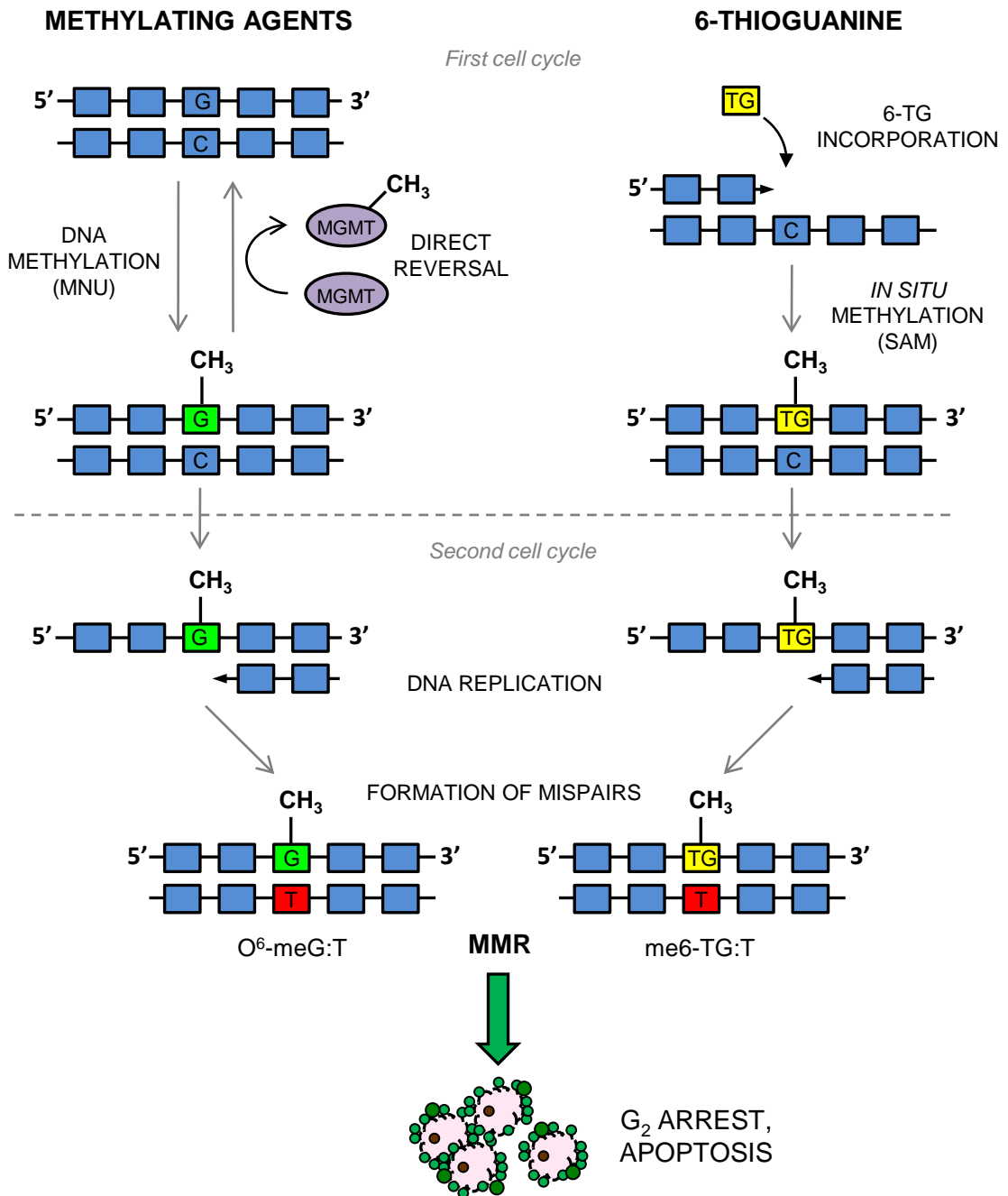


Figure 1.4. DNA mispair formation following exposure to methylating agents or 6-thioguanine.

Methylated guanine nucleotides are formed during the first cell cycle by the action of methylating agents (left). This can be directly reversed prior to DNA replication, but only in cells expressing MGMT. In the case of 6-TG (right), following intracellular metabolism, 6-TG nucleotides become incorporated into DNA by replicative polymerases. Incorporated 6-TG becomes rapidly methylated *in situ* by the methyl donor, S-adenosyl methionine (SAM). In both cases, during the following round of DNA replication, polymerase can incorrectly insert a thymine opposite the methylated lesions, resulting in O⁶-meG:T and me6-TG:T mismatches respectively, which are a substrate for MutS α binding. Subsequent processing requires functional DNA MMR, resulting in G₂ cell cycle arrest and apoptosis.

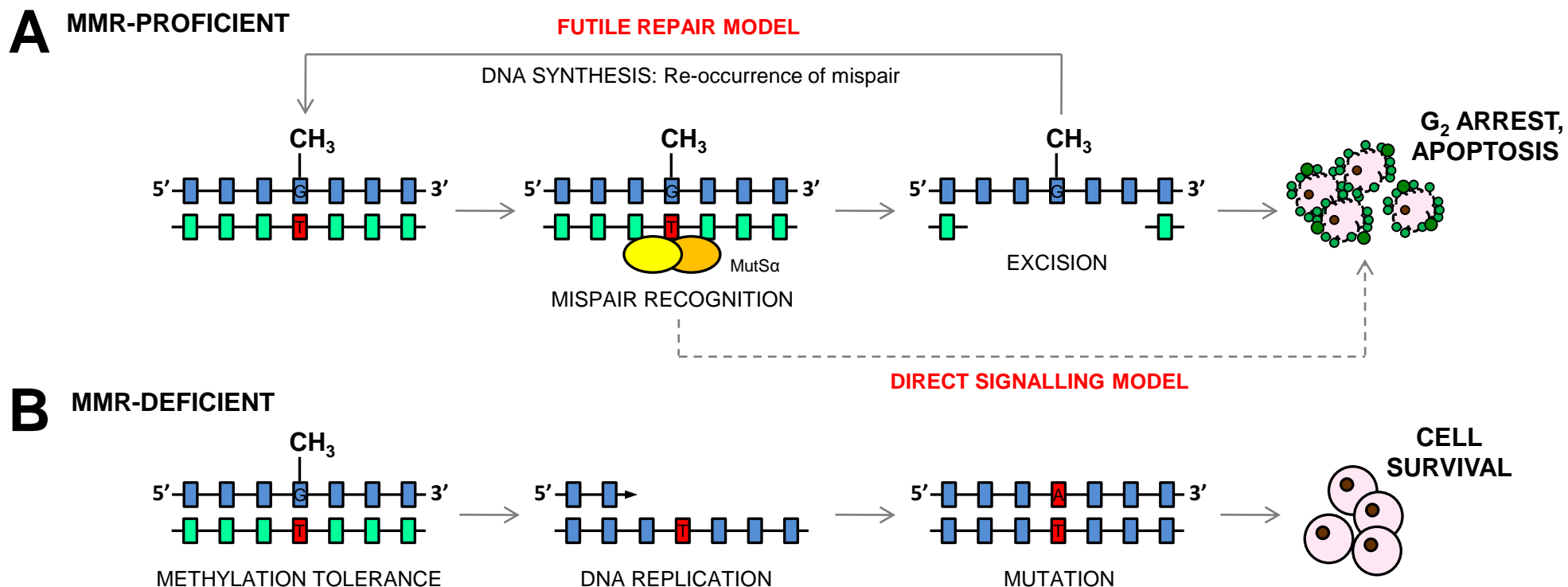


Figure 1.5. Involvement of DNA MMR in signalling cell cycle arrest/apoptosis in response to methylating agent- or 6-thioguanine-induced DNA damage.

A. Two proposed models could explain the role of DNA MMR in signalling G₂ cell cycle arrest and subsequent apoptosis. In the futile repair model (top), MutSα binds to mispaired lesions and mediates repair, however the placement of the methylated lesion in the parental DNA strand leads to re-insertion of the incorrect base, hence initiating repeated repair. Generation of aberrant repair intermediates provides the signal for cell cycle arrest and initiation of other DNA repair pathways. The direct signalling model (bottom) suggests that DNA MMR components can communicate the presence of DNA damage to mediators of the checkpoint and/or apoptosis without the requirement for lesion processing. **B.** In MMR-defective cells, there is no detection of mispaired lesions, allowing them to persist in DNA without triggering cell cycle arrest or apoptosis. Conversion of mispairs to mutations occurs at subsequent rounds of replication, therefore cells survive but demonstrate a mutator phenotype.

The alternative model, referred to as the 'direct signalling' model, suggests that MMR components are general DNA damage sensors and have the ability to signal cell cycle arrest and/or apoptosis without the requirement for futile lesion processing. In support of this model are studies which demonstrate rapid induction of damage signalling pathways following drug exposure, which are described below, as well as physical interaction between MMR components and mediators of cell cycle arrest, particularly between MSH2 and ATR (Carethers et al., 1996; Yoshioka et al., 2006; Pabla et al., 2011). Intriguing findings also in support of a direct damage signalling function of MMR components come from reports of separation of function mutations in *Msh2* and *Msh6* in murine models (Lin et al., 2004; Yang et al., 2004a). These mutations disable the mismatch repair function of the Msh2 and Msh6 proteins, however the mice remain sensitive to methylating agents, demonstrating that the ability to mediate cell death remains unaffected.

Multiple redundant pathways can signal G₂ cell cycle arrest and cell death following DNA damage; evidence suggests a number of these pathways may be activated in an MMR-dependent manner (Figure 1.6). Arrest at the G₂ checkpoint following methylating agent or 6-TG exposure is accompanied by activation of ATR (Caporali et al., 2004; Stojic et al., 2004a; Yamane et al., 2004; Yan et al., 2004; Yoshioka et al., 2006). ATR is primarily responsible for cell cycle arrest as a result of stalled replication forks (Kastan and Bartek, 2004), hence its activation in response to these agents argues in favour of the generation of aberrant repair intermediates which block replication. Concomitant with ATR activation is the appearance of nuclear foci, containing phosphorylated H2AX, RPA and other DNA repair proteins, which may represent sites of DNA damage (Stojic et al., 2004a). ATM, primarily activated in response to DSBs (Shiloh, 2006), is also activated in response to methylating agents and 6-TG (Caporali et al., 2004; Stojic et al., 2004a; Yan et al., 2004; Adamson et al., 2005). In the case of methylating agents, this has been shown to occur later than ATR activation (Caporali et al., 2004), suggesting that some repair intermediates resulting from processing of O⁶-meG:T mispairs might be converted to DSBs. Reports that MMR-proficient cell lines display a higher frequency of chromosomal aberrations and sister chromatid exchange than MMR-deficient subclones also provides evidence for the formation of DSBs (Armstrong and Galloway, 1997; Vernole et al., 2003).

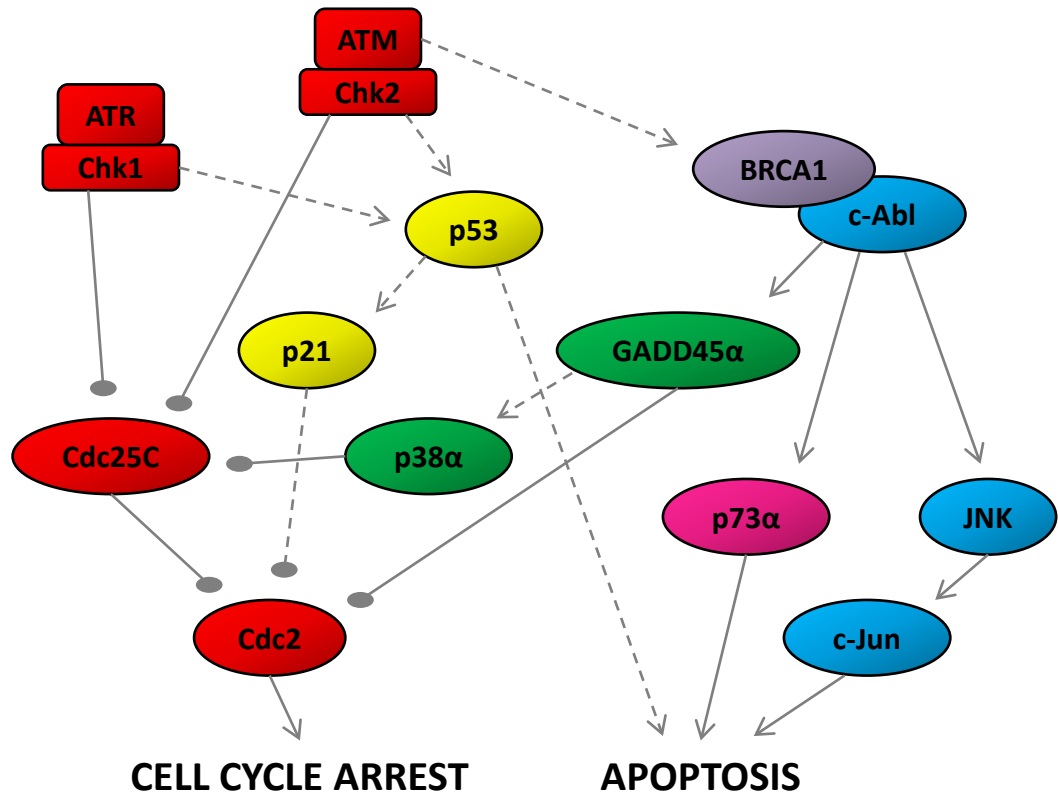


Figure 1.6. Pathways which may mediate MMR-dependent G₂ cell cycle arrest and apoptosis in response to methylating agents or 6-thioguanine.

The serine-threonine protein kinases ATR and ATM mediate the major checkpoint signalling pathway in response to DNA damage (red). Upon activation, ATR and ATM phosphorylate and activate their respective substrates Chk1 and Chk2. The activated complexes signal cell cycle arrest through phosphorylation of the Cdc25C phosphatase, leading to its inhibition via sequestration in the cytoplasm. This prevents Cdc25C from dephosphorylating Cdc2, which is required to permit progression to mitosis. ATR/Chk1 and ATM/Chk2 can also phosphorylate p53 which contributes to cell cycle arrest by transcriptional activation of p21, a direct inhibitor of Cdc2 activity (yellow). In addition, p53 can act as a transcription factor for several pro-apoptotic genes. It is unclear however, whether either of these responses occur following treatment with methylating agents or 6-TG (indicated by dashed lines) (Li et al., 2008). A pathway involving MAPK signalling could also link damage detection with apoptosis (blue). Genotoxic insult results in ATM-dependent activation of the non-receptor tyrosine kinase c-Abl, causing a MAPK signalling cascade leading to activation of Jun-N-terminal kinase (JNK), which in turn directly phosphorylates c-Jun, a transcription factor with roles in promoting apoptosis. Other investigations have demonstrated c-Abl-mediated activation of GADD45 α in response to methylation damage (green) (Li et al., 2008; Wagner et al., 2008). p38 α , also a member of the MAPK family, is activated in an MMR-dependent manner following methylating agent exposure and promotes cell cycle arrest through phosphorylation of Cdc25C (Hirose et al., 2003). It is not clear how p38 α is activated, although evidence suggests it may occur downstream of GADD45 α activation (Wagner et al., 2008). GADD45 α can also directly dephosphorylate Cdc2 to contribute to cell cycle arrest and is implicated in pro-apoptotic signalling (Li et al., 2008). p73 α (pink), also activated by c-Abl (Yuan et al., 1999), has been implicated in direct promotion of apoptosis, which is independent of G₂ arrest, following exposure to methylating agents or 6-TG (Li et al., 2008). The DNA repair protein and transcription factor, BRCA1 (purple) has recently been identified as a potential candidate in activation of c-Abl-mediated responses, through DNA MMR and ATM-dependent phosphorylation (Yamane et al., 2007).

ATR/Chk1 and ATM/Chk2 can phosphorylate and activate p53, a key transcription factor capable of promoting both cell cycle arrest and apoptosis. Although methylating agent-induced cell death occurs primarily via apoptosis (Kaina et al., 1997; Meikrantz et al., 1998), and p53 is phosphorylated and stabilised in an MMR-dependent manner (Davis et al., 1998; Duckett et al., 1999), it has been shown that p53 does not play a key role in G₂ arrest responses or apoptosis after methylating agent exposure (Li et al., 2008b).

Mitogen activated protein kinase (MAPK) signalling is another prominent pathway activated in response to cellular stress (see Figure 1.6), including exposure to methylating agents (Kim et al., 2007). Furthermore, activation in response to methylating agents appears dependent on functional MMR (Kim et al., 2007), suggesting a potential signalling pathway linking detection of O⁶-meG:T mismatches with induction of apoptosis. In addition, a direct interaction between MLH1, PMS2 and c-Abl was identified which argues in favour of a direct signalling role for the MutL α complex (Kim et al., 2007).

Recent studies have shown that a mutation in the *BRCA1* gene can almost completely abolish G₂ cell cycle arrest in response to 6-TG, causing *BRCA1* mutant cells to be more resistant than isogenic wild-type counterparts (Yamane et al., 2007). *BRCA1* can be phosphorylated by ATM, disrupting its interaction from a dormant complex with c-Abl, allowing both proteins to become active (Foray et al., 2002). Furthermore, *BRCA1* can directly interact with MSH2 and ATM (Wang et al., 2000). Taken together, this identifies *BRCA1* as a potential candidate that could bridge the gap between DNA MMR and c-Abl signalling responses.

p73 α and GADD45 α , also downstream targets of c-Abl (see Figure 1.6), are rapidly activated in an MMR-dependent manner following methylating agent exposure (Li et al., 2008b; Wagner et al., 2008). Down-regulation of GADD45 α blocked both G₂ arrest and apoptosis in response to methylating agents (Li et al., 2008b), possibly through activation of p38 α MAPK (Hirose et al., 2003), demonstrating a key role in these processes. Interestingly, down-regulation of p73 α only affected apoptosis, providing the first evidence that MMR may be able to signal an apoptotic response independently of cell cycle arrest (Li et al., 2008b). It should be noted that these same studies also report observation of single strand regions and DSBs following methylating

agent exposure (Wagner et al., 2008), hence evidence which apparently supports the direct signalling model for MMR-dependent arrest and apoptosis does not rule out MMR-mediated futile cycling, merely that it is not the trigger required to initiate damage signalling.

Taking all of the available evidence into account, it appears that a number of cellular MMR-dependent processes can signal cell cycle arrest and/or apoptosis following methylating agent or 6-TG exposure. It still remains uncertain however, exactly how detection of DNA damage results in their initiation, and ongoing studies are required to delineate this.

One of the purposes of G₂ cell cycle arrest is to allow DNA repair pathways an opportunity to repair DNA damage sustained during DNA replication, prior to the onset of mitosis (Kastan and Bartek, 2004). Given that at least some O⁶-meG:T and me6-TG:T mispairs appear to be converted into DSBs as a result of MMR-mediated processing, a likely candidate repair pathway is HRR. Consistent with this model, HRR is activated in response to methylating agents (Zhang et al., 1996) through a mechanism that is dependent on functional DNA MMR (Zhang et al., 2000). Rajesh and colleagues (2011) provided direct evidence that HRR is required in the cellular response to 6-TG-induced, and by extension methylating agent-induced DNA damage downstream of DNA MMR. Specifically, MEFs deficient in Rad51 were found to be hypersensitive to 6-TG, show an enhanced G₂ arrest and a substantial increase in chromosomal aberrations following exposure (Rajesh et al., 2011). Furthermore, this phenotype was almost completely rescued by deletion of *Mlh1*, strongly suggesting that HRR is involved in the repair of 6-TG-induced DSBs generated by DNA MMR. This is also consistent with previous findings that cells and tumours deficient in the HRR genes *BRCA1*, *BRCA2* or *XRCC3* are hypersensitive to 6-TG (Issaeva et al., 2010).

1.2.1.3. Methylation Tolerance in MMR-defective Cells

Concomitant resistance to methylating agents and 6-TG occurs in cells in which components of the DNA MMR pathway are defective (Aquilina et al., 1989; Aquilina et al., 1990; Hawn et al., 1995; Shin et al., 1998; Humbert et al., 1999). In MMR-deficient cells, O⁶-meG:T or me6-TG:T mispairs accumulate in DNA but do not trigger G₂ cell cycle arrest or apoptosis (Karran and Bignami, 1994). This phenomenon, referred to as

methylation 'tolerance', is a hallmark of MMR-defective cells and represents a mechanism by which DNA damage can be uncoupled from cell death, thus conferring a cellular survival advantage (Karran, 2001). Tolerance to DNA damage however, comes at the cost of significantly increased mutability due to uncorrected mispairs (Branch et al., 1993; Branch et al., 1995) (Figure 1.5B). This has been referred to as a 'super mutator phenotype', and is also considered a hallmark of MMR-defective cells (Karran et al., 2003). These phenotypes have clear implications for both the aetiology and treatment of DNA MMR-defective cancer, and these are discussed in the context of therapy-related leukaemia in Section 1.4.1.1.

1.2.2. 5-Fluorouracil

5-fluorouracil (5-FU) is an analogue of the nucleobase, uracil, which has a fluorine atom substituted in place of hydrogen at the 5-position of the pyrimidine ring. It is widely employed in the treatment of solid cancers, most notably colorectal cancer, as it exhibits tumour-selective toxicity (Longley et al., 2003). A number of cellular DNA repair processes have been implicated as mediators of response to 5-FU, including DNA MMR, although the extent of MMR contribution and the mechanistic details of this response remain largely unclear.

1.2.2.1. MMR and 5-FU Cytotoxicity

Because 5-FU is a structural analogue of uracil, once it has been transported into cells, it can readily participate in uracil metabolism, culminating in the generation of fraudulent DNA and RNA precursors (Longley et al., 2003), similar to 6-TG described above. Cellular metabolism of 5-FU also results in inhibition of thymidylate synthetase, causing nucleotide pool imbalances which can favour nucleotide misincorporation during replication (Longley et al., 2003).

The triphosphate of 5-FU is a good substrate for some replicative polymerases, leading to incorporation into genomic DNA (Tanaka et al., 1981). Biochemical evidence demonstrates incorporation most frequently opposite adenine (Tanaka et al., 1981), although nucleotide pool imbalance has been shown to cause misinsertion opposite guanine (Meyers et al., 2005). A number of studies have reported that cells deficient in MMR components, particularly MSH2 and MLH1, demonstrate decreased cell cycle arrest and apoptosis in response to 5-FU (Carethers et al., 1999; Tokunaga et al., 2000;

Meyers et al., 2001; Meyers et al., 2005). Furthermore, 5-FU:G mispairing is higher in MMR-defective cells, implying that loss of MMR leads to cellular tolerance of this lesion (Meyers et al., 2005). These findings are consistent with a model in which MMR-dependent recognition of 5-FU lesions is required to initiate cytotoxicity.

Unlike methylating agents and 6-TG, in which arrest occurs in the second cell cycle, MMR-dependent cell cycle arrest in response to 5-FU takes place in the first cell cycle (Meyers et al., 2005; Liu et al., 2008). This suggests MMR components detect 5-FU inserted in the daughter strand during the first round of DNA replication following treatment. Consistently, biochemical assays have demonstrated that MutS α can recognise 5-FU mispaired opposite guanine but not when paired opposite adenine (Tajima et al., 2004; Meyers et al., 2005; Fischer et al., 2007). How this affects cell cycle arrest and apoptosis however, is unclear.

Cell-free assays demonstrate that 5-FU:G mispairs can be efficiently corrected by MMR components, although it is unlikely repair would be successful *in vitro* or *in vivo* given that nucleotide pool imbalance would favour re-insertion of 5-FU (Fischer et al., 2007). Futile repair cycling leading to generation of pro-apoptotic replication intermediates and/or DSBs is therefore a possibility. Consistent with this model, DSBs (Meyers et al., 2001) and ATR activation (Liu et al., 2008) have been reported in MMR-proficient cells following 5-FU treatment. Other evidence suggests that direct signalling by MMR components to the c-Abl/p73 α /GADD45 α arrest/apoptosis pathway occurs in response to 5-FU:G mispairs, and this does not involve either ATR or ATM (Meyers et al., 2001). It is clear, as in the case of methylating agents and 6-TG, that multiple models could account for MMR-mediated cell death following 5-FU treatment, and further studies are required to delineate exact mechanisms.

As stated above, 5-FU is used in the treatment of colorectal cancer, including hereditary non-polyposis colorectal cancer (HNPCC), a condition characterised by defective DNA MMR (see Section 1.4.1.1). Similar to *in vitro* studies described above, clinical studies examining 5-FU responses in these patients do not provide a clear picture of the specific involvement of MMR. Early reports suggested that patients with defective MMR might selectively benefit from 5-FU treatment (Hemminki et al., 2000). Subsequent studies however report either no difference in response between MMR-proficient and deficient patients (Popat et al., 2005; Lamberti et al., 2007), or in some

cases, an unfavourable response in MMR-deficient patients (Ribic et al., 2003; Carethers et al., 2004; Jover et al., 2006). Prolonged exposure to 5-FU, such as would occur clinically, has been reported to result in MMR-independent cytotoxic responses involving other DNA repair pathways (Liu et al., 2008). The apparent discrepancies in the response of patients with MMR defects to 5-FU may therefore reflect the fact that the status of other DNA repair pathways were not assessed.

1.2.3. Crosslinking Agents

Crosslinking agents damage DNA by forming numerous intra and interstrand crosslinks (ICLs) between bases. These bulky lesions block DNA polymerases resulting in replication fork stalling, sustained G₂ cell cycle arrest and apoptosis. The nucleotide excision repair (NER) pathway, as well as the HRR pathway, are the primary mechanisms which respond to ICLs (Vasquez, 2010). Early studies demonstrating that MMR-defective cell lines display a low level of cisplatin resistance compared to isogenic MMR-proficient counterparts (Aebi et al., 1996; Fink et al., 1996) suggested DNA MMR was also involved.

1.2.3.1. MMR and Cisplatin Cytotoxicity

Cisplatin is one of the most effective chemotherapeutics for the treatment of testicular and ovarian cancers. This platinating agent modifies predominantly the N7-position of purine bases, giving rise to monoadducts as well as crosslinks when two purines are in close proximity. Of the numerous bulky adducts formed, 1,2-ICLs occurring between the N7 atoms of two adjacent guanine bases can be bound by MutS α with high affinity (Duckett et al., 1996; Yamada et al., 1997). Unlike 5-FU, methylating agents and 6-TG, there is no evidence to suggest that this results in subsequent MutL α recruitment and further processing (Karran, 2001). Instead, resistance to cisplatin in DNA MMR-defective cells appears to be linked to the failure of these cells to directly activate damage signalling pathways that trigger apoptosis.

Activation of c-Abl and downstream JNK kinase following cisplatin exposure is completely absent in MMR-defective cells (Nehme et al., 1997; Nehme et al., 1999). Additionally, cellular p73 α protein is increased in response to cisplatin, but only in cells which have a functional DNA MMR system (Gong et al., 1999). A direct interaction between PMS2 and p73 α has also been demonstrated following cisplatin exposure,

abrogation of which resulted in a diminished apoptotic response (Shimodaira et al., 2003). Taken together, these findings revealed the existence of an MMR-dependent apoptosis pathway which contributes to cisplatin-induced cytotoxicity. It has been suggested that this may well be the same c-Abl mediated MMR-dependent pathway reported to occur following exposure to methylating agents (Li et al., 2008b) (see Section 1.2.1.2), in which case this would support the theory that MMR components can act as general DNA damage sensors with essential roles in signalling cell cycle arrest and/or apoptosis responses, and which does not necessarily depend on lesion processing.

Whereas tolerance to methylating agents and 6-TG is accompanied by acquisition of a supermutator phenotype with implications for genomic stability, this is not observed in MMR-defective cells displaying low-level cisplatin resistance, presumably because other DNA repair pathways can efficiently process cisplatin damage (Stojic et al., 2004b). Nevertheless, cisplatin treatment can lead to the emergence/selection of MMR-deficient cell clones (Fink et al., 1998); the clinical significance of this is described in Section 1.4.1.1.

1.2.3.2. MMR and Repair of ICLs

As stated above, NER and HRR are the primary mechanisms which respond to ICLs, and both pathways cooperate in the repair of these lesions (Vasquez, 2010). Early observations that MMR-defective human cell lines demonstrated hypersensitivity to the ICL-inducing agents N-(2-chloroethyl)-N'-cyclohexyl-N-nitrosourea (CCNU) and mitomycin C (MMC) suggested that DNA MMR might also contribute to the repair of certain ICLs (Aquilina et al., 1998; Aquilina et al., 2000; Fiumicino et al., 2000). A possible mechanism has been explored in the case of CCNU.

CCNU, like many other ICL-inducing agents, induces DSBs in proliferating cells through processing involving NER proteins (De Silva et al., 2000). Studies using a PMS2-deficient cell line demonstrated that γ -H2AX foci (a sensitive indicator of DSB formation) persist in cells lacking a functional MutL α complex, and that these cells demonstrate a higher frequency of CCNU-induced chromosomal damage (Casorelli et al., 2008). This implicates active MMR in repair of CCNU-induced DSBs by HRR, possibly

through stabilisation of RAD51-containing repair intermediates, given that this protein was also inefficiently localised in PMS2-deficient cells (Casorelli et al., 2008).

Further evidence implicating MMR components in the repair of ICLs comes from the response of MMR-defective cells to psoralens, photoactivatable ICL-inducing agents (Cimino et al., 1985) which can be used to target ICLs to particular genomic sites (Liu et al., 2009). The MutS β complex plays a role in initial processing of psoralen-induced ICLs via interaction with NER proteins, leading to removal or uncoupling of these lesions (Zhang et al., 2002; Lan et al., 2004; Zhao et al., 2009). Additionally, deficiency of MSH2 renders cells hypersensitive and hypermutable in response to psoralen-induced ICLs, suggesting a role in error-free repair of these lesions (Wu et al., 2005). A mechanism has been speculated in which processing involving MutS β and NER proteins gives rise to DSBs which are channelled into HRR for efficient recombination-mediated repair (Zhang et al., 2007). Surprisingly, whereas MSH2-deficient cells are hypersensitive to psoralen, MLH1 deficiency confers resistance and inefficient induction of apoptosis by psoralen ICLs, through lack of G₂ checkpoint activation (Wu and Vasquez, 2008). It appears therefore, that DNA MMR components have distinct and unique functions in the repair of and response to psoralen and CCNU-induced ICLs, which lie outside of their defined roles in DNA MMR.

1.2.4. Ionising Radiation

Available evidence is conflicting regarding the influence of cellular MMR status on radiosensitivity. Initial studies aimed at elucidating a role for DNA MMR in response to IR demonstrated that MEFs deficient in either MSH2, MLH1 or PMS2 showed increased survival following exposure to IR compared to MMR-proficient counterparts (Fritzell et al., 1997; DeWeese et al., 1998). Subsequent studies using strictly isogenic cell lines however, show no differences in cytotoxicity, arguing against an involvement of DNA MMR in cell death induced by IR (Papouli et al., 2004).

1.2.4.1. MMR and IR-Induced Cell Cycle Checkpoint Activation

IR induces a spectrum of lesions that can cause structural damage to DNA, including single strand nicks, DSBs, cross-links, oxidative base modifications and clustered base damage. Of these, unrepaired DSBs are thought to be the main lesion associated with cell killing following exposure to IR (Martin et al., 2010). Unlike all of

the agents previously described, it has not been established whether DNA MMR components can recognise IR-induced DNA damage directly (with the possible exception of oxidative base modifications as described below). IR-induced accumulation of cells in G₂ phase of the cell cycle however, is reported to be diminished in MMR-deficient cells (described below), suggesting MMR components may have roles in cell cycle regulation following IR exposure.

Two distinct G₂ checkpoints are activated following exposure to IR (Xu et al., 2002). The first occurs early after IR (referred to as the early G₂ checkpoint), is very transient and appears to be dependent on ATM (Xu et al., 2002). Its function is to prevent cells which were in G₂ phase at the time of irradiation from progressing to mitosis. Loss of MSH2 has been reported to result in inefficient activation of this checkpoint following IR exposure (Franchitto et al., 2003). Furthermore, this checkpoint is also reported to be absent following cisplatin exposure in MMR-defective cells (Marquez et al., 2003), hence MutS α has been proposed as a trigger of early checkpoint activation in response to DNA damage.

The second checkpoint occurs several hours after irradiation and represents the accumulation of cells that had been in earlier phases of the cell cycle at the time of exposure. This checkpoint is ATM independent, and likely to be primarily activated by the ATR kinase which phosphorylates Chk1 (Xu et al., 2002). Both the early and late checkpoints involve inhibition of Cdc25C, which provides a block to progression into mitosis through failure to activate Cdc2 (see Figure 1.6).

The role of MMR proteins in the late G₂ arrest is uncertain. In one study, cell lines deficient in MLH1 demonstrated reduced late G₂ arrest compared to MMR-proficient counterparts, which resulted in hypersensitivity to IR (Davis et al., 1998). A further study by the same investigators demonstrated a similar reduced late G₂ arrest in MSH2-deficient cells, although this had no effect on cell survival (Yan et al., 2001b). Conversely, other investigations demonstrated a prolonged G₂ arrest in response to IR in MutS α -deficient cells, which had no apparent effect on cytotoxicity (Aquilina et al., 1999). The differing effects of MMR deficiency observed between studies may reflect an inability to clearly distinguish between the two G₂ checkpoints using particular experimental systems, a caveat reported for certain cell cycle checkpoint assays (Xu et al., 2002).

In addition to arrest in G₂ phase, an intra-S phase checkpoint is also activated in response to IR, but only in MMR-proficient cell lines (Brown et al., 2003). This checkpoint is also mediated by ATM activation and phosphorylation of Chk2, resulting in targeting of the Cdc25A phosphatase for degradation, meaning it can no longer dephosphorylate its substrate Cdk2, hence blocking replicating cells in S phase (Falck et al., 2001) (see Figure 1.12). MLH1 and MSH2 have been shown to interact with ATM and Chk2 respectively, and assembly of the MMR complex at damage sites has been suggested to provide a molecular scaffold that allows ATM to phosphorylate and activate Chk2, hence initiating S phase arrest (Brown et al., 2003). This, however, is contended by studies using strictly isogenic cell lines, in which no differences in phosphorylation of Chk2 (or other checkpoint kinases) are observed as a result of MMR deficiency, suggesting they may in fact be MMR-independent events (Cejka et al., 2004).

1.2.4.2. MMR and Removal of 8-Oxoguanine

Reactive oxygen species (ROS) are generated by exposure to IR as well as a variety of exogenous genotoxic agents, but also by endogenous metabolic functions such as mitochondrial respiration (Cooke et al., 2003). Intracellular ROS are highly damaging and oxidise bases in DNA and RNA as well as in the cellular dNTP pool (Cooke et al., 2003). Among several base lesions which have been identified, oxidation of guanine appears to occur most readily (Cooke et al., 2003). The resulting oxidised base, 8-oxoguanine (8-oxoG), is highly mutagenic and miscoding during DNA replication (Shibutani et al., 1991). Given this major threat to genomic stability, cells possess a number of mechanisms which prevent the accumulation of 8-oxoG in DNA, most notably the base excision repair (BER) pathway mediated by the OGG1 and MYH DNA glycosylases (Slupska et al., 1999; Boiteux and Radicella, 2000). Both *in vitro* and *in vivo* studies demonstrate that loss of MMR components results in accumulation of 8-oxoG (and other oxidative lesions) in DNA (DeWeese et al., 1998; Colussi et al., 2002; Russo et al., 2007), illustrating that DNA MMR also contributes to the control of DNA oxidation.

During DNA replication, 8-oxoG in the parental DNA strand most often directs incorporation of adenine or cytosine opposite the lesion, although guanine and thymine misincorporation can also occur (Shibutani et al., 1991). Of the possible

resulting mispairs, MutS α has been shown to bind to 8-oxoG:T and 8-oxoG:G with high affinity, but not to the 8-oxoG:C and 8-oxoG:A mispairs most likely to arise (Mazurek et al., 2002; Larson et al., 2003). Given that 8-oxoG:C and 8-oxoG:A mispairs can be efficiently repaired by BER proteins (Slupska et al., 1999; Boiteux and Radicella, 2000), a mechanism was proposed in which resynthesis following MMR-mediated excision of guanine or thymine would allow another chance for insertion of adenine or cytosine, thus generating substrates which could be addressed by BER (Larson et al., 2003).

The cellular dNTP pool also provides a source of 8-oxoG, in the form of 8-oxodGTP, which can be incorporated into daughter DNA strands by replicative polymerases (Colussi et al., 2002). The enzyme MTH1 provides protection against this by hydrolysis of 8-oxodGTP, preventing its incorporation during replication (Mo et al., 1992). Loss of either MSH2 or MLH1 results in increased levels of incorporated 8-oxodGTP *in vitro* (Colussi et al., 2002; Macpherson et al., 2005), suggesting another role of MMR may be in excision of this lesion, hence providing supplementary protection against 8-oxodGTP incorporation.

Expression of transfected hMTH1 into *Msh2*^{-/-} MEFs, as well as reducing the level of DNA 8-oxodGTP, decreases their mutator phenotype to almost wild-type levels (Russo et al., 2004). This finding implicates oxidised bases in the mutator phenotype and genomic instability of MMR-defective cells, and furthermore suggests that they could significantly contribute to carcinogenesis associated with loss of DNA MMR (described in Section 1.4.1.1).

1.3. Acute Myeloid Leukaemia

Acute myeloid leukaemia (AML) is a malignant disorder of the blood and bone marrow which arises as a result of de-regulation of haematopoiesis, the process by which the cellular components of blood are formed (Figure 1.7). It is a relatively rare cancer, with an incidence of approximately 2,300 cases annually in the UK [www.hmrn.org]. The median age of patients at diagnosis is 68 years [www.hmrn.org], hence AML is considered mainly a disease of adults, although it can present at any age.

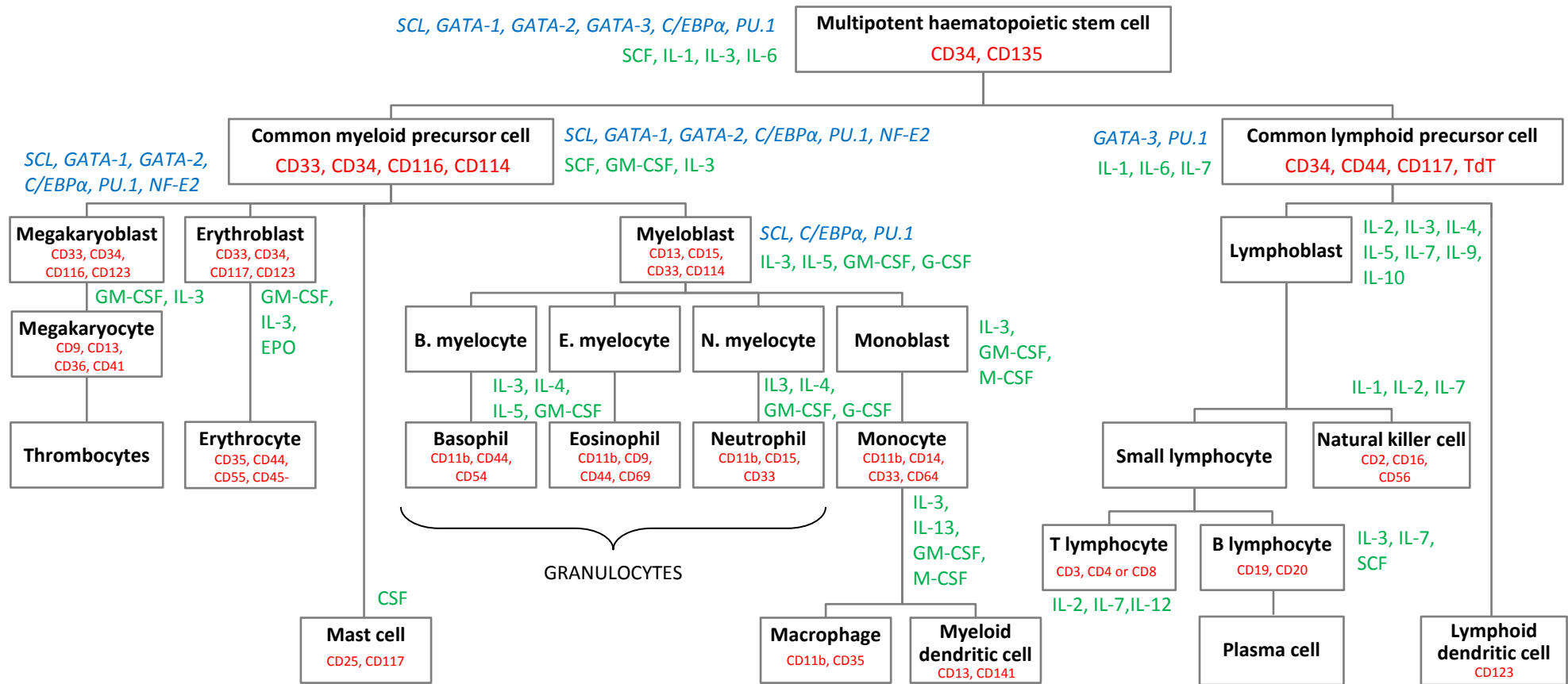


Figure 1.7. Simplified representation of human haematopoiesis.

Haematopoietic stem cells differentiate into lineage committed common myeloid and lymphoid precursors which give rise to all myeloid and lymphoid lineages respectively. In the bone marrow, precursors differentiate into immature lineage-restricted blast cells which rapidly develop into mature cells, each possessing the ability to perform specialised functions. Haematopoiesis is regulated by numerous inter- and intra-cellular signalling factors (green text) such as growth factors, cytokines and cell cycle regulatory proteins. Active genes associated with cell growth, signal transduction and transcriptional regulation during early stages of differentiation are also shown (blue text). Specific cell types express characteristic surface markers (red text) which are functional to the cell, but also allow identification and isolation of specific cell populations.

AML manifests as a differentiation block of one or more myeloid cell lineages, leading to the accumulation of immature myeloblast cells in the bone marrow and diminished production of normal circulating erythrocytes and/or leukocytes. This is the cause of the characteristic clinical symptoms of AML which include fatigue and shortness of breath, accompanied by inability to fight infection and in some cases, haemorrhaging. It is unclear within the haematopoietic cell hierarchy, which cell constitutes the target for leukaemic transformation leading to AML. Evidence suggests the multipotent haematopoietic stem cell (HSC) as the likely target, as only HSCs isolated from AML patients were able to transfer AML to immunocompromised mice, whereas more committed progenitor cells could not, despite demonstrating a leukaemic blast phenotype (Bonnet and Dick, 1997).

AML can occur *de novo*, described in this section, or as a secondary malignancy following cytotoxic therapy, termed therapy-related AML (t-AML; see Section 1.4). In rare cases, a predisposition to AML may be inherited as part of a more complex illness or syndrome.

AML has historically been classified into 8 subtypes depending on the specific cell lineage(s) affected, which is determined by morphological appearance of the myeloblasts populating the leukaemic bone marrow (Table 1.1). In addition to morphological classification, detection of certain genetic mutations (cytogenetic and molecular genetic) can also delineate specific AML subtypes. Furthermore, many commonly detected genetic mutations are prognostically relevant and, in some cases, can direct therapeutic choice.

FAB Subtype	% of AML cases	Description	Morphology
M0	<5	Acute myeloblastic leukaemia, minimally differentiated	Immature myeloblasts without definite myeloid differentiation
M1	20	Acute myeloblastic leukaemia without maturation	Immature myeloblasts, Auer rods may be present
M2	30	Acute myeloblastic leukaemia with maturation	Immature myeloblasts (more mature than M1), Auer rods often present
M3	10	Acute promyelocytic leukaemia	Hypergranular promyelocytes, bundles of Auer rods
M4 M4 ^{eo}	25	Acute myelomonocytic leukaemia	Mixture of abnormal monocytes and myeloblasts/promyelocytes (eosinophil precursors in M4 ^{eo})
M5 ^a M5 ^b	10	Acute monocytic leukaemia	M5 ^a 80% immature monoblasts M5 ^b 20% differentiated monocytes
M6	<5	Acute erythroleukaemia	Abnormal multinucleated erythroblasts, characterised by ringed sideroblasts
M7	<5	Acute megakaryoblastic leukaemia	Megakaryoblasts, often myelofibrils, increased bone marrow reticulin

Table 1.1. Overview of the French-American-British (FAB) classification system of AML (Bennett et al., 1976)

1.3.1. Genetic Mutations in AML Leukaemogenesis

Cytogenetically-detectable abnormalities are present in approximately 55% of *de novo* AML cases (Sanderson et al., 2006). Those most commonly observed are balanced translocations, which do not involve gain or loss of genetic material but cause aberrant localisation of a gene or part of a gene, usually resulting in either its de-regulated expression or generation of a novel fusion protein with oncogenic properties. The remaining 45% of AML diagnoses demonstrate a cytogenetically normal karyotype (Sanderson et al., 2006). Such patients were previously poorly characterised with respect to genetic changes, however recent improvements in molecular diagnostic techniques have led to the identification of a number of molecular genetic mutations. In both cases, affected genes are often involved directly or indirectly in haematopoiesis, aberrant (or lost) expression of which can de-regulate proliferation, differentiation and/or apoptosis of various immature myeloid cells.

The cytogenetic and molecular genetic mutations commonly detected in AML can be grouped into at least two broad classes: Class I mutations which confer a proliferative and/or survival advantage to cells, and class II mutations which primarily impair haematopoietic differentiation. It is hypothesised that AML likely follows a 'two-hit' model of leukaemogenesis, with leukaemic transformation being the consequence of collaboration between members of both classes of mutation (Deguchi and Gilliland, 2002; Kelly and Gilliland, 2002). Thus far, it has not been firmly established which mutations are primary events, and which occur later in AML development, if such an order indeed exists (Pedersen-Bjergaard et al., 2008).

The incidences of the most common class I and II mutations observed in *de novo* AML (as well as t-AML; see Section 1.4.1.2) are summarised in Table 1.2. Probable roles in leukaemogenesis are described below.

Gene	Mutation	Incidence (%) ^a	
		<i>de novo</i> AML	t-AML
Class I mutations			
<i>FLT3</i>	Internal tandem duplication	22 ^b	12 ^b
	Point mutations	6 ^b	2 ^b
<i>N-RAS, K-RAS</i>	Point mutations	10	10
Class II mutations			
<i>AML1</i>	t(8;21)(q22;q22)	7-10	5-7
	Point mutations	10 ^c	16 ^d
<i>CBFβ</i>	inv(16)(p13q22)	5-8	2-3
<i>EVI1</i>	inv(3)(q21q26)	2-3	2-3
<i>MLL</i>	Balanced rearrangements affecting 11q23	2-3 ^e	9-10 ^e
	Partial tandem duplication	6 ^b	3 ^b
<i>RARα</i>	t(15;17)(q22;q21)	5-10	2-3
<i>NPM1</i>	Point mutations	40-50	15
<i>C/EBPα</i>	Point mutations	15-20	rare
Class III mutations?			
<i>TP53</i>	Point mutations	10-15	20-25

Table 1.2. Summary of genetic mutations observed in *de novo* and therapy-related AML.

^a Incidences obtained from Pedersen-Bjergaard et al., (2007) unless otherwise stated.

^b Incidences obtained from Bacher et al., (2007).

^c Incidence obtained from Harada and Harada (2009).

^d Incidence obtained from Christiansen et al., (2004).

^e Incidences obtained from Schoch et al., (2003).

1.3.1.1. Class I Mutations

FLT3

The *fms-related tyrosine kinase 3 (FLT3)* gene on chromosome 13q12 encodes a membrane-bound receptor involved in the regulation of proliferation, differentiation and apoptosis of haematopoietic cell progenitors (Stirewalt and Radich, 2003). Internal tandem duplications (ITDs) which affect the juxtamembrane domain of the receptor are among the most prevalent mutations in *de novo* AML, being detected in around 22% of cases (Bacher et al., 2007). An additional 5-6% of cases demonstrate missense point mutations within the tyrosine kinase domain of the gene (Bacher et al., 2008). Both mutations result in a protein that is constitutively activated, promoting proliferation and decreasing apoptosis of leukaemic blasts (Gilliland and Griffin, 2002). Due to the relatively high frequency of *FLT3* mutations in AML, much concentration focuses on the development of *FLT3* inhibitors for treatment of this AML subgroup (see Section 1.3.2.3).

RAS

Mutations of *RAS* genes (*N-RAS*, *K-RAS* and *H-RAS*) are frequent observations in several cancer types. In AML, point mutations in *N-RAS* and *K-RAS* collectively are found in approximately 10% of patients (Pedersen-Bjergaard et al., 2007), with *N-RAS* codon 12 mutations being the most common (Renneville et al., 2008). These genes encode a family of guanine-nucleotide binding proteins that regulate intracellular signal transduction. Mutations abrogate intrinsic GTPase activity and thus confer constitutive activation of *RAS* proteins and their downstream effectors, which play an important role in proliferation, differentiation and apoptotic processes (Beaupre and Kurzrock, 1999).

1.3.1.2. Class II Mutations

AML1

A balanced translocation between chromosomes 8 and 21, which fuses the *RUNX1 (AML1)* gene at 21q22 with the *RUNX1T1 (ETO)* gene at 8q22, represents the most common chromosomal abnormality in AML. The resulting fusion oncoprotein consists of the N-terminal DNA-binding domain of *AML1*, a subunit of the core binding

factor (CBF) transcription activator essential for haematopoiesis (Okuda et al., 1996), and almost all of ETO, a protein thought to function as a co-repressor for a variety of transcription factors (Davis et al., 2003). AML1/ETO promiscuously targets a number of haematopoietic transcription factors including PU.1, GATA-1 and C/EBP α ; the consequence being de-regulated haematopoietic differentiation (Petrie and Zelent, 2007). AML1/ETO can be detected in HSCs from AML patients, meaning the translocation probably occurs at the stem cell level and hence represents an early event in AML leukaemogenesis (Miyamoto et al., 2000). Despite this, it is not sufficient alone to cause leukaemic transformation and subsequent mutations are required (Yuan et al., 2001).

Point mutations of the *AML1* gene are detected in approximately 10% of AML patients, with an even higher frequency detected in t-AML (see Section 1.4.1.2) (Harada and Harada, 2009). Surprisingly, numerous mutations are observed in *AML1* and are distributed throughout the full length of the gene (Harada and Harada, 2009). Despite this diversity, they can roughly be grouped into two subtypes: those affecting the N-terminal runt homology domain of the protein, and those affecting the C-terminal 'activation' domain (Harada and Harada, 2009). Investigations of the effects of forced expression of *AML1* mutants in human CD34+ cells demonstrate a pivotal role in early AML leukaemogenesis. Mutations affecting the C-terminal domain result in a block in cell differentiation and increased proliferation and self-renewal capacity, suggesting these mutations alone may be sufficient to drive AML development (Harada and Harada, 2009). N-terminal mutations on the other hand, block differentiation and slightly increase self-renewal capacity but block proliferation, hence additional mutations that induce proliferation activity appear necessary for transformation to AML (Harada and Harada, 2009). Consistently, cytogenetic abnormalities and mutations of other genes are more frequently detected in patients with N-terminal *AML1* mutations compared to patients with C-terminal mutations (Harada and Harada, 2009).

CBFB

An inversion within chromosome 16 represents another commonly reported chromosomal aberration in AML, particularly in subtype M4 (Le Beau et al., 1983). The breakpoints of the inversion lie within the *MYH11* gene at 16p13 and the *CBFB* gene at

16q22, which encodes the β unit of CBF (Liu et al., 1993). The resulting CBF β /MYH11 fusion product, like AML1/ETO causes impaired haematopoietic differentiation (Reilly, 2005). Accordingly, AMLs with t(8;21) or inv(16) are often grouped together and referred to as CBF leukaemias, given that they seem to share a common pathogenic mechanism.

EVI1

Another chromosomal inversion, which is observed in a small number of AML cases, affects the 3q26 locus, harbouring the *EVI1* gene (Testoni et al., 1999). Although the exact pathogenic mechanism of the rearrangement remains unclear, it appears that over-expression of *EVI1* as a result of the inversion also interferes with differentiation of immature progenitor cells, particularly of the erythroid and granulocytic lineages (Barjesteh van Waalwijk van Doorn-Khosrovani et al., 2003).

MLL

Balanced rearrangements, the majority of which are reciprocal translocations, involving band 11q23 occur in approximately 2% of cases of AML (Schoch et al., 2003). The 11q23 locus contains the mixed lineage leukaemia (*MLL*) gene, encoding a transcription factor with a role in regulation of haematopoietic development (Hess et al., 1997). Translocations affecting this locus result in fusion of the 5' component of *MLL* with one of a number of partner genes, creating a fusion protein with transforming properties (Ayton and Cleary, 2001). Unlike AML1/ETO described above, it has been demonstrated using murine models that certain *MLL* fusion proteins are sufficient to cause leukaemic transformation without the requirement for co-operating mutations (Forster et al., 2003).

In addition to cytogenetic rearrangements, the *MLL* gene can also undergo partial tandem duplication (PTD) spanning multiple exons, which occurs in approximately 6% of AML patients (Bacher et al., 2007). The leukaemogenic mechanism of the *MLL*-PTD is thought to be distinct from that of *MLL* fusion proteins, and may involve suppression of the remaining wild-type *MLL* allele by the mutant allele, resulting in a lack of normal *MLL* protein (Whitman et al., 2005).

RAR α

AML of subtype M3, or acute promyelocytic leukaemia (APL), is characterised by the occurrence of a specific translocation between chromosomes 15 and 17, fusing the promyelocyte gene (*PML*; 15q22) with the retinoic acid receptor alpha gene (*RAR α* ; 17q12) (de The et al., 1990; Kakizuka et al., 1991). The hybrid protein created by the fusion targets and represses transcription of a number of genes containing retinoic acid response elements, ultimately resulting in a block in myeloid differentiation, as well as conferring a survival and proliferative advantage and genetic instability on the expressing cells (Pandolfi, 2001). Like t(8;21) however, the translocation alone is not sufficient for transformation to overt leukaemia and co-operating mutations are required (Pandolfi, 2001).

NPM1

Point mutations in the nucleophosmin 1 (*NPM1*) gene have been identified in a number of haematological disorders, and are thought to occur in as many as 50% of *de novo* AML diagnoses (Pedersen-Bjergaard et al., 2007). NPM is a multi-functional shuttling protein, one role of which is regulation of p53 activity (Grisendi et al., 2006). Mutation of *NPM1* results in improper localisation of the protein (Mariano et al., 2006), and is probably an early event in AML leukaemogenesis (Thiede et al., 2006). The pathogenic mechanism however remains unclear, despite it being such a common observation in haematological malignancy (Baldus et al., 2007).

C/EBP α

The *CCAAT/enhancer binding protein alpha* (*C/EBP α*) gene encodes a member of a family of transcription regulators with an essential role in granulocyte differentiation (Zhang et al., 1997). Mutations of *C/EBP α* occur in 15-20% of cytogenetically normal AML patients (Pedersen-Bjergaard et al., 2007) and are usually associated with AML of FAB subtype M1 or M2 (Pabst and Mueller, 2009). Two types of mutation are predominantly observed: N-terminal frameshift mutations which result in a truncated form of the protein, and C-terminal insertions or deletions which affect DNA binding (Pabst et al., 2001). Interestingly, the majority of patients have more than one mutation, most commonly a combination of an N-terminal frameshift and a C-terminal insertion or deletion, usually located on different alleles (Pabst and Mueller, 2007). The role of *C/EBP α* mutation in leukaemogenesis remains to be clarified, however

microarray analysis demonstrates upregulation of genes involved in erythroid differentiation (such as *GATA-1*), as well as downregulation of genes involved in myeloid differentiation (such as *AML1* and *PU.1*) and proliferation signalling pathways (such as *FLT3*) in *C/EBPα*-mutated AML patients (Marcucci et al., 2008b).

1.3.1.3. Class III Mutations

Inactivating mutations of genes involved in regulation of cell cycle and/or apoptosis, such as the *TP53* tumour suppressor gene, possibly constitute a third class of mutation in AML leukaemogenesis (Pedersen-Bjergaard et al., 2007). Point mutations of *TP53* are detected in 10-15% of *de novo* AML patients (Pedersen-Bjergaard et al., 2007), but appear to be significantly more frequent in t-AML (see Section 1.4.1.2). Patients with *TP53* mutation are generally resistant to chemotherapy and have very short survival (Wattel et al., 1994).

1.3.1.4. Other Genetic Abnormalities

In addition to balanced chromosome rearrangements, certain deletions affecting either whole chromosomes or specific regions are often observed in AML, and also may be associated with leukaemic transformation and/or prognosis. Deletions of the long arms of chromosomes 5 and 7 (*del(5q)* and *del(7q)* respectively), or entire loss of these chromosomes are observed most frequently. As these deletions are significantly associated with t-AML, they are described below (Section 1.4.1.2). Loss of chromosomes in AML generally predicts for an adverse prognosis, especially combined loss of more than one chromosome (termed a monosomal karyotype) which is detected in approximately 10% of cases (Breems et al., 2008).

A limited number of recurrent chromosomal trisomies are also reported in AML. Although rare as sole abnormalities, these are usually observed in conjunction with other abnormalities. The most common is trisomy 8, accounting for around 10% of *de novo* AML cases (4% as a sole abnormality) (Mrozek et al., 2004). Trisomy 8 has been reported to confer a proliferative advantage to leukaemic cells, hence it may be involved in promoting clonal expansion (Yan et al., 2001a). Other recurrent trisomies reported in AML are +11, +13, +21 and +22 (Mrozek et al., 2004).

Non-coding microRNAs (miRNAs) have also recently been found to be involved in myeloid leukaemogenesis, as well as in transformation of several other human malignancies (Marcucci et al., 2009). miRNAs are 19-25 nucleotide RNA molecules which can hybridise to imprecisely complementary mRNA targets, thereby inhibiting translation of the corresponding proteins (Ambros, 2004). They are present in all cell types and, by affecting gene regulation, are likely to be involved in most biological processes (Ambros, 2004). Genome-wide miRNA-expression profiling has demonstrated that specific subtypes of AML have unique miRNA expression signatures, capable of distinguishing them from other AML subtypes (Dixon-Mclver et al., 2008; Jongen-Lavrencic et al., 2008; Li et al., 2008c). Furthermore, a growing body of evidence suggests that miRNA expression can influence clinical outcome in AML (Dixon-Mclver et al., 2008; Garzon et al., 2008; Marcucci et al., 2008a). Functional studies of miRNA expression are currently in their infancy but will likely provide important insights into AML leukaemogenesis and pathogenesis.

1.3.2. Treatment Strategies for Acute Myeloid Leukaemia

1.3.2.1. Standard Chemotherapeutic Approaches in AML

Treatment of patients with AML typically consists of at least one course of intensive myelosuppressive induction chemotherapy, followed by a consolidation phase usually involving higher drug doses, and subsequently an extended period of lower intensity maintenance therapy. Historically, the nucleoside analogue cytarabine (Ara-C; Section 1.5) has formed the backbone of all phases of AML treatment, and remains a mainstay in current AML therapeutic regimes. Ara-C is usually administered in combination with the anthracycline daunorubicin (or in some cases idarubicin), a DNA intercalating agent. Other agents sometimes used in combination with Ara-C and daunorubicin include the base analogue 6-TG and topoisomerase inhibitors (such as etoposide or topotecan).

Overall, with standard chemotherapy, approximately 60-80% of adult AML patients will achieve complete remission (CR), however many will relapse within 2 years, often with chemoresistant disease (Shiple and Butera, 2009). The treatment of relapsed and refractory AML remains a major challenge, as does the treatment of t-AML, in which the CR rate has been reported to be as low as 28% (Larson, 2007).

Relapsed, refractory and t-AML patients are also treated with Ara-C, although the low CR rate demonstrates the poor success of this approach. Novel regimens which include the use of fludarabine, mitoxantrone and G-CSF with high dose Ara-C are currently being trialled and are showing favourable early results (Robak and Wierzbowska, 2009).

Treatment of elderly AML patients (those aged 60 years and over) also currently poses a significant challenge which is due, in large part, to an inability to tolerate aggressive therapeutic regimens. Strategies such as liposomal encapsulation of Ara-C and daunorubicin, which can reduce drug-associated toxicity and decrease dosage, have showed promise in elderly *de novo* AML patients (Feldman et al., 2011).

1.3.2.2. *Alternative Nucleoside Analogues for AML Treatment*

Clofarabine (Section 1.5.4), a next generation nucleoside analogue which is licensed for the treatment of acute lymphoblastic leukaemia (ALL), is currently being trialled in patients with AML, particularly elderly patients who are unsuitable for conventional chemotherapy, and those with relapsed or refractory AML who do not typically respond well. Indications suggest that using clofarabine in combination with high dose Ara-C in relapsed/refractory AML patients (Faderl et al., 2005), or with low dose Ara-C in elderly patients (Faderl et al., 2008) is capable of achieving an improved CR rate as well as demonstrating a favourable toxicity profile.

Fludarabine (Section 1.5.4), an adenosine nucleoside analogue commonly used to treat chronic lymphocytic leukaemia (CLL), is currently being trialled for the treatment of relapsed/refractory AML (in combination with high dose Ara-C), with favourable early results being demonstrated in small scale studies (Jackson, 2004). Other nucleoside analogues also being investigated include troxacitabine and sapacitabine, both of which are similar in structure and function to Ara-C (Robak and Wierzbowska, 2009).

Certain nucleoside analogues which can act as hypomethylating agents also demonstrate efficacy in the treatment of AML. Endogenous DNA methylation occurs when a methyl group is attached to a cytosine base in a CpG dinucleotide by a DNA methyltransferase (DNMT) enzyme. This leads to remodelling of the chromatin structure thus preventing access by DNA binding proteins. DNA methylation of

promoter regions occurs often in cells and provides a mechanism by which genes can be epigenetically silenced when their expression is not required. Aberrant DNA methylation has been reported in AML and several other malignancies (Ellis et al., 2009). Azacytidine (AZA) and decitabine (DEC), like Ara-C, are nucleoside analogues of cytidine which are readily incorporated into DNA and RNA and are able to inhibit DNMTs, hence providing a block to DNA methylation. Both agents have been used in the past to treat relapsed/refractory AML, although the treatment-related toxicity was considerable (Robak and Wierzbowska, 2009). However, more recent small-scale trials have demonstrated that lower doses of AZA and DEC may be just as effective as higher doses, and furthermore are well tolerated in elderly patients (Sudan et al., 2006; Blum et al., 2007). It has been suggested that AML patients with the t(8;21) translocation may particularly benefit from the use of these agents given that one of the mechanisms by which the AML1/ETO fusion protein blocks gene expression is through aberrant recruitment of DNMTs (Petrie and Zelent, 2007). This however remains to be formally tested.

1.3.2.3. Targeted Therapies for Treatment of AML

Recent years have seen the advent of so called 'targeted therapies' which interfere with specific molecules unique to leukaemic cells, rather than targeting all dividing cells in the way traditional chemotherapeutic agents do. All-trans retinoic acid (ATRA) was the first example of targeted therapy, which revolutionised treatment of patients with APL. ATRA is a vitamin A derivative which specifically affects the function of the fusion protein encoded by the characteristic t(15;17) translocation. Disruption of the fusion protein abrogates the differentiation block and enables cells to mature along the granulocyte lineage (Raelson et al., 1996). Using ATRA in combination with standard chemotherapy can induce CR in over 90% of APL patients, with 95% of patients remaining in remission at 5 years (Hu et al., 2009).

The immunotoxin gemtuzumab ozogamycin (GO) is another example of a targeted therapy which is being trialled in the treatment of AML. GO consists of an anti-CD33 antibody conjugated to calicheamicin, a potent cytotoxic antibiotic. It binds to the CD33 antigen, which is expressed on the surface of AML cells in 80-90% of patients, following which the antibiotic is internalised and causes cytotoxic DNA DSBs (Stasi et al., 2008). GO monotherapy is approved for treatment of relapse in elderly

AML patients who are unfit for standard cytotoxic chemotherapy, and can induce CR in 26% of cases (Larson et al., 2005). GO has also shown remarkable activity in APL patients, probably owing to the high expression of CD33 on APL blasts (Estey et al., 2002; Lo-Coco et al., 2004). Combinations of GO with standard chemotherapy are still under investigation in other AML patient subgroups (Stasi et al., 2008).

Other examples of targeted therapies which are currently under trial for efficacy in AML treatment include *FLT3* inhibitors which may be effective in patients with *FLT3* mutations, and farnesyl-transferase inhibitors which can block constitutively activated Ras signalling in *RAS*-mutated AML patients. In both cases, small scale trials have showed encouraging results and larger multicentre trials are underway (Robak and Wierzbowska, 2009).

1.4. Therapy-Related Acute Myeloid Leukaemia

Therapy-related acute myeloid leukaemia (t-AML) is recognised as a specific form of AML which arises as a direct consequence of therapy (chemotherapy or radiotherapy) for a primary malignancy, or non-malignant condition in some cases. Primary disorders commonly preceding t-AML include Hodgkin lymphoma (HL), non-Hodgkin lymphoma (NHL), multiple myeloma, breast cancer, ovarian cancer and prostate cancer (Smith et al., 2003). A number of distinct subtypes of t-AML are recognised and these are associated with the nature of the therapy received for the preceding malignancy. Unlike the majority of other cancers, t-AML is considered unique in the respect that its aetiology, and the genetic events involved in disease progression, are well defined. This is especially true in the case of methylating agent-related t-AML, as described below.

Currently, t-AML is estimated to account for around 2% of AML diagnoses in the UK [www.hmrn.org], although the incidence is predicted to rise due to the increasing number of cancer survivors (Travis et al., 2006). Survival times of t-AML patients are often short, and the CR rate is as low as 28% (Larson, 2007). This is attributed to t-AML being less responsive to current forms of therapy than *de novo* AML, a complication which may be due to the underlying genetics of the condition, but may also reflect other factors, such as patient age (as t-AML patients are often elderly and hence

expected to demonstrate decreased tolerance to intensive therapy) or immunosuppression persisting following the primary disorder (Godley and Larson, 2008).

1.4.1. Methylating Agent-Related Acute Myeloid Leukaemia

The most common subtype of t-AML, accounting for 75% of cases (Yin et al., 2010), arises in patients who have been treated with chemotherapeutic regimes involving the use of DNA methylating agents. Patients who develop methylating agent-related t-AML generally show a long latency period of 3-7 years (median 5 years) from initial methylating agent exposure, often present with a preceding myelodysplastic phase and usually demonstrate a complex karyotype with loss of genetic material (Allan and Travis, 2005). Typically, multiple haematopoietic cell lineages are affected which suggests the disease may arise in a multipotent HSC or progenitor cell (Qian et al., 2010). Prognosis for methylating agent-related t-AML is particularly poor and median survival following disease presentation is typically less than 9 months (Smith et al., 2003).

1.4.1.1. DNA MMR Dysfunction and t-AML Carcinogenesis – The ‘Genomic Instability’ Model

The aetiology of methylating agent-related t-AML is particularly well defined and involves a complex series of events leading to leukaemic transformation (Figure 1.8A). Accumulating evidence suggests that, because of its interaction with chemotherapeutic methylating agents, DNA MMR may play a role in the early stages of this process.

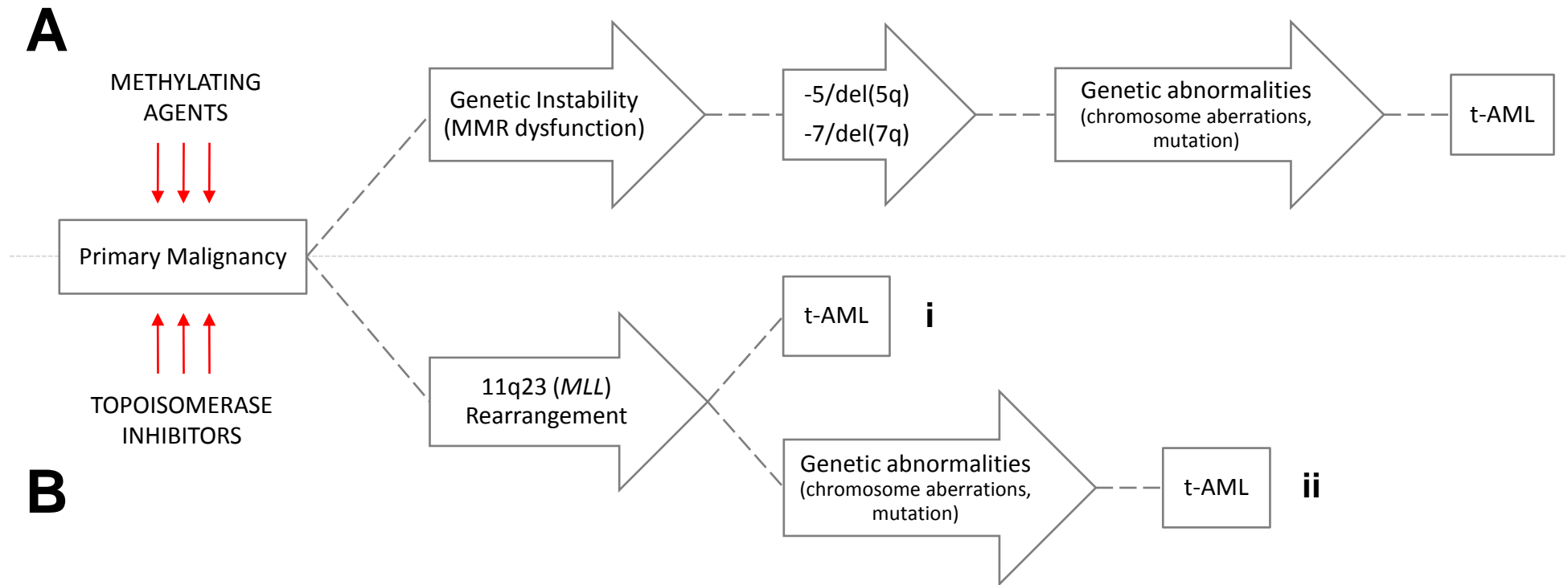


Figure 1.8. Genetic pathways in t-AML pathogenesis.

A. Exposure to chemotherapeutic methylating agents may give rise to genetic instability through dysfunction of the DNA MMR system (see Section 1.4.1.1). Downstream events include loss of all or part of chromosomes 5 and/or 7 as well as acquisition of other chromosomal and molecular genetic abnormalities, leading to eventual leukaemic transformation. Note that the exact order in which these events occur remains unclear.

B. Chemotherapy involving topoisomerase inhibitors results in balanced chromosomal rearrangements, commonly affecting the *MLL* locus at 11q23. Abnormal proteins resulting from these rearrangements may themselves be sufficient for leukaemic transformation (i). However, subsequent genetic aberrations may also be required for transformation to t-AML (ii). These events occur over a shorter timescale (2 - 3 years) compared to those occurring as a result of methylating agent exposure (3 - 7 years).

The main evidence for an association between DNA MMR and t-AML comes from several studies which have demonstrated high-grade microsatellite instability (MSI) in patients with t-AML following exposure to methylating agent chemotherapy. MSI refers to alterations in the length of short repetitive DNA sequences dispersed throughout the genome (termed microsatellites) that arises due to slippage of DNA polymerase during DNA replication. DNA MMR can repair polymerase slippage events, and biochemical evidence has directly linked the development of MSI to defective DNA MMR (Umar et al., 1994; Boyer et al., 1995). Detection of MSI is therefore considered a marker of MMR dysfunction. Figure 1.9 summarises key studies which have assessed MSI in t-AML and *de novo* AML. Consistent observation of high levels of MSI in t-AML strongly implicates loss of normal DNA MMR function in the pathogenesis of this disease. Further support is provided by the direct identification of defects affecting *MSH2* or *MLH1* expression, preferentially in t-AML patients (Horiike et al., 1999; Zhu et al., 1999; Casorelli et al., 2003). In addition, a small number of studies have investigated MSI status in relapsed and secondary AML (also included in Figure 1.9). The finding of MSI in these AML subtypes suggests they could share similarities in disease pathogenesis with t-AML (discussed further in Chapter 7). By contrast, MSI is relatively rare in *de novo* AML, suggesting MMR defects have little involvement in the aetiology of AML arising as a primary malignancy, except perhaps in the elderly (Das-Gupta et al., 2001).

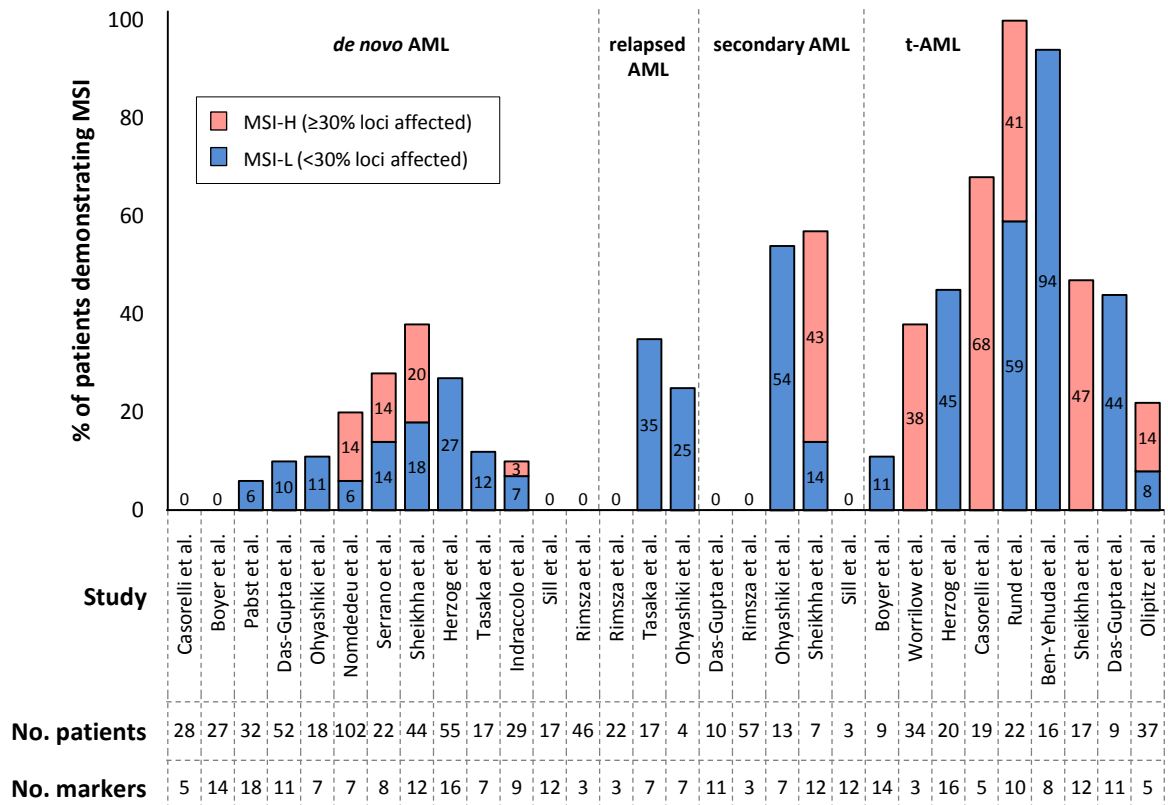


Figure 1.9. Frequency of microsatellite instability in AML.

The bar chart summarises studies reporting microsatellite instability (MSI) frequency in *de novo* AML, relapsed AML, secondary AML (defined as AML transformed from prior myelodysplastic syndrome) and t-AML. Data is presented as the percentage of study patients defined as positive for MSI according to criteria specified in each study. Where possible, data is separated according to patients demonstrating MSI-high (MSI observed at 30% or more of loci examined) and those demonstrating MSI-low (MSI at less than 30% of loci examined). Note that this data could be somewhat confounded due to the use of different microsatellite loci among the studies cited. References: Ben-Yehuda et al., 1996; Boyer et al., 1998; Casorelli et al., 2003; Das Gupta et al., 2001; Herzog et al., 2005; Indraccolo et al., 1999; Nomdedeu et al., 2005; Ohyashiki et al., 1996; Olipitz et al., 2002; Pabst et al., 1996; Rimza et al., 2000; Rund et al., 2005; Serrano et al., 2008; Sheikhha et al., 2002; Sill et al., 1996; Tasaka et al., 1997; Worrillow et al., 2003.

Predicted models for the role of DNA MMR in methylating agent-related t-AML development are shown in Figure 1.10. As described in Section 1.2.1.3, dysfunction of DNA MMR represents a mechanism by which malignant cells could evade the cytotoxic effects of methylating agent chemotherapy. One possibility therefore, is that chemotherapeutic agents themselves cause abrogation of DNA MMR function, giving rise to a cell clone that can survive treatment. This has been demonstrated to occur in response to cisplatin chemotherapy for ovarian cancer (Fink et al., 1998; Samimi et al., 2000). Alternatively, a pre-existing MMR-defective myeloid cell clone could be enriched during chemotherapy. In either case, positive selection during further rounds of chemotherapy would promote the emergence of an MMR-deficient population (Allan and Travis, 2005). This has been shown to occur following exposure to the chemotherapeutic methylating agent temozolomide using a murine model of t-AML (Reese et al., 2003) and has also been demonstrated *in vivo* in ovarian cancer patients treated with cisplatin (Fink et al., 1997; Samimi et al., 2000).

MMR deficiency itself is not sufficient for leukaemic transformation (Reese et al., 2003). One consequence of DNA MMR dysfunction however, is acquisition of a mutator phenotype as described in Section 1.2.1.3. A mutator phenotype is presumed to have genome-wide consequences, increasing the likelihood of additional transforming mutations which contribute to leukaemic transformation (hence the model of t-AML carcinogenesis as a result of DNA MMR loss is often referred to as the 'genomic instability' model (Allan and Travis, 2005)). Furthermore, as well as demonstrating genomic instability and a mutator phenotype, the survival advantage also afforded to MMR-defective cells may allow avoidance of apoptosis, leading to an expanded cell clone susceptible to tumourigenic mutation (Fishel, 2001).

Dysfunction of DNA MMR is not unique to t-AML and has been identified in a number of other malignancies such as HNPCC, in which heritable germline mutations in MMR genes (most commonly *MSH2* and *MLH1* (Peltomaki, 2003)) constitute a pre-disposing factor for development of cancer, often at a young age. Sporadic cancers in which somatic MMR dysfunction is observed include breast, skin, lung, prostate and bladder cancers, although its role is not well understood in many cases (Peltomaki, 2003).

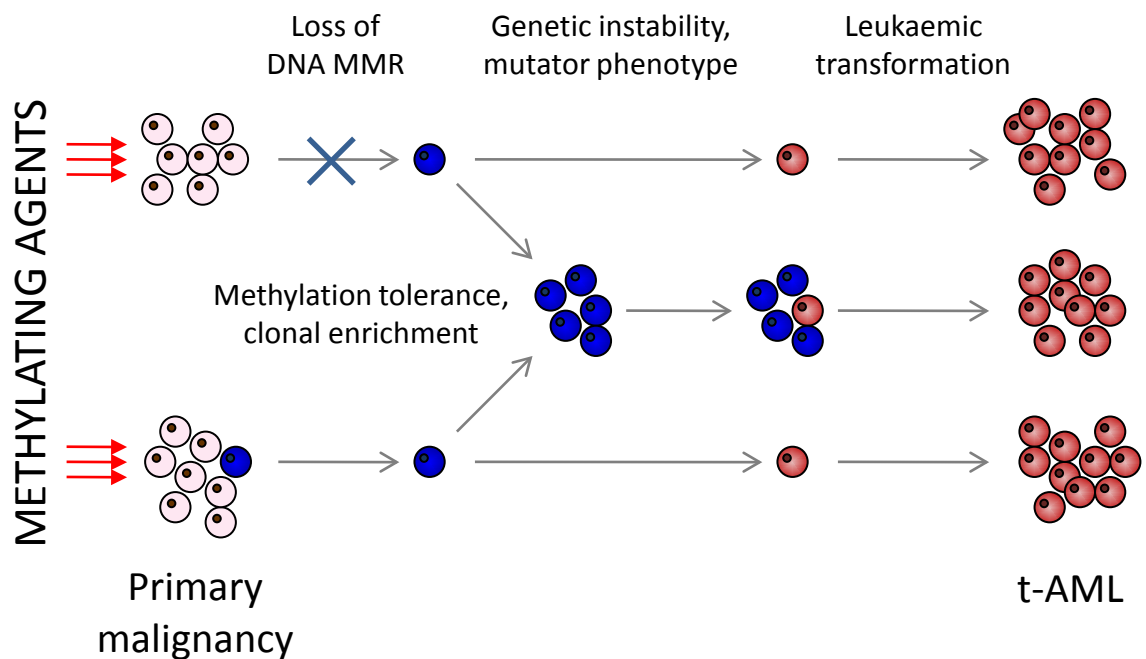


Figure 1.10. DNA MMR loss in methylating agent-related t-AML carcinogenesis.

Treatment of a primary malignancy with methylating agents (or other chemotherapeutic agents known to interact with DNA MMR) may promote generation of (top pathway), or emergence of a pre-existing (bottom pathway) MMR-defective cell clone. Loss of MMR may also confer tolerance to the cytotoxic effect of methylating agents and allow avoidance of apoptosis, leading to clonal enrichment (middle pathway). In each case, MMR loss results in genetic instability and a mutator phenotype, increasing the possibility of subsequent genetic aberrations leading to eventual leukaemic transformation. Note that only one mutational event is depicted prior to leukaemic transformation, however multiple events are likely required. Adapted from Allan and Travis (2005).

1.4.1.2. Cooperating Genetic Aberrations in t-AML Aetiology

A number of mutational events are probably required for eventual transformation to t-AML, consistent with the long latency period associated with this disease. Of particular significance are -5/del(5q) and -7/del(7q). Such abnormalities, when grouped together, are observed in more than 80% of methylating agent-related t-AML cases (Smith et al., 2003). Del(5q) is the most common abnormality, and it is believed that the commonly deleted region (5q31-33) contains at least one leukaemia-specific tumour suppressor gene (TSG) (Qian et al., 2010). Attempts to elucidate the identity of TSGs on 5q has proved challenging, although some candidates include the transcriptional regulator early growth response 1 (*EGR1*) (Joslin et al., 2007), the adenomatous polyposis coli (*APC*) gene (Qian et al., 2008) and the gene encoding alpha-catenin (*CTNNA1*) (Liu et al., 2007). Similarly, it is likely that the commonly deleted region on chromosome 7 (7q22-31) harbours a TSG (Le Beau et al., 1996), although candidates have so far remained elusive.

As in *de novo* AML, a growing body of evidence suggests that point mutations in genes responsible for regulation of haematopoiesis may be involved in the progression and pathogenesis of methylating agent-related t-AML. Interestingly, although the spectrum of observed molecular mutations is similar, many of the mutations common in *de novo* AML, such as mutations within *FLT3*, *NPM1* and *C/EBP α* , are rare observations in methylating agent-related t-AML (see Table 1.2) (Side et al., 2004; Christiansen et al., 2005; Kayser et al., 2011). Conversely, mutations affecting *AML1* or *TP53* appear to be more common in therapy-related disease than *de novo* AML and are reported to be significantly associated with -7/del(7q) and -5/del(5q) respectively (Horiike et al., 1999; Christiansen et al., 2001; Harada et al., 2003; Christiansen et al., 2004; Side et al., 2004; Pedersen-Bjergaard et al., 2008).

1.4.1.3. Deregulation of Other DNA Repair Pathways

Accumulating evidence suggests that MSI-related abrogation of other key DNA repair genes, in particular those involved in the HRR pathway, may contribute to t-AML leukaemogenesis. MSI occurring within the coding region of the *MRE11* gene (a component of the MRE11/RAD50/NBS1 (MRN) complex), resulting in aberrant splicing, has been reported in MMR-defective cell lines (Ham et al., 2006) and in a small subset

of t-AML patients (Casorelli et al., 2003), as well as in other cancers displaying MSI, including colorectal, gastric, and endometrial cancer (Giannini et al., 2002; Giannini et al., 2004; Ottini et al., 2004). Furthermore, Worrillow and Allan (2006) demonstrated de-regulation of the expression of *Mre11* (with concurrent deregulation of a number of other HRR genes) in *Msh2*-deficient murine ES cells. These findings suggest a model whereby de-regulation of HRR occurs as a consequence of DNA MMR loss, and this is predicted to contribute to genomic instability and t-AML carcinogenesis (Worrillow and Allan, 2006). These observations are consistent with DNA MMR as a negative regulator of HRR, as described in Section 1.1.2.1.

Similarly, MSI affecting a coding microsatellite within the *FANCD2* gene has recently been reported in t-AML patients and in leukaemic cell lines displaying MSI (Offman et al., 2005). The *FANCD2* gene product is a member of the Fanconi Anaemia complementation group of proteins, and has a probable role in HRR (Taniguchi et al., 2002; Thompson and Hinz, 2009), providing further evidence that this pathway is a target for de-regulation following DNA MMR loss.

1.4.2. DNA Topoisomerase Inhibitor-Related Acute Myeloid Leukaemia

The second major subtype of t-AML (accounting for 20-30% of t-AML cases (Rowley and Olney, 2002)) arises following treatment with chemotherapeutic inhibitors of DNA topoisomerase enzymes; such inhibitors include etoposide and mitoxantrone. Compared to methylating agent-related t-AML, patients who develop topoisomerase inhibitor-related t-AML are generally younger, have a shorter latency period (2-3 years) and rarely present with MDS (Allan and Travis, 2005). Prognosis is also generally more favourable, with response rates similar to patients with *de novo* AML (Godley and Larson, 2008).

Almost all cases of topoisomerase inhibitor-related t-AML present with balanced translocations, most commonly involving 11q23 (affecting *MLL*) (Rowley and Olney, 2002). Other abnormalities include t(8;21) (affecting *AML1*), t(15;17) (affecting *RAR α*) and inv(16) (affecting *CBF β*) (Rowley and Olney, 2002). The mechanism of formation of these abnormalities has been directly linked to the action of DNA topoisomerase inhibitors (Libura et al., 2005). Topoisomerase enzymes uncoil DNA, via generation of transient DSBs, to enable DNA replication or transcription (Wang, 2002).

Topoisomerase inhibitors trap the enzymes before re-ligation, thus generating DSBs which have the potential to participate in translocations (Richardson and Jasin, 2000).

It is thought that translocations are an early event in topoisomerase inhibitor-related t-AML carcinogenesis (Figure 1.8B), and some may even be sufficient alone to cause leukaemic transformation (Allan and Travis, 2005). For example, in the case of 11q23 rearrangements, some of the resulting MLL fusion proteins are sufficient to cause leukaemia in mouse models (Forster et al., 2003). In other cases, however, it is likely that the acquisition of additional genetic alterations is required for complete transformation to t-AML (Yuan et al., 2001).

1.4.3. Therapy-Related Acute Myeloid Leukaemia Following Radiotherapy

Certain investigations have identified radiotherapy as a risk factor for development of t-AML, particularly when used as a pre-conditioning treatment for autologous stem cell transplant (Krishnan et al., 2000; Pedersen-Bjergaard et al., 2000). It is difficult to determine however, to what extent t-AML development can be attributed to radiation alone given that it is often administered in combination with chemotherapeutic regimes involving methylating agents or topoisomerase inhibitors (Smith et al., 2003). Furthermore, in the case of stem cell transplant, chemotherapy for the malignancy necessitating transplant may also influence outcome (Hake et al., 2007).

Radiotherapy (ionising radiation) causes DNA damage in the form of DSBs (as well as other less cytotoxic forms of DNA damage), hence it is conceivable that exposure would increase the likelihood of genetic aberrations (for example, chromosomal deletions or translocations) which could contribute to leukaemic transformation. Consistently, t-AML has been observed in patients who received radiotherapy alone (Kantarjian et al., 1986; Krishnan et al., 2000; Smith et al., 2003; Christiansen et al., 2005).

Overall, no specific clinical or cytogenetic differences appear to separate t-AML following radiotherapy from chemotherapy-related t-AML (Smith et al., 2003). Similarly, no specific molecular genetic abnormalities have been significantly associated with t-AML following radiotherapy, with the potential exception of *FLT3*

mutations, reported by a single study, although the clinical significance remains unknown (Christiansen et al., 2005).

1.4.4. Therapy-Related Acute Myeloid Leukaemia Following Organ Transplantation

In addition to cancer patients, t-AML has been observed in patients who have received solid organ transplants, with an aetiology associated with the use of immunosuppressive therapies administered to minimise organ rejection, such as azathioprine (Arnold et al., 1999; Offman et al., 2004).

Azathioprine is a thiopurine prodrug, related to 6-TG. As described in Section 1.2.1.2, the DNA MMR system plays an important role in mediating the cytotoxicity of these drugs, via interaction with thiopurine nucleotides incorporated into DNA (Waters and Swann, 1997). Given this similarity between azathioprine and methylating agents with regards to interactions with DNA MMR, it is probable that t-AML following organ transplantation is closely related, if not identical, to methylating agent-related t-AML. Frequent observation of loss of all or part of chromosomes 5 and 7 in transplant-related t-AML (Offman et al., 2004) is also consistent with this notion.

1.4.5. Atypical Therapy-Related Acute Myeloid Leukaemia

Although the vast majority of t-AML cases can be classified into one of the subtypes described above, a small number of clinically atypical cases are reported which do not appear to associate with any specific type of previous therapy (Pedersen-Bjergaard et al., 2007). Little is known about the molecular biology of these leukaemias, however a normal karyotype is commonly observed, as are mutations affecting the RTK/RAS-BRAF signalling pathway (Christiansen et al., 2005). It has been suggested that these leukaemias may be considered identical to *de novo* AML with a normal karyotype (Pedersen-Bjergaard et al., 2007). It is therefore possible that AML observed in these patients is in fact a *de novo* disease representing a second primary cancer, rather than a therapy-induced secondary disorder.

1.4.6. Genetic Predisposition to Therapy-Related Acute Myeloid Leukaemia

The major risk factor for t-AML is high-dose chemotherapy (or radiotherapy), however risk is variable and not all patients exposed to leukaemogenic therapy will

develop t-AML. Inherent differences in drug response exist between individuals due to genetic variability in enzymes that metabolise chemotherapeutic agents and those that repair drug-induced DNA damage, some of which have been identified as potential modifiers of t-AML susceptibility (summarised in Table 1.3).

Metabolism of chemotherapeutic agents in humans is mediated by two groups of enzymes. Phase I enzymes, including the cytochrome p450 (CYP) enzymes, activate substrates into electrophilic intermediates, whereas phase II enzymes, including glutathione S-transferase (GST) and NAD(P)H:quinone oxoreductase 1 (NQO1), function to inactivate genotoxic substrates.

A large number of single nucleotide polymorphisms (SNPs) have been identified in genes encoding CYP enzymes, several of which have been studied in t-AML, although the majority do not appear to be significantly associated with development of the disease (Seedhouse and Russell, 2007). Of potential interest is an A>G polymorphism in the promoter region of the *CYP3A4* gene (located 293bp upstream of the transcription start site (Rebbeck et al., 1998)) which has been proposed to protect against t-AML development, particularly following treatment with topoisomerase II inhibitors (Rund et al., 2005). It is postulated that the variant (G) allele may modify the rate of metabolism and reduce the risk of DNA damage associated with these agents (Felix et al., 1998), however larger studies are required to confirm this hypothesis.

Homozygous deletion polymorphisms have been identified in the genes encoding phase II GST enzymes (Seidegard et al., 1988; Pemble et al., 1994). These constitutional deletions result in absence of functional protein, with the apparent consequence being a higher level of DNA damage (Wiencke et al., 1995). As in the case of the CYP enzymes, the majority do not demonstrate a significant association with t-AML, however one study did report a significant increase in the likelihood of developing t-AML in *GSTT1*-null Caucasians (Sasai et al., 1999). Given that approximately 30-40% of Caucasians are thought to be *GSTT1*-null (Pemble et al., 1994), this also may warrant further investigation. In another of the GST enzymes, *GSTP1*, a common G>A polymorphism at codon 105 affecting protein activity has also been significantly associated with t-AML development in a substrate-specific manner (Allan et al., 2001).

Gene	Variant /SNP	Patient Cohort	Odds Ratio (95% CI ^a) of t-AML	Study
Phase I metabolising enzymes				
<i>CYP3A4</i>	A>G 293bp upstream of transcription start site	44 t-AML, 134 controls	Not given. Variant allele under-represented in t-AML (P<0.025)	Rund et al., 2005
Phase II metabolising enzymes				
<i>GSTT1</i>	Null	18 t-AML, 43 controls	4.62 (1.48-14.4)	Sasai et al., 1999
<i>GSTP1</i>	G>A polymorphism affecting codon 105 (Ile105Val)	89 t-AML, 1022 controls	Any chemotherapy 2.66 (1.39-5.09) Known GSTP1 substrate 4.34 (1.43-13.2)	Allan et al., 2001
<i>NQO1</i>	C609T (Pro187Ser)	58 t-AML, 150 controls	Heterozygote 0.98 (0.28-1.68) Homozygote 2.62 (2.16-3.08)	Naoe et al., 2000
Folate metabolism				
<i>MTHFR</i>	C677T A1298C	81 t-AML, 64 controls	15.71 (1.63-151.07) 5.5 (1.06-28.42)	Guillem et al., 2007

Table 1.3. Genetic polymorphisms reported to modify risk of t-AML (continued on next page).

^a CI, confidence interval.

Gene	Variant /SNP	Patient Cohort	Odds Ratio (95% CI ^a) of t-AML	Study
DNA mismatch repair				
<i>MSH2</i>	-6 exon 13 T>C (splice acceptor site)	91 t-AML, 837 controls	4.02 (1.4-11.37)	Worrillow et al., 2003
<i>MLH1</i>	G>A 93bp upstream of transcription start site	133 t-AML, 1177 controls	5.31 (1.4-20.15)	Worrillow et al., 2008
Homologous recombination repair				
<i>RAD51</i>	G135C (within 5'-UTR)	51 t-AML, 186 controls	2.66 (1.17-6.02)	Seedhouse et al., 2004
Nucleotide excision repair				
<i>ERCC2</i>	Lys751Gln	41 t-AML, 729 controls	2.22 (1.04-4.74)	Allan et al., 2004
Base excision repair				
<i>XRCC1</i>	Arg399Gln	34 t-AML, 178 controls	0.44 (0.20-0.93)	Seedhouse et al., 2002

Table 1.3. Genetic polymorphisms reported to modify risk of t-AML (continued from previous page).

^a CI, confidence interval.

NQO1 is also a phase II enzyme which functions to prevent the generation of damaging ROS during detoxification processes (Seedhouse and Russell, 2007). A common polymorphism in the *NQO1* gene (C609T substitution resulting in a proline to serine change at codon 187 (Traver et al., 1992)) which reduces protein activity has been significantly associated with t-AML, particularly following methylating agent chemotherapy (Naoe et al., 2000). It is believed that people carrying the polymorphism are at increased risk of telomere shortening and oxidative stress as a result of chemotherapeutic exposure, leading to genetic instability (Fern et al., 2004).

Another genetic variant which has been significantly associated with development of t-AML exists in the gene encoding methylenetetrahydrofolate reductase (MTHFR), a member of the folate metabolism pathway. Two SNPs within the gene (C677T and A1298C) have been reported to confer increased risk of t-AML following treatment of primary breast cancer with the antimetabolite 5-FU, although the cellular mechanisms underlying this association are unclear (Guillem et al., 2007).

Given the high rate of MSI in t-AML, particularly in methylating agent-related disease, there has been a lot of interest in whether variations in genes encoding components of DNA repair pathways could be associated with increased risk of t-AML development. Mutations causing loss of MMR function (commonly involving *MSH2* and *MLH1* genes) are known to be a susceptibility factor for HNPCC, although these mutations do not seem to be common somatic events in t-AML (Sheikhha et al., 2002). There are however, reports of genetic variants in certain MMR genes which may predispose individuals to t-AML. A T>C SNP has been identified in a splice acceptor site within the *MSH2* gene (-6 exon 13) which appears to be significantly associated with t-AML development following methylating agent chemotherapy (Worrillow et al., 2003). Similarly a G>A SNP within the promoter of *MLH1* (93bp upstream from transcription start site) has been reported in a high number (75%) of patients who received methylating chemotherapy for HL (Worrillow et al., 2008). Although the functional significance of these polymorphisms is unknown, one possibility is that they result in a reduction in the levels of the respective protein, conferring tolerance to methylating agent chemotherapy and concurrent susceptibility to t-AML development. Consistent with this, Claij and te Riele (2002) reported that murine ES cells expressing a reduced

level of Msh2 protein are tolerant to the cytotoxic effects, but highly sensitive to the mutagenic effects of methylating agents *in vitro*.

Variants within genes involved in the HRR pathway have also been associated with an increased risk of t-AML development in some studies. For example, a G>C substitution within the 5' untranslated region of the *RAD51* gene (G135C) has been shown to be significantly over-represented in t-AML patients compared to normal controls (Seedhouse et al., 2004). *RAD51* is one of the central proteins in the HRR pathway, and is essential in the maintenance of genetic stability (Sonoda et al., 1998). The polymorphism significantly enhances promoter activity leading to increased levels of *RAD51* mRNA (Hasselbach et al., 2005), and is postulated to have a dominant negative effect on initiation of HRR (Seedhouse and Russell, 2007). This finding, in combination with the reports of MSI within the *MRE11* gene in t-AML patients (described in Section 1.4.1.3), further suggest HRR de-regulation as a likely factor in t-AML pathogenesis.

Polymorphic variants within other DNA repair genes, such as *ERCC2 (XPD)*, which is involved in NER, and *XRCC1*, a component of the BER pathway, have also been associated with risk of t-AML (Seedhouse et al., 2002; Allan et al., 2004). The latter, which carries a SNP within the coding region of the gene (*XRCC1*-Arg399Gln), appears to protect against t-AML carcinogenesis, possibly because the variant allele results in reduced BER capacity and might drive damaged cells towards apoptosis rather than attempted repair (Seedhouse et al., 2002).

1.5. Cytarabine (Ara-C)

Ara-C is a mainstay of treatment for AML, as described in Section 1.3.2.1. This section focuses on the structure of Ara-C, the current understanding of the cytotoxic mechanism of the drug, and the factors thought to be associated with resistance to Ara-C chemotherapy. In addition, some other therapeutic nucleoside analogues which share mechanistic similarities with Ara-C are also described.

1.5.1. Structure of Ara-C

Ara-C belongs to a class of compounds known as nucleoside analogues, so-called due to their structural and/or functional resemblance to normal DNA precursor nucleosides. Ara-C is a pyrimidine nucleoside analogue bearing structural resemblance to deoxycytidine, and is distinguished by the presence of a hydroxyl group in β -D-configuration on the 2'-carbon of the deoxyribose ring of the drug (Figure 1.11). Crystallographic studies with free nucleoside reveal that the presence of the hydroxyl group does not significantly alter the conformation of Ara-C from deoxycytidine (Sundaralingam, 1975).

1.5.2. Cytotoxic Mechanisms of Ara-C

1.5.2.1. Incorporation into Replicating DNA Leading to Chain Termination

A prerequisite for the cytotoxicity of Ara-C is penetrance of the drug into cells and subsequent conversion to Ara-C triphosphate (Ara-CTP) (Figure 1.11). The cytotoxic mechanism of Ara-CTP is multifaceted but is understood primarily to involve fraudulent incorporation into replicating DNA (due to its structural similarity to dCTP) during S phase of the cell cycle, resulting in chain termination.

DNA replication in eukaryotic cells requires three DNA polymerases: DNA polymerase α (pol α), DNA polymerase δ (pol δ) and DNA polymerase ϵ (pol ϵ). Primase, which is tightly associated with pol α , synthesises short RNA primers at replication origins which are then extended by pol α . Following limited DNA synthesis by pol α , a switch occurs to processive DNA synthesis by pol ϵ (leading strand) or pol δ (lagging strand) (for a recent review, see (Pavlov and Shcherbakova, 2010). Molecular analyses demonstrate that Ara-CTP is a substrate for DNA pol α and can be incorporated in place of dCTP during DNA synthesis (Perrino and Mekosh, 1992; Gandhi et al., 1997; Richardson et al., 2004). When incorporated, the hydroxyl group on the 2'-carbon of the deoxyribose ring of Ara-C causes major conformational perturbations of DNA at the site of incorporation (Gao et al., 1991; Schweitzer et al., 1994) which is proposed to hinder binding of pol α , hence inhibiting further chain elongation (Perrino and Mekosh, 1992; Gandhi et al., 1997). Ara-CTP can also inhibit activity of the other major replicative polymerases, pol δ (Han et al., 2000; Jiang et al., 2000) and pol ϵ (Huang et al., 1991), although the effects are less pronounced.

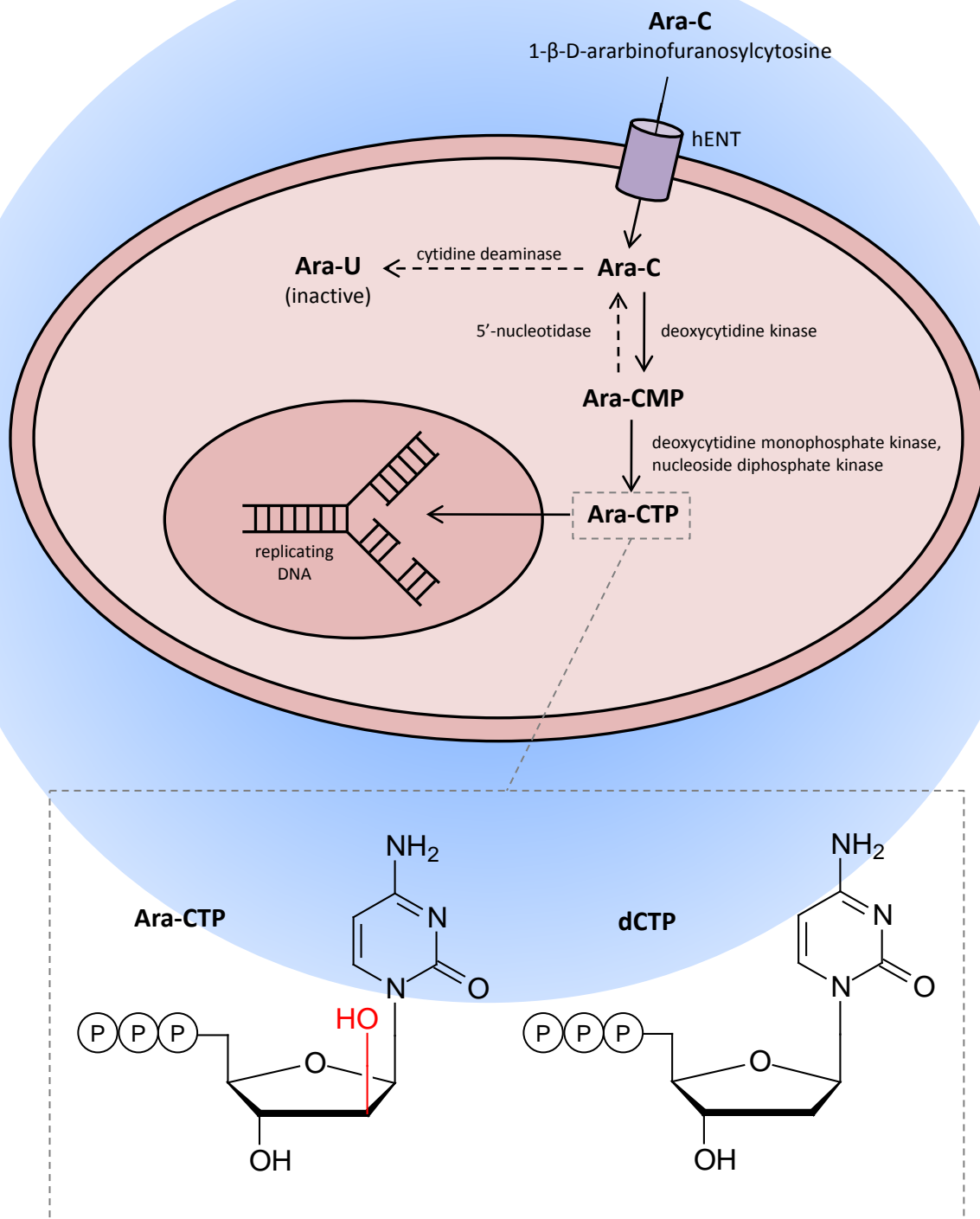


Figure 1.11. Uptake and intracellular metabolism of cytarabine.

Interaction of cytarabine (Ara-C; 1-β-D-arabinofuranosylcytosine) with specialised membrane-bound nucleoside transporters is required for penetration of Ara-C into cells. The human equilibrative nucleoside transporter I (hENT1) is the primary transporter responsible for cellular uptake of Ara-C (Wiley et al., 1985). Once inside cells, the enzyme deoxycytidine kinase phosphorylates Ara-C, giving rise to Ara-C monophosphate (Ara-CMP), after which further phosphorylation events mediated by deoxycytidine monophosphate kinase and nucleoside diphosphate kinase result in Ara-CTP (Matsuda and Sasaki, 2004) which can enter the nucleus and interfere with DNA replication. Inset shows the structure of Ara-CTP, compared to the normal deoxynucleoside triphosphate, dCTP (substituted hydroxyl group is shown in red).

The incorporation of Ara-C at 3'-terminal positions in DNA was correlated with reduced clonogenic survival in early studies (Kufe et al., 1980; Major et al., 1981), however the exact mechanisms by which this chain termination mediates cell death still remain uncertain. Ara-C-induced stalled replication forks lead to activation of an intra-S phase checkpoint which results in S-phase cell cycle arrest (Shi et al., 2001; Mesa et al., 2005) (Figure 1.12A). One of the consequences of this may be to permit attempted removal of Ara-C lesions to allow DNA replication to continue. Studies generally suggest that the exonuclease activities associated with replicative DNA polymerases are inefficient at removal of Ara-C from 3'-termini (Huang et al., 1991; Perrino et al., 1999). Unassociated 3'→5' exonucleases capable of excision of Ara-C in template assays however, have been identified (Perrino et al., 1994; Skalski et al., 2000). Additionally, the human APE1 endonuclease, whose major function is excision of damage during BER (Wilson and Barsky, 2001), has also been shown to have exonuclease activity towards nucleoside analogues, however its affinity for Ara-C was low (Chou et al., 2000).

It has recently been suggested that DSBs form as a result of unresolved stalled replication forks (Ewald et al., 2008b). Consistent with this model, the appearance of chromosome aberrations (Jones et al., 1976; Sekizawa et al., 2007), as well as phosphorylation of γ -H2AX and localisation of ATM and the MRN complex (Ewald et al., 2008a), also suggests the formation of DSBs in response to Ara-C. These proteins may recruit other repair pathways, such as HRR, providing an opportunity to rescue the replication fork (Figure 1.12B).

Ara-C initiates cells to die by apoptosis (Gunji et al., 1991; Bullock et al., 1995), which appears to be dependent on functional c-Abl (Huang et al., 1997), a tyrosine kinase which mediates apoptosis through p73 (Yuan et al., 1999). Failure of repair pathways to recover the replication fork represents the likely apoptotic signal (Roos and Kaina, 2006), which could be mediated by ATM given that it can activate c-Abl (Baskaran et al., 1997; Shafman et al., 1997) (Figure 1.12B), as well as other cell death signalling proteins.

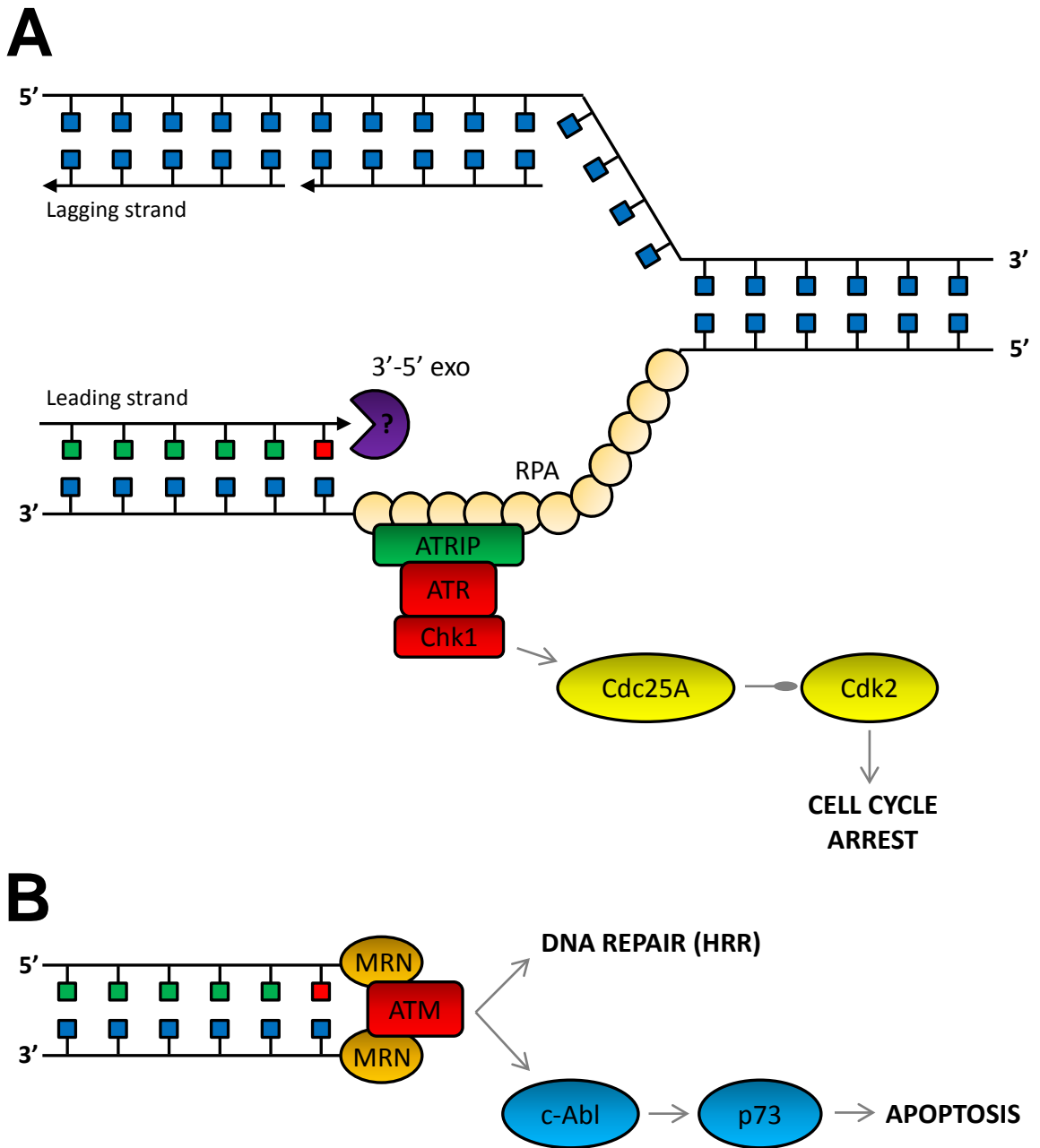


Figure 1.12. Replication fork stalling and S phase arrest in response to Ara-C

A. ATR is attracted to single stranded regions of DNA at stalled replication forks through interactions with replication protein A (RPA) and ATR-interacting protein (ATRIP) (Zou and Elledge, 2003). Following its recruitment, ATR activates Chk1 kinase (Feijoo et al., 2001), which in turn phosphorylates and activates Cdc25A phosphatase (Bartek and Lukas, 2003). Activation of Cdc25A prevents it from dephosphorylating cyclin-dependent kinase 2 (Cdk2), a positive regulator of cell cycle progression, thus cell cycle arrest is induced (Hu et al., 2001). One consequence of cell cycle arrest may be removal of Ara-C by exonuclease enzymes. **B.** Collapsed replication forks could be converted to DSBs. ATM and MRN complex localisation might recruit DNA repair pathways to attempt to rescue the replication fork. It may also signal p73-mediated apoptosis through interaction with c-Abl.

1.5.2.2. Inhibition of DNA Repair

There is a growing body of evidence demonstrating that Ara-C can interfere with the DNA re-synthesis step of certain DNA repair pathways, highlighting another potential mechanism of Ara-C-mediated cytotoxicity. In fact, it has been suggested that under normal conditions, the majority of Ara-C nucleotide observed in DNA is as a result of incorporation during DNA repair re-synthesis, and only in cases where the pool of available deoxynucleotides is reduced is the incorporation of Ara-C into DNA by replicative synthesis favoured (Iwasaki et al., 1997).

Early studies demonstrated that stimulation of DNA repair activity by ultra violet (UV) irradiation enhanced the incorporation of Ara-C into DNA, which had the effect of inhibiting repair of UV-induced damage (Kufe et al., 1984; Mirzayans et al., 1993). Similarly, more recent studies demonstrated that single strand DNA gap filling during NER could be inhibited by treatment of cells with Ara-C (Matsumoto et al., 2007).

Consistent with these findings, some of the polymerases associated with DNA repair are capable of mediating incorporation of Ara-C into DNA, including polymerase β (pol β) and polymerase λ (pol λ), which are specialised polymerases responsible for re-synthesis of DNA during the BER pathway (Shcherbakova et al., 2003). Template assays demonstrate that Ara-CTP is an efficient substrate for both pol β (Ohno et al., 1988; Prakasha Gowda et al., 2010) and pol λ (Garcia-Diaz et al., 2010) suggesting that the BER pathway might be capable of mediating the cytotoxicity of Ara-C.

1.5.2.3. Inhibition of Topoisomerase Enzymes

The cytotoxicity of Ara-C may also be enhanced through effects on the action of DNA topoisomerases, enzymes responsible for relaxing the torsion of DNA, through controlled generation of strand breaks, during replication and transcription (Wang, 2002). Ara-C treatment can result in trapping of topoisomerase I (topo I) cleavage complexes on DNA in leukaemic cell lines, due to the localised structural effects of Ara-C incorporation into DNA, causing inhibition of the DNA religation reaction catalysed by topo I (Chrencik et al., 2003). Similarly it has been shown that the presence of Ara-C at particular positions in DNA can 'poison' topoisomerase II (topo II) resulting in an increase in cytotoxic DSBs (Cline and Osheroff, 1999). Consistently, cells deficient in

topo I or topo II are more resistant to Ara-C than parental cells with normal levels of the enzymes (Goz and Bastow, 1997; Pourquier et al., 2000).

1.5.3. Mechanisms of Resistance to Ara-C

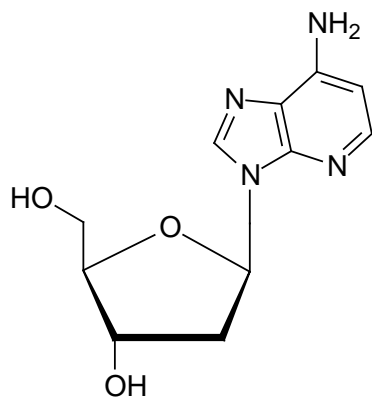
A number of mechanisms of cellular resistance to Ara-C have been identified *in vitro*, as well as *in vivo* in AML patients showing poor response to Ara-C chemotherapy. The majority of Ara-C resistance mechanisms are related to expression of genes associated with uptake and cellular metabolism of Ara-C. These include deficiency of hENT1 resulting in decreased cellular uptake of Ara-C (Takagaki et al., 2004; Hubeek et al., 2005; Kanno et al., 2007; Cai et al., 2008), reduced expression of deoxycytidine kinase (dCK) thus limiting the activation of Ara-C into Ara-C triphosphate (Veuger et al., 2003; Cai et al., 2008; Rathe and Largaespada, 2010), overexpression of the gene encoding cytidine deaminase which is responsible for deamination of Ara-C to an inactive form (Neff and Blau, 1996) and increased expression of 5'-nucleotidase, capable of dephosphorylation of Ara-C monophosphate (Dumontet et al., 1999). Furthermore, correlation of these mechanisms with poor outcome in AML patients has been demonstrated (Galmarini et al., 2002; Cros et al., 2004), suggesting their potential responsibility for Ara-C resistance *in vivo*.

Some proteins not associated with Ara-C metabolism have also been implicated in Ara-C resistance, in particular those associated with regulation of apoptosis. Insulin-like growth factor 1 (IGF1), a potent inhibitor of apoptosis, was overexpressed in Ara-C-resistant cell lines as well as in AML patients with refractory disease (Abe et al., 2006). Loss of expression of Nf1, an upstream regulator of RAS signalling (Maruta and Burgess, 1994), has also been reported in Ara-C-resistant cell lines (Yin et al., 2006). Similarly, loss of p53 expression is also associated with decreased sensitivity to the cytotoxic effects of Ara-C in cell line models (Decker et al., 2003; Kanno et al., 2004; Yin et al., 2006).

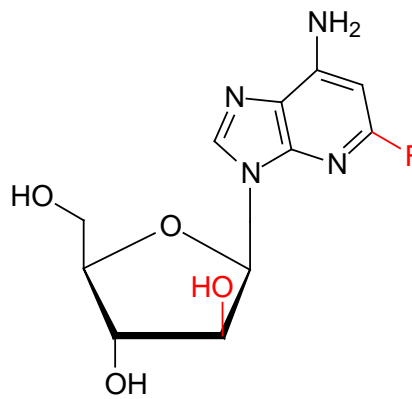
1.5.4. Other Therapeutic Nucleoside Analogues

Fludarabine and clofarabine are both analogues of 2'-deoxyadenosine currently being evaluated for the treatment of AML (see Section 1.3.2.2). Fludarabine, like Ara-C, is distinguished by the presence of a 2'-hydroxyl group in β -D-conformation on the deoxyribose sugar ring, but in addition it also has substitution of a fluorine atom in place of hydrogen at the 2-position of the purine ring (Figure 1.13). Clofarabine is distinguished from the parent nucleoside by the presence of a fluorine atom at the 2'-position of the deoxyribose sugar, as well as substitution of chlorine at the 2-position of the purine ring (Figure 1.13). Clofarabine, by virtue of its structure, is more stable and is associated with a reduction in off-target toxic effects that compromise the use of other nucleoside analogues, affording it a higher degree of efficacy and a wider clinical spectrum (Zhenchuk et al., 2009). Cladribine is also an anti-leukaemic 2'-deoxyadenosine analogue, modified solely on the purine ring where it has substitution of a chlorine at the 2-position (Figure 1.13).

The primary mechanism of fludarabine, clofarabine and cladribine-induced cytotoxicity appears to be similar to Ara-C in that cell death depends primarily on fraudulent incorporation of the triphosphate into replicating DNA, and subsequent inhibition of DNA synthesis (Hentosh et al., 1990; Huang et al., 1990; Parker et al., 1991). Unlike Ara-C however, fludarabine, cladribine and clofarabine also possess an additional mechanism of action which contributes to their cytotoxicity. The triphosphates have inhibitory actions towards ribonucleotide reductase (Parker et al., 1988; Xie and Plunkett, 1996), a key enzyme involved in the formation of deoxyribonucleotides from ribonucleotides. Inhibition of ribonucleotide reductase results in a decrease in deoxynucleotide pools, leading to enhanced incorporation of the fraudulent nucleotides into DNA, an action known as self-potential (Heinemann et al., 1992).

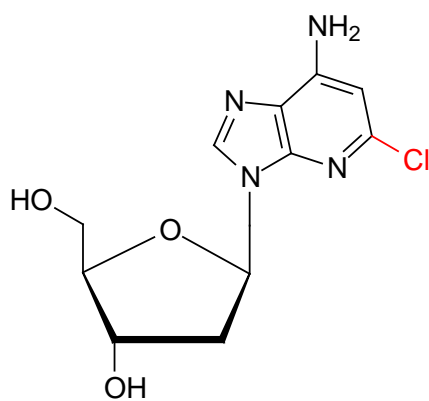


2'-Deoxyadenosine



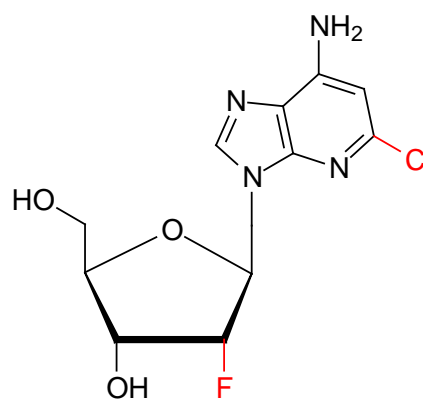
Fludarabine

9-β-D-arabinofuranosyl-2-fluoroadenine



Cladribine

2-chloro-deoxyadenosine



Clofarabine

2-chloro-2'-fluoro-arabinosyladenine

Figure 1.13. Structures of the normal nucleoside, 2'-deoxyadenosine and its analogues fludarabine, cladribine and clofarabine.

Substituted groups are shown in red.

1.6. Aims of Project

Failure to achieve complete remission and disease relapse are major clinical problems in AML, and often lead to poor outcome in patients. Numerous factors can contribute to poor response to therapy, including presence (or acquisition) of mutations which allow cancer cells to evade the cytotoxic mechanisms of drugs (chemoresistance) or an inability to tolerate necessary aggressive therapeutic approaches (particularly in elderly patients). Of the many factors affecting therapeutic response, chemoresistance remains the major obstacle to successful treatment of AML, and understanding the underlying mechanisms is an important goal for researchers and treating clinicians.

It is well established that defects in the DNA MMR pathway confer cellular resistance to certain chemotherapeutic agents *in vitro*, namely methylating agents, 6-TG and cisplatin, and may also modulate response to other agents including IR and 5-FU. Although typically chemoresistant subtypes of AML, such as relapsed AML and t-AML, have been reported to demonstrate MMR defects in a high percentage of cases, a direct link between MMR loss and chemoresistance *in vivo* has yet to be established.

The primary objective of this project was to investigate the role of DNA MMR in mediating therapeutic response to agents used to treat AML. The strategies for achieving this were:

- To determine whether defects of the DNA MMR pathway (loss or overexpression of MMR components) affect *in vitro* response to chemotherapeutic agents used in the treatment of AML, particularly Ara-C and other nucleoside analogues.
- To determine if prolonged exposure of myeloid cells to either a methylating agent, 6-TG or Ara-C could result in loss of functional DNA MMR, effectively recapitulating the postulated development of t-AML, and investigate the effects on chemotherapeutic response.
- To investigate the DNA-directed mutagenicity of Ara-C, including characterisation of the spectrum of drug-induced mutations, in order to identify potential substrates for interaction with DNA MMR components.

- To perform genome-wide molecular analysis (via high density SNP arrays) of a small cohort of matched presentation and relapsed AML patients, in order to investigate clonal architecture of AML, and whether there was evidence of AML evolving as the disease progresses from presentation to relapse.

Chapter 2. Materials and Methods

2.1. Chemicals and Reagents

All chemicals and reagents used were of Analar grade and were purchased from Sigma-Aldrich Co. Ltd. (Dorset, UK) unless otherwise stated. Phosphate buffered saline (PBS) was prepared from PBS tablets (Invitrogen Life Technologies, Paisley, UK) and was autoclaved prior to use for sterility. Preparation of reagents for use in specific investigations are described in relevant sections below.

2.2. Cell Lines

The lymphoblastoid TK6 cell line and its subline, MT-1 were a kind gift from Prof. W. Thilly (MIT, MA, USA). A second culture of TK6 and its paired subline, TK6 MTXr, as well as the precursor B-cell line PreB697 and its subline PreB697 MTXr, were provided by E. C. Matheson (Northern Institute for Cancer Research (NICR), Newcastle, UK). The myeloid leukaemic cell line HL-60 and its subline HL-60R were a kind gift from Prof. T. Shimada (Nippon Medical School, Tokyo, Japan). The myeloid leukaemic cell lines KG-1 and EoL-1 were obtained from the American Type Culture Collection (ATCC, VA, USA). In addition, the cell lines HeLa and LoVo were used as controls for certain experiments, and were provided in the form of frozen cell pellets by E. C. Matheson.

Specific features of cell lines are described in more detail in relevant results chapters.

2.3. General Cell Culture Methods

2.3.1. Routine Cell Culture

All cell culture reagents were purchased from Invitrogen Life Technologies (Paisley, UK) unless otherwise stated. Tissue culture plasticware was from Corning-Costar (supplied by VWR International Ltd., Leicestershire, UK). All cell culture was carried out in a class II microbiological safety cabinet (BIOMAT-2, Medical Air Technology Ltd., Oldham, UK) using aseptic technique.

All cell lines were maintained as suspension cultures in 5ml RF10 medium [Roswell Park Memorial Institute (RPMI) 1640 medium supplemented with 10% (v/v) foetal bovine serum (FBS) and 50µg/ml penicillin/streptomycin] in 25cm³ sterile cell culture flasks. Cultures were incubated at 37°C in a humidified 5% CO₂ incubator

(Heraeus Equipment Ltd., Essex, UK). Cell cultures were passaged as required, according to Table 2.1, in order to maintain cells in exponential growth phase. Cell lines were passaged a maximum of 25 times, after which fresh stocks were resuscitated from liquid nitrogen storage (see Section 2.3.4). Testing for mycoplasma was performed by E. C. Matheson at 2 month intervals using a MycoAlert kit (Lonza Biologics, Slough, UK).

2.3.2. Cell Counting and Determination of Cell Density

An aliquot of cell suspension was mixed with a 0.4% solution of trypan blue (Life Technologies, Paisley, UK) in a 1:1 ratio and 10µl of the mixture was loaded onto a Neubauer haemocytometer (VWR International Ltd.) and a minimum of 100 cells were recorded for each cell count.

2.3.3. Cryopreservation of Cell Stocks

Following determination of cell concentration, appropriate volume of cell suspension containing 5×10^6 cells was dispensed into sterile BD Falcon™ centrifuge tubes (BD Biosciences, Oxford, UK) and centrifuged at 230 x g for 5 min. Supernatant was discarded, after which cell pellets were resuspended in 1ml freezing medium [FBS supplemented with 10% (v/v) dimethyl sulphoxide (DMSO)] and transferred to sterile polypropylene cryovials (Invitrogen Life Technologies). Cells were frozen slowly (approximately 1°C per minute) to -80°C and transferred to liquid nitrogen for long term storage.

2.3.4. Resuscitation of Frozen Cell Stocks

Cryopreserved cell aliquots were thawed rapidly and transferred to 5ml pre-warmed RF10 medium. Suspensions were then centrifuged at 230 x g for 5 min, after which supernatant was completely removed and discarded. Resulting cell pellets were resuspended in 5ml RF10 culture medium, transferred to 25cm³ sterile cell culture flasks and incubated at 37°C/5% CO₂. Cell cultures were checked daily for growth and were not used in any experimental procedures until normal exponential cell growth had resumed.

Cell Line	Optimum Density (x10⁶ cells/ml)	Approximate Doubling Time (hours)	No. of Days between Passage	Split
HL-60	0.5 - 1.0	30	3	1:5
HL-60R	0.5 - 1.0	30	3	1:5
TK6	0.2 - 1.0	18	2	1:8
MT-1	0.2 - 1.0	18	2	1:8
TK6	0.2 - 1.0	18	2	1:8
TK6 MTX ^R	0.2 - 1.0	18	2	1:8
PreB697	0.5 - 1.0	24	3	1:5
PreB697 MTX ^R	0.5 - 1.0	24	3	1:5
KG-1	0.2 - 1.0	38	4	1:4
EoL-1	1.5 - 2.0	50	6	1:4

Table 2.1. Routine passage schedule of cell lines.

2.3.5. Preparation of Cell Pellets

Five million cells were dispensed into sterile BD Falcon™ centrifuge tubes and centrifuged at 230 x g for 5 min. Supernatant was discarded and cell pellets were resuspended in 3ml sterile PBS. Washed cells were then centrifuged and resuspended in 1ml sterile PBS and centrifuged again at 230 x g for 5 min. Supernatant was completely removed and the resulting cell pellets were stored at -80°C until required.

2.4. Generation of Stable DNA MMR-Defective Cell Lines using Short Hairpin RNA-Mediated Gene Knockdown

Stable MMR-defective subclones of the cell lines TK6 and HL-60 were generated using short hairpin RNA (shRNA)-mediated gene knockdown. In this process, lentiviral particles are used to deliver shRNA constructs into cells which become incorporated into the host genome. Translation by RNA polymerase III (due to the H1 promoter sequence included in the construct) results in continual production of shRNA molecules which are cleaved to produce small interfering RNA (siRNA) molecules. The siRNA molecules become bound to the RNA-induced silencing complex (RISC) which subsequently binds to and cleaves mRNA molecules which match the siRNA, hence permanently blocking expression of the target gene.

2.4.1. shRNA Constructs, Controls and Reagents

Pre-packaged lentiviral transduction particles containing verified MISSION® shRNA constructs targeting the coding domain sequence (CDS) of *MSH2*, *MSH3* or *MSH6* (in pLKO.1-puro plasmid vectors) were purchased from Sigma-Aldrich, UK. The sequences of the shRNA constructs were as follows:

MSH2: CCGGGCCTTGCTGAATAAGTGTAAGTCTCGAGTTTACACTTATTCAGCAAGGCTTTTTG

MSH3: CCGGGCAAGGAGTTATGGATTAAATCTCGAGATTTAATCCATAACTCCTTGCTTTTTG

MSH6: CCGGGCCAGAAGAATACGAGTTGAACTCGAGTTCAACTCGTATTCTTCTGGCTTTTTG

In addition, lentiviral transduction particles containing an empty pLKO.1 plasmid vector (MISSION® pLKO.1-puro Control Transduction Particles), as well as particles containing a random shRNA construct confirmed not to target any known human or

mouse gene (MISSION® Non-Target shRNA Control Transduction Particles), were also purchased to use as negative controls for transduction.

Lentiviral transduction particles containing a pLKO.1 plasmid vector expressing a green fluorescent protein (GFP) gene (MISSION® TurboGFP™ Control Transduction Particles) were also purchased to determine the transduction efficiency of cell lines (Section 2.4.4).

All purchased lentiviral particles were received as frozen stock and stored at -80°C. Upon first use, particles were aliquoted appropriately and stored at -80°C until required.

An 800µg/ml stock solution of hexadimethrine bromide was prepared by dissolving 800µg hexadimethrine bromide in 1ml sterile dH₂O. Stock solution was filter sterilised using a 0.2µm filter (VWR International Ltd.), stored at 4°C and used neat as required.

2.4.2. Assessment of Puromycin Sensitivity

The pLKO.1-puro plasmid used as a vector for the shRNA constructs contains a puromycin resistance gene, meaning the antibiotic can be used to select cells which have been successfully transduced. However, many cell lines are inherently sensitive to the effects of puromycin, hence preliminary investigations were necessary to establish the minimum puromycin concentration required to kill all non-transduced cells. The following investigation was performed for TK6 and HL-60 cells:

A cell suspension at a density of 7.5×10^3 cells/ml was established in RF10 medium (20ml). For administration of puromycin, a 2ml aliquot of cell suspension was transferred to a sterile BD Falcon™ centrifuge tube and centrifuged at 230 x g for 5 min. Supernatant was discarded, cells were resuspended in 2ml RF10 medium supplemented with appropriate volume of working puromycin solution and transferred to a well of a sterile 6-well culture plate. Puromycin concentrations of 0 (control), 2, 4, 6, 8 or 10 µg/ml were tested, as recommended by the manufacturer (Sigma-Aldrich). Plates were incubated at 37°C/5% CO₂ and assessed microscopically each day for cell death.

In the case of both TK6 and HL-60 cells, after approximately 72 hours in culture following puromycin administration, all cells in all treated cultures were found to be

dead upon microscopic inspection (confirmed using trypan blue dye, see Section 2.3.2). Therefore for both cell lines, selection of transduced cells was performed using media supplemented with puromycin at a concentration of 2µg/ml.

2.4.3. Assessment of Hexadimethrine Bromide Sensitivity

Hexadimethrine bromide is a cationic polymer which can be used to increase the efficiency of transduction of mammalian cell lines. Growth of certain cell lines however is detrimentally affected by hexadimethrine bromide, hence it was necessary to determine whether TK6 or HL-60 would be affected by its inclusion in media used for transduction. The following investigation was performed for TK6 and HL-60 cells:

A cell suspension at a density of 5×10^4 cells/ml was established in RF10 medium (5ml). For administration of hexadimethrine bromide, a 1ml aliquot of cell suspension was transferred to a sterile BD Falcon™ centrifuge tube and centrifuged at 230 x g for 5 min. Supernatant was discarded, cells were resuspended in 1ml RF10 medium supplemented with 8µg/ml hexadimethrine bromide (the concentration routinely used in transduction protocols) and transferred to a well of a sterile 6-well culture plate. A 1ml aliquot of untreated cell suspension was transferred to a second well as a control. Plates were incubated at 37°C/5% CO₂ for 72 hours.

After 72 hours in culture, cell density and viability of the control and hexadimethrine bromide-treated cultures were assessed by counting cells using a haemocytometer and trypan blue dye (Section 2.3.2). In the case of both TK6 and HL-60 cells, hexadimethrine bromide had no effect on cell growth and viability compared to the untreated control cultures (data not shown), and 8µg/ml was deemed suitable for use in transduction.

2.4.4. Assessment of Transduction Efficiency

Prior to performing transduction with lentiviral particles containing shRNA constructs, it was necessary to determine the optimum multiplicity of infection (MOI) required for transduction of each cell line using MISSION® TurboGFP™ Control Transduction Particles. This also served as a control to determine whether the transduction process itself had any effect on cell growth, so that these could be separated from effects of shRNA-mediated gene knockdown.

Lentiviral transduction of TK6 and HL-60 cells was performed using MISSION® TurboGFP™ Control Transduction Particles according to Section 2.4.5 below. MOIs of 0 (control), 0.5, 1, 2 and 5 were prepared as recommended by the manufacturer (Sigma-Aldrich).

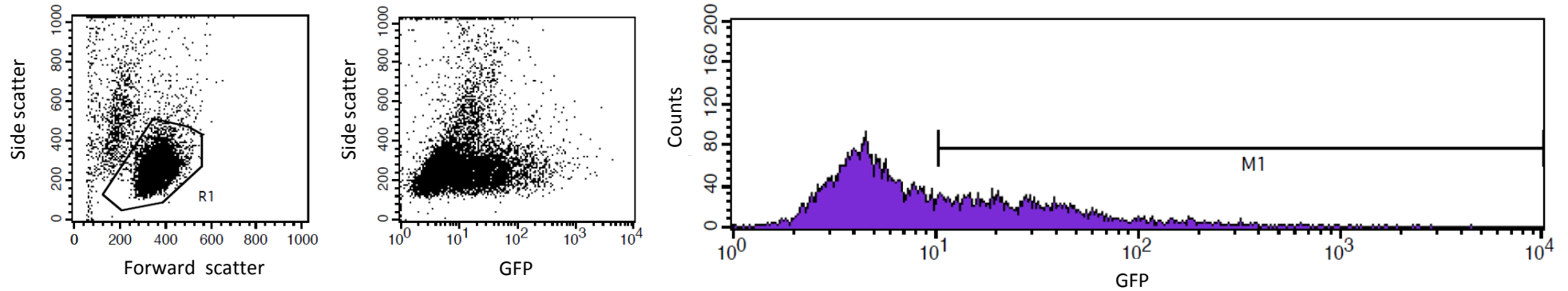
2.4.4.1. Assessment of GFP Expression by Flow Cytometry

Once cell populations transduced with MISSION® TurboGFP™ Control Transduction Particles had resumed normal exponential growth following puromycin selection (see Section 2.4.6 below), transduction efficiency was determined by assessment of the expression of GFP by flow cytometry (the principles of flow cytometry are described in Section 2.12.1).

For each transduced cell population, a suspension containing 2×10^5 cells was dispensed into a BD Falcon™ capped polystyrene tube. Cells were centrifuged at 450 x g for 4 min, supernatant discarded and cells resuspended in 500µl PBS. Flow cytometry was kindly performed by V. Forster (NICR) using a FACSCalibur flow cytometer with BD CellQuest Pro software (BD Biosciences) using pre-optimised instrument settings for detection of GFP fluorescence. A total of 10,000 cells were assessed from each transduced cell population. For assessment of GFP-expressing cells, cell debris and dead cells were first excluded from the analysis based on forward and side scatter signals. Percentage of GFP-expressing cells in the remaining cell population was then determined based on detection of GFP fluorescence.

Figure 2.1 shows the results of flow cytometric assessment of GFP expression in TK6 cells transduced at an MOI of 2. Expression of GFP was similar for all MOIs tested, in both HL-60 and TK6 cells (data not shown). It was therefore decided, based on time to recover exponential cell growth (approximately 4 days for MOIs 2 and 5, approximately 6 days in the case of MOIs 0.5 and 1), to use an MOI of 2 for subsequent lentiviral transductions.

TK6 MOI 2



TK6 (non-transduced)

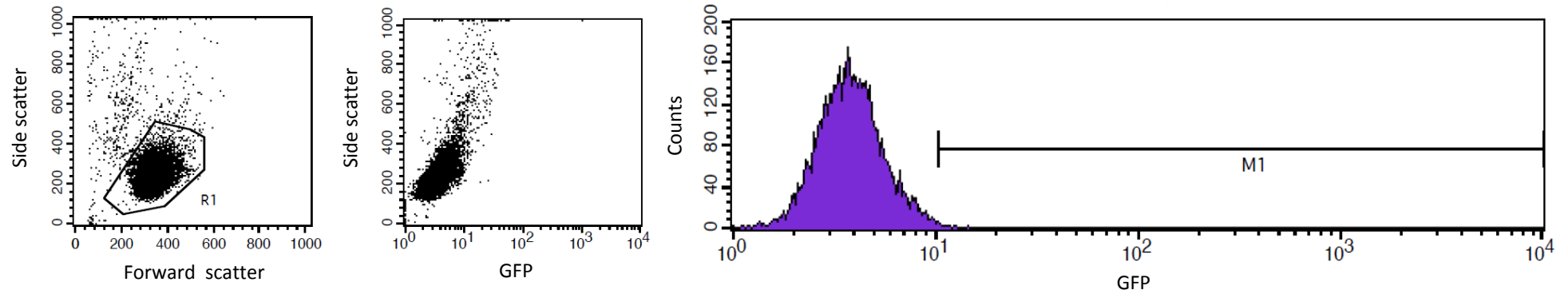


Figure 2.1. Flow cytometric assessment of transduction efficiency of TK6 with Mission® TurboGFP™ Control Transduction Particles.

10,000 cells transduced with an MOI of 2 were assessed for expression of GFP using a FACSCalibur flow cytometer (top). Left hand dot plot shows forward scatter and side scatter profiles which were used to determine viable cells (R1 gate). Right hand dot plot (gated to contain only viable cells) shows GFP fluorescence. The histogram displays the numbers of cells expressing GFP at increasing intensities. Those within the M1 region are positively expressing GFP. The same analysis was also performed on non-transduced TK6 cells for comparison (bottom).

It was also noted at this point that the growth kinetics of transduced cells was not significantly different from non-transduced cells (MOI 0) (data not shown), demonstrating that the transduction process itself has no apparent effect on the growth of TK6 or HL-60 cells.

2.4.5. Lentiviral Transduction

A suspension of exponentially growing cells was established at a density of 5×10^4 cells/ml using RF10 culture medium (10ml) supplemented with $8\mu\text{g/ml}$ hexadimethrine bromide. For addition of lentiviral particles, a 1ml aliquot of cell suspension was transferred to a sterile 15ml BD Falcon™ centrifuge tube and appropriate volume of thawed lentiviral particle suspension was added directly to the cell suspension. The following formula was used to calculate appropriate volume of lentiviral particles to give the required MOI:

$$\text{Volume required} = \frac{\text{Total no. of cells} \times \text{required MOI}}{\text{viral titre (TU/ml)}^*}$$

Following addition of lentiviral particles, cell suspensions were centrifuged at 800 x g for 30 min at 32°C. After centrifugation, supernatant was carefully removed and discarded, cells were re-suspended in 2ml RF10 culture medium and transferred to a sterile 6-well cell culture plate. Plates were incubated at 37°C/5% CO₂ for 72 hours.

A normal control was prepared for each cell line/shRNA combination according to the same procedures, but without the addition of lentiviral particles.

2.4.6. Puromycin Selection of Transduced Cells

After 72 hours incubation, transduced cell populations were transferred to sterile BD Falcon™ centrifuge tubes and centrifuged at 230 x g for 5 min. Supernatant was discarded, cells were resuspended in 2ml selection media [RF10 media supplemented with $2\mu\text{g/ml}$ puromycin] and transferred to a fresh 6 well cell culture plate. Cultures were incubated at 37°C/5% CO₂ and selection media was replaced according to the above procedure every 72 hours until normal exponential cell growth had resumed (assessed by counting cells using a haemocytometer and trypan blue dye). At this point, cell populations were deemed to consist entirely of transduced cells, given that

* Viral titre was supplied by manufacturer for each vial of lentiviral particles received.

only cells which had taken up a plasmid could survive in selection media due to acquired puromycin resistance.

Control non-transduced parental cell populations were treated in the same way as above (in order to keep cell lines paired), except normal RF10 culture media was used in place of selection media.

2.4.7. Selection of TK6 Knockdown Clones by Limiting Dilution

Individual clones of transduced TK6 cells were selected and expanded prior to assessment of knockdown efficiency as follows:

A cell suspension at a density of 1×10^4 cells/ml was established using selection medium and 10-fold serial dilution (using selection medium) was performed to give a cell suspension at a density of 1 cell/ml. This was transferred to a sterile 96-well plate (200 μ l per well) and incubated at 37°C/5% CO₂.

Following sufficient time in culture (approximately 10 days), a number of wells in which clonal populations had become established (assessed microscopically) were selected at random and each transferred to a sterile 6-well culture plate with 3ml selection medium. Following a further 72 hours in culture, 7ml selection medium was added to each culture, which was then split between two 25cm³ sterile cell culture flasks. These were incubated for a further 48 hours, after which each cell suspension was transferred to a sterile 75cm³ culture flask with 30ml selection medium. After another 72 hours in culture, for each knockdown cell population, the contents of one flask was used to prepare cell pellets, according to Section 2.3.5, for assessment of knockdown efficiency. The contents of the second flask was used to freeze viable cell aliquots, according to Section 2.3.3, for use in cytotoxicity assays.

The same procedures were also performed with control non-transduced TK6 cells (using normal RF10 culture medium), including preparation of cell pellets and cryopreservation of viable cell aliquots, in order to maintain paired cell clones as best as possible.

2.4.8. Expansion of HL-60 Knockdown Populations

Cloning of HL-60 cells is not possible by limiting dilution due to the low cloning efficiency of this cell line. Populations of HL-60 knockdown cells were therefore expanded from a small number of cells as follows.

Cell suspensions at a density of 2×10^3 cells/ml were established using selection medium (2 flasks per knockdown cell line) and were incubated at 37°C/5% CO₂. After 72 hours in culture, each cell population (5ml) was transferred to a 75cm³ cell culture flask and 30ml selection medium was added. After a further 72 hours in culture, the contents of one flask was used to prepare cell pellets, according to Section 2.3.5, for assessment of knockdown efficiency. The contents of the second flask was used to freeze viable cell aliquots, according to Section 2.3.3, for use in cytotoxicity assays.

Populations of control non-transduced HL-60 cells were also expanded in the same manner (using normal RF10 medium) alongside knockdown cell populations in order to maintain paired cell lines as best as possible. Cell pellets and cryopreserved cell aliquots were also prepared as above.

2.4.9. Assessment of Knockdown Efficiency

Efficiency of shRNA-mediated knockdown of target genes, relative to control non-transduced cells, was assessed by western immunoblotting according to the protocols described below (Section 2.7). Effect of gene knockdown on the cellular levels of other DNA MMR protein components was also assessed in the same way.

The cellular amounts of DNA MMR proteins were also assessed in cells transduced with the pLKO.1-puro control or the non-target shRNA control to exclude any effects of transduction and shRNA processing, respectively, on target gene expression (see Figure 3.7).

2.4.10. Routine Culture of Knockdown Cell Lines for use in Cytotoxicity Assays

For use in cytotoxicity assays, cryopreserved aliquots of knockdown cell lines and their paired control non-transduced cell lines were thawed and cultured in RF10 medium according to Sections 2.3.4 and 2.3.1 above. In order to minimise cell stress, it was deemed not necessary to culture knockdown cell lines in selection media given

that they were only cultured for short periods to allow use in cytotoxicity assays. Furthermore, plasmid DNA should be stably incorporated into the host cell genome, meaning shRNA expression should be stable and permanent without the requirement for continuous selection.

Non-transduced control cell populations were always routinely passaged alongside knockdown cells in order to maintain paired cell lines for assessment of relative cytotoxicity.

Once normal exponential growth had resumed (assessed by counting cells using a haemocytometer and trypan blue dye), cytotoxicity assays were performed according to Section 2.6 below. Fresh cell aliquots were used each time a subsequent cytotoxicity assay was performed in order to minimise culture time and hence the risk of mutations occurring due to the mutator phenotype of MMR-deficient cells.

2.5. Generation of Drug Resistant Cell Lines by Escalating Dosage

In order to model the development of t-AML *in vitro* (Chapter 5), myeloid cell lines were cultured in the presence of escalating doses of either MNU, 6-TG or Ara-C, in an attempt to generate drug-resistant subclones for analysis of DNA MMR status. The myeloid cell lines HL-60, KG-1 and EoL-1 were used (described in Chapter 5), as well as the B-lymphoblastoid cell line TK6.

2.5.1. Dose Finding Assay

In order to identify a suitable starting dose for each drug in each cell line, dose finding assays were performed by treating the cell lines with a range of doses of each drug (data not shown), and the dose which resulted in death of approximately 70-80% of cells was selected as a starting dose (see Table 2.2). Dose finding assays were performed using growth inhibition in all cases, as described in Section 2.6.3.

Cell Line	Normal Doubling Time (Hrs)	Drug	Initial Dose (μM)	Dose Increment (μM)	Final Dose (μM)
HL-60	24-36	MNU	0.05	0.05	0.5 ^a
		6-TG	0.5	0.5, rising to 1, rising to 2	20
		Ara-C	0.01	0.01, rising to 0.05, rising to 0.2	1
EoL-1	40-48	MNU	0.01	0.01	0.1
		6-TG	0.1	0.1	No recovery from second drug dose (0.2)
		Ara-C	0.02	0.02	No recovery from second drug dose (0.04)
KG-1	36-38	MNU	0.05	0.05, rising to 0.1	1
		6-TG	0.1	0.1	No recovery from second drug dose (0.2)
		Ara-C	0.1	0.1	0.5 ^b
TK6	16-20	MNU	0.01	0.01, rising to 0.05	0.5
		6-TG	0.5	0.5, rising to 1, rising to 2	20
		Ara-C	0.04	0.04, rising to 0.1, rising to 0.5	2

Table 2.2. Dosing schedule for generation of drug-resistant sub-cultures from myeloid (HL-60, EoL-1 and KG-1) and lymphoblastoid (TK6) cell lines.

^a Further dosing was attempted using a dose of 0.55 μM , however cells consistently failed to recover.

^b Further dosing was attempted using a dose of 0.6 μM , however cells consistently failed to recover.

2.5.2. Drug Dosing

For each cell line and drug combination, to administer the initial drug dose, 1×10^5 cells were centrifuged at $230 \times g$ for 5 min, then resuspended in 5ml RF10 medium supplemented with the appropriate volume of drug (dosed culture) and transferred to a sterile 25cm^3 cell culture flask. At the same time, a similar culture was setup using RF10 medium supplemented with appropriate solvent but no drug (parental culture). Cultures were incubated at $37^\circ\text{C}/5\% \text{CO}_2$ and assessed at regular intervals for resumption of normal exponential growth (by counting cells using a haemocytometer and trypan blue dye). Once normal growth had resumed in the dosed culture, the next drug dose was applied using the same procedure. The parental culture was treated in the same manner, using appropriate solvent but no drug. The dosing schedules which were used are shown in Table 2.2 for each cell line and drug combination.

2.5.3. Assessment of Resistance

Following recovery of exponential cell growth after the final drug dose, acquired resistance to the drug with which cells were dosed was assessed relative to respective parental cultures (data not shown). In the case of HL-60, KG-1 and EoL-1 this was achieved via growth inhibition assay (Section 2.6.3), and in the case of TK6, via 96-well clonogenic assay (Section 2.6.2).

For TK6 sub-cultures, a single cell clone was selected via limiting dilution (see Section 2.4.7) and expanded in normal RF10 medium for several passages. This was not possible in the case of HL-60, KG-1 and EoL-1 cultures as these cells demonstrate a low cloning efficiency. The dosed sub-cultures were therefore passaged as normal in drug-free RF10 medium for several passages. In all cases, parental cultures were passaged alongside dosed cultures according to the same schedule.

Following several passages in drug-free RF10 medium, cytotoxicity assays were repeated, as described above, to confirm that acquired drug-resistance was stable.

Subsequently, cross-resistance to other agents, was assessed relative to parental cultures as detailed in Chapter 5. Resistance was assessed via growth inhibition assay (HL-60, KG-1, EoL-1) or 96-well clonogenic assay (TK6).

2.6. Cytotoxicity Assays

Cytotoxicity assays were used throughout the project (Chapters 3, 4 and 5) to assess drug (or radiation) response in MMR-deficient cells (or drug-resistant cells), relative to respective normal parental counterparts. Cell lines were assessed in pairs (i.e. parental cell line and relevant subclone), or sets of 5 in the case of MMR knockdown lines (i.e. non-transduced control (parental) cell line, MSH2, MSH3 and MSH6 knockdown subclones and non-target shRNA control subclone).

2.6.1. Reagents and Exposures

Stock solutions of chemotherapeutic agents for use in cytotoxicity assays were prepared according to Table 2.3 using appropriate solvents. All stock solutions were aliquoted and stored at -80°C. Working solutions were prepared immediately prior to use by dilution of stock solutions in RF10 culture medium, or sterile PBS in the case of MNU.

Exposure to UV radiation was performed using a Stratalinker 2400 UV Crosslinker (Agilent Technologies UK Ltd., Berkshire, UK) at a wavelength of 254nm.

Exposure to IR was performed using a D3300 X-ray system (Gulmay Medical Ltd., Surrey, UK) at a dose rate of 2.4Gy/min, 310kV, 10mA.

Agent	Molecular Weight (g)	Solvent	Stock Solution (mM)
Methylnitrosourea <i>[N-methyl-N-nitrosourea]</i>	103.8	PBS	100
6-thioguanine <i>[2-amino-2-mercaptapurine]</i>	167.2	DMSO	15
Cytarabine <i>[1-β-D-arabinofuranosylcytosine]</i>	243.2	DMSO	50
Clofarabine <i>[2-chloro-2'-fluoro-arabinosyladenine]</i>	303.7	Sterile dH ₂ O	5
Fludarabine <i>[9-β-D-arabinofuranosyl-2-fluoroadenine]</i>	285.2	DMSO	50
Cladribine <i>[2-chloro-deoxyadenosine]</i>	285.7	DMSO	50

Table 2.3. Preparation of stock solutions of cytotoxic agents.

2.6.2. 96-Well Clonogenic Assay

Cytotoxicity of TK6 and its derivative subclones was assessed using a 96-well plate clonogenic assay. This technique was originally developed as a method of determining the mutability of suspension cell lines which are capable of growth at a very low density (i.e. 10^1 cells per ml and below) (Furth et al., 1981). The assay was adapted for use in assessment of cytotoxicity, with the following procedures performed for each cell line.

An exponentially growing cell suspension at a density of 1×10^5 cells/ml was established using RF10 culture medium. From this, suspensions at densities of 10^3 , 10^2 and 10^1 cells/ml were prepared by 10-fold serial dilution, using RF10 medium. In the case of assessment of cytotoxicity in response to drug treatment, for each drug dose, a 30ml aliquot of the appropriate density cell suspension was transferred to a sterile BD Falcon™ centrifuge tube and centrifuged at $230 \times g$ for 5 min. Supernatant was discarded and cells were resuspended in 30ml RF10 medium supplemented with appropriate volume of drug to give the required dose. 200 μ l of dosed cell suspension was then transferred to each well of a 96-well plate. The lowest doses were applied to cell suspensions at a density of 10^1 cells/ml (2 cells/well), mid range doses were applied to cell suspensions at a density of 10^2 cells/ml (20 cells/well) and the highest doses were applied to cell suspensions at a density of 10^3 cells/ml (200 cells/well). A vehicle-only control plate was also setup, in the same way, containing cells at a density of 10^1 cells/ml treated with appropriate solvent but no drug.

Clonogenic assays for assessment of cytotoxic response to IR or UV radiation exposure were setup in a similar manner. For each radiation dose, 200 μ l of appropriate density cell suspension was transferred to each well of a 96-well plate and the plate was exposed to radiation for the appropriate length of time to give the required dose. As above, the lowest doses were applied to cell suspensions at a density of 10^1 cells/ml, mid range doses were applied to cell suspensions at a density of 10^2 cells/ml and the highest doses were applied to cell suspensions at a density of 10^3 cells/ml. A negative control plate was also setup using cells at a density of 10^1 cells/ml (200 μ l per well) but not exposed to any radiation source. In all cases, plates were incubated at $37^\circ\text{C}/5\% \text{CO}_2$ for 20 days.

Following the 20 day growth period, cloning efficiency (CE) was calculated at each drug or radiation dose. For each plate, wells in which a viable colony had formed were determined microscopically. The number of negative wells was counted for each plate and CE was then calculated using the following Poisson relationship (Furth et al., 1981):

$$CE = \frac{-\ln P_0^\dagger}{\text{No. cells per well}}$$

The survival fraction at each dose was then determined by calculating the mean CE of the dosed cells as a percentage of the mean CE of the vehicle-only or negative control cells.

Survival fractions at each drug or radiation dose were plotted on an X-Y scatter graph (using Microsoft Excel) to generate kill curves for each cell line, thus enabling comparison of cytotoxicity between the paired (or 5) cell lines.

Each individual experiment was performed in triplicate and mean survival fractions at each drug or radiation dose were used to generate the kill curves. Standard error of the mean (SEM) was also calculated for each dose to enable inclusion of error bars on kill curves.

2.6.3. Growth Inhibition Assay

Cytotoxicity of all other cell lines (which do not grow readily at very low densities) was assessed using a flask-based growth inhibition assay. The following procedures were performed for each cell line.

An exponentially growing cell suspension at a density of 1×10^4 cells/ml was prepared using RF10 medium. In the case of assessment of cytotoxicity in response to drug treatment, for each dose, a 5ml aliquot of cell suspension was transferred to a sterile BD Falcon™ centrifuge tube and centrifuged at $230 \times g$ for 5 min. Supernatant was discarded, cell pellet was resuspended in 5ml RF10 medium supplemented with appropriate volume of drug to give the required dose, then transferred to a sterile 25cm^3 cell culture flask. A vehicle-only control flask was also setup in the same way, by

[†] P_0 represents the fraction of negative wells per plate (i.e. No. negative wells / 96)

resuspending cells in 5ml RF10 medium supplemented with appropriate solvent but no drug. Flasks were incubated at 37°C in a humidified 5% CO₂ incubator for 4 days.

In the case of assessment of cytotoxicity in response to IR or UV radiation, for each dose, a 5ml aliquot of cell suspension was transferred to one well of a sterile 6-well cell culture plate. This was then exposed to radiation for the appropriate amount of time to give the required dose. A negative control plate was also prepared using 5ml of cell suspension but not exposed to any radiation source. Plates were incubated at 37°C/5% CO₂ for 4 days.

Following the 4 day growth period, the number of viable cells in each culture was determined using a haemocytometer and trypan blue dye. The survival fraction at each dose was then determined by calculating the viable cell density of the dosed culture as a percentage of the viable cell density of the vehicle-only or negative control culture.

Kill curves were prepared as described in Section 2.6.2. Each individual experiment was performed in triplicate and mean (and SEM) survival fractions at each drug or radiation dose were used to generate the kill curves.

2.7. Western Immunoblotting

To determine whether the levels of particular proteins differed in MMR-defective cell lines and their paired parental MMR-proficient counterparts (Chapters 3 and 4), or in drug-resistant subclones and their respective parental cells (Chapter 5), quantitation of protein expression was performed by western immunoblotting. This technique involves extraction of total cytosolic proteins, separation of proteins according to size followed by immobilisation onto a membrane, and subsequent detection of target proteins of interest using labelled antibodies. The number of antibody molecules which can bind to each protein (and hence the amount of label detected) is proportional to the amount of protein present, therefore protein expression levels can be compared between cell lines.

2.7.1. Cytosol Preparation

A frozen cell pellet containing 5×10^6 cells (see Section 2.3.5) was thawed, resuspended in 100µl sodium dodecyl sulphate (SDS) sample buffer [62.5M Tris-HCl pH 6.8, 2% (w/v) SDS, 20% (v/v) glycerol] and passed through a 21 gauge needle (attached

to a 1ml syringe) several times to disrupt cell membranes. The homogenised sample was boiled at 100°C for 5 min, then centrifuged at 14,000 x g for 10 min to pellet cell debris. Protein concentration of the supernatant was estimated via Pierce BCA assay as described in Section 2.7.2.

Following estimation of protein concentration, 250µg of protein was transferred to a 1.5ml Eppendorf tube and made up to 450µl using SDS sample buffer. To this was added 25µl β-mercaptoethanol (final concentration 20% v/v) and 25µl 0.2% bromophenol blue aqueous solution (final concentration 0.01% v/v), resulting in a cytosolic extract at a protein concentration of 0.5mg/ml (500µl volume). Extracts were divided into 50µl aliquots for storage at -80°C until required.

2.7.2. Estimation of Protein Concentration by Pierce BCA Assay

Estimation of protein concentration was performed using a Pierce® BCA Protein Assay Kit (Fisher Scientific UK Ltd., Leicestershire, UK). This kit combines reduction of copper cations (Cu^{+2} to Cu^{+1}) by protein with colourimetric detection of Cu^{+1} using an agent containing bicinchoninic acid (BCA). The coloured complex produced exhibits strong absorbance at 562nm that increases linearly with increasing protein concentrations, hence intensity of the coloured complex can be used to estimate protein concentration. The assay was performed according to manufacturers protocols which are briefly described as follows:

An aliquot of each extract was diluted 1:10 using dH₂O to bring protein concentrations within the range of detection of the kit (0.2 – 1.2 mg/ml). For each diluted extract, 10µl was transferred to a 96-well optical plate (VWR International Ltd.) in quadruplicate. To each well, 190µl of BCA Working Reagent (Reagent A + Reagent B in a 50:1 ratio, according to manufacturers protocol) was added, well contents were mixed by gentle agitation using a plate shaker and plate was incubated at 37°C for 30 min.

Following incubation, absorbance at 562nm was read using a Spectromax® 250 Microplate Spectrophotometer System (Molecular Devices Corporation, Crawley, UK). Protein concentration was estimated from the corrected mean absorbance values by the spectrophotometer software (SOFTmax Pro 3.0, Molecular Devices Corporation), via comparison to a bovine serum albumin (BSA) standard curve which was also

prepared each time the assay was performed. Values generated were multiplied by 10 (to account for dilution factor) to give protein concentration in each extract.

2.7.3. SDS PAGE and Electrophoretic Transfer

Sodium dodecyl sulphate polyacrylamide gel electrophoresis (SDS-PAGE) was used to separate proteins in the cytosolic extracts according to size. Novex® 4-20% Tris-glycine gels (Invitrogen Life Technologies) were used for protein separation and were placed in an XCell SureLock™ Mini-Cell electrophoresis system (Invitrogen Life Technologies) filled with SDS electrode buffer [41.2mM Tris-HCl pH 6.8, 192 mM glycerol, 0.1% (w/v) SDS]. For every gel, 5µl of Benchmark Pre-stained Protein Ladder (Invitrogen Life Technologies) was loaded into the first lane. For each cell line, 20µl cytosolic extract (10µg protein) was loaded per well (aliquots of cytosolic extract were thawed in a heating block immediately prior to loading). Electrophoresis was performed using a constant voltage of 200V until the bromophenol blue dye front reached the bottom of the gel (approximately 1 hour).

Following separation, proteins were transferred electrophoretically from the gels onto polyvinylidene fluoride (PVDF) membrane (Bio-Rad Laboratories Ltd., Hertfordshire, UK). Gels were removed from their casing and placed in transfer cassettes with PVDF membrane (permeabilised in 100% methanol immediately prior to use), sandwiched between 3mm Whatman® chromatography papers (supplied by VWR International Ltd.) and transfer sponges, all of which had been pre-soaked in transfer buffer [10mM CAPS-NaOH pH 11, 10% (v/v) methanol]. Cassettes were placed in a Mini Trans Blot Electrophoretic Transfer Cell (Bio-Rad Laboratories Ltd.) filled with transfer buffer and electrophoresis was performed overnight at a constant voltage of 30V using a magnetic stirrer to maintain ion distribution in the buffer.

2.7.4. Antibody Detection and Visualisation of Bound Proteins

Antibodies used for detection of DNA MMR (and other) proteins are listed in Table 2.4.

PVDF membranes with bound proteins were removed from transfer cassettes and immersed in 5% blocking solution [TBS-Tween (see below), 5% (w/v) dried non-fat skimmed milk powder] with constant agitation for one hour at room temperature to

block non-specific antibody binding sites. Following blocking, membranes were cut into appropriate sections (depending on which proteins were to be detected) and transferred to 50ml BD Falcon™ centrifuge tubes containing 5ml primary antibody solution (prepared according to dilution specified in Table 2.4). Incubation in most cases was for 1 hour at room temperature with gentle agitation (using a roller mixer), however in some cases an overnight incubation at 4°C was performed (with constant gentle agitation).

After incubation in primary antibody, membranes were washed in 5ml TBS/Tween [0.01M Tris-HCl pH 7.5, 0.1M NaCl, 0.05% (v/v) Tween-20] at room temperature for 10 min (with gentle agitation). This wash step was repeated twice more to ensure removal of any unbound primary antibody. Membranes were then transferred to fresh 50ml Falcon tubes containing 5ml appropriate horseradish peroxidase-conjugated secondary antibody (prepared according to Table 2.4) and incubated for a minimum of 30 min at room temperature (with gentle agitation). Following this, a total of 4 washes were performed, as above, to ensure any unbound antibody was completely removed.

Detection of bound antibodies was performed using Visualizer™ Spray & Glow™ ECL Western Blotting Detection System (Upstate Pharmaceuticals, VA, USA) according to manufacturers protocol. Visualisation of chemiluminescence was achieved via exposure of membranes to Kodak BioMax Light film (VWR International Ltd.) for appropriate length of time (10 seconds – 5 min, depending on target protein). Films were developed using a Mediphot 937 X-Ray Filmprocessor (Colenta Lobortechnik, Austria). Membranes were then either stripped as described below (Section 2.7.5) for re-probing, or rinsed with TBS/Tween and stored moistened in cling film at 4°C for future use.

Protein	Molecular Weight (kDa)	Antibody Type	Clone	Isotype	Supplier	Cat No.	Dilution
Primary Antibodies							
MSH2	102	Monoclonal	G219-1129	Mouse IgG ₁	BD Biosciences	556349	1:250
MSH3	127	Monoclonal	52	Mouse IgG ₁	BD Biosciences	611390	1:250
MSH6	160	Monoclonal	44	Mouse IgG ₁	BD Biosciences	610919	1:2,000
MLH1	85	Monoclonal	G168-15	Mouse IgG ₁	BD Biosciences	551092	1:500
PMS2	100	Monoclonal	A16-4	Mouse IgG ₁	BD Biosciences	556415	1:500
MGMT	25	Monoclonal	MT3.1	Mouse IgG ₁	Millipore (UK) ^a	MAB16200	1:500
ERK-2	42	Monoclonal	G263-7	Mouse IgG ₁	BD Biosciences	554095	1:500
pERK	42	Monoclonal	12D4	Mouse IgG ₁	Santa Cruz Biotechnology Inc. ^b	sc-81492	1:1,000
TPMT	32	Monoclonal	31-J	Mouse IgG ₁	Santa Cruz Biotechnology Inc.	sc-100874	1:500
Actin (loading control)	46	Monoclonal	JLA20	Mouse IgM	Calbiochem ^{®c}	CP01	1:20,000
Secondary Antibodies							
Goat Anti-Mouse IgG, HRP conjugate	-	Polyclonal	-	Goat IgG	Millipore (UK)	12-349	1:3,750
Goat Anti-Mouse IgM, HRP conjugate	-	Polyclonal	-	Goat IgM	Calbiochem [®]	JA 1200	1:1,000

Table 2.4. Antibodies used in western immunoblotting

^a Watford, UK

^b Heidelberg, Germany

^c Supplied by Merck Chemicals Ltd., Nottingham, UK

2.7.5. Stripping PVDF Membranes for Re-Probing

In order to remove bound antibodies to allow re-probing with a different primary antibody, membranes were immersed in stripping buffer [62.5mM Tris-HCl pH6.7, 2% (w/v) SDS, 100mM β -mercaptoethanol] with constant agitation for 40 min at 60°C. The high stringency of the buffer forces antibodies to become unbound from proteins, however the binding of proteins to the membrane is unaffected.

Following stripping, membranes were washed twice in 5ml TBS/Tween with gentle agitation at room temperature for 10 min. Membranes were then transferred to 5% blocking solution and re-probed according to Section 2.7.4.

2.8. Gene Expression Analysis by Quantitative Real-Time PCR

In order to determine whether the expression of particular genes involved in DNA MMR was altered in MMR-defective cell lines, relative to paired parental MMR-proficient counterparts (Chapters 3 and 4), gene expression analysis was performed by real-time quantitative PCR using Taqman[®] chemistry. This technique involves two stages. Firstly, mRNA is reverse transcribed to cDNA. Secondly, PCR is performed using primers specific for the gene of interest, during which accumulation of the PCR product is detected in real-time. This is achieved through the use of specially designed probes which bind within the target sequence and fluoresce as the sequence is amplified. The amount of fluorescence detected (the cycle threshold (Ct) value) is therefore proportional to the level of expression of the target gene. Quantitation of expression of the target gene can either be performed in one sample relative to another (relative quantitation), as in these studies, or relative to a standard expression curve constructed from RNA of known concentration (absolute quantitation).

2.8.1. RNA Extraction and Quantitation

For each cell line, a frozen cell pellet consisting of 5×10^6 cells was thawed on ice. Total RNA was extracted from thawed cells using an RNeasy Mini kit (Qiagen, Crawley, UK) according to the supplied manufacturers protocol. Briefly, cells were lysed and homogenised, then RNA was bound to a RNeasy[®] silica gel membrane in spin-column format, after which contaminants were removed by washing in provided buffers. RNA

was eluted in 50µl nuclease-free distilled water (dH₂O) (Invitrogen Life Technologies). Quantitation of RNA was performed using a NanoDrop® ND-1000 spectrophotometer (Thermo Scientific, DE, USA) which measures the absorbance of UV light at 260nm passed through a 1µl aliquot of extracted RNA, and performs the necessary calculations according to the Beer Lambert Law to provide RNA concentration (in ng/µl).

Following quantitation, appropriate volume of eluate containing 10µg of RNA was transferred to a 1.5ml Eppendorf tube and made up to 20µl using nuclease-free dH₂O, resulting in an RNA extract at a concentration of 200ng/µl. Any remaining neat RNA extract were stored at -80°C.

2.8.2. Reverse Transcription of RNA into cDNA

Preparation of cDNA was performed using a High Capacity cDNA Reverse Transcription Kit (Applied Biosystems, Warrington, UK). This kit uses the random primer method for initiating reverse transcriptase (RT)-mediated cDNA synthesis of all RNA molecules present.

Appropriate volume of RT mastermix was prepared according to manufacturer's protocol and 10µl was dispensed into appropriate number of 0.2ml MicroAmp® Reaction Tubes (Applied Biosystems). For each sample, 10µl of 200ng/µl total RNA extract was added. A blank reaction was also prepared using nuclease-free dH₂O in place of RNA, to ensure no contamination of reagents. The following single cycle was performed using a GeneAmp® PCR System 9700 (Applied Biosystems):

25°C	10 min
37°C	120 min
85°C	5 min

Assuming a reverse transcription efficiency of 100%, this yielded 20µl of cDNA at a concentration of 100ng/µl. This was subsequently adjusted to 5ng/µl by addition of 380µl nuclease-free dH₂O and stored at 4°C until required.

Gene	TaqMan® Gene Expression Assay ID
MSH2	Hs00953523_m1
MSH3	Hs00989003_m1
MSH6	Hs00264721_m1
MLH1	Hs00179866_m1
PMS2	Hs00241053_m1
MGMT	Hs00172470_m1
β -actin (endogenous control)	Cat no. 4333762F

Table 2.5. TaqMan® Gene Expression Assays used in RT-PCR assessment of DNA MMR gene expression

2.8.3. Real-Time PCR Setup

Inventoried and validated TaqMan® Gene Expression Assays (each containing forward and reverse primers and 5'-FAM (carboxyfluorescein)-labelled internal probes for the target gene) were purchased from Applied Biosystems (Table 2.5). Assays were received as 20x concentrated stocks, which were aliquoted appropriately at first use and stored at -20°C.

For preparation of PCR mastermixes, appropriate volume of TaqMan® Universal PCR Master Mix (Applied Biosystems) was added to thawed aliquots of 20x Gene Expression Assay (as well as β -actin), according to the manufacturers protocol. 11 μ l of each mastermix was dispensed into appropriate number of wells of a 96-well Optical PCR Plate (Applied Biosystems). For each reaction, 9 μ l of 5ng/ μ l cDNA (total amount, 45ng) was added. Controls were also prepared using either a blank reverse transcription reaction or nuclease free dH₂O in place of cDNA, to ensure no contamination of reagents. Assays (and controls) were setup in quadruplicate for each gene in each cell line.

The following thermal cycle was performed using a 7300 Real Time PCR System (Applied Biosystems):

50°C	2 min	
95°C	10 min	
95°C	15 s	} 40 cycles
60°C	1 min	

Following completion of thermal cycling, detected fluorescence was converted to a Ct value for each reaction using the supplied PCR system software (SDS version 1.4, Applied Biosystems) using standard parameters. The means of the quadruplicate Ct values generated for each gene (in each cell line) were used for quantitation of gene expression, as described below.

2.8.4. Data Analysis

Relative quantitation using the $2^{-\Delta\Delta Ct}$ method (Livak and Schmittgen, 2001) was performed to determine the expression level of each gene of interest in MMR-deficient cell lines, relative to paired parental MMR-proficient counterparts. Briefly, analysis by this method first involved normalisation of the expression of each gene of

interest to expression of β -actin (a constitutively expressed house-keeping gene) in all cell lines. Normalised expression levels of genes of interest were then compared in MMR-defective cell lines and parental MMR-proficient cells, generating values representing fold change in expression for each gene. All calculations were performed using Microsoft Excel.

The entire investigation was repeated a total of three times, using new frozen cell pellets each time. Bar charts showing the mean (and SEM) fold-changes in gene expression (relative to respective parental cell lines) were generated for MMR-defective cell lines using Microsoft Excel.

2.9. Genomic DNA Sequencing (For *N-RAS* and *K-RAS* Mutations)

Sequencing of commonly mutated exons of *N-RAS* and *K-RAS* was performed in TK6 and MT-1 to exclude potential mechanisms of Ara-C sensitivity (Chapter 3). The following procedures were performed for each cell line:

2.9.1. DNA Extraction and Quantitation

Frozen cell pellets consisting of 5×10^6 cells were thawed and resuspended in 100 μ l PBS. Genomic DNA was extracted using a QIAamp DNA Mini Kit (Qiagen) according to the supplied manufacturers protocol. Briefly, DNA extraction was achieved through binding of DNA to a QIAamp[®] silica gel membrane (in spin-column format) after which contaminants were removed by washing using provided buffers. DNA was eluted in 200 μ l Buffer AE [10 mM Tris-HCl, 0.5 mM EDTA, pH 9.0]. Quantitation of DNA was performed using a NanoDrop[®] ND-1000 spectrophotometer which measures the absorbance of UV light at 260 nm passed through a 1 μ l aliquot of extracted DNA, and performs the necessary calculations according to the Beer Lambert Law to provide DNA concentration (in ng/ μ l).

For each sample, a 20 μ l aliquot of DNA at a concentration of 100ng/ μ l was prepared using Buffer AE and stored at 4°C for use in PCR reactions. Remaining DNA was stored at -20°C.

Gene/Exon	Primer Sequences	Amplicon Length (bp)	Annealing Temp. (°C)
<i>N-RAS</i> exon 1	Forward: CCAAATGGAAGGTCACACTA Reverse: AGAGACAGGATCAGGTCAGC	276	54
<i>N-RAS</i> exon 2	Forward: TGCCCCCTTACCCTCCACA Reverse: CCTCATTTCCCCATAAAGATTCAGA	272	52
<i>K-RAS</i> exon 1	Forward: TACTGGTGGAGTATTTGATAGT Reverse: CATGAAAATGGTCAGAGAAACC	286	55
<i>K-RAS</i> exon 2	Forward: TCTTTTCAAGTCCTTTGCC Reverse: GCAAATACACAAAGAAAGCC	256	53

Table 2.6. Sequences of oligonucleotide primers used for PCR amplification of *RAS* exons for sequencing.

2.9.2. PCR Amplification

PCR primers for amplification of specific *N-RAS* and *K-RAS* exons were provided as reconstituted stocks (100pmol/ μ l in TE buffer [10mM Tris-HCl pH 8, 1mM EDTA]) by E. C. Matheson. Primer sequences are shown in Table 2.6. PCR reaction conditions were the same for each gene/exon and consisted of 1x ReddyMix PCR buffer (Thermo Scientific), 1.5mM MgCl₂, 10pmol primers, 0.2mM (each) dNTPs (Invitrogen Life Technologies), 0.5 units ThermoPrime *Taq* DNA polymerase (Thermo Scientific) and 100ng cDNA in a total volume of 20 μ l. For setup of reactions, appropriate volume of PCR mastermix was initially prepared (consisting of all reagents except DNA) and 19 μ l was dispensed into appropriate number of 0.2ml MicroAmp[®] Reaction Tubes on ice. To this, 1 μ l of 100ng/ μ l DNA was added. Controls were also prepared using nuclease free dH₂O in place of DNA, to ensure no contamination of reagents. Thermal cycles were performed as follows:

94°C	1 min	} 30 cycles
94°C	30 s	
54/52/55/53°C [‡]	30 s	
72°C	60 s	
72°C	7 min	

2.9.3. Agarose Gel Electrophoresis

In order to confirm successful PCR amplification of exons, an aliquot of each reaction was assessed using agarose gel electrophoresis as follows:

2.9.3.1. Gel Preparation

A 2% agarose gel was prepared by melting 700mg of Ultrapure™ agarose (Invitrogen Life Technologies) in 35ml TBE buffer [89mM Tris-HCl pH 8, 89mM boric acid, 2mM EDTA] in a conical flask. This was allowed to cool to 'hand heat' and 3.5 μ l of 1mg/ml ethidium bromide solution was added (final concentration in gel, 0.1 μ g/ml). Ethidium bromide is a DNA intercalating agent which, when exposed to UV light, fluoresces brightly with an orange colour when incorporated in nucleic acids. Its inclusion in the gel therefore allows visualisation of the DNA following separation, as

[‡] See Table 2.6 for annealing temperatures for specific primers.

described below (Section 2.9.3.3). Gel solution was mixed thoroughly, poured into a gel cassette and allowed to set at room temperature.

2.9.3.2. Electrophoresis

The gel cassette was placed in a Sub-Cell® GT Agarose Gel Electrophoresis System (Bio-Rad Laboratories Ltd.) filled with TBE buffer. To allow estimation of the size of PCR products, 5µl of Quick-Load® 100bp DNA Ladder (New England BioLabs (UK) Ltd., Hitchin, UK) was loaded in to the first well. For each reaction, 7µl of PCR products was loaded directly into subsequent wells (loading dye was already present in the ReddyMix PCR buffer). A 7µl aliquot of each control reaction was also loaded into remaining wells to ensure no DNA contamination of reagents. Electrophoresis was performed at 100V for an appropriate length of time, as indicated by the position of the dye front (approximately 45 minutes).

2.9.3.3. Visualisation of DNA

Following electrophoresis, the gel was removed from the cassette and placed in a Gel Doc™ XR (Bio-Rad Laboratories Ltd.) for visualisation of PCR products using a UV light source. The Gel Doc software (Quantity One® V4.5.0) was used to capture an image of the gel and the gel was discarded. Presence of DNA bands of expected size (as estimated using the DNA ladder) confirmed successful PCR reactions.

2.9.4. Cleanup of PCR Products for Sequencing

Cleanup of remaining PCR products (approximately 13µl) for DNA sequencing was performed using a QIAquick® PCR Purification kit (Qiagen) according to manufacturers supplied protocol. Briefly, reaction mixtures are applied to a silica membrane (in spin-column format) which binds double stranded DNA, enabling residual PCR buffer to be washed away using supplied buffers. PCR products were eluted in 20µl buffer EB [10mM Tris-HCl pH 8.5] and concentration was determined using a Nanodrop spectrophotometer, as described above (Section 2.9.1).

Concentration of PCR products was adjusted to 10ng/µl using nuclease-free H₂O and 10µl of each was sent to Source BioScience LifeSciences (Nottingham, UK) (with appropriate primers; see Table 2.6) for forward and reverse sequencing.

2.9.5. Sequence Analysis

Sequences received in FASTA format were viewed using EditSeq (DNASTAR Inc, WI, USA) and compared to published human *N-RAS* and *K-RAS* exon sequences using nucleotide BLAST (<http://blast.ncbi.nlm.nih.gov/Blast.cgi>). Both forward and reverse sequences were analysed to ensure accurate coverage of entire exons. In addition, sequence traces (chromatogram format) were viewed using FinchTV (Geospiza Inc., WA, USA) in order to assess quality of sequence reads.

2.10. In Vitro Mutation Assays

In vitro mutation assays were used to investigate the DNA mutagenic potential of Ara-C (and MNU as a positive control) in an MMR proficient (TK6) and an MMR deficient (TK6 *MSH2i*) cell line (Chapter 6). The principles of the thymidine kinase (TK) and hypoxanthine-guanine phosphoribosyltransferase (HPRT) mutation assays used are described in more detail in Section 6.1. The workflow for setup of the assays is summarised in Figure 2.2 and specific details of each step are described below.

2.10.1. Removal of Spontaneous Mutants using CHAT Medium

Prior to performing mutation assays, cell populations were purged of any existing spontaneous *TK* or *HPRT* mutants by culture in CHAT (cytidine, hypoxanthine, aminopterin, thymidine) medium. Components in CHAT medium (aminopterin) result in cellular inhibition of purine nucleotide biosynthesis, forcing cells to rely on purine salvage pathways (using thymidine or hypoxanthine as substrates). This is therefore cytotoxic to mutants because they lack key components of these pathways.

For each cell line, 5×10^5 cells were centrifuged at 230 x g for 5 min, resuspended in 25ml CHAT medium [RF10 medium supplemented with 10 μ M 2-deoxycytidine, 17.5 μ M thymidine, 200 μ M hypoxanthine and 0.2 μ M aminopterin] and transferred to a 75cm³ cell culture flask. Cultures were incubated at 37°C/5% CO₂ for 48 hours.

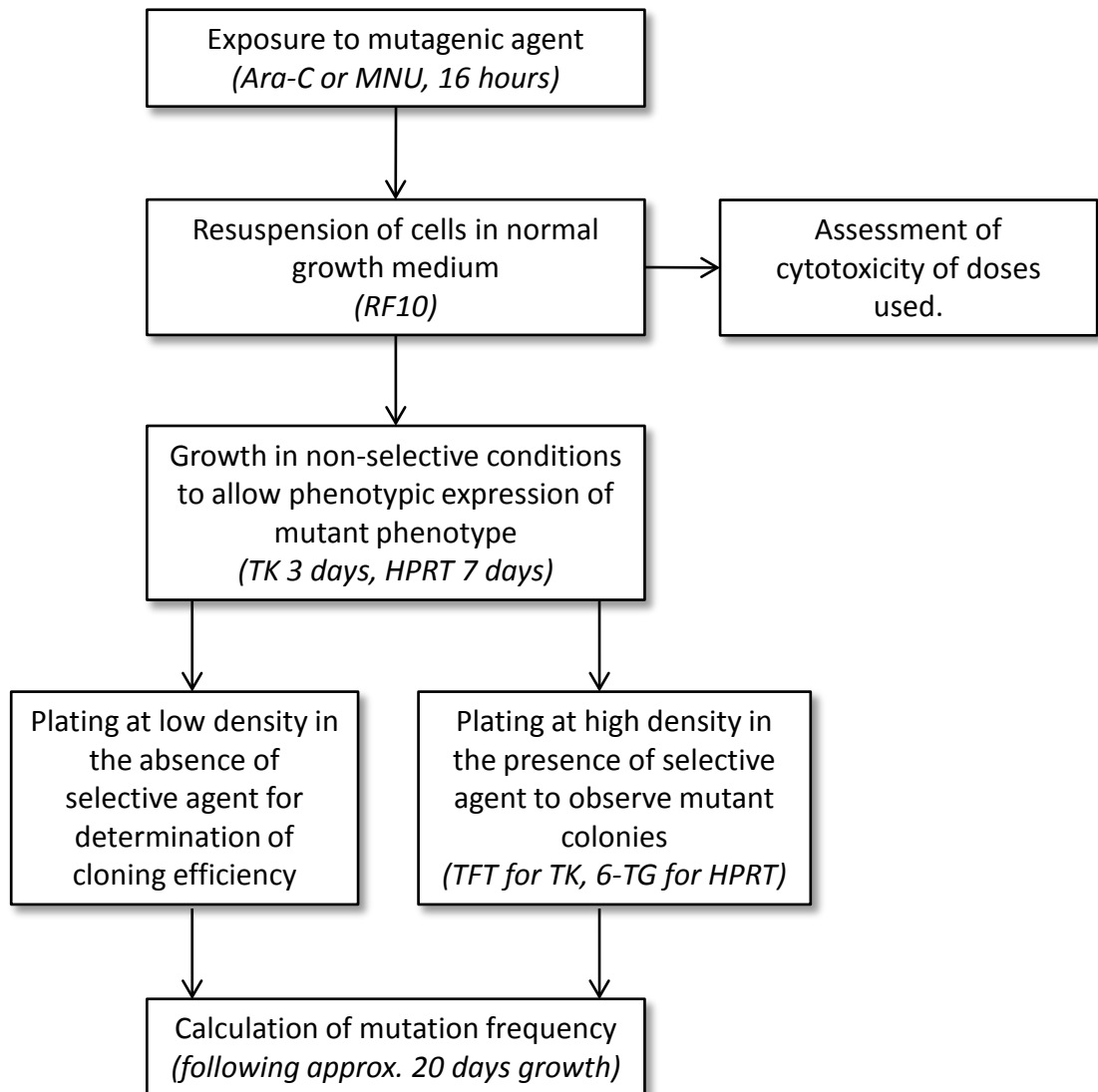


Figure 2.2. General workflow of mutation assays (TK and HPRT) in TK6 cells

Following 48 hours in culture, 5×10^5 viable cells were centrifuged at 230 x g for 5 min and resuspended in sterile PBS to wash cells. Following a second wash in sterile PBS, cells were resuspended in 25ml THC medium [as CHAT medium but without aminopterin] and transferred to a fresh 75cm³ culture flask. Cell cultures in THC medium were incubated at 37°C/5% CO₂ for 72 hours.

Following this culture period, the above procedure was repeated using normal RF10 medium to resuspend cells, which were now ready for immediate use in mutation assays.

2.10.2. Drug Exposure

For each cell line (TK6 and TK6 *MSH2i*), a suspension of exponentially growing cells at a density of 1×10^5 cells/ml was prepared using RF10 medium. For drug dosing, a 50ml aliquot of cell suspension was transferred to a sterile BD Falcon™ centrifuge tube and centrifuged at 230 x g for 5 min. Supernatant was discarded, cells were resuspended in 50ml RF10 medium supplemented with appropriate volume of drug and transferred to 175cm³ cell culture flasks. Each drug dose was prepared in triplicate. In addition, a vehicle-only control (for calculation of spontaneous mutation frequency) was also setup in the same way (in triplicate), by resuspending cells in 50ml RF10 medium supplemented with appropriate solvent but no drug. Cultures were incubated for 16 hours at 37°C/5% CO₂.

Following 16 hours incubation, cell populations were washed twice using sterile PBS, after which appropriate volume of each cell suspension containing 5×10^5 cells was transferred to a sterile Falcon tube for assessment of cytotoxicity as below. Remaining cell suspensions were transferred to sterile 175cm³ cell culture flasks and incubated at 37°C/5% CO₂. Cell suspensions were counted daily and diluted to a density of 4.5×10^5 cells/ml (in a volume of 50ml) as required, using RF10 medium.

2.10.3. Assessment of Cytotoxicity

For each dosed suspension, the aliquot containing 5×10^5 cells was diluted (using RF10 medium) to give a cell suspension at a density of 1×10^5 cells/ml. From this, cell suspensions at 10^4 , 10^3 , 10^2 and 10^1 cells/ml were prepared by 10-fold serial dilution. The 10^1 , 10^2 and 10^3 suspensions were then each transferred to a sterile 96-well cell

culture plate (200µl per well). Plates were incubated at 37°C/5% CO₂ for approximately 20 days.

Following the 20 day growth period, survival fraction at each dose was determined according to Section 2.6.2. Kill curves were generated according to Section 2.6.2, using the mean and SEM of the triplicate results for each dose.

2.10.4. Selection of TK Mutants

TK mutants were selected based on resistance to trifluorothymidine (TFT) following 3 days in culture, the time required for expression of the *TK* mutant phenotype (Liber and Thilly, 1982). The following procedures were performed for all dosed (and control) cell populations:

A cell suspension at a density of 1×10^5 cells/ml (155ml) was established using RF10 culture medium (remainder was returned to the incubator for subsequent selection of *HPRT* mutants). From this suspension, a 5ml aliquot was removed and a 10-fold serial dilution was performed (using RF10 culture medium), to result in a cell suspension at a density of 10^1 cells/ml. This was then transferred to a 96-well culture plate (200µl per well, average 2 cells/well). Plates prepared in this way for each dose were to enable calculation of CE in the absence of selection.

To the remainder of the cell suspension (150ml), 37.5µl of a 4mg/ml TFT solution [prepared using sterile dH₂O immediately prior to use] was added (giving a final TFT concentration of 1µg/ml). Cell suspension was then transferred to 6 96-well culture plates (200µl per well, average 20,000 cells/well). All plates were incubated at 37°C/5% CO₂ for approximately 20 days.

2.10.5. Selection of HPRT Mutants

Seven days in culture following removal of drug is required for expression of the *HPRT* mutant phenotype (Liber and Thilly, 1982). After this time period, *HPRT* mutants were selected based on resistance to 6-TG according to the following procedures:

A cell suspension at a density of 1×10^5 cells/ml (155ml) was established using RF10 culture medium. From this suspension, a 5ml aliquot was removed and a plate for calculation of CE was prepared as above. To the remainder of the cell suspension (150ml), 120µl of a 2.5mg/ml 6-TG solution [prepared using DMSO and filter sterilised

immediately prior to use] was added (giving a final 6-TG concentration of 2µg/ml). Cell suspension was then transferred to 6 96-well culture plates (200µl per well). All plates were incubated at 37°C/5% CO₂ for approximately 20 days.

2.10.6. Calculation of Mutation Frequency

After appropriate time for proliferation of any mutant colonies (approximately 20 days), all plates were assessed microscopically for growth and the number of wells in which a mutant colony had grown was scored per plate. The total number of mutants from the 6 plates setup for each dose was used for calculation of mutation frequency, according to the formula below.

For calculation of CE in the absence of selection, the CE plate prepared for each dose was assessed microscopically and the number of negative wells was determined. CE was calculated according to the formula in Section 2.6.2.

Mutation frequency at each dose was calculated according to Liber and Thilly, (1982) using the following formula:

$$MF = \frac{\text{Total No. Mutant Colonies}}{CE \times \text{Total No. Cells Plated}}$$

All calculations were performed using Microsoft Excel. Bar charts representing the mean and SEM of the triplicate results at each dose in each cell line were prepared using Microsoft Excel. Calculation of induced MF at each drug dose was performed by subtracting the spontaneous MF (i.e. the MF observed in the vehicle-only treated cell population). These values (mean and SEM of triplicate results) were plotted on an X-Y scatter graph (using Microsoft Excel).

2.10.7. Statistical Analysis

One-way and two-way analysis of variance (ANOVA) testing was used as described in Section 6.2.1 to assess effects of drug dose and DNA MMR dysfunction on MF. A significance level of 0.05 was used in all cases. All statistical analyses were performed using Minitab 15 (Minitab Ltd., Coventry, UK) statistical software package.

2.11. Molecular Analysis of *HPRT* Mutants

To investigate particular classes of DNA mutation that Ara-C can induce (Chapter 6), a number of drug-induced (and spontaneous) *HPRT* mutant TK6 colonies from the above assay were selected and subjected to molecular analysis as follows.

2.11.1. Expansion of Mutant Cell Populations

From the *HPRT* mutant TK6 colonies generated with the highest dose of Ara-C (30nM), 40 colonies were selected at random from each of the triplicate drug treatments (120 total). Similarly, 20 mutant colonies generated from the vehicle-only treated (spontaneous) TK6 cells were also randomly selected from each of the triplicate populations (60 total). For each colony selected, the entire contents of the well (approximately 200 μ l) was transferred to a well of a sterile 24-well cell culture plate containing 1ml RF10 medium supplemented with 2 μ g/ml 6-TG. Plates were incubated at 37°C/5% CO₂ and assessed daily for cell growth (indicated by a change in colour of culture medium and confirmed microscopically). As required, another 1ml of RF10 medium supplemented with 2 μ g/ml 6-TG was added to each well. Once sufficient cell numbers were generated (after approximately 7 days in culture), as estimated microscopically, each population was divided equally into 2 and washed cell pellets were prepared according to Section 2.3.5 (without performing cell counts) and stored at -80°C.

2.11.2. Multiplex PCR for *HPRT* Exon Deletions

2.11.2.1. DNA Extraction

For each *HPRT* mutant, one of the cell pellets was used for DNA extraction, quantitation and dilution to 100ng/ μ l according to Section 2.9.1, for use in genomic multiplex PCR reactions.

Exon	Primer Sequences	Amplicon Length (bp)
1	Forward: TGGGACGTCTGGTCCAAGGATTCA Reverse: CCGAACCCGGGAAACTGGCCGCCC	627
2	Forward: TGGGATTACACGTGTGAACCAACC Reverse: GACTCTGGCTAGAGTTCCTTCTTC	572
3	Forward: CCTTATGAAACATGAGGGCAAAGG Reverse: TGTGACACAGGCAGACTGTGGATC	1059
4	Forward: TAGCTAGCTAACTTCTCAAATCTTCTAG Reverse: ATTAACCTAGACTGCTTCCAAGGG	335
5	Forward: CAAATCCCAGCAGATGGGCCACTTG Reverse: TCACTCCTTTAGAACACAAGCCCAC	317
6	Forward: GACAGTATTGCAGTTATACATGGGG Reverse: CCAAATCCTCTGCCATGCTATTC	443
7/8	Forward: GATCGCTAGAGCCCAAGAAGTCAAG Reverse: TATGAGGTGCTGGAAGGAGAAAAC	1535
9	Forward: GAGGCAGAAGTCCCATGGATGTGT Reverse: CCGCCCAAAGGGAAGTACTGATAGTC	1279

Table 2.7. Sequences of oligonucleotide primers used for multiplex PCR amplification of *HPRT* exons.

^a Due to the close proximity of exons 7 and 8, they are co-amplified in a single amplicon.

2.11.2.2. Multiplex PCR Setup

Sequences of primers for PCR amplification of all 9 *HPRT* exons were obtained from Gibbs et al., (1990) and are shown in Table 2.7. Primers were ordered from Sigma-Aldrich, reconstituted to 100pmol/ μ l using TE buffer upon receipt and stored at -20°C. Working stocks of primers at a concentration of 10pmol/ μ l were prepared using nuclease-free dH₂O and stored at 4°C.

25x concentrated multiplex PCR buffer was prepared according to Gibbs et al., (1990) and consisted of 1.675M Tris-HCl pH 8.8, 170 μ M EDTA, 125mM β -mercaptoethanol, 415mM ammonium sulphate ((NH₄)₂SO₄) and 167.5mM MgCl₂. Sufficient volume for all reactions was prepared in advance and stored at 4°C.

PCR amplification of *HPRT* exons was performed in 2 multiplex reactions. Reaction 1 contained primers for exons 1, 3, 4, 7/8 and 9. Reaction conditions were 1x multiplex PCR buffer (67mM Tris-HCl pH 8.8, 6.8 μ M EDTA, 5mM β -mercaptoethanol, 16.6mM (NH₄)₂SO₄, 6.7mM MgCl₂), 10% (v/v) DMSO, 10pmol exon 1 primers, 16pmol exon 3 primers, 25pmol exon 4 primers, 18pmol exon 7/8 primers, 16pmol exon 9 primers, 1.5mM (each) dNTPs, 4 units ThermoPrime *Taq* DNA polymerase and 250ng genomic DNA in a total volume of 40 μ l. Reaction 2 contained primers for exons 2, 5 and 6. Reaction conditions were 1x multiplex PCR buffer, 10% (v/v) DMSO, 20pmol exon 2 primers, 20pmol exon 5 primers, 10pmol exon 6 primers, 1mM (each) dNTPs, 4 units ThermoPrime *Taq* DNA polymerase and 250ng genomic DNA in a total volume of 30 μ l.

For setup of PCR reactions, appropriate volume of PCR mastermix was prepared (containing all reagents except template DNA) and appropriate volume was dispensed into appropriate number of wells of an Abgene® PCR Plate (Thermo Scientific) on ice. An appropriate volume of 100ng/ μ l DNA was then added. Controls were also prepared using nuclease free dH₂O in place of DNA, to ensure no contamination of reagents. Thermal cycles (identical for both reactions) were performed as follows:

94°C	4.5 min	} 28 cycles
94°C	30 s	
61°C	50 s	
68°C	60 s	
68°C	7 min	

2.11.2.3. Analysis of PCR Products

1.4% agarose gels were prepared by melting 1.4g of Ultrapure™ agarose in 100ml TBE buffer. Following cooling to 'hand heat', 10µl of 1mg/ml ethidium bromide solution was added (final concentration in gels, 0.1µg/ml). Gel solutions were mixed thoroughly, poured into large gel cassettes and allowed to set at room temperature.

Gel cassettes were placed in Sub-Cell® GT Agarose Gel Electrophoresis Systems filled with TBE buffer. To allow estimation of the size of PCR products, 5µl of Quick-Load® 100bp DNA Ladder was loaded in to the first well of each gel. For each reaction, 10µl of PCR products was mixed with 2µl of Blue/Orange Loading Dye 6x (Promega UK, Southampton, UK) and loaded into the gel. Products from reaction 1 and 2 were loaded side by side for each mutant. Control reactions were loaded in the same way into the last wells of each gel. Electrophoresis was performed at 100V for an appropriate length of time, as indicated by the position of the dye front (approximately 45 minutes).

Gels were visualised and images captured for analysis according to Section 2.9.3.3. Exon deletions were determined based on absence of bands of expected size (see Figure 6.4 for a representative gel image).

2.11.3. Sequencing of HPRT cDNA for Detection of Point Mutations

2.11.3.1. RNA Extraction and cDNA Preparation

For each *HPRT* mutant which did not demonstrate exon deletion, the remaining cell pellet was used for total RNA extraction, quantitation and dilution to 200ng/µl according to Section 2.8.1. Reverse transcription to generate cDNA (at a concentration of 100ng/µl) from total mRNA was performed according to Section 2.8.2.

2.11.3.2. Amplification and Sequencing of HPRT cDNA

Sequences of PCR primers for amplification of *HPRT* cDNA were obtained from Meng et al., (2002) and were as follows:

Forward: CCTGAGCAGTCAGCCCGCGC

Reverse: CAATAGGACTCCAGATGTTT

Primers were ordered from Sigma-Aldrich, reconstituted to 100pmol/ μ l using TE buffer upon receipt and stored at -20°C. Working stocks of primers at a concentration of 10pmol/ μ l were prepared using nuclease-free dH₂O and stored at 4°C.

PCR reaction conditions were 1x ReddyMix PCR buffer, 1.5mM MgCl₂, 10pmol primers, 0.2mM (each) dNTPs, 0.5 units ThermoPrime *Taq* DNA polymerase and 100ng cDNA in a total volume of 20 μ l. For setup of PCR reactions, an appropriate volume of PCR mastermix was prepared and appropriate volume was dispensed into an appropriate number of wells of an Abgene® PCR Plate on ice. Appropriate volume of cDNA was added. Controls were also prepared using either a blank reverse transcription reaction or nuclease free dH₂O in place of cDNA, to ensure no contamination of reagents. Thermal cycle was as follows:

94°C	1 min	} 36 cycles
94°C	30 s	
55°C	30 s	
72°C	45 s	
72°C	7 min	

To confirm successful amplification of *HPRT* cDNA, an aliquot of each reaction (7 μ l) was assessed using agarose gel electrophoresis according to Section 2.9.3. The remainder of PCR products were prepared and sent for sequencing to Source BioScience LifeSciences according to Section 2.9.4. Sequence analysis was performed according to Section 2.9.5.

2.11.4. Amplification of *HPRT* Exons for Sequencing of Putative Splice Mutants

Primers used for multiplex PCR amplification of *HPRT* exons (Table 2.7) are designed to also amplify sequences directly flanking exons, hence can be used to amplify individual *HPRT* fragments for sequencing of splice sites. Exons 7 and 8 and their associated splice sites were amplified and sequenced from genomic DNA in a number of *HPRT* mutants as follows:

Reaction conditions for PCR amplification consisted of 1x ReddyMix PCR buffer, 1.5mM MgCl₂, 10pmol primers, 0.2mM (each) dNTPs, 0.5 units ThermoPrime *Taq* DNA polymerase and 100ng genomic DNA in a total volume of 20 μ l. For setup of PCR reactions, appropriate volume of PCR mastermix was prepared and appropriate volume was dispensed into appropriate number of 0.2ml MicroAmp® Reaction Tubes on ice. Appropriate volume of genomic DNA was added. A control was also prepared

using nuclease free dH₂O in place of DNA, to ensure no contamination of reagents.

Thermal cycle was as follows:

94°C	2 min	} 36 cycles
94°C	30 s	
56°C	30 s	
72°C	90 s	
72°C	7 min	

To confirm successful amplification, an aliquot of each reaction (7µl) was assessed using agarose gel electrophoresis according to Section 2.9.3. The remainder of PCR products were prepared and sent for sequencing to Source BioScience LifeSciences according to Section 2.9.4. Sequence analysis was performed according to Section 2.9.5.

2.11.5. Calculation of Absolute and Ara-C-Induced Mutant Fractions

Following characterisation, *HPRT* mutants were grouped into classes (point mutations (including splice site mutations), internal exon deletions, 3' partial gene deletions, 5' partial gene deletions or complete deletions) and the frequency of each class of mutation was used to estimate the fraction of total *HPRT* mutants represented by each class (i.e. the absolute mutant fraction). The following calculation was performed for each class of mutation for both the spontaneous and Ara-C-treated mutant populations:

$$\text{Absolute mutant fraction} = \% \text{ mutants in class} \times \text{mean MF}^{\S}$$

From these results, the fraction of each class of mutation which was attributable to Ara-C (i.e. the Ara-C-induced mutant fraction) was estimated by subtraction of the spontaneous absolute mutant fractions from the Ara-C-treated absolute mutant fractions for each mutation class.

Absolute mutant fractions (spontaneous and Ara-C-treated) and Ara-C-induced mutant fractions for each class of mutation were plotted on a stacked bar graph (using Microsoft Excel) in order to demonstrate the *HPRT* mutational spectra (see Figure 6.8).

[§] Refers to the mean MF observed at 30nM Ara-C (or at 0nM Ara-C in the case of spontaneous mutants) (see Section 2.10.6).

2.11.6. Statistical Analysis

A Chi-squared test was performed to determine if there was any significant difference between the overall spectra of Ara-C induced and spontaneously occurring *HPRT* mutants, as described in Section 6.2.3.4. Fisher's exact testing was used to determine whether the frequencies of specific classes of mutant differed significantly between Ara-C induced and spontaneous mutants. A significance level of 0.05 was used in all cases. Bonferroni correction was applied in cases where multiple tests were performed on the same data. All statistical analyses were performed using Minitab 15 statistical software package.

2.12. Leukaemic Blast Quantitation and Enrichment from AML Patient Samples

Matched presentation and relapsed material (cryopreserved mononuclear cells purified from peripheral blood) from a number of adult AML patients was received from the Newcastle Haematology Biobank (Newcastle University, REC reference 07/H0906/109) for investigation of the clonal origins of relapsed AML via comparative SNP array analysis (Chapter 7). Prior to extraction and preparation of DNA for SNP array analysis (see Section 2.13 below), it was necessary to determine the percentage of leukaemic blasts in AML patient samples to ensure sufficient purity for array analysis. In cases where the percentage of leukaemic blasts was below the required threshold (85%), blasts were purified from the sample. The following processes were performed for AML patient samples at both presentation and relapse:

2.12.1. Immunophenotyping

Immunophenotyping is a technique used to identify and characterise cells according to lineage and stage of differentiation based on the expression of particular surface or intracellular markers. The process involves labelling of specific markers, commonly cluster of differentiation (CD) antigens, using fluorescence-conjugated monoclonal antibodies which can then be quantified by flow cytometry. Flow cytometry allows rapid analysis of fluorescently labelled markers, as well as other characteristics of single cells suspended in a stream of fluid as they pass through a beam of light (emitted by a laser). Emitted light signals are detected and digitised for computer analysis.

Immunophenotyping was used to quantitate the leukaemic blast population in each patient sample, based on the expression of CD33 and CD34 antigens (use of these particular antigens is described in Section 7.2.2) as follows:

2.12.1.1. Antibody Labelling

Fluorescence-conjugated monoclonal antibodies used for immunophenotyping are listed in Table 2.8.

For antibody labelling of cells, cryopreserved mononuclear cells were rapidly thawed and transferred to 5ml pre-warmed RF10 culture medium. Cells were centrifuged at 230 x g for 5 min and resuspended in 5ml RF10 culture medium. Viable cells were counted using a haemocytometer and trypan blue dye (Section 2.3.2), following which 2×10^5 cells were dispensed into 2 BD Falcon™ capped polystyrene tubes (remaining cell suspension was incubated at 37°C/5% CO₂).

Cells were centrifuged at 450 x g for 4 min, supernatant was discarded and cells were resuspended in 100µl sterile PBS. To the first tube, 10µl each of CD34-FITC, CD33-PE and CD45-PerCP antibodies were added. To the second tube, 10µl each of the 3 isotype controls (see Table 2.8) were added in order to determine background levels of fluorescence and optimise flow cytometer settings, described below. Tubes were incubated in the dark at room temperature for 15 min.

Following incubation, cells were washed by addition of excess PBSA [Dulbecco's PBS (Invitrogen Life Technologies) containing 0.2% (w/v) BSA] and centrifuged at 450 x g for 4 min. Supernatant was discarded, wash step was repeated and cells were finally resuspended in 400µl PBSA.

Antibody	Clone	Isotype	Conjugate^a	Supplier	Cat No.
CD45	2D1	Mouse IgG ₁	PerCP	BD Biosciences	345809
CD33	AC104.3E3	Mouse IgG ₁	PE	Miltenyi Biotec	130-091-732
CD34	AC136	Mouse IgG _{2a}	FITC	Miltenyi Biotec	130-081-001
Mouse IgG ₁ isotype control	X40	Mouse IgG ₁	PerCP	BD Biosciences	345817
Mouse IgG ₁ isotype control	IS5-21F5	Mouse IgG ₁	PE	Miltenyi Biotec	130-092-212
Mouse IgG _{2a} isotype control	S43.10	Mouse IgG _{2a}	FITC	Miltenyi Biotec	130-091-837

Table 2.8. Fluorescence-conjugated antibodies used in flow cytometric assessment of blast immunophenotype.

^a PerCP, peridinin chlorophyll protein; PE, phycoerythrin; FITC, fluorescein isothiocyanate.

2.12.1.2. Flow Cytometry

Flow cytometry was kindly performed by J. Irving (NICR) using a FACSCalibur flow cytometer with BD CellQuest Pro software. Prior to analysis of fluorescently-labelled cell surface markers, for each sample the isotype control mixture was used to optimise instrument settings (adjust voltages of fluorescence detectors to remove background fluorescence and adjust compensation settings for overlap of fluorescent spectra). Following optimisation, a total of 10,000 cells were assessed from the antibody-labelled cell sample.

For determination of blast percentage in the sample, cell debris and dead cells were first excluded based on forward and side scatter signals. Any residual red blood cells in the sample were then excluded based on lack of expression of CD45 (i.e. no detected PerCP fluorescence). Percentage of leukaemic blasts in the remaining cell population was determined based on positive expression of CD33 and/or CD34 (by detection of PE and FITC fluorescence, respectively).

2.12.2. Magnetic-Activated Cell Sorting

Magnetic Activated Cell Sorting (MACS[®]) is a method by which cells can be separated based on expression of specific cell surface markers. Cells are first labelled with magnetic MicroBeads specific for the marker of choice, following which cell suspension is loaded onto a MACS Column placed in the magnetic field of a MACS Separator. Magnetically labelled cells are retained on the column whilst unlabelled cells are washed through (the negative fraction). Removal of the column from the magnetic field allows elution of the labelled cells (the positive fraction). For this investigation, MACS was used for positive selection of CD33+ or CD34+ AML blasts from patient samples in which the blast percentage of the sample determined by immunophenotyping was less than the threshold required for SNP array analysis (85%).

2.12.2.1. MicroBead Labelling

CD33 and CD34 MicroBeads were purchased from Miltenyi Biotec (Bisley, UK) and stored at 4°C for use as required. For labelling of cells, cell populations were centrifuged at 300 x g for 10 min, supernatant was completely removed and cells were

resuspended in appropriate volume of MACS buffer [PBS pH 7.2, 0.5% (w/v) BSA, 2mM EDTA] according to manufacturer's protocol. Appropriate volume of either CD33 or CD34 MicroBeads was added and suspensions were incubated at 4°C for 15 min. Following incubation, cells were washed by the addition of excess MACS buffer, centrifuged at 300 x g for 10 min and resuspended in 500µl MACS buffer.

2.12.2.2. Cell Separation

MACS MS Columns were purchased from Miltenyi Biotec. MACS Separators were kindly provided by H. McNeill (NICR).

For separation of labelled cells, a MACS Column was placed into a MACS Separator and rinsed with 500µl MACS buffer. Cell suspension was then applied to the column and unlabelled cells which passed through were collected. Column was then washed 3 times using 500µl MACS buffer. Following washing, column was removed from the MACS separator, immediately placed on a sterile collection tube and 1ml MACS buffer was added in order to elute labelled cells.

Due to the limited nature of patient material, separation efficiency could not be assessed on a case by case basis. It was deemed with confidence however, that separation efficiency would be high (> 98%) based on the results of a preliminary investigation in which a CD33+ cell line (KG-1) was efficiently separated from a mixture of CD33- cells (EoL-1) (data not shown).

2.12.3. Storage of Cell Populations

Remaining cell populations (either whole populations or separated fractions as appropriate) were divided equally between two sterile 1.5ml Eppendorf tubes and microfuged at 230 x g for 5 min. For one pellet, supernatant was completely removed and the pellet was stored at -80°C for future DNA extraction. For the other pellet, supernatant was removed and cells were resuspended in 350µl Buffer RLT (Qiagen) supplemented with 1% (v/v) β-mercaptoethanol for storage at -80°C (in order to preserve RNA integrity for possible future investigation of gene expression).

2.13. SNP Array Analysis

SNP arrays were performed on matched presentation and relapsed AML samples in order to investigate clonal evolution of relapsed AML (Chapter 7). SNP arrays assess the expression of both SNPs and non-polymorphic sites distributed throughout the entire genome using probes hybridised to a chip. This data can be used to demonstrate copy number aberrations (CNAs) in individual patient samples, indicated by deletion or amplification of particular probes. It can also reveal regions of copy-neutral loss of heterozygosity (cn-LOH) (also referred to as acquired uniparental disomy (UPD)) by comparison of SNP genotype to those of either matched germline DNA (if available) or a pooled reference sample.

SNP arrays were performed offsite by Almac Diagnostics Ltd (Craigavon, UK) using the Affymetrix SNP 6.0 platform. The SNP 6.0 array includes more than 906,600 SNPs and 946,000 non-polymorphic probes, representing the highest level of detection of genetic variation currently available.

2.13.1. Preparation of DNA for SNP Array

Frozen cell pellets (see Section 2.12.3) were thawed and DNA was extracted using a QIAamp DNA Mini Kit (with DNA eluted in 50µl of buffer AE) and quantitated using a Nanodrop ND-1000 spectrophotometer as described in Section 2.9.1. For each sample a minimum of 10µl of DNA at a concentration above 100ng/µl was analysed (this required vacuum concentration of DNA samples in some cases using a Genevac SF50 Vacuum centrifuge (Genevac Ltd., Ipswich, UK)).

2.13.2. Data Analysis

Raw array-generated data in the form of .CEL files were received from Almac Diagnostics Ltd. Processing of raw data to identify CNAs and regions of cn-LOH in each sample was kindly performed by V. Rand (NICR) using Genotyping Console v4.0 (Affymetrix, CA, USA).

The workflow for data processing briefly involved initial generation of SNP genotype calls using the birdseed v2 algorithm (performed using all 14 samples in one batch to maximise efficiency of the clustering algorithm). This was followed by quantile

normalisation of data and copy number (CN) and LOH analyses (via Hidden Markov Model) using default software settings (with regional GC correction applied). HapMap270 data (SNP genotype calls for the 270 normal samples which comprise the International HapMap project) was used as a reference model for LOH analysis given that matched germline DNA was not available for the patients included in the study. Segment analysis of CN data was performed to identify regions of CNA (with detection thresholds set to exclude regions smaller than 100kb) and involving fewer than 5 markers). Detected regions of CNA which mapped to regions of known (published) genetic variation were identified by the software (using annotations obtained from the Database of Genomic Variants [<http://projects.tcag.ca/variation/>]) and were excluded from further analysis.

Remaining CNAs and regions of LOH were compared in matched presentation and relapsed samples from individual patients using Affymetrix Genotyping Console Browser (v1.0.12). This also allowed identification of genes within affected regions (of CNA or LOH) based on annotations taken from the NCBI RefSeq database.

Quality control assessment of data was performed by determination of call rate at control SNPs (median 96.93%, range 94.34 – 99.21) and by measurement of concordance between presentation and relapse samples in individual patients (median 99.23%, range 98.41 – 99.78).

**Chapter 3. Loss of DNA MMR Components Mediates Response
to Chemotherapeutic Nucleoside Analogues *in vitro***

3.1. Introduction

Ara-C is a nucleoside analogue used extensively in the treatment of AML. Its major mode of cytotoxicity involves incorporation of Ara-CTP into replicating DNA, leading to chain termination via inhibition of further polymerisation, as described in Section 1.5.2.1. Despite this, there is evidence from cell-free systems that chain termination is not 100% efficient and that chain extension can occur following Ara-CTP incorporation (Ohno et al., 1988). The presence of Ara-C residues at internucleotide linkage positions in leukaemic cells from treated patients and leukaemic cell lines treated *in vitro* (Major et al., 1981), provides further evidence of incorporation and extension.

Certain antimetabolites which, like Ara-C, are metabolised to DNA precursors, are incorporated within DNA whereupon they represent substrates for DNA MMR components (MutS α) due to their miscoding properties. The most noted examples are the base analogues 6-TG and 5-FU, as described in Sections 1.2.1.2 and 1.2.2.1, respectively. Paradoxically, although DNA MMR mediates repair of accidental polymerase-mediated errors arising during normal DNA replication, in the case of drug-induced lesions, the MMR system initiates cell cycle arrest and apoptosis following their detection. Cells with dysfunctional DNA MMR, due to loss of key pathway components, lack the capacity to recognise or respond to lesions occurring due to the incorporation of 6-TG or 5-FU into DNA. Consequently cell cycle arrest and apoptosis are not initiated, leading to cell survival, but at the expense of an increased mutation rate due to tolerance of the lesions in the genome.

Cellular resistance to cisplatin and IR, which are not themselves incorporated into DNA, but cause damage via the formation of crosslinks and/or strand breaks, can also be conferred by loss of certain DNA MMR components (see Sections 1.2.3.1 and 1.2.4.1). The DNA MMR pathway cannot directly process these lesions however, illustrating that MMR components probably have roles in signalling DNA damage and initiating checkpoint responses unique from their roles in classical mismatch repair.

Although originally proposed as a mechanism by which cells acquire resistance to DNA damaging drugs (Irving and Hall, 2001), emerging *in vitro* evidence suggests that loss of DNA MMR components may in fact also be able to confer increased sensitivity to the cytotoxic effects of certain chemotherapeutic agents. One such example is

methotrexate (MTX), the primary cytotoxic effect of which is through inhibition of folate metabolism (see Section 4.1 for further details). In addition to its major cytotoxic mechanism, MTX can also induce 8-oxo-G lesions in DNA (Martin et al., 2009). Persistence of these lesions in the DNA of MSH2-deficient cells increases cytotoxicity, presumably due to increased mutational load (Martin et al., 2009), which is consistent with the purported role of DNA MMR in 8-oxo-G repair (described in Section 1.2.4.2). Similarly curcumin, a dietary pigment showing promise in clinical trials for colorectal cancer (Chauhan, 2002), is also selectively cytotoxic to MSH2 (or MLH1) deficient cells through the induction of oxidative damage (Jiang et al., 2010). In this case, the purported mechanism involves loss of a DNA MMR-dependent checkpoint response following conversion of oxidative damage to DSBs, the result being extensive cell death due to mitotic catastrophe (Jiang et al., 2010).

Gemcitabine (2',2'-difluorodeoxycytidine)-induced cytotoxicity can also be modulated by cellular mismatch repair status. Like Ara-C, gemcitabine is a 2'-deoxycytidine analogue which is active in a broad spectrum of solid tumours including pancreatic and bladder cancer (Burriss et al., 1997; von der Maase, 2000). Gemcitabine is metabolised by the same cellular mechanisms as Ara-C, resulting in accumulation of its triphosphate (dFdCTP) which competes with dCTP for incorporation into DNA (Huang et al., 1991). Whereas Ara-C is primarily a chain terminating agent, treatment of human lymphoblastoid cell lines with gemcitabine demonstrates that greater than 90% of dFdCTP is incorporated at internal positions in DNA (Huang et al., 1991). Furthermore, template assays reveal that DNA polymerases can extend from dFdCTP lesions with greater efficiency than is observed for Ara-C (Richardson et al., 2004), suggesting gemcitabine is a weaker chain terminator. One study has demonstrated that cells deficient in either MSH2 or MLH1 are hypersensitive to the cytotoxic effects of gemcitabine compared to MMR-proficient counterparts, although a mechanism has yet to be established (Takahashi et al., 2005).

3.1.1. Aims of Chapter 3

Despite the DNA damaging nature of Ara-C, there have been no published studies which have determined whether MMR components can interact with incorporated Ara-C nucleotides, or whether cellular DNA MMR status can mediate response to the drug either *in vitro* or *in vivo*. The objectives of the studies described in

this chapter were therefore to determine whether loss of key components of the DNA MMR pathway can affect *in vitro* response to the cytotoxic effects of Ara-C, similar to other antimetabolites. This was investigated using an established MMR proficient and deficient cell line pair, and cells in which DNA MMR components have been 'knocked down' using shRNA-mediated RNA interference.

Specifically, the experimental aims of this chapter were as follows:

- In the MMR-deficient cell line MT-1, determine the exact nature and extent of defects of the DNA MMR pathway at protein and gene expression levels.
- Determine whether loss of MMR function in MT-1 affects response to treatment with Ara-C, and other therapeutic nucleoside analogues, using cytotoxicity assays.
- Generate isogenic MMR-deficient cell lines using shRNA-mediated gene interference and determine whether loss of MMR function affects response to treatment with Ara-C, and other therapeutic nucleoside analogues.

3.2. Results

3.2.1. Phenotypic Characterisation of the MMR-Defective Cell Line MT-1

MT-1 is a subclone of the B-lymphoblastoid cell line TK6. It was generated in 1986 by exposure of the parental cell line to the potent acridine mutagen, ICR-191, resulting in cells highly resistant to killing, but hypermutable by the methylating agent, MNNG (Goldmacher et al., 1986). This phenotype was later attributed to dysfunction of the DNA MMR pathway when it was found that MT-1 was unable to repair base:base mispairs (Kat et al., 1993). Subsequently, MT-1 was found to possess 2 different missense mutations, one in each allele of the gene coding for the MutS α component, MSH6, accounting for the MMR-deficient phenotype (Papadopoulos et al., 1995).

3.2.1.1. Expression Levels of MMR Proteins Determined by Western Immunoblotting

To further characterise the MMR-deficient phenotype of MT-1, western immunoblotting was performed to determine the levels of the MMR proteins, MSH2, MSH3 and MSH6, which form the heterodimeric MutS α and MutS β damage recognition complexes (Figure 3.1A). MT-1 expressed almost negligible levels of MSH6 compared to parental TK6 cells. This was accompanied by a slight reduction in MSH2 but no difference in MSH3. MSH6 heterodimerises with MSH2 to form the MutS α complex; loss of MSH6 causes deficiency of the MutS α complex in the MT-1 cell line, resulting in a proportion of partnerless MSH2 which is likely susceptible to proteolysis, explaining the concomitant reduction in MSH2 levels.

The MutL α complex is a heterodimer of MLH1 and PMS2. The levels of these proteins were also assessed in MT-1 via western immunoblotting, with no difference observed for either protein compared to parental TK6 cells (Figure 3.1B).

MGMT is responsible for removal of methyl groups from O⁶-meG lesions which occur as a result of exposure to methylating agents (Margison and Santibanez-Koref, 2002). Loss of MGMT expression correlates with increased sensitivity to the cytotoxic effects of methylating agents (Yarosh et al., 1983). Furthermore, reactivation of MGMT has been demonstrated as a mechanism by which cells can acquire resistance to these agents (Hampson et al., 1997). TK6 is deficient in MGMT due to hypermethylation of

the promoter region of the gene (Danam et al., 2005). Western immunoblotting confirmed lack of MGMT protein in TK6 and demonstrated that MT-1 also lacks the protein (Figure 3.1C).

3.2.1.2. Expression Levels of MMR Genes Determined by Quantitative RT-PCR

In addition to characterisation of MMR components at the protein level, quantitative RT-PCR was performed to assess gene expression in MT-1 relative to parental TK6 cells (Figure 3.2). Expression of *MSH2*, *MSH3* and *MSH6* was not significantly different in MT-1 cells relative to TK6. Bi-allelic *MSH6* mutation in MT-1 therefore does not affect transcription, and loss of expression is presumably due to an inability to produce functional *MSH6* at the translational level. Similarly, reduction in *MSH2* in MT-1 appears not to be due to down-regulated expression, suggesting that degradation of partnerless protein occurs as stated above.

Relative expression of *PMS2* was also unchanged in MT-1 cells, however an apparent reduction in the expression of *MLH1* was observed (Figure 3.2). The significance of this finding remains unclear given that the levels of the *MLH1* protein were not altered in MT-1 relative to the parental TK6 line (see Figure 3.1B).

Quantitative RT-PCR of *MGMT* indicated a complete lack of expression in both TK6 and MT-1, presumably due to the methylation of the promoter which blocks transcription.

3.2.1.3. Cytotoxicity in Response to MNU and 6-TG

Tolerance to the cytotoxic effects of methylating agents and 6-TG is a hallmark of MMR deficiency (Karran, 2001). To confirm the MMR-deficient phenotype of MT-1, cytotoxicity in response to treatment with the methylating agent, MNU and 6-TG was compared in MT-1 and parental TK6 cells via 96-well clonogenic assay, as described in Section 2.6.2. MT-1 demonstrated increased tolerance to the cytotoxic effects of MNU (Figure 3.3A) and 6-TG (Figure 3.3B) relative to parental TK6 cells. This was consistent with previous reports of tolerance to these agents in MT-1 (Goldmacher et al., 1986; Kat et al., 1993) and the observed loss of MutS α activity.

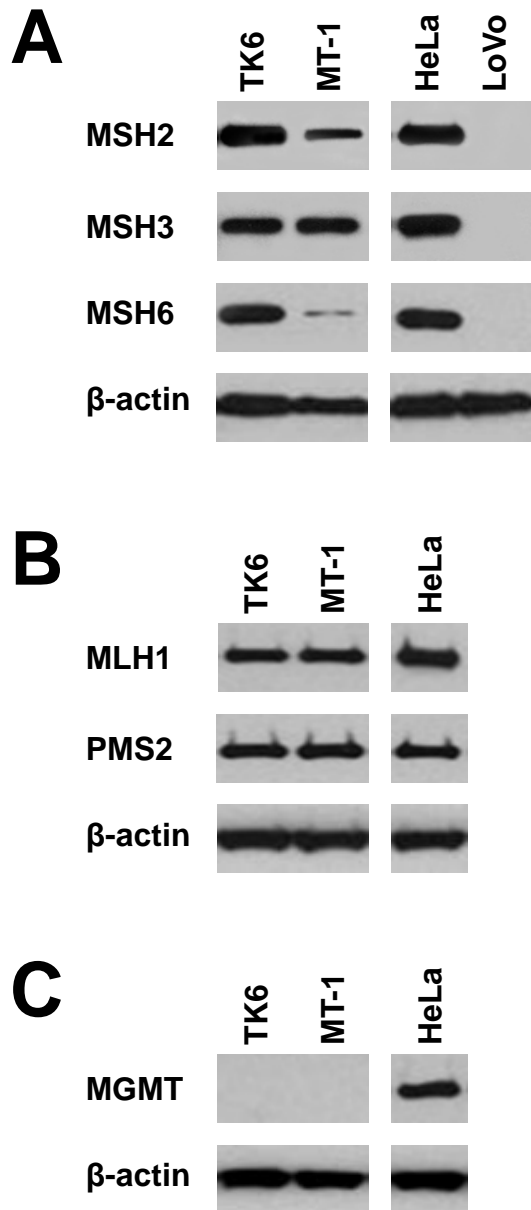


Figure 3.1. MMR protein expression in TK6 and MT-1 cell lines.

Western immunoblotting was performed to determine protein expression of DNA MMR components in the MMR-proficient cell line TK6 and its MMR-deficient subclone MT-1 as follows: **A.** MutS components (MSH2, MSH3 and MSH6). **B.** MutL α components (MLH1 and PMS2). **C.** MGMT. The MMR proficient HeLa cell line was included as a positive control in each case. The MutS deficient LoVo cell line was included as a negative control in the case of MSH2, MSH3 and MSH6. β -actin was used as a loading control for all blots. Each blot is representative of three independent experiments.

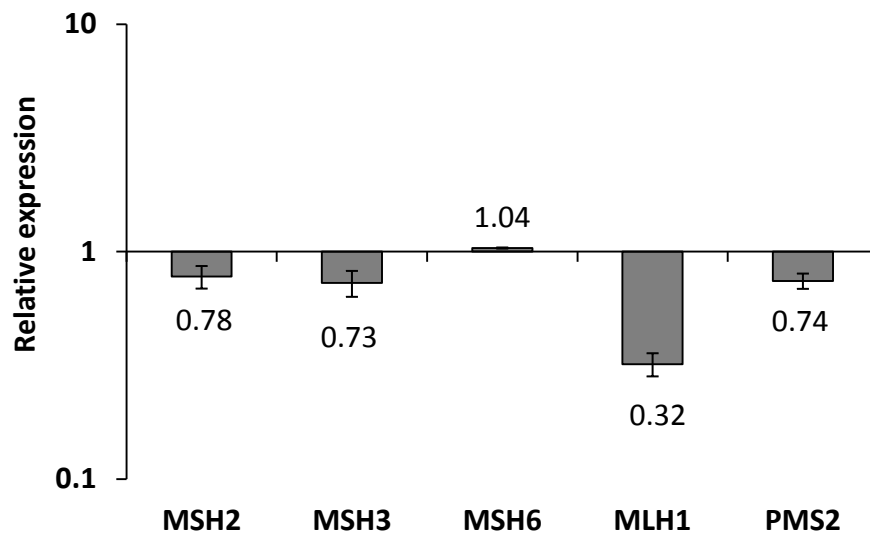


Figure 3.2. Relative expression of DNA MMR components in MMR-deficient MT-1 cells.

RT-PCR was performed to determine changes in gene expression of the MutS (*MSH2*, *MSH3* and *MSH6*) and MutL (*MLH1* and *PMS2*) components in MMR-defective MT-1 cells relative to parental MMR-proficient TK6 cells. Expression of each gene was calculated relative to the parental cell line with the expression of β -actin used as endogenous control. Values represent fold change in expression calculated from the mean and standard error of three independent experiments.

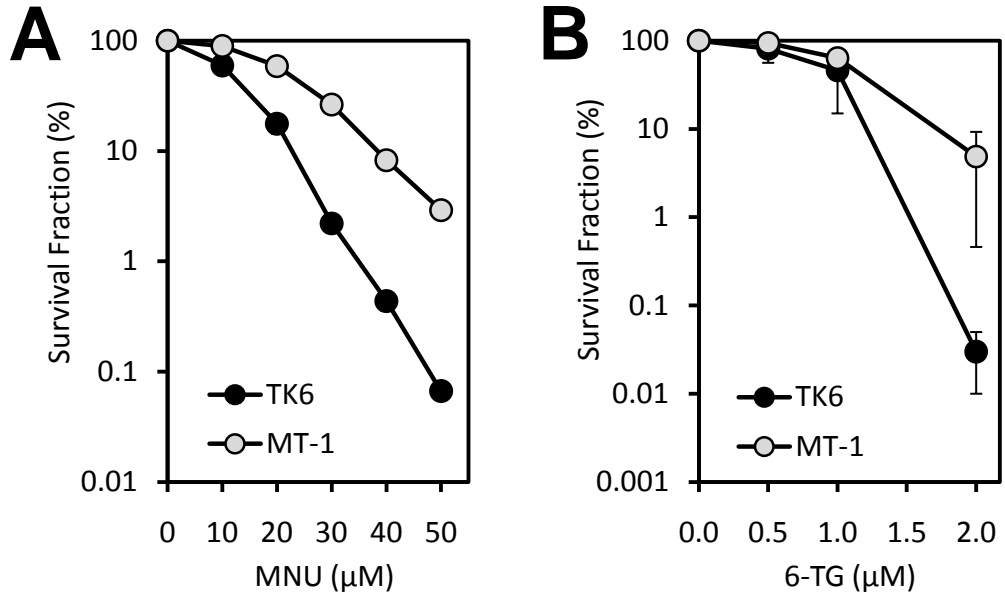


Figure 3.3. Cytotoxicity in response to MNU and 6-TG in TK6 and MT-1 cell lines.

Cell survival in response to MNU (A) and 6-TG (B) was compared in MMR-proficient TK6 cells (black circles) and MMR-deficient MT-1 cells (grey circles) via clonogenic assay. Data is presented as the number of viable colonies from dosed cell suspensions as a percentage of the number of viable colonies from vehicle-only treated cell suspensions. Data represents the mean and standard error of three independent experiments.

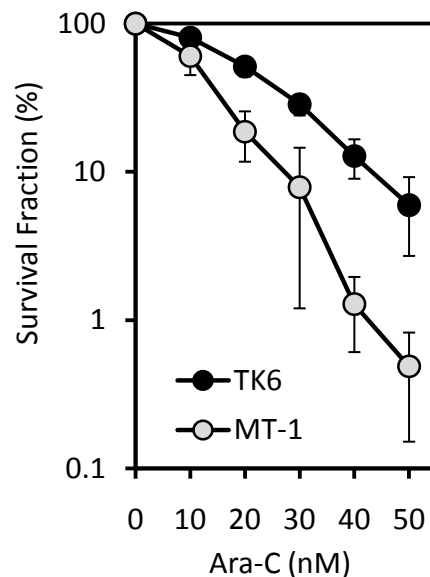


Figure 3.4. Cytotoxicity in response to Ara-C in TK6 and MT-1 cell lines.

Cell survival in response to Ara-C was compared in MMR-proficient TK6 cells (black circles) and MMR-deficient MT-1 cells (grey circles) via clonogenic assay. Data is presented as described in the legend to Figure 3.3 above.

3.2.2. Cytotoxicity in TK6 and MT-1 Cells Following Treatment with Ara-C

Cytotoxicity in response to Ara-C was assessed in MT-1 relative to TK6 via clonogenic assay. Whereas MT-1 demonstrated tolerance to the cytotoxic effects of MNU and 6-TG, a different phenotype was observed in response to Ara-C. Specifically, MT-1 cells were significantly more sensitive to cell killing mediated by Ara-C than the MMR-proficient parental TK6 cells (Figure 3.4). These data are consistent with a role for the DNA MMR pathway in modulating cellular response to Ara-C, however the mechanism of interaction is likely different to that reported for methylating agents and 6-TG given the differential drug response phenotypes observed following treatment with these agents and with Ara-C.

3.2.3. Cytotoxicity in TK6 and MT-1 Cells Following Treatment with Fludarabine, Cladribine and Clofarabine

In order to determine whether the increased sensitivity of MT-1 to Ara-C was also seen in response to other therapeutic nucleoside analogues, cytotoxicity in response to fludarabine, cladribine and clofarabine was assessed in MT-1 relative to TK6.

Like Ara-C, the triphosphates of fludarabine, cladribine and clofarabine can be fraudulently incorporated into replicating DNA resulting primarily in chain termination (Hentosh et al., 1990; Huang et al., 1990; Parker et al., 1991), although there is also evidence for internucleotide incorporation (Hentosh et al., 1990; Xie and Plunkett, 1995). In the case of clofarabine, at low concentrations, incorporation is mainly in internal positions within DNA, which has been reported to have inhibitory effects on DNA repair (Xie and Plunkett, 1995; Zhenchuk et al., 2009).

MT-1 cells were hypersensitive to fludarabine (Figure 3.5A), cladribine (Figure 3.5B) and clofarabine (Figure 3.5C) compared to parental TK6 cells, which was consistent with the phenotype observed in response to Ara-C. These data suggest that the role of DNA MMR as a modulator of cellular response to nucleoside analogues is not limited to Ara-C, but can also be extended to other arabinosyl nucleoside analogues.

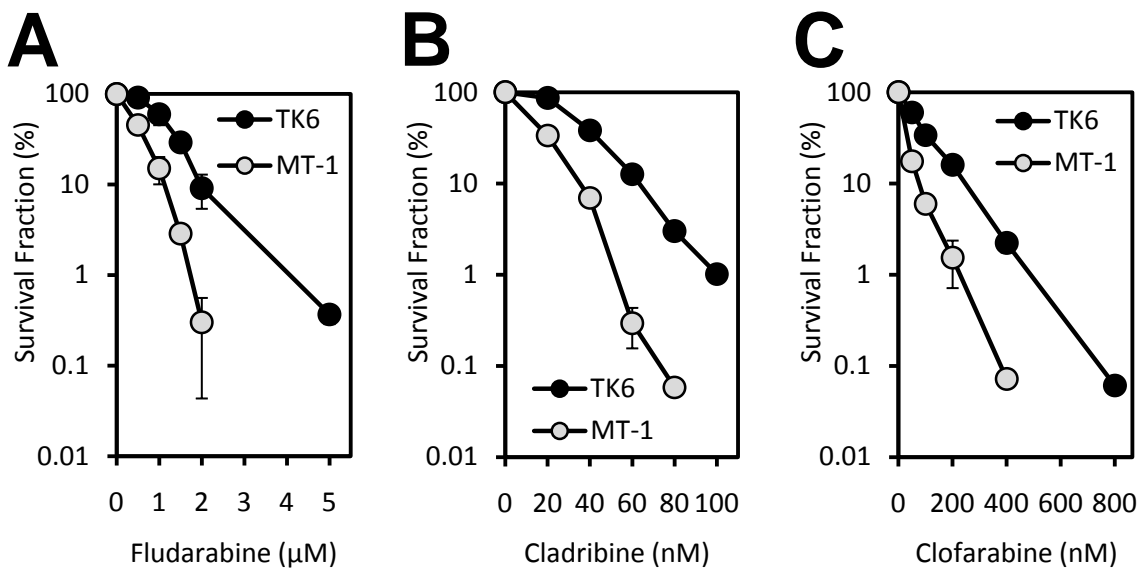


Figure 3.5. Cytotoxicity in response to adenosine nucleoside analogues in TK6 and MT-1 cell lines.

Cell survival in response to fludarabine (A), cladribine (B) and clofarabine (C) was compared in MMR-proficient TK6 cells (black circles) and MMR-deficient MT-1 cells (grey circles) via clonogenic assay. Data is presented as the number of viable colonies from dosed cell suspensions as a percentage of the number of viable colonies from vehicle-only treated cell suspensions. Data represents the mean and standard error of three independent experiments.

3.2.4. Assessment of RAS Mutation Status and Activity in TK6 and MT-1 Cells

3.2.4.1. Sequencing of N-RAS and K-RAS Exons

Activating mutations of *RAS* proto-oncogenes can sensitise cells to Ara-C *in vitro* (Koo et al., 1999; Meyer et al., 2009). Furthermore, patients with *RAS* mutations have been reported to benefit most from Ara-C therapy, particularly at high doses (Neubauer et al., 2008).

Coding sequences of commonly mutated exons of *N-RAS* and *K-RAS* in MT-1 were wild-type (sequencing data not shown), indicating that mutation was not responsible for the Ara-C sensitivity observed in this cell line.

3.2.4.2. Quantification of Activated ERK via Western Immunoblotting

Activation of *RAS* is observed in a subset of AML patients in which detectable *RAS* mutations are not found, and this has also been correlated with improved CR rates following treatment with Ara-C, as well as improved overall survival (Illmer et al., 2005). It is possible therefore, that *RAS* could be activated in MT-1 via a mechanism other than point mutation.

ERK-2 is a downstream effector of *RAS* activation, and is phosphorylated to its active form, pERK-2, via a kinase signalling cascade (Meloche and Pouyssegur, 2007). Quantification of pERK-2 was performed in MT-1 cells relative to TK6 via western immunoblotting to determine if *RAS* activation had occurred despite there being no detectable *N-RAS* or *K-RAS* mutations. Parental TK6 cells did not demonstrate any phosphorylation of ERK-2 (Figure 3.6), consistent with absence of *RAS* activation in this cell line. A low level of pERK-2 was detectable in MT-1 cells (Figure 3.6), however it remains unknown whether this would be sufficient to confer hypersensitivity to Ara-C.

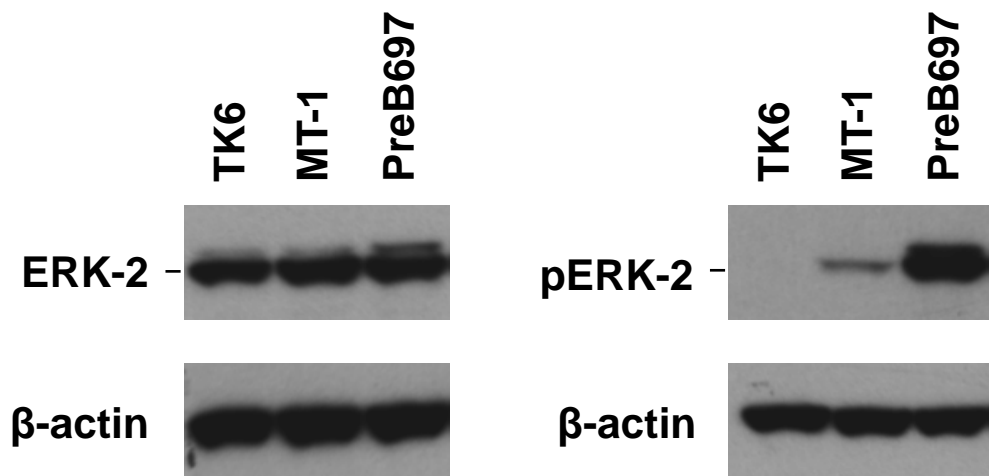


Figure 3.6. ERK-2 and pERK-2 protein levels in TK6 and MT-1 cell lines.

Western immunoblotting was performed to assess protein levels of ERK-2 (left) and pERK-2 (right) in the MMR-deficient MT-1 cell line and its MMR-proficient parental cell line TK6. PreB697 cells were included as a positive control. In both cases, the major band corresponds to ERK-2 (42kDa). The minor band above corresponds to ERK-1 (44kDa), an alternate ERK isoform. β -actin was used as a loading control.

3.2.5. Assessment of MMR Status in shRNA Knockdown Cell Lines

Because MT-1 was generated from TK6 by exposure to a mutagenic compound, and has a mutator phenotype (Goldmacher et al., 1986; Kat et al., 1993), it is possible that MT-1 has acquired additional genomic mutations not present in the parental cell line. Consistent with this model, an investigation of methylating agent-induced transcriptome changes in TK6 and MT-1 revealed differences in the basal gene expression profile (di Pietro et al., 2003). TK6 and MT-1 therefore cannot be considered strictly isogenic, which highlighted a requirement for confirmation of the results described above in a truly isogenic system. To this end, cell lines were generated from TK6, and also from the myeloid leukaemic cell line, HL-60, in which MutS components (MSH2, MSH3 and MSH6) were stably knocked down using shRNA-mediated RNA interference (see Section 2.4). These cell lines were then characterised for their DNA MMR status, following which cytotoxicity in response to nucleoside analogues was assessed relative to their respective parental cell lines as follows.

3.2.5.1. Expression Levels of MutS Protein Components Determined by Western Immunoblotting

Western immunoblotting was used to determine the protein levels of MSH2, MSH3 and MSH6 in each of the shRNA knockdown cell lines (Figure 3.7). Knockdown of *MSH6* completely abolished MSH6 protein in TK6 *MSH6i* and HL-60 *MSH6i*, accompanied by a slight decrease in MSH2 but no difference in MSH3 relative to the respective parental cell lines. Knockdown of *MSH2* resulted in complete loss of MSH2 protein in both TK6 (TK6 *MSH2i*) and HL-60 (HL-60 *MSH2i*), accompanied by complete loss of both MSH3 and MSH6. Degradation of MSH3 and MSH6, due to instability in the absence of their binding partner (Drummond et al., 1997) is the probable explanation for this phenotype. *MSH3* knockdown resulted in a reduction in MSH3 protein levels of approximately 95% in both cell lines (TK6 *MSH3i* and HL-60 *MSH3i*) but there was no observed effect on MSH2 or MSH6. In human cells, the ratio of MutS α to MutS β is approximately 6:1 (Drummond et al., 1997), therefore loss of MSH3 would not be expected to have a significant impact on the stability of MSH2 because the majority is partnered with MSH6 in the MutS α complex.

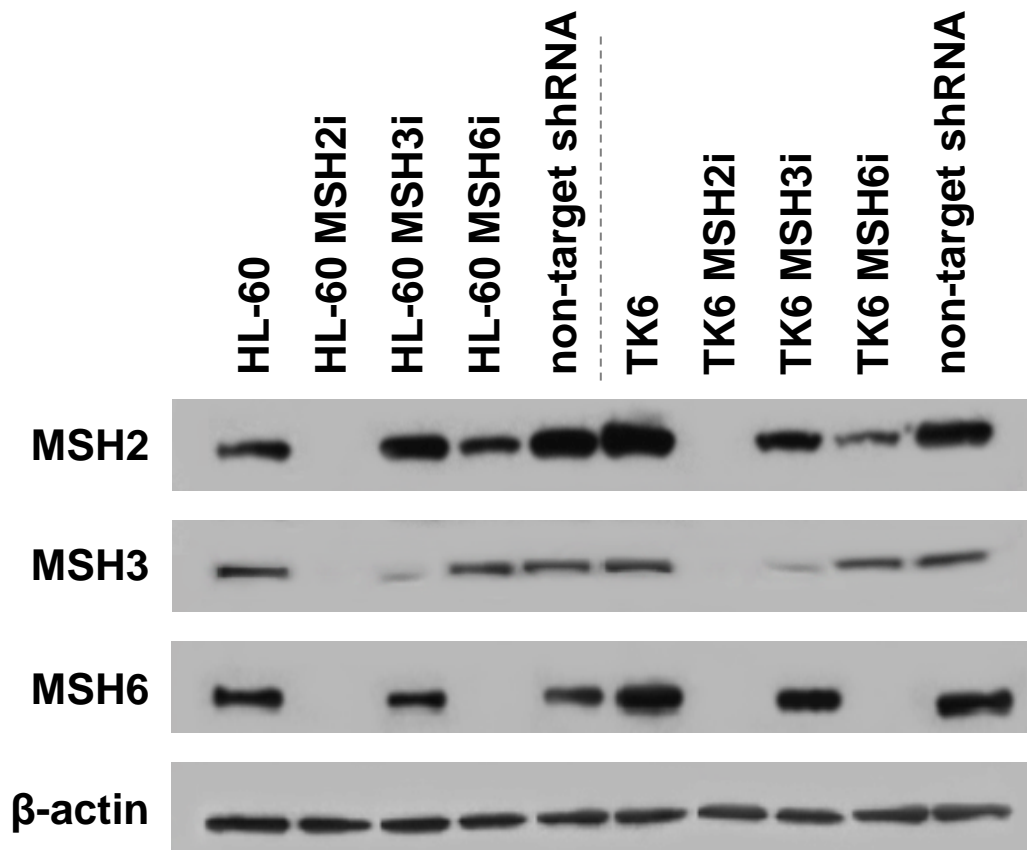


Figure 3.7. MutS protein expression in MMR knockdown cell lines.

Western immunoblotting was performed to assess protein expression of MutS components (MSH2, MSH3 and MSH6) as a result of shRNA-mediated knockdown of *MSH2*, *MSH3* or *MSH6* in HL-60 and TK6 cell lines. Non-target shRNA was used to control for effects of the transduction process on protein expression. β -actin was used as a loading control.

3.2.5.2. Cytotoxicity Following Treatment with MNU and 6-TG

To determine the effects of knockdown of MutS components on DNA MMR status, cytotoxicity in response to MNU and 6-TG was assessed in knockdown cell lines relative to their MMR-proficient parental counterparts (Figure 3.8). TK6 *MSH6i* and HL-60 *MSH6i* cells demonstrated tolerance to the cytotoxic effects of MNU and 6-TG compared to their respective parental cell lines, as did TK6 *MSH2i* and HL-60 *MSH2i* cells. This is consistent with the phenotype expected in MutS α defective cells when exposed to these agents, and confirms major perturbation of the DNA MMR pathway.

MSH3 heterodimerises with MSH2 to form the MutS β complex, which is responsible for detection of IDLs and extrahelical loops but is not thought to possess activity towards base:base mismatches (Palombo et al., 1996). Depletion of MSH3 protein alone in TK6 *MSH3i* and HL-60 *MSH3i* therefore results in deficiency of MutS β , but this is not expected to affect MutS α . Consistently, TK6 *MSH3i* and HL-60 *MSH3i* demonstrated no difference in cytotoxicity in response to MNU or 6-TG compared to their respective parental cell lines (Figure 3.8). This demonstrates that MutS α function is not affected in these cell lines, and furthermore confirms that the MutS β complex has no role in mediating cytotoxicity in response to MNU and 6-TG.

3.2.6. Cytotoxicity in MMR Knockdown Cell Lines Following Treatment with Nucleoside Analogues

Cytotoxicity in response to Ara-C, fludarabine and clofarabine was assessed in MMR knockdown cell lines relative to respective MMR-proficient parental cells (Figure 3.9). Consistent with the results observed in the MT-1, TK6 *MSH6i* and HL-60 *MSH6i* cells demonstrated increased sensitivity to cytotoxicity induced by Ara-C, fludarabine and clofarabine compared to their parental counterparts. Additionally, TK6 *MSH2i* and HL-60 *MSH2i* also demonstrated increased cytotoxicity in response to these nucleoside analogues relative to their parental cells.

Conversely, loss of MSH3 protein alone in TK6 *MSH3i* and HL-60 *MSH3i* cells conferred tolerance to the cytotoxic effects of Ara-C, fludarabine and clofarabine relative to parental cells (Figure 3.9).

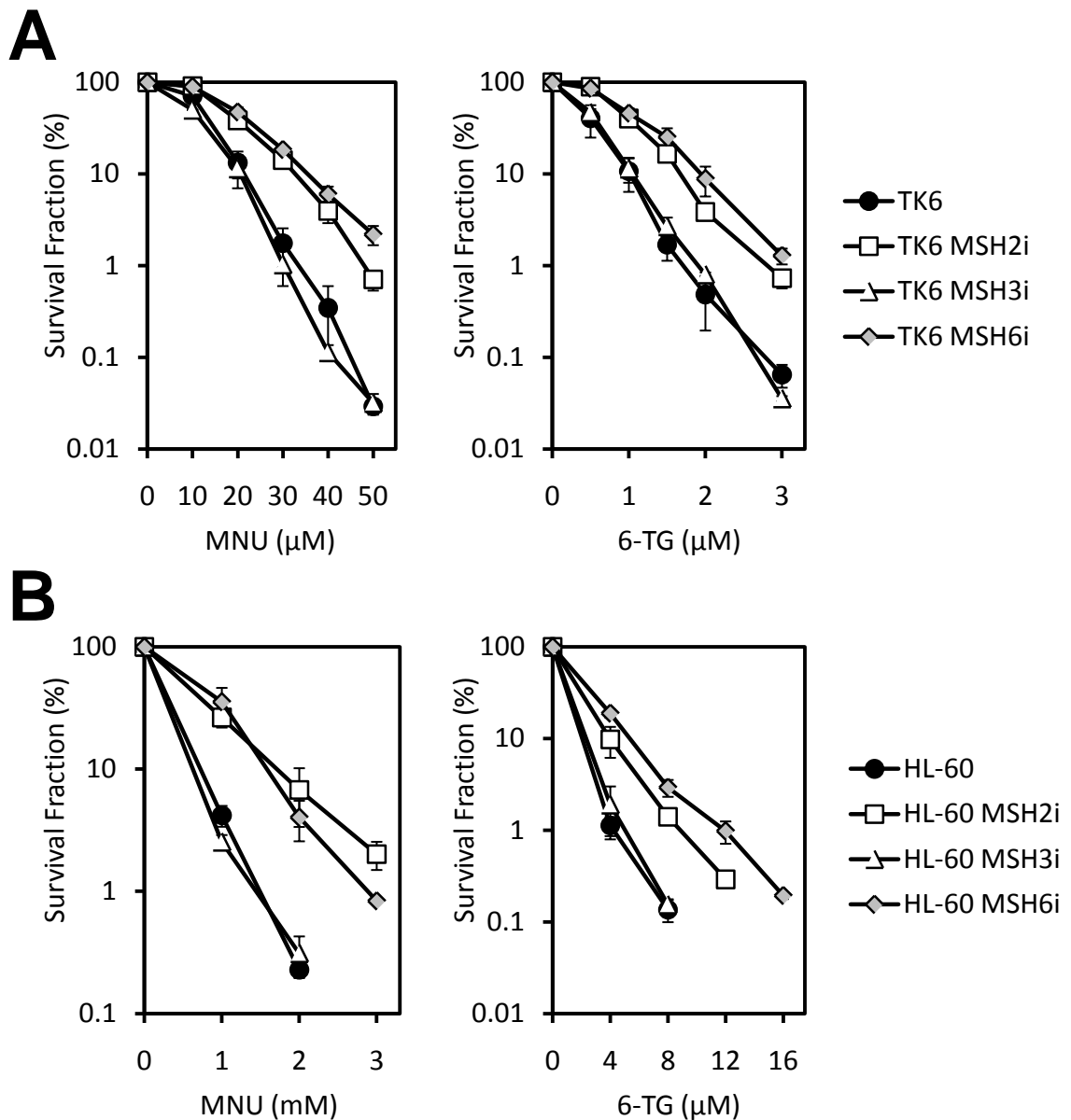
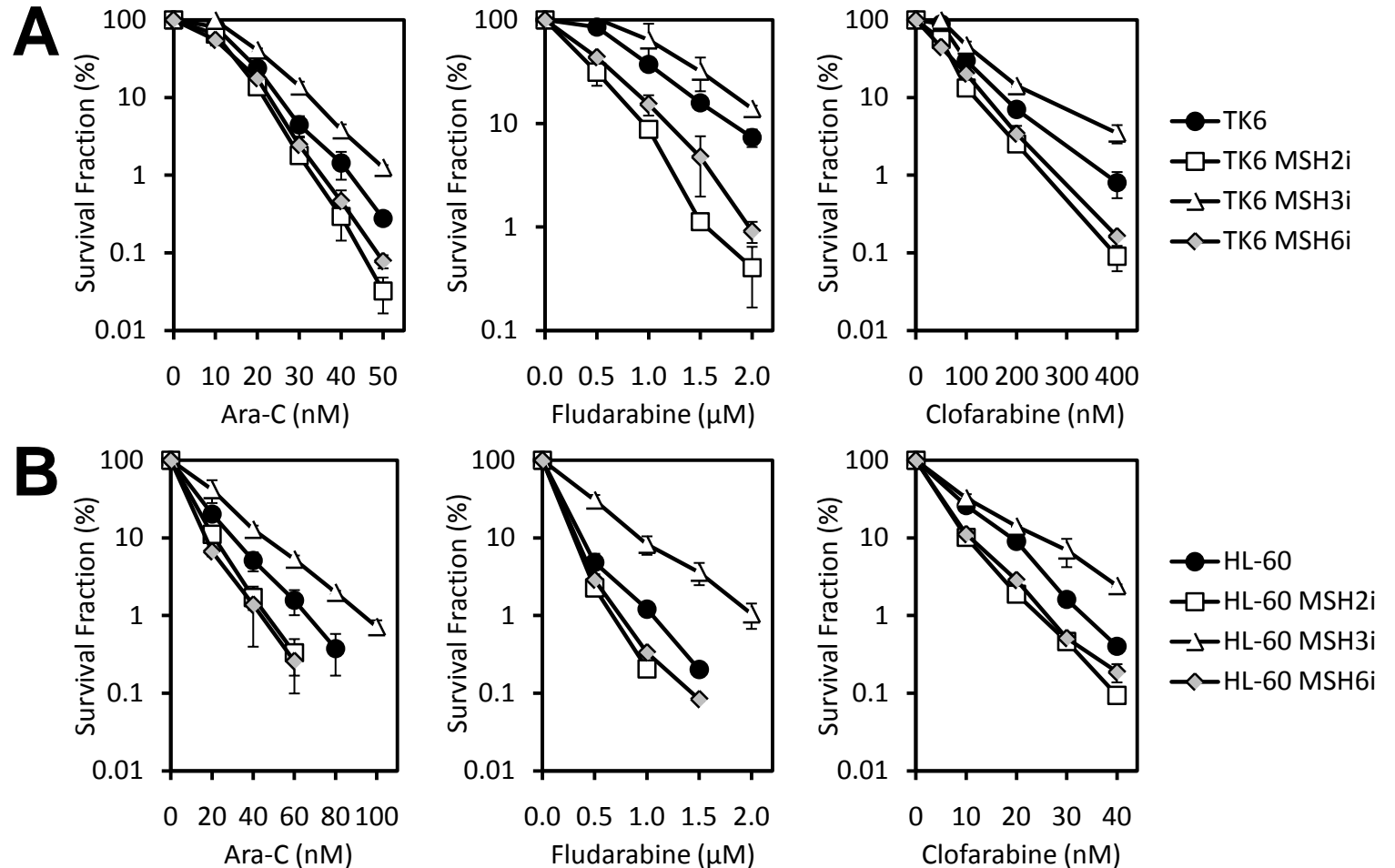


Figure 3.8. Cytotoxicity in response to MNU and 6-TG in MMR knockdown cell lines. **A.** Cytotoxicity in response to MNU (left) and 6-TG (right) was compared in TK6 and its MMR knockdown subclones via clonogenic assay. Data is presented as the number of viable colonies from dosed cell suspensions as a percentage of the number of viable colonies from vehicle-only-treated cell suspensions. **B.** Cytotoxicity in response to MNU and 6-TG was compared in HL-60 and its MMR knockdown subclones via growth inhibition assay. Data are presented as the number of surviving cells from dosed cell suspensions as a percentage of surviving cells from vehicle-only-treated cell suspensions. In each case, data represents the mean and standard error of three independent experiments. Cytotoxicity in TK6 and HL-60 cells transduced with non-target shRNA was also assessed in response to MNU and 6-TG to confirm that the transduction process itself did not affect drug response (data not shown).

Figure 3.9. Cytotoxicity in response to Ara-C, fludarabine and clofarabine in MMR knockdown cell lines.

A. Cytotoxicity in response to Ara-C (left), fludarabine (centre) and clofarabine (right) was compared in TK6 and its MMR knockdown subclones via clonogenic assay. Data is presented as the number of viable colonies from dosed cell suspensions as a percentage of the number of viable colonies from vehicle-only-treated cell suspensions.

B. Cytotoxicity in response to Ara-C, fludarabine and clofarabine was compared in HL-60 and its MMR knockdown subclones via growth inhibition assay. Data are presented as the number of surviving cells from dosed cell suspensions as a percentage of surviving cells from vehicle-only-treated cell suspensions.



from dosed cell suspensions as a percentage of surviving cells from vehicle-only-treated cell suspensions. In each case, data represents the mean and standard error of three independent experiments. Cytotoxicity in TK6 and HL-60 cells transduced with non-target shRNA was also assessed in response to Ara-C, fludarabine and clofarabine to confirm that the transduction process itself did not affect drug response (data not shown).

Taken together, these data further support a role for DNA MMR in mediating cellular response to Ara-C and other nucleoside analogues. Moreover it appears that the specific nature of MMR defects is important in influencing outcome, suggesting that MutS α and MutS β components have different roles in modulating response to these agents.

3.2.7. Cytotoxicity in MMR-Deficient Cell Lines Following Exposure to IR and UV Radiation

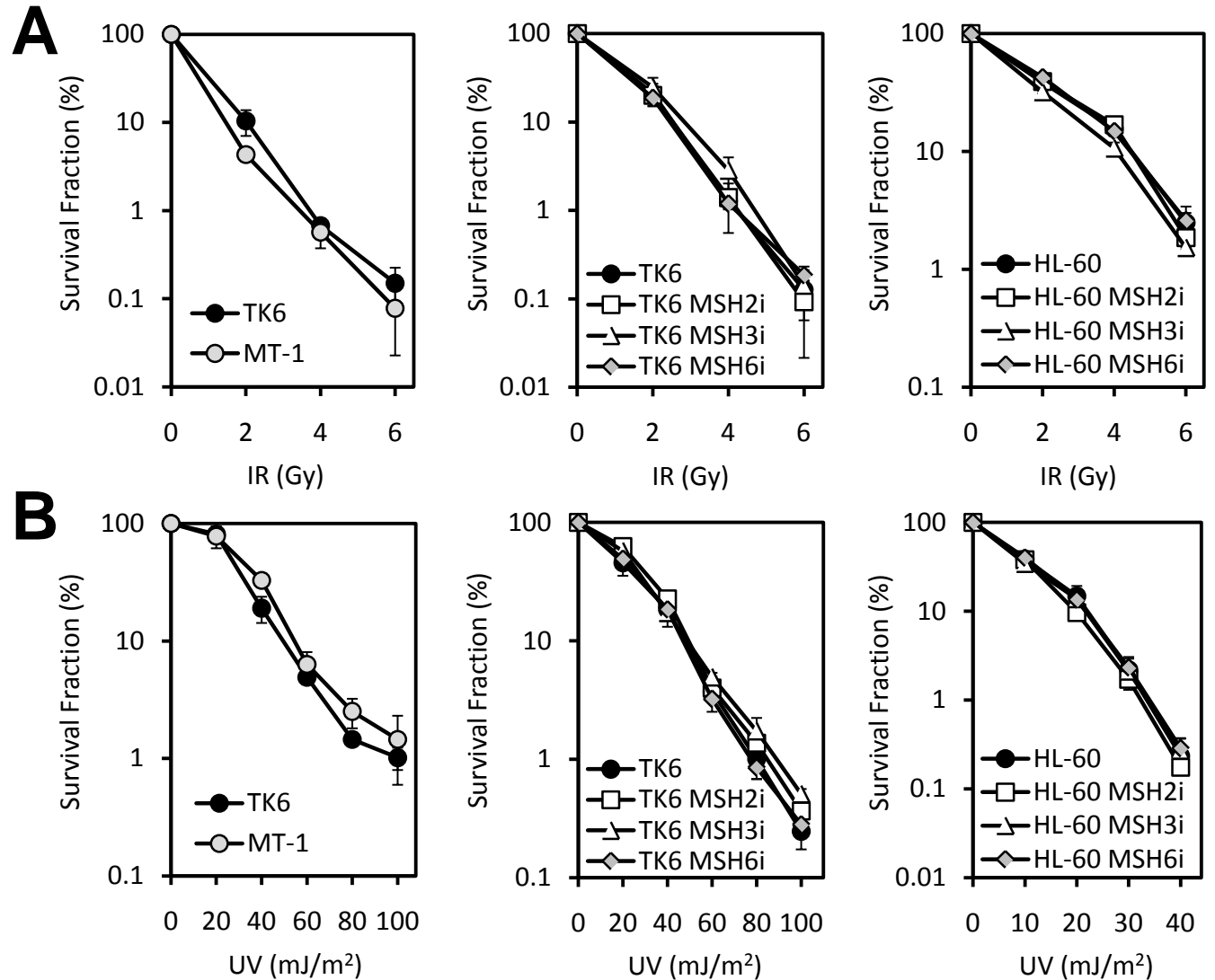
It has been reported that certain defects of the DNA MMR pathway can affect cytotoxicity following exposure to IR, although results are conflicting and the exact role of MMR in response to IR is unclear (see Section 1.2.4). To determine whether loss of MutS components in MT-1 or in MMR knockdown cells could affect response to IR, cytotoxicity following acute IR exposure was assessed in all lines relative to their parental counterparts. No differential cytotoxic response to IR was observed in any of the MMR-deficient cells relative to their respective MMR-proficient parental cells (Figure 3.10A). This is consistent with previous studies using strictly isogenic cell line pairs (Cejka et al., 2004) and suggests that neither MutS α nor MutS β loss can significantly influence cytotoxicity in response to IR. It should be noted however, that cell cycle-related effects, for instance differences in activation of checkpoint proteins, cannot be excluded.

It is possible that the difference in response to nucleoside analogues observed between MMR-proficient and MMR-deficient cell lines could be attributed to a defect affecting other DNA repair pathways, although this is unlikely given the isogenic nature of the cell line pairs. Nevertheless, to exclude this possibility, cytotoxicity in response to UV exposure was assessed, as UV radiation causes DNA lesions which are substrates for repair pathways acting independently of DNA MMR. There was no observable difference in cytotoxicity resulting from exposure to UV radiation in any of the MMR-defective cells relative to parental lines (Figure 3.10B), therefore excluding a generic DNA repair defect.

Figure 3.10. Cytotoxicity in response to IR and UV exposure in MMR-deficient cell lines.

A. Cytotoxicity following exposure to IR was compared in TK6 and MT-1 (left) and in TK6 and its MMR knockdown subclones (centre) via clonogenic assay. Data is presented as the number of viable colonies from exposed cell suspensions as a percentage of the number of viable colonies from unexposed control cell suspensions. Cytotoxicity following exposure to IR was compared in HL-60 and its MMR knockdown subclones (right) via growth inhibition assay. Data are presented as the number of surviving cells from exposed cell suspensions as a percentage of surviving cells from unexposed control cell suspensions.

B. Cytotoxicity following exposure to UV radiation was compared in TK6 and MT-1 (left), in TK6 and its MMR knockdown subclones (centre) and in HL-60 and its MMR knockdown subclones (right) as described above. In all cases, data represents the mean and standard error of three independent experiments.



CELL LINE	MMR PROTEIN EXPRESSION ^a						MMR STATUS	DRUG RESPONSE PHENOTYPE ^b						
	MSH2	MSH3	MSH6	MLH1	PMS2	MGMT		MNU	6-TG	ARA-C	FLUD	CLAD	CLOF	IR/UV
MT-1	-	NE	--	NE	NE	---	MutS α deficient	Resistant	Resistant	Sensitive	Sensitive	Sensitive	Sensitive	ND
TK6 <i>MSH2i</i>	---	---	---	U	U	U	MutS α / β deficient	Resistant	Resistant	Sensitive	Sensitive	U	Sensitive	ND
HL-60 <i>MSH2i</i>	---	---	---	U	U	U	MutS α / β deficient	Resistant	Resistant	Sensitive	Sensitive	U	Sensitive	ND
TK6 <i>MSH3i</i>	NE	--	NE	U	U	U	MutS β deficient	ND	ND	Resistant	Resistant	U	Resistant	ND
HL-60 <i>MSH3i</i>	NE	--	NE	U	U	U	MutS β deficient	ND	ND	Resistant	Resistant	U	Resistant	ND
TK6 <i>MSH6i</i>	-	NE	---	U	U	U	MutS α deficient	Resistant	Resistant	Sensitive	Sensitive	U	Sensitive	ND
HL-60 <i>MSH6i</i>	-	NE	---	U	U	U	MutS α deficient	Resistant	Resistant	Sensitive	Sensitive	U	Sensitive	ND

Table 3.1. Summary of MMR protein expression, MMR status and drug response phenotypes in MMR-deficient cells (relative to MMR-proficient parental cells).

^a --- complete loss of protein expression -- significantly reduced expression - slight reduction in expression; NE, no effect; U, undetermined

^b ND, no difference in response; U, undetermined.

3.2.8. Summary of Relative Cytotoxic Responses in MMR-Deficient Cell Lines Following Exposure to DNA Damaging Agents

For ease of reference, a summary of the cellular defects, MMR status and drug response phenotypes observed in MT-1 and in each of the isogenic MMR knockdown cell lines is presented in Table 3.1.

3.3. Discussion

The requirement for functional DNA MMR in mediating response to methylating agents and the base analogue antimetabolite 6-TG is well established. In the case of 6-TG, incorporation of the fraudulent nucleotide triphosphate (6-thio-dGTP) into DNA and subsequent *in situ* methylation and replication of the lesion results in mispairs which are a substrate for the damage recognition complex MutS α (Swann et al., 1996; Waters and Swann, 1997) (see Figure 1.4). Following damage recognition by MutS α , cells are arrested in G₂ phase of the second cell cycle and apoptosis is initiated (Hawn et al., 1995). This may be due to repeated abortive repair attempts coordinated by MMR components which results in the formation of pro-cytotoxic strand breaks. Alternatively it could be due to an ability of MMR proteins to signal directly to cell cycle and/or apoptosis-mediating factors, implicating DNA MMR components as general DNA damage sensors, although this remains to be firmly established. Loss of key DNA MMR components (MutS α or MutL α) results in tolerance to 6-TG-induced DNA damage due to lack of MMR-mediated cell cycle arrest and/or apoptosis initiation (Aquilina et al., 1989; Aquilina et al., 1990).

Using cell lines harbouring defined defects affecting specific MMR components, this study demonstrates a role for DNA MMR in mediating cytotoxicity in response to several therapeutic antimetabolite nucleoside analogues. Additionally, the data suggests that the mode of interaction of MMR components with nucleoside analogues differs from that with 6-TG. Furthermore, differences in the cytotoxic response to nucleoside analogues were observed when different MMR components were dysfunctional, demonstrating that the specific nature of MMR defects is important in influencing response to these agents.

Loss of the MutS α complex in MT-1 (through MSH6 mutation), and in TK6/HL-60 MSH2i and TK6/HL-60 MSH6i (through gene knockdown) conferred tolerance to the cytotoxic effects of the methylating agent MNU and 6-TG as expected. Rather than being cross-tolerant to the cytosine nucleoside analogue Ara-C, MutS α -deficient cells were acutely sensitive. This initial finding was then extended to include other therapeutic nucleoside analogues, namely fludarabine, cladribine and clofarabine, which are each analogues of 2'-deoxyadenosine (see Section 1.5.4). These findings therefore add to a growing body of evidence that loss of DNA MMR components can confer sensitivity to specific DNA damaging agents.

Despite differences in the metabolism, mechanism of action and clinical activity of the nucleoside analogues used in this study, the cytotoxic responses observed in MMR-deficient cells were consistent. This suggests a common mechanism (or mechanisms) by which DNA MMR interacts with the lesions caused by these agents. The following sub-sections outline a number of mechanisms which might account for the observations herein.

S phase checkpoint abrogation

Each of the nucleoside analogues used in this investigation causes stalling of the replication fork, eliciting activation of the S phase checkpoint (through ATR-Chk1-Cdk2 signalling; see Figure 1.12), causing cells to accumulate in S phase (Ewald et al., 2008b). The involvement of DNA MMR components at the G₂M checkpoint in response to methylating agents, 6-TG and IR is well characterised (see Sections 1.2.1.2 and 1.2.4.1 respectively). Similarly, Brown et al. demonstrated that functional DNA MMR is required for S phase checkpoint activation in response to IR through an interaction between MSH2 and Chk2 (Brown et al., 2003). These findings led to the proposition that damage-enhanced association of checkpoint signalling molecules (such as Chk1 and Chk2) with MMR complexes assembled at sites of DNA damage may be a key step in the activation of signalling cascades in response to genotoxic stress (Brown et al., 2003; Wang and Qin, 2003). A possible explanation for these findings therefore (which could also extend to gemcitabine), is that such an MMR-mediated 'molecular scaffold' also forms at nucleoside analogue-induced stalled replication forks to mediate damage signalling, loss of which confers sensitivity to these agents. Abrogation of the S phase

checkpoint has previously been identified as a mechanism by which cells can be sensitised to nucleoside analogues via an increase in lethal DNA damage. This has been demonstrated *in vitro* in the case of Ara-C (Loegering et al., 2004; Cho et al., 2005; Karnitz et al., 2005; Mesa et al., 2005) as well as gemcitabine (Shi et al., 2001; Karnitz et al., 2005; Ewald et al., 2007). Furthermore, in response to IR exposure, cells deficient in MSH2 (or MLH1) demonstrate abrogation of the S phase checkpoint such that cells continue to replicate their DNA despite the presence of damage (Brown et al., 2003). This would presumably lead to mitotic catastrophe and increased cell death. Loss of MSH2 in MT-1, TK6/HL-60 *MSH2i* and TK6/HL-60 *MSH6i* in this study could similarly cause checkpoint failure, allowing cells to continue through the cell cycle despite the presence of nucleoside analogue-induced DNA damage and subsequently undergo increased cell death due to mitotic catastrophe. Further investigations to delineate the mode of nucleoside analogue-induced cytotoxicity in these cell lines, as well as the timing of cell death, are required to test these models.

Deficiency in repair/removal of nucleoside analogues

As well as initiating cell cycle arrest, activation of the ATR-Chk1-Cdk2 response also promotes replication fork stabilisation (Paulsen and Cimprich, 2007), likely allowing DNA repair mechanisms an opportunity to remove fraudulent nucleotides from DNA. Another possible explanation for the observations in this study is that DNA MMR components are involved in signalling to, or recruitment of, factors which facilitate removal of nucleoside analogues from stalled replication forks, for example unassociated 3'→5' exonucleases, or BER and NER components. In particular, BER is capable of removing fludarabine nucleotides from DNA both *in vitro* and *ex vivo*, and inhibition of this response sensitises cells to the cytotoxic effects of fludarabine (Bulgar et al., 2010). It remains to be established whether DNA MMR components could directly or indirectly recruit BER components to stalled replication forks. Alternatively, it is possible that MMR components themselves might be involved in the removal of terminal nucleoside analogues hence permitting resumption of DNA replication, however this has yet to be investigated. In either case, dysfunction of DNA MMR would result in sensitisation of cells to nucleoside analogue-mediated cytotoxicity,

consistent with the observations herein and those previously reported with gemcitabine (Takahashi et al., 2005).

Deregulation of HRR

ATM kinase, the damage responsive histone γ -H2AX, and the MRN complex are also localised to sites of stalled replication forks in response to nucleoside analogues (Ewald et al., 2007; Ewald et al., 2008a). These molecules are classically associated with response to DSBs (Fernandez-Capetillo et al., 2004; Shiloh, 2006; Lamarche et al., 2010); consistently, there is some evidence to suggest that DSBs form as a result of stalled replication forks which are not repaired (Arnaudeau et al., 2000; Arnaudeau et al., 2001). This appears to allow other repair pathways such as HRR an opportunity to rescue the replication fork (Arnaudeau et al., 2001; Lundin et al., 2002; Rothkamm et al., 2003). DNA MMR components have a role in HRR (described in Section 1.1.2.1), and deregulation of HRR has been demonstrated as a consequence of MMR-dysfunction (Worrillow and Allan, 2006). Deregulation of HRR-mediated processing of nucleoside analogue-induced DSBs could therefore represent another potential explanation for increased sensitivity observed in MT-1, TK6/HL-60 *MSH2i* and TK6/HL-60 *MSH6i*. Also consistent with this proposed theory, MSH2 deficiency sensitises cells to camptothecin (Pichierri et al., 2001), an agent which causes DSBs selectively at stalled replication forks, in this case through topoisomerase I inhibition (Hsiang et al., 1989).

There is some evidence to suggest that non-homologous end joining (NHEJ), an error-prone alternative DSB repair pathway, may also be involved in repair of DSBs at stalled replication forks, for example following exposure to fludarabine (de Campos-Nebel et al., 2008). Additionally, a role for MSH2 (and MLH1) in regulation of NHEJ at a step involving pairing of terminal DNA tails has been suggested (Bannister et al., 2004; Smith et al., 2005). The observed sensitivity of MT-1, TK6/HL-60 *MSH2i* and TK6/HL-60 *MSH6i* to fludarabine, and by extension other nucleoside analogues, could therefore also potentially be attributed to deregulation of NHEJ. This is speculative however, as deregulation of NHEJ as a consequence of DNA MMR-dysfunction has not been demonstrated.

Dysfunction of MutS β -mediated damage signalling

In contrast to the phenotype seen with loss of MSH2, loss of MSH3 (through *MSH3* gene knockdown in TK6/HL-60 *MSH3i*) conferred increased tolerance to the cytotoxic effects of Ara-C and other nucleoside analogues. MSH3 loss however, did not affect response to MNU or 6-TG, presumably because MutS α function remains unaffected. Loss of MSH3 results in lack of functional MutS β complex, demonstrating a potential role for this complex in response to nucleoside analogue-induced DNA damage. In turn, this would suggest that these agents can induce DNA lesions which are substrates for MutS β . Consistent with this suggestion, *in vitro* cell-free translesion synthesis experiments demonstrate that replication of an oligonucleotide containing an internal Ara-C lesion can give rise to a daughter DNA product containing an extrahelical base (Figure 3.11, unpublished observations courtesy of J.M. Allan), generating a legitimate substrate for MutS β . It is also conceivable that this could occur *in vivo* given that nucleoside analogues can become incorporated at internucleotide positions within DNA (Major et al., 1981; Ohno et al., 1988). Furthermore, there is evidence to suggest, at least in the case of Ara-C, that specialised translesion DNA polymerases can replicate across incorporated Ara-C nucleotides (Chen et al., 2006), although whether this occurs with low fidelity giving rise to extrahelical bases has yet to be determined.

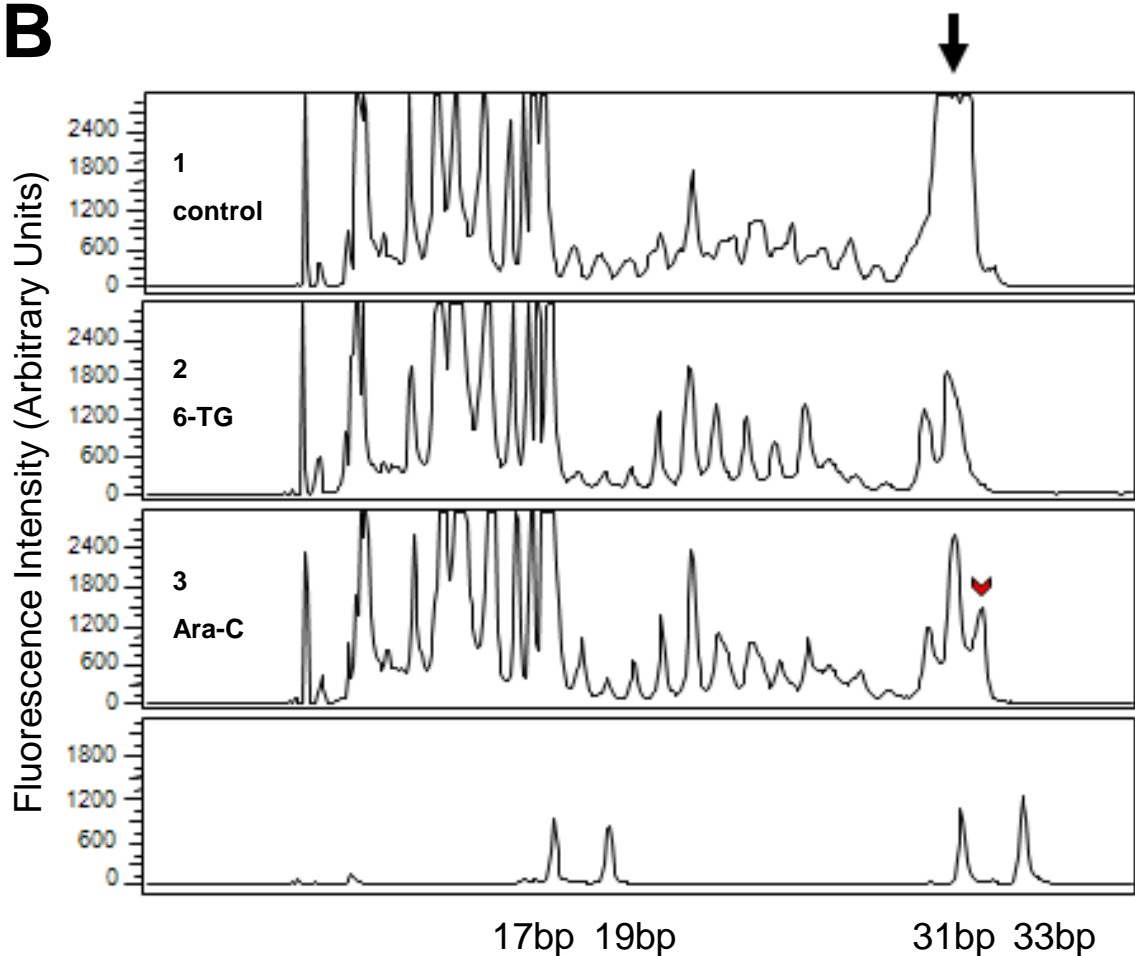
A**Substrate**

1 3' – CGGCTTAAAGATCTTAGCTTTTGAACGATCG – 5'

2 3' – CGGCTTAAAGATCTTA(6-TG)CTTTTGAACGATCG – 5'

3 3' – CGGCTTAAAGATCTTAG(Ara-C)TTTTCGAACGATCG – 5'

Primer 5' – GCCGAATTTCTA – 3'

B**Figure 3.11. Ara-C lesions induce replication slippage in cell-free assays.**

(A) Single stranded 31-mer oligonucleotides were used as substrates in translesion synthesis experiments (performed by JMA), and were either unmodified (1), or contained a 6-TG lesion (2) or an Ara-C lesion (3). (B) Products generated following replication of the individual substrates with Klenow fragment from *E. coli*. The large arrow demonstrates the 31 base pair full length product generated in each reaction. The smaller (red) arrowhead demonstrates the additional 32 base pair product generated by replication of the Ara-C containing substrate (3). Similar results were also obtained using DNA pol α (data not shown).

Given that loss of MutS β confers tolerance to nucleoside analogues, a model is proposed in which MutS β -mediated detection of DNA lesions signals cell cycle arrest and apoptosis (either through futile repair cycles or direct signalling), analogous to the MutS α -mediated response to 6-TG (and other agents). The 'futile cycling' model requires the presence of the lesion in the parental strand following two rounds of replication. It remains possible that MutS β can detect nucleoside analogues incorporated within the daughter DNA strand following a single round of DNA replication. It is expected however, that this would result in removal of the lesion, conferring sensitivity, rather than the observed resistance, with loss of DNA MMR. One possible approach to investigating this model is to perform cell cycle analysis in order to determine whether nucleoside analogue-mediated cytotoxicity in MSH3-deficient cells occurs in the first or second cycle following exposure. It would also be interesting to determine whether loss of MSH3 alone confers tolerance to gemcitabine given that this drug is primarily observed at internucleotide positions (Huang et al., 1991).

The finding that MSH3 deficiency as a sole abnormality confers tolerance to the cytotoxic effects of nucleoside analogues is in contrast to recent evidence that MSH3 loss (in a strictly isogenic system) can sensitise colorectal carcinoma cells to platinum drugs (Takahashi et al., 2011). It is thought that the sensitivity conferred by MSH3 loss is due to dysfunction of HRR, given that MSH3 loss in the same study was also found to sensitise cells to an inhibitor of poly(ADP-ribose) polymerase 1 (PARP-1), a phenotype characteristic of HRR-defective cells (Martin et al., 2008). This implicates the MutS β complex in the regulation of HRR-mediated repair of platinum agent-induced DSBs, a role which has previously been suggested for other cross-linking agents (see Section 1.2.3.2). This report is therefore consistent with the observations of nucleoside analogue sensitivity in TK6/HL-60 *MSH2i*, and suggests that the observed phenotype is due to deregulation of HRR as suggested above, but mediated through loss of MutS β rather than MutS α . Deregulation of HRR through MutS β loss however, would not explain the nucleoside analogue sensitivity in MT-1 or TK6/HL-60 *MSH6i*, given that this complex is apparently unaffected in these cell lines as demonstrated by western immunoblotting (Figure 3.1 and Figure 3.7). Rather, evidence suggests that MutS α loss is primarily responsible for nucleoside analogue sensitivity in MT-1, TK6/HL-60 *MSH2i* and TK6/HL-60 *MSH6i*.

In conclusion, DNA MMR components might have multiple roles in cellular response to nucleoside analogues (summarised in Figure 3.12), dysfunction of which could account for the data generated in these investigations. Importantly, it should be noted that such roles are not necessarily mutually exclusive. For instance, MutS β might have a role in mediating cell cycle arrest and/or apoptosis in response to internal nucleoside analogue-induced lesions, however cellular phenotype could be determined by dysfunction of MutS α in S phase checkpoint signalling and/or HRR regulation at the stalled replication fork. Furthermore, the contrasting findings between Ara-C and other agents (such as platinum drugs) that may ultimately generate the same damage (i.e. DSBs), highlights the complexity of MMR-mediated responses to DNA damage, which appear to be agent specific.

Although highly unlikely given the reproducibility of the observed drug response phenotypes in multiple cell lines, and that cytotoxicity in response to IR and UV radiation was unaffected, it cannot be completely excluded that factors independent of DNA MMR are responsible for the findings of this study. For instance, the mutator phenotype conferred by MMR dysfunction could permit mutation in a gene or genes which could subsequently affect response to nucleoside analogues. This possibility applies particularly to MT-1 given its mechanism of generation. Indeed, modest ERK2 activation in MT-1 cells relative to TK6 might be a consequence of the mutator phenotype of this cell line. Although considered isogenic, it should also be noted that the MMR knockdown lines themselves will have acquired a mutator phenotype, however by using them at a very early passage, the risk of acquiring additional mutations is minimised. The most efficient way of confirming these findings would be to use a strictly isogenic model in which MMR status can be altered without the need for cell passage, for example the Tet-Off system.

Despite not investigating specific mechanisms responsible for the observed phenotypic response to nucleoside analogues, these findings have clear implications for the use of nucleoside analogues in the treatment of AML, especially in those subtypes which are associated with DNA MMR dysfunction, such as relapsed and t-AML. This will be discussed in Chapter 8.

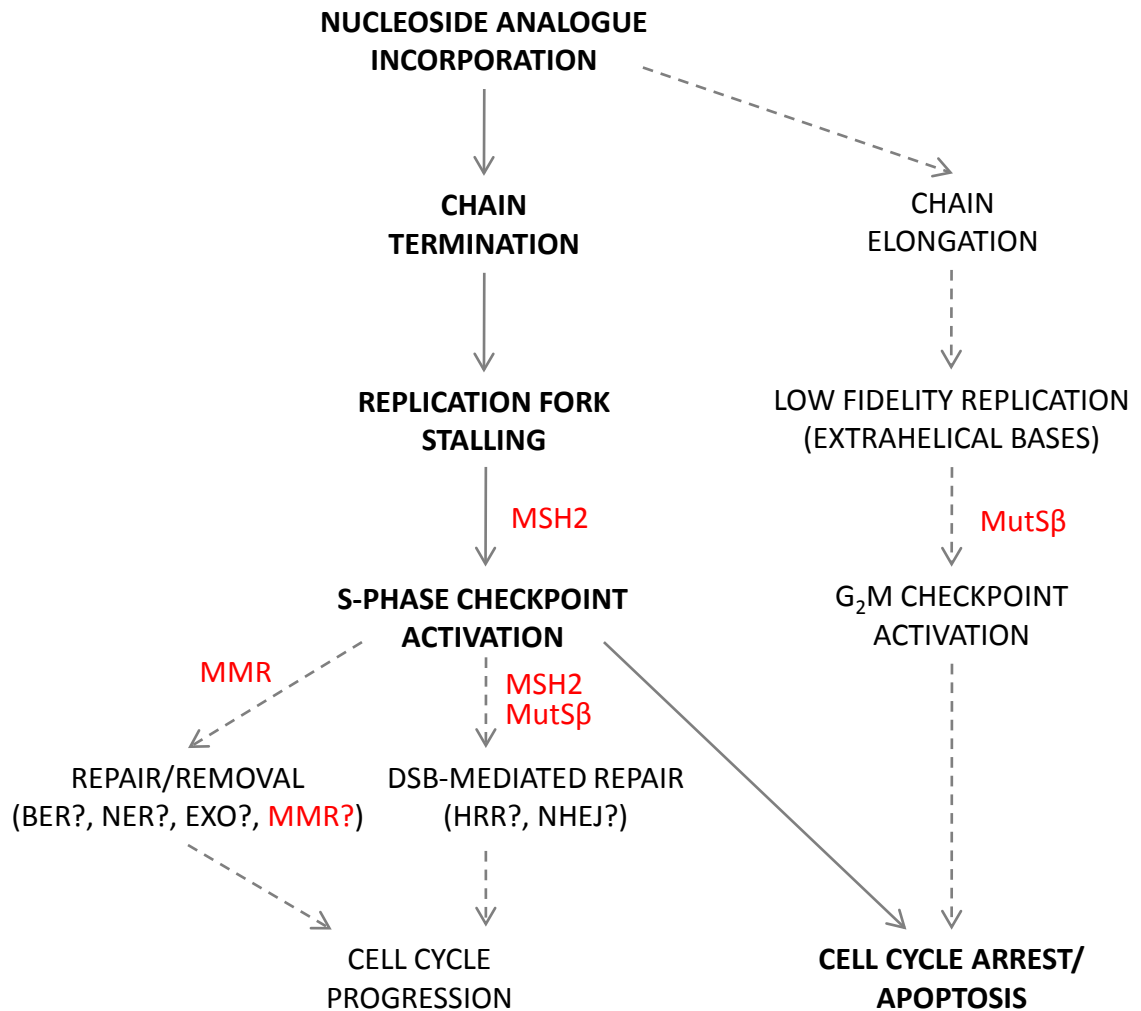


Figure 3.12. Possible roles for DNA MMR components in cellular response to nucleoside analogues.

Incorporation of nucleoside analogues into replicating DNA primarily results in chain termination, in turn resulting in replication fork stalling, activation of the S-phase checkpoint and subsequent cell cycle arrest and cell death via apoptosis (bold text, solid arrows). Other processes which could occur (as described in the text) are indicated by plain text/dashed arrows. DNA MMR components are highlighted in red, alongside steps in which they are speculated to be involved.

3.3.1. Summary of Chapter

In summary, the studies described in this chapter demonstrate:

- Deficiency of the DNA MMR pathway via loss of MutS α activity confers cellular sensitivity to the nucleoside analogues Ara-C, fludarabine, cladribine and clofarabine.
- A number of mechanisms could be responsible for this phenotype including S phase checkpoint abrogation or deregulation of downstream repair pathways at the stalled replication fork, such as HRR.
- Loss of MSH3 protein does not significantly perturb the function of the MMR pathway but is able to confer tolerance/resistance to the cytotoxic effects of the nucleoside analogues Ara-C, fludarabine and clofarabine.
- Incorporation of nucleoside analogues into DNA may result in lesions that can act as substrates for the MutS β complex, which mediates their cytotoxicity. This could explain the tolerance to these agents observed in MSH3-deficient cells.

**Chapter 4. Overexpression of *MSH3* Confers Resistance to
Nucleoside Analogues *in vitro***

4.1. Introduction

Loss of MMR-mediated DNA damage signalling, through absence of functional gene products, results in the characteristic methylation (and 6-TG) tolerance phenotype of MMR-defective cells *in vitro* (Karran, 2001). Investigations described previously (Chapter 3) have extended these findings and demonstrated that loss of MMR components can also mediate response to chemotherapeutic nucleoside analogues. In particular, loss of MSH3 (through gene knockdown), and hence the MutS β complex, confers tolerance to the cytotoxic effects of these agents (see Figure 3.9).

MMR dysfunction can arise not only through lack of a functional gene product, but also as a result of imbalance in the relative amounts of MMR proteins due to gene amplification. The best example of this phenomenon is provided by the cell line HL-60R, an MMR-dysfunctional subclone of the myeloid leukaemic cell line HL-60. Relative to parental HL-60 cells, HL-60R demonstrates gross over-production of MSH3 protein, resulting in sequestration of virtually all cellular MSH2 protein into the MutS β complex (Drummond et al., 1997). Lack of MSH6 (and hence the MutS α complex) is postulated to be due to proteasome-mediated degradation of the protein in the absence of any free MSH2 with which to heterodimerise (Drummond et al., 1995; Drummond et al., 1997). Consequently, HL-60R cells are unable to repair mismatches as determined by *in vitro* assay (Drummond et al., 1997; Marra et al., 1998), and are hypermutable in comparison to parental HL-60 cells (Drummond et al., 1997).

The overproduction of MSH3 protein in HL-60R is a direct result of overexpression of the *MSH3* gene, located on chromosome 5q14.1. Interestingly, the promoter region of the *MSH3* gene is shared with another gene, *dihydrofolate reductase (DHFR)*, transcribed in the opposite direction (Figure 4.1). The protein product of the *DHFR* gene is an essential metabolic enzyme which catalyses reduction of dihydrofolate to tetrahydrofolate, essential for *de novo* synthesis of purines and certain amino acids (Schnell et al., 2004). The action of DHFR can be blocked by treatment with the antifolate drug MTX, leading to inhibition of cell growth and proliferation (Schweitzer et al., 1990), however resistance can develop via a number of mechanisms, including *DHFR* gene amplification (Banerjee et al., 2002). The HL-60R subclone was generated by treatment of HL-60 cells with prolonged, escalating doses

of MTX (up to 1 μ M). This considerable selective pressure caused gross amplification of the *DHFR* gene (leading to MTX resistance), which was accompanied by co-amplification of *MSH3* (Fujii and Shimada, 1989). Subsequently, MTX-resistant HL-60R cells were demonstrated to be cross-resistant to the cytotoxic effects of methylating agents and 6-TG (Pepponi et al., 2001) by virtue of the effects of MSH3 protein overproduction on assembly of DNA MMR damage recognition complexes as described above.

Whereas defective DNA MMR caused by protein loss (either through mutation or promoter hypermethylation) has been observed in t-AML (Horiike et al., 1999; Zhu et al., 1999; Casorelli et al., 2003), as well as other cancers, MSH3 amplification leading to protein overproduction (or indeed amplification of other MMR genes) has yet to be documented *in vivo*.

4.1.1. Aims of Chapter 4

Loss of key DNA MMR components through either lack of gene expression or imbalances in cellular amounts of protein components is able to confer characteristic tolerance to the cytotoxic effects of methylating agents and 6-TG as described. The overall objective of this chapter was to determine whether amplification of MSH3 gives rise to concomitant MutS complex imbalance and whether this affects *in vitro* response to chemotherapeutic nucleoside analogues.

Specifically, the experimental aims were as follows:

- Using cell lines in which *MSH3* is overexpressed to varying degrees (HL-60R, TK6 MTX^R and PreB697 MTX^R), determine the effect on key DNA MMR components (and MutS complex formation) at protein and gene expression levels.
- Determine whether overproduction of MSH3 protein affects response to Ara-C, clofarabine, fludarabine and cladribine using cytotoxicity assays.

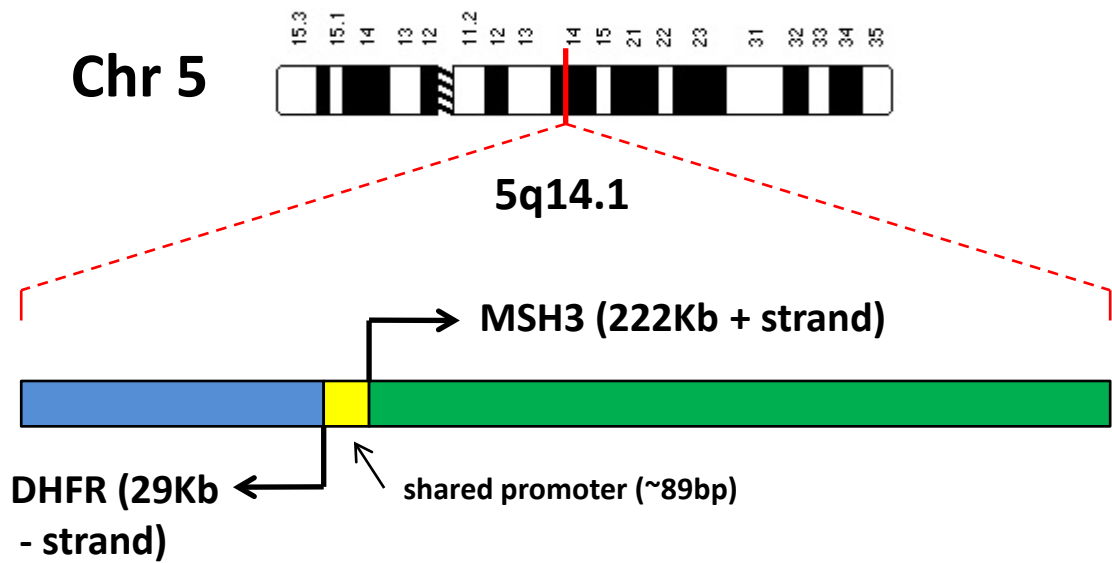


Figure 4.1. Structural organisation of human *DHFR* and *MSH3* loci.

The human *MHS3* gene is divergently transcribed from a promoter region shared with the *DHFR* gene on chromosome 5q14.1. The relative orientation of the two loci is shown, as well as the approximate total lengths of the genes (not drawn to scale). Numbers above the chromosome 5 ideogram indicate cytogenetic bands.

4.2. Results

4.2.1. Phenotypic Characterisation of MSH3-Overexpressing Cell Lines

HL-60R is a subclone of the myeloid leukaemic cell line, HL-60. As described above, it was generated by treating parental HL-60 with increasing concentrations of MTX over a period of several weeks, resulting in a 200-fold increase in *DHFR* and concomitant *MSH3* copy number (Fujii and Shimada, 1989).

TK6 MTX^R and PreB697 MTX^R are both subclones of the lymphoblastoid cell lines, TK6* and Preb697, respectively, also generated by treatment of the parental cells with escalating doses of MTX (Matheson et al., 2007). The doses used were much lower than those used to generate HL-60R and resulted in approximately 7-fold and 3-fold amplification of *DHFR* and *MSH3* in TK6 MTX^R and PreB697 MTX^R, respectively (Matheson et al., 2007).

4.2.1.1. Expression Levels of MMR Proteins Determined by Western Immunoblotting

The relative amounts of MSH3 protein, as well as the other mismatch recognition proteins, MSH2 and MSH6, were compared in parental cells and their MTX-resistant subclones via western immunoblotting (Figure 4.2A). The HL-60R cell line demonstrated significantly higher levels of MSH3 protein relative to parental HL-60 cells. This was accompanied by a slight increase in the levels of MSH2 protein and complete loss of MSH6 protein, consistent with previous studies which have assessed the levels of DNA MMR protein components in this cell line (Drummond et al., 1997; Marra et al., 1998). TK6 MTX^R and PreB697 MTX^R both demonstrated modest over-production of MSH3 protein relative to their respective parental cells, consistent with previous investigations (Matheson et al., 2007). There was no effect however, on the levels of MSH2 or MSH6 protein in either cell line.

In addition to the damage recognition proteins, relative levels of MLH1 and PMS2, which form the MutL α complex, were also assessed in MTX-resistant sublines, with no difference observed for either protein relative to respective parental counterparts (Figure 4.2B).

* Note that due to the paired nature of the cell lines used, the parental TK6 cell line described in this chapter is from a different source to the TK6 line used in all other investigations (see Section 2.2).

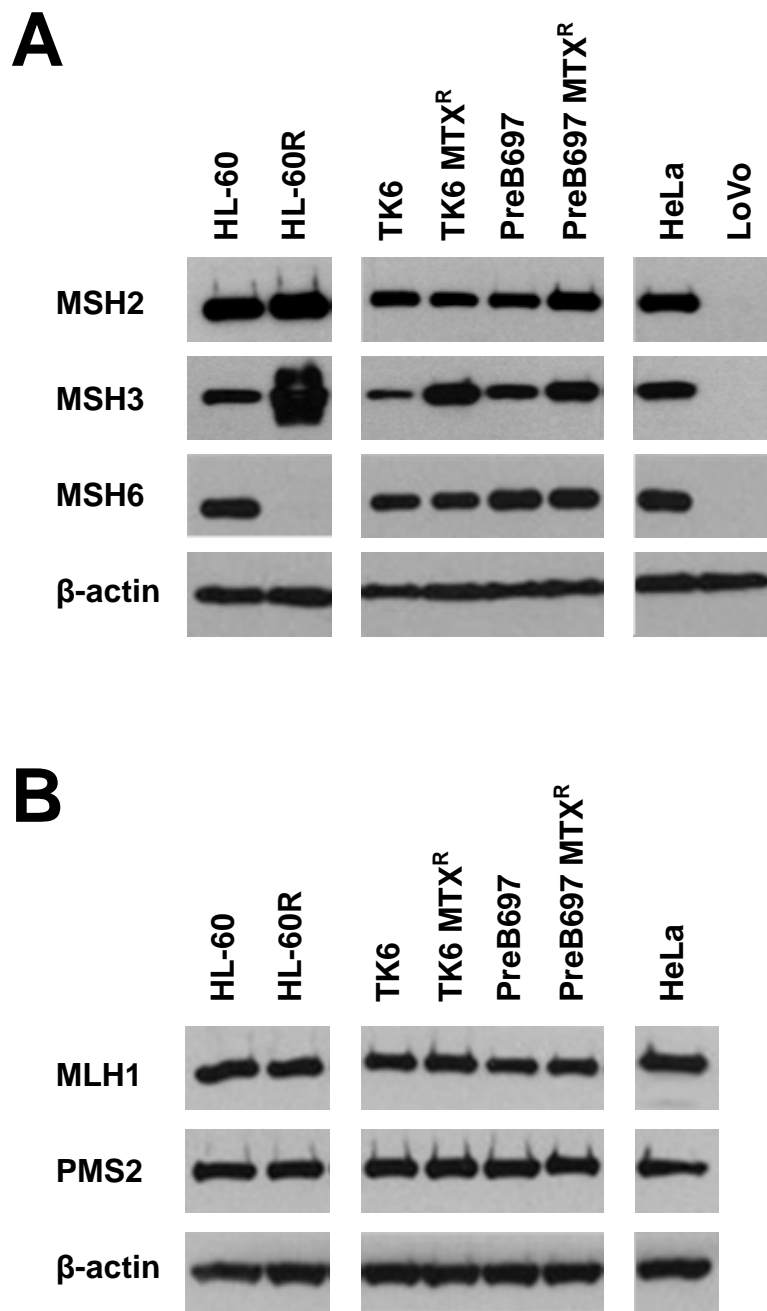


Figure 4.2. MMR protein expression in methotrexate-resistant cell lines.

Western immunoblotting to determine protein expression of DNA MMR components in HL-60R, TK6 MTX^R and PreB697 MTX^R, relative to their respective parental counterparts as follows: **A.** MutS components (MSH2, MSH3 and MSH6). **B.** MutL α components (MLH1 and PMS2). The MMR proficient HeLa cell line was included as a positive control in each case. The MutS deficient LoVo cell line was included as a negative control for MSH2, MSH3 and MSH6 proteins. β -actin was used as a loading control for all blots. Each blot is representative of three independent experiments.

4.2.1.2. Expression Levels of MMR Genes Determined by Quantitative RT-PCR

To determine whether the observed relative changes in MMR protein levels stemmed from changes at the transcriptional level, relative expression of *MSH2*, *MSH3* and *MSH6* was determined in parental and corresponding MTX-resistant sublines (Figure 4.3). Consistent with previous reports (Fujii and Shimada, 1989; Matheson et al., 2007), approximate 200-fold, 5-fold and 2.5-fold increased *MSH3* expression was observed in HL-60R, TK6 MTX^R and PreB697 MTX^R respectively. There was no change however, in expression of *MSH2* or *MSH6* in any of the MTX-resistant cell lines relative to their respective parental counterparts. These findings demonstrate that loss of *MSH6* protein in HL-60R cells is due to post-translational regulation, probably proteasome-mediated degradation, as previously suggested (Drummond et al., 1995; Drummond et al., 1997).

Relative expression of the *MLH1* and *PMS2* genes was also unchanged in MTX-resistant subclones relative to parental cell lines (Figure 4.3).

4.2.1.3. Cytotoxicity in Response to MNU and 6-TG

To determine the MMR status of the MTX-resistant cell lines, response to treatment with MNU and 6-TG, was assessed, given that tolerance to the cytotoxic effects of these agents is indicative of a defective DNA MMR pathway.

Previous studies have shown that HL-60R is tolerant to treatment with these agents, relative to parental HL-60 cells (Pepponi et al., 2001), and this was confirmed in the present study (Figure 4.4A). Conversely, neither TK6 MTX^R nor PreB697 MTX^R displayed differential sensitivity to MNU or 6-TG compared to their respective parental cells (Figure 4.4B-C), suggesting that MutS α -mediated DNA damage signalling is apparently unaffected in these cell lines.

These data suggest that cellular DNA MMR status is dependent on the severity of the specific MMR defect. Whereas gross over-expression of *MSH3* results in non-functional DNA damage signalling via loss of the MutS α complex, as shown in HL-60R (Drummond et al., 1997; Marra et al., 1998), modest *MSH3* over-production as observed in TK6 MTX^R and PreB697 MTX^R is not sufficient to perturb DNA damage signalling function and affect sensitivity to MNU and 6-TG.

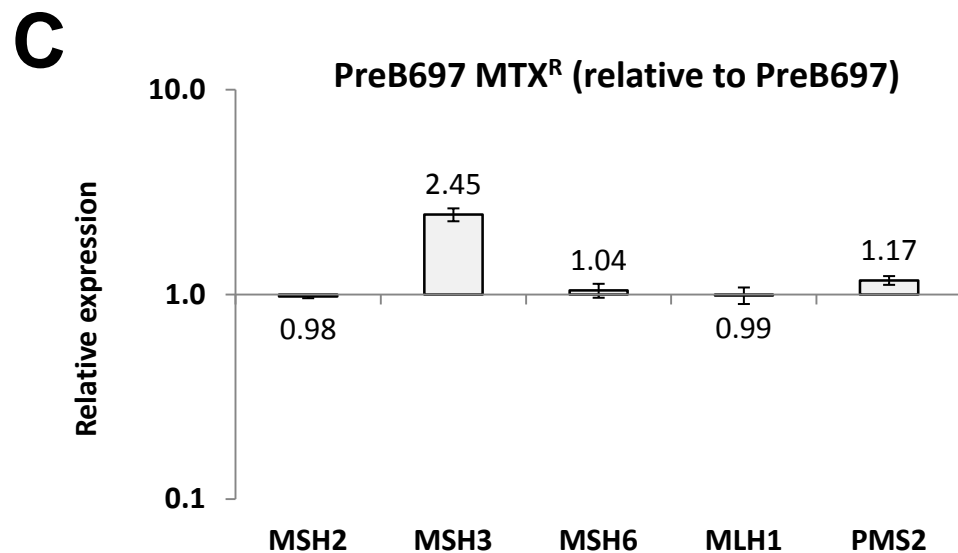
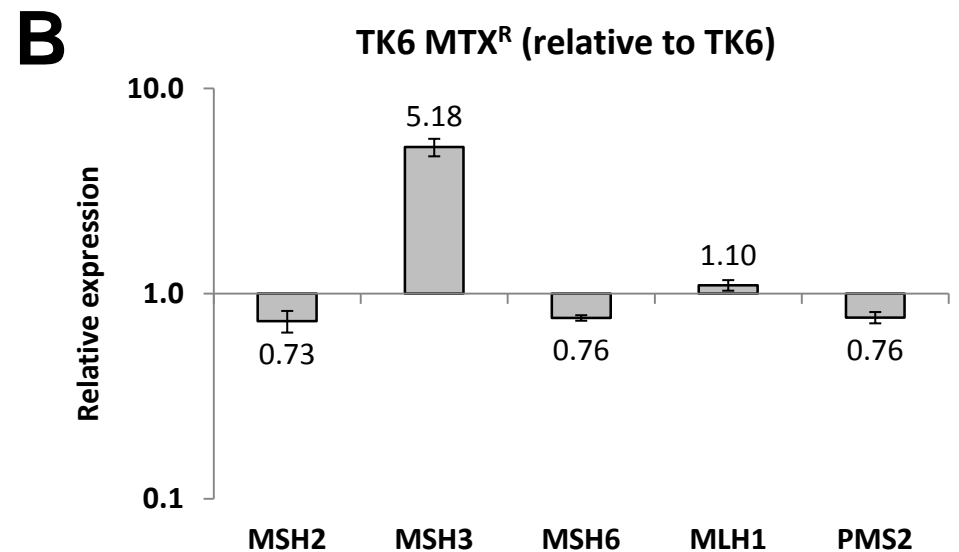
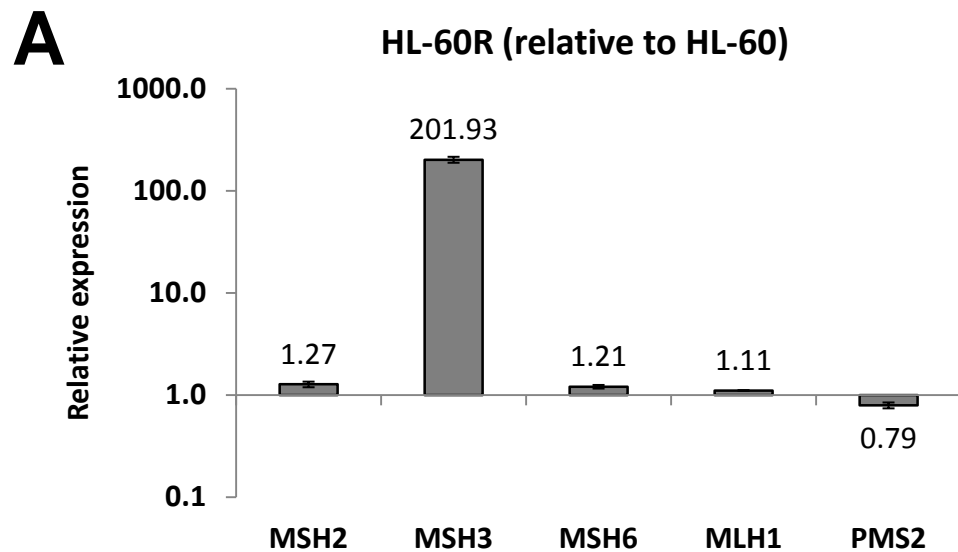


Figure 4.3. Relative expression of DNA MMR components in methotrexate-resistant cell lines.

RT-PCR to determine changes in gene expression of the MutS (*MSH2*, *MSH3* and *MSH6*) and MutL (*MLH1* and *PMS2*) components in HL-60R (**A**), TK6 MTX^R (**B**) and PreB697 MTX^R (**C**) cells relative to their respective parental cell lines. Expression of each gene was calculated relative to the parental cell line with the expression of *β-actin* used as endogenous control. Values represent fold change in expression calculated from the mean and standard error of three independent experiments.

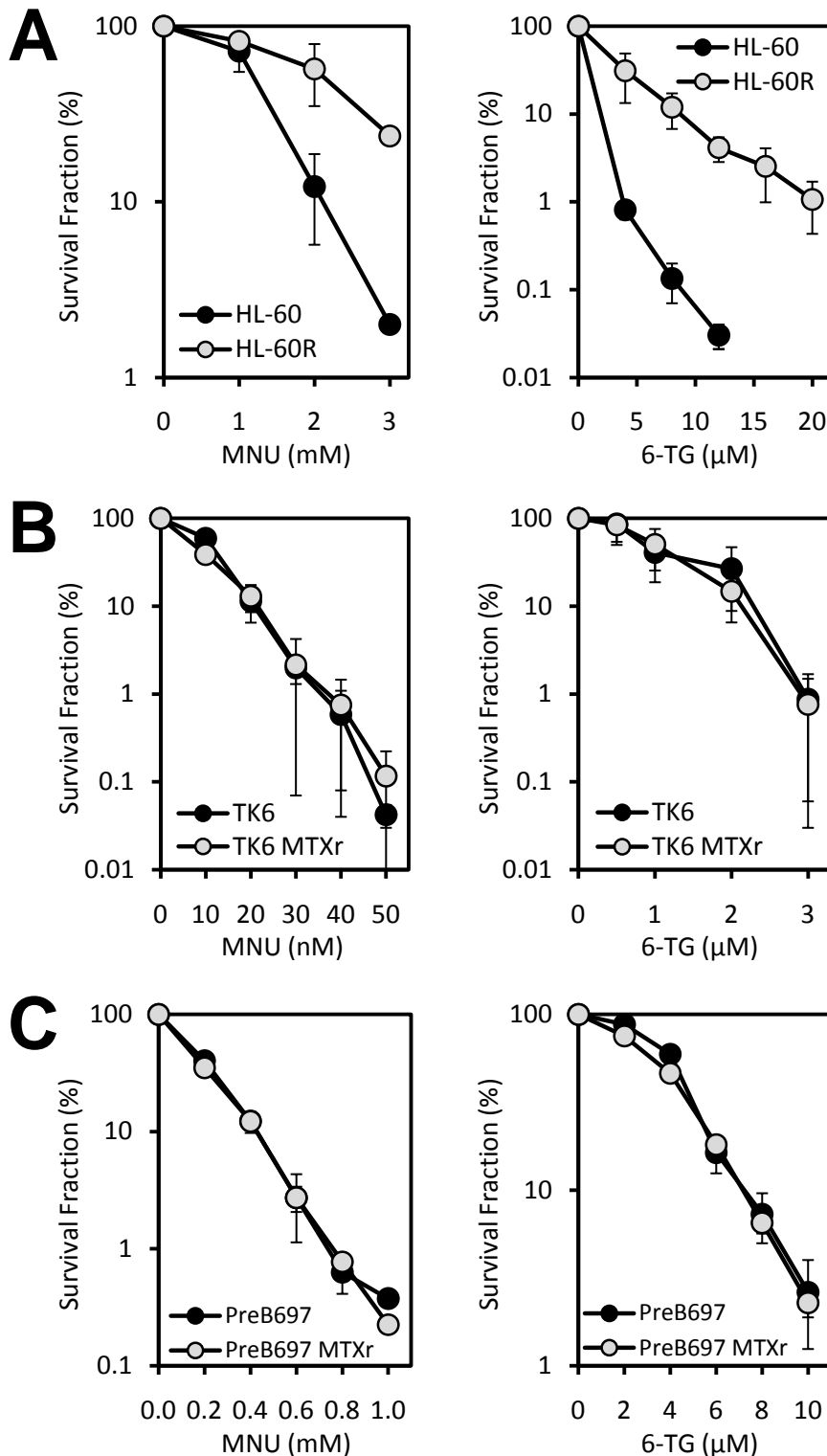


Figure 4.4. Cytotoxicity in response to MNU and 6-TG in *MSH3*-overexpressing cell lines.

Cytotoxicity in response to MNU (left) and 6-TG (right) was compared in HL-60 (A), TK6 (B), PreB697 (C) and their respective *MSH3*-overexpressing subclones. For HL-60 and PreB697, cytotoxicity was assessed via growth inhibition assay, with data presented as the number of surviving cells from dosed cell suspensions as a percentage of surviving cells from vehicle-only-treated cell suspensions. For TK6 and TK6 MTX^R, cytotoxicity was assessed via clonogenic assay. Data is presented as the number of viable colonies from dosed cell suspensions as a percentage of the number of viable colonies from vehicle-only-treated cell suspensions. In each case, data represents the mean and standard error of three independent experiments.

4.2.2. Cytotoxicity in *MSH3*-Overexpressing Cells Following Treatment with Nucleoside Analogues

Cytotoxicity assays were performed to assess response of the MTX-resistant subclones, relative to their respective parental cell lines, following treatment with the nucleoside analogues, Ara-C, clofarabine, fludarabine and cladribine (Figure 4.5).

HL-60R was tolerant to the cytotoxic effects of each of the nucleoside analogues relative to parental HL-60 cells (Figure 4.5A). TK6 MTX^R and PreB697 MTX^R however, were not differentially sensitive to any of these agents, relative to their respective parental lines (Figure 4.5B-C).

Taken together, these data demonstrate that overexpression of *MSH3* can confer resistance to treatment with therapeutic nucleoside analogues, but only when *MSH3* amplification is substantial.

4.2.3. Cytotoxicity in *MSH3*-Overexpressing Cells Following Exposure to IR and UV Radiation

In addition to investigating the effect of *MSH3* overexpression on response to nucleoside analogues, cytotoxicity in response to IR exposure was also assessed in MTX-resistant/*MSH3* amplified cell lines, given that certain DNA MMR defects have been reported to affect response to IR. Neither HL-60R, TK6 MTX^R nor PreB697 MTX^R demonstrated differential sensitivity to IR relative to normal parental cell lines (Figure 4.6A), which is consistent with the other cell lines tested (Section 3.2.7) and would argue against a role for DNA MMR in the cytotoxic response to IR. As previously stated however, defects in responses such as checkpoint activation cannot be excluded.

Cytotoxicity following exposure to UV radiation was also assessed in order to control for generic DNA repair defects (see Section 3.2.7). No difference in sensitivity to UV radiation was observed in any of the MTX-resistant cell lines relative to their respective parental counterparts (Figure 4.6B).

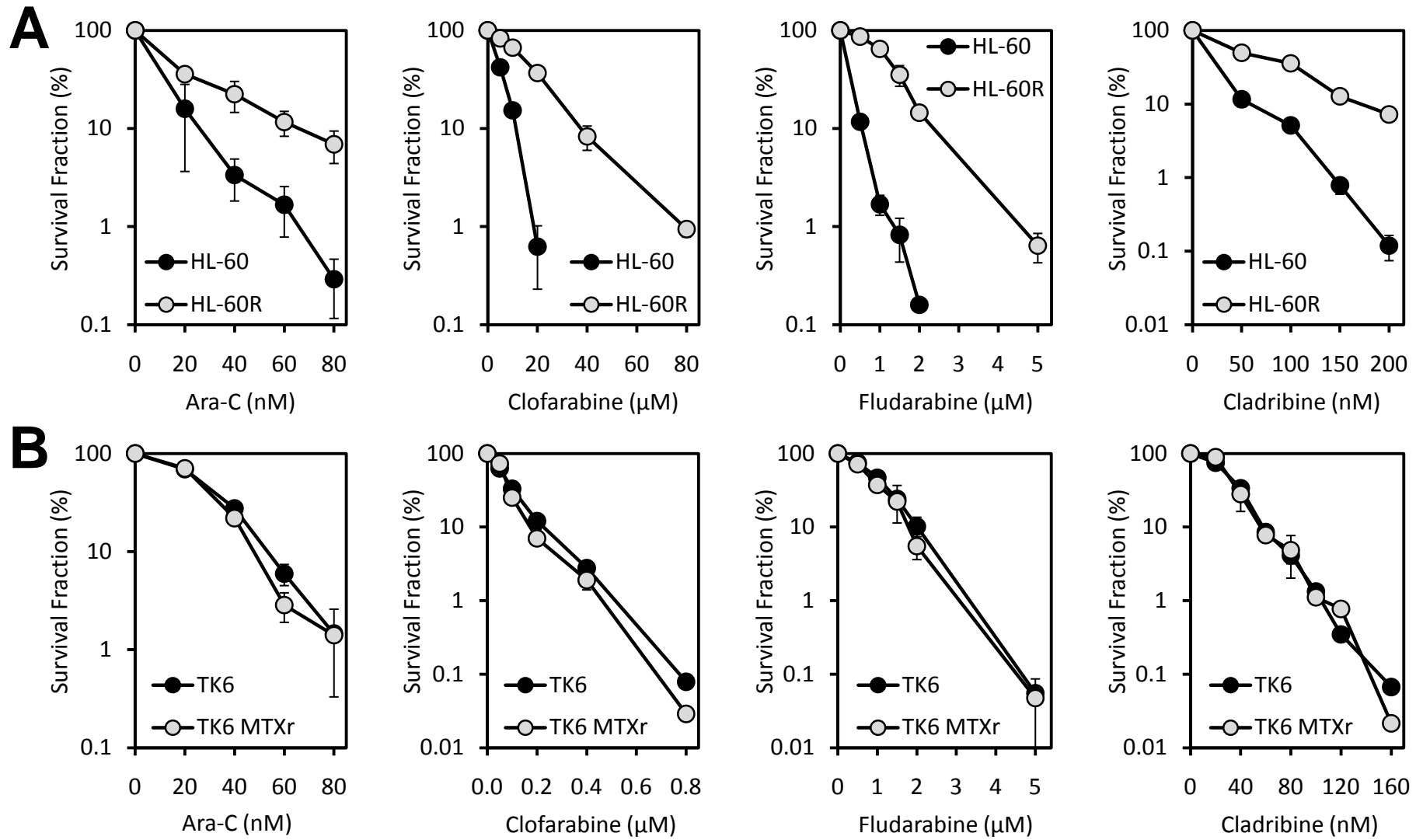


Figure 4.5. Cytotoxicity in response to nucleoside analogues in MSH3-overexpressing cell lines (continued on next page).

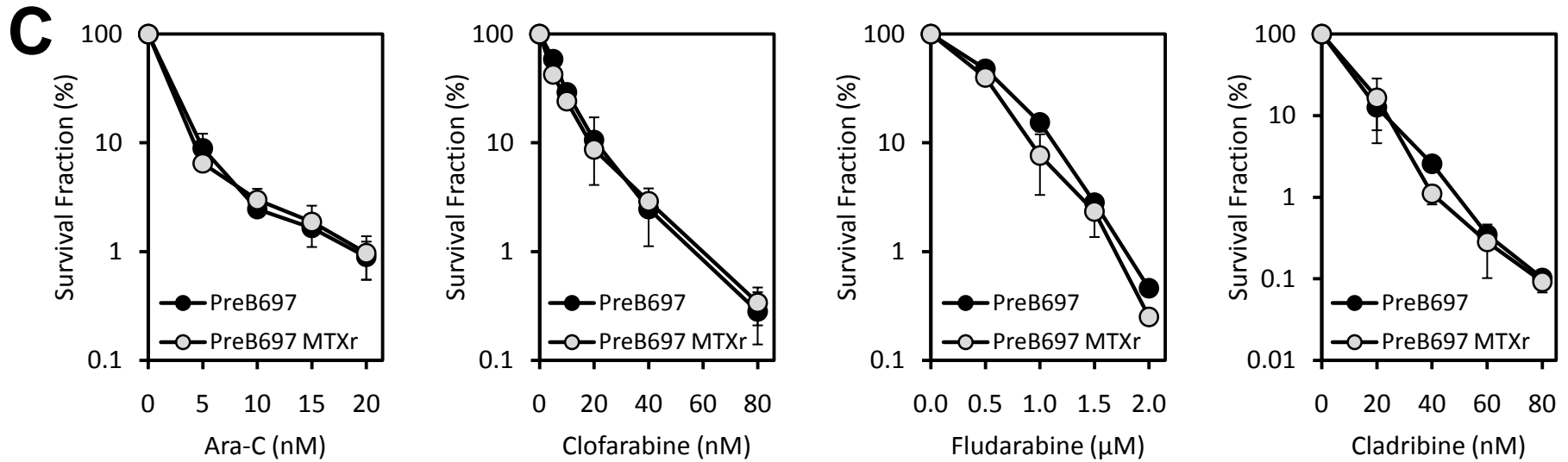
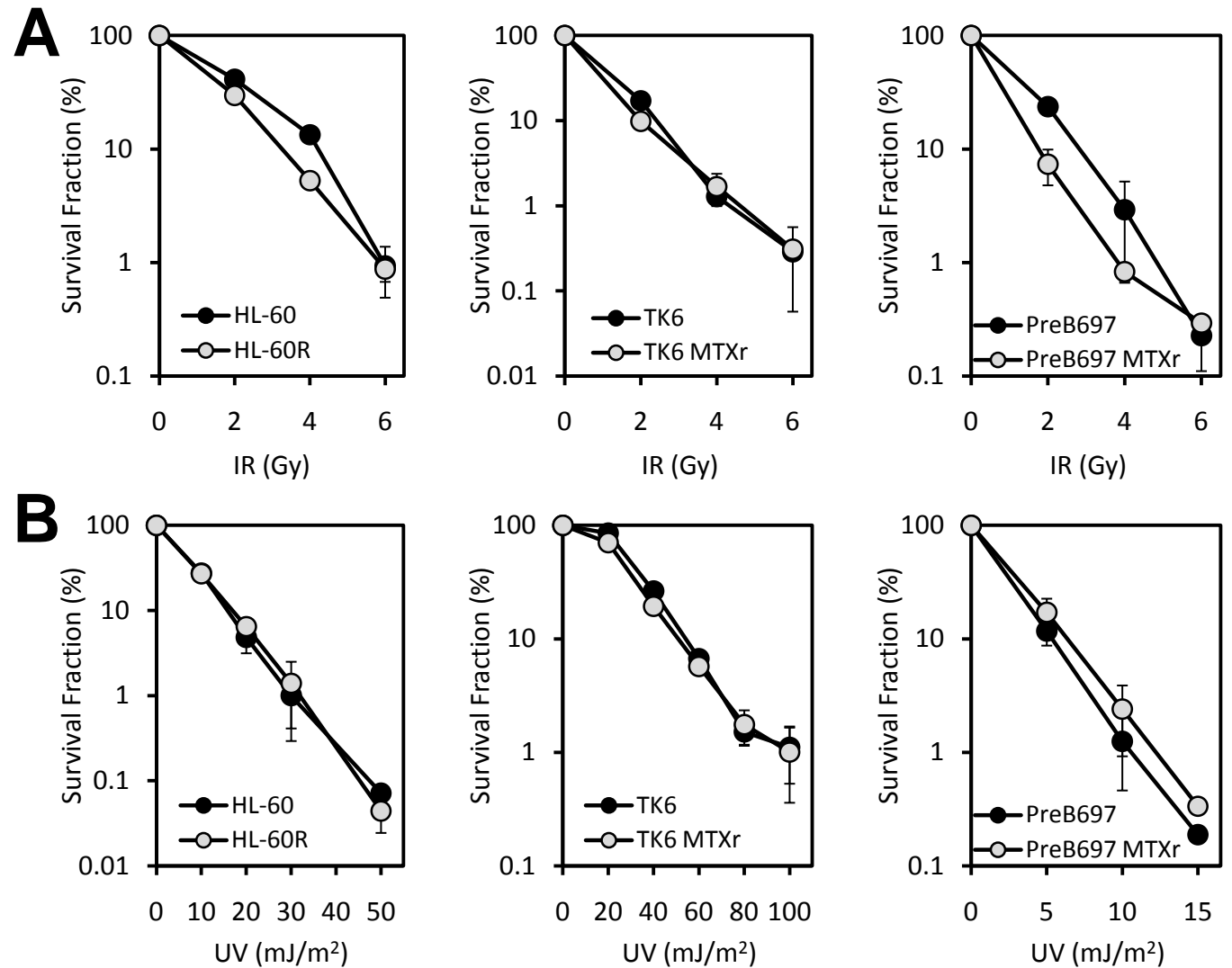


Figure 4.5. Cytotoxicity in response to nucleoside analogues in *MSH3*-overexpressing cell lines (continued from previous page).

Cytotoxicity in response to Ara-C (far left), clofarabine (left), fludarabine (right) and cladribine (far right) was compared in HL-60 (A), TK6 (B), PreB697 (C) and their respective *MSH3*-overexpressing subclones. For HL-60 and PreB697, cytotoxicity was assessed via growth inhibition assay, with data presented as the number of surviving cells from dosed cell suspensions as a percentage of surviving cells from vehicle-only-treated cell suspensions. For TK6 and TK6 MTX^R, cytotoxicity was assessed via clonogenic assay. Data is presented as the number of viable colonies from dosed cell suspensions as a percentage of the number of viable colonies from vehicle-only-treated cell suspensions. In each case, data represents the mean and standard error of three independent experiments.

Figure 4.6. Cytotoxicity following exposure to IR and UV in *MSH3*-overexpressing cell lines.

A. Cytotoxicity following IR exposure was compared in HL-60 (left), TK6 (centre), PreB697 (right) and their respective *MSH3*-overexpressing subclones. For HL-60 and PreB697, cytotoxicity was assessed via growth inhibition assay, with data presented as the number of surviving cells from dosed cell suspensions as a percentage of surviving cells from vehicle-only-treated cell suspensions. For TK6 and TK6 MTX^R, cytotoxicity was assessed via clonogenic assay. Data is presented as the number of viable colonies from dosed cell suspensions as a percentage of the number of viable colonies from vehicle-only-treated cell suspensions. **B.** Cytotoxicity following exposure to UV radiation was compared in HL-60, TK6, PreB697 and their respective *MSH3*-overexpressing cell lines as described above. In all cases, data represents the mean and standard error of three independent experiments.



4.3. Discussion

Prolonged exposure to MTX can cause amplification of the *DHFR* gene and co-amplification of *MSH3* due to its close proximity (Fujii and Shimada, 1989). Investigations using the myeloid cell line, HL-60R, confirm the findings of others and demonstrate that gross *MSH3* protein overexpression, due to *MSH3* amplification, results in loss of MutS α and consequently tolerance to methylating agents and 6-TG. This study, in addition, has extended these findings and demonstrates that extensive *MSH3* overproduction can also confer tolerance to the cytotoxic effects of the nucleoside analogues Ara-C, clofarabine, fludarabine and cladribine.

The observation that HL-60R demonstrates tolerance to the cytotoxic effects of nucleoside analogues is unexpected given that *MSH3* knockdown also confers tolerance to these agents (as demonstrated by TK6/HL-60 *MSH3i*; see Figure 3.9). As such, amplification of *MHS3* is expected to confer sensitivity, hence it is unclear how two seemingly opposing defects can result in a similar phenotype. Previous studies have demonstrated that the efficiency of repair of extrahelical loop substrates, mediated by the MutS β complex, is reduced to approximately 40% in HL-60R cells, relative to parental HL-60 cells (Drummond et al., 1997). Single base extrahelical loops are proposed to occur following replication of Ara-C lesions (see Figure 3.11). It is possible therefore that dysfunctional MutS β in HL-60R leads to diminished detection of and tolerance to nucleoside analogue-induced lesions as previously suggested (Section 3.3). How the cellular ratios of MMR damage recognition proteins influence the efficiency of DNA repair remains to be fully understood. It is also important to note that the observations herein may reflect the inability of one or more DNA MMR components to participate in a damage response specific to nucleoside analogues, which is independent from routine DNA repair. This finding therefore exemplifies the previous suggestion that the involvement of DNA MMR in the response to nucleoside analogues, as well as to other DNA damaging agents, is complex and likely is only one factor in an interwoven network of pathways.

The observed tolerance to nucleoside analogues in *MSH3*-amplified HL-60R adds to a small body of evidence that overexpression of a single DNA MMR component results in a phenotype that is traditionally assigned to MMR deficiency. For example,

forced over-expression of MLH1 in *S. cerevisiae* leads to compromised MMR function and a mutator phenotype (Shcherbakova and Kunkel, 1999). Similarly, over-expression of *PMS2* in murine cells confers tolerance to MNU, as well as an increase in both spontaneous and MNU-induced mutation frequency (Gibson et al., 2006). Mechanisms are unclear but may involve formation of either MLH1 or PMS2 homodimers that inhibit formation of the MutL α complex (MLH1 + PMS2) (Shcherbakova and Kunkel, 1999; Gibson et al., 2006). It would be interesting to determine whether overexpression of MutL α components could also confer tolerance to nucleoside analogues, or whether this response is restricted to dysfunction of damage recognition complexes.

It is possible that the observed Ara-C-resistance (as well as resistance to other nucleoside analogues) in HL-60R is in fact not due to defective DNA MMR, but rather due to a common resistance mechanism that is shared with MTX. Resistance to MTX in HL-60R is due primarily to gross overexpression of DHFR, the target for the inhibitory effects of the drug (Fujii and Shimada, 1989). The intracellular metabolism of Ara-C, as well as the purine nucleoside analogues, does not involve DHFR, hence it is improbable that this would confer cross-resistance to these agents. It is also possible that other uncharacterised resistance mechanisms are operating in HL-60R, affecting drug transport or metabolism for instance. Again however, it is unlikely that this would affect response to Ara-C given that these drugs do not appear to share any intracellular pathways. It is remotely possible that other factors common to the metabolism of these drugs have yet to be discovered.

Additionally, because of the selection method used to generate HL-60R, this line and HL-60 cannot be classed as an isogenic cell line pair. Furthermore, relative to HL-60, HL-60R is a hypermutable cell line (Drummond et al., 1997) and could readily acquire mutations anywhere in its genome. It is possible that this cell line is mutated in a gene (unrelated to DNA MMR) which could confer resistance to nucleoside analogues, although this is unlikely in the absence of any selective pressures. Nevertheless, a strictly isogenic system in which MMR protein levels can be up-regulated without the need for cell division would be useful to confirm whether these observations are directly attributable to defective DNA MMR.

In contrast to HL-60R, cell lines demonstrating a significantly lower level of *MSH3* amplification (~ 5-fold in TK6 MTX^R and ~ 2.5-fold in PreB697 MTX^R) were found to be proficient in DNA MMR by virtue of unaffected protein stoichiometry. Furthermore, these cell lines were not differentially sensitive to the cytotoxic effects of Ara-C and other therapeutic nucleoside analogues. The implications of these observations are two-fold: firstly they demonstrate that, in the case of over-expression of MMR genes, the extent of perturbation of DNA MMR components is important in determining whether the function of the pathway is significantly affected. It should be noted however, that although not sufficient to confer tolerance to the cytotoxic effects of methylating agents or 6-TG (or the nucleoside analogues), it is unknown whether the anticipated modest effects on the ratio of MutS α to MutS β could affect MMR efficiency. Secondly, given that these cell lines did not differ in response to Ara-C relative to their parental counterparts, despite demonstrating resistance to MTX (Matheson et al., 2007), further weight is added to the model that Ara-C resistance is due to dysfunction of DNA MMR and is independent of MTX resistance.

Despite being unable to delineate mechanisms at this point, these findings have clinical implications, particularly regarding the combined chemotherapeutic use of MTX and nucleoside analogues (or other drugs which are less effective in MMR-defective cells). Additionally, it has also been suggested that overexpression of DNA MMR components may represent a mechanism by which cells become genetically unstable, contributing not only to drug resistance, but also to carcinogenesis (Gibson et al., 2006). These factors will be discussed in Chapter 8.

4.3.1. Summary of Chapter

In summary, the investigations described in this chapter have shown that:

- Although significant overproduction of MSH3 protein can cause MutS α deficiency through protein imbalance, modest increases in the cellular amount of MSH3 protein do not significantly perturb DNA MMR-mediated damage signalling, as demonstrated by lack of tolerance to the cytotoxic effects of MNU and 6-TG (in TK6 MTX^R and PreB697 MTX^R).

- Gross overproduction of MSH3 in HL-60R confers tolerance to the nucleoside analogues Ara-C, clofarabine, fludarabine and cladribine, possibly by affecting MutS β function.
- Modest MSH3 over-production in TK6 MTX^R and PreB697 MTX^R does not result in differential nucleoside analogue sensitivity relative to parental cell lines.

**Chapter 5. Development of *in vitro* Cellular Model Systems of
Therapy-Related Acute Myeloid Leukaemia**

5.1. Introduction

Many agents routinely used in cancer chemotherapy, despite being highly cytotoxic to malignant cells, are carcinogenic, mutagenic and toxic to other non-malignant tissues. This can give rise to one of the most significant side effects associated with successful cancer therapy, which is development of a therapy-related malignancy (defined as a second primary malignancy pathologically independent from the first primary cancer, and which arises as a consequence of chemotherapy). Therapy-related malignancy can occur following treatment with a diverse range of chemotherapeutic agents, most notably methylating agents, topoisomerase inhibitors and thiopurine anti-metabolites, and can occur at almost all sites in the body. Compared to therapy-induced solid cancers, the relative risk of developing t-AML is considered highest due to the inherent sensitivity of the bone marrow to the toxic and mutagenic effects of several chemotherapeutic agents (Allan and Travis, 2005). For this reason extensive research efforts have been directed towards delineating the genetic and molecular mechanisms associated with development of t-AML.

Methylating agents such as procarbazine, dacarbazine and temozolomide are used to treat numerous cancers, including HL and NHL. High incidence of t-AML (as well as other secondary malignancies) in survivors of HL and NHL (Armitage et al., 2003; Josting et al., 2003; Schonfeld et al., 2006) is indicative of a causal link between the use of methylating agents in chemotherapy and the development of t-AML. A high incidence of t-AML is also observed in organ transplant patients who received the thiopurine anti-metabolite azathioprine as an immunosuppressive agent (Offman et al., 2004) (see Section 1.4.4). Additionally, t-AML has been identified as a potential complication of thiopurine therapy for ALL (Karran 2008). These findings suggest a causative association between the use of thiopurine anti-metabolites and t-AML development.

The aetiology of t-AML following methylating agent chemotherapy, and by extension t-AML following the use of thiopurines, is particularly well defined and likely follows a 'genomic instability' pathway, whereby a mutator phenotype predisposes target cells to accumulate mutations in multiple genes that will eventually lead to leukaemic transformation, as described in Section 1.4.1.1. Because of the well established interaction between methylating agents (and 6-TG) and DNA MMR

components, coupled with the observation of high levels of MSI indicative of defective MMR in t-AML patients (see Figure 1.9), loss of activity of this pathway is postulated to be the causative event giving rise to genomic instability in methylating agent-related t-AML carcinogenesis (Allan and Travis, 2005).

Loss of DNA MMR activity *in vitro* provides a mechanism by which cells can tolerate the cytotoxic effects of methylating agents (Karran, 2001). It follows therefore, that dysfunction of DNA MMR *in vivo* would provide a selective advantage allowing cells to circumvent methylating agent-induced cell death, although this has not been firmly established. It is possible that this could occur due to methylating agents themselves inducing abrogation of DNA MMR activity, resulting in a sub-clone of MMR-defective cells in an otherwise MMR-proficient population. It is not clear however, why this would be selectively advantageous to haematopoietic cells within the bone marrow, given that they are non-malignant at the time chemotherapy is administered for the primary malignancy. It has been suggested that MMR-proficient cells which express low levels of MMR components may be particularly susceptible to methylating agent-induced mutations (Claij and Te Riele, 2002). An alternative possibility is that an MMR-defective sub-clone may already exist in an early myeloid progenitor population within the bone marrow, and methylating agent chemotherapy promotes expansion of this clone due to the survival advantage afforded by MMR loss. Evidence in support of this has been demonstrated in murine models using temozolomide (Reese et al., 2003), as well as *in vivo* following cisplatin chemotherapy (Fink et al., 1997; Samimi et al., 2000), as outlined in Section 1.4.1.1. In both cases, the highly proliferative nature of the bone marrow would mean MMR-defective cells would be rapidly expanded.

There is some limited evidence to suggest that patients treated with chemotherapeutic nucleoside analogues are also at risk of developing t-AML. In particular, a number of studies have reported cases of t-AML with abnormalities of chromosome 7 following fludarabine therapy for CLL (Coso et al., 1999; Morrison et al., 2002; McLaughlin et al., 2005; Carney et al., 2010). Similarly, a recent small study has reported 5 cases of t-AML with abnormalities of chromosome 7 arising in patients who received Ara-C during treatment for *de novo* AML (Arana-Yi et al., 2008). Mechanisms by which nucleoside analogues could contribute to t-AML development have yet to be

investigated but could involve MMR defects, given the evidence suggesting DNA MMR status can mediate response to these agents (Chapters 3 and 4).

Therapy-related malignancies, by virtue of their aetiology, are generally difficult to treat and do not respond favourably to routine chemotherapeutic regimes. This is particularly exemplified in the case of t-AML in which the CR rate is as low as 28% (Larson, 2007). A direct link between DNA MMR loss and chemoresistance has yet to be firmly identified in t-AML, although the *in vitro* studies outlined in this work (Chapters 3 & 4) support a role for MMR-dysfunction in resistance to Ara-C and other nucleoside analogues routinely used in AML treatment.

5.1.1. Aims of Chapter 5

The purpose of these investigations was to determine whether treatment of myeloid cells with either a methylating agent, 6-TG or Ara-C *in vitro* could result in generation of DNA MMR-defective sub-clones, effectively re-capitulating early events in the postulated development of t-AML. Furthermore, to investigate whether drug-resistant sub-clones demonstrate cross-resistance to chemotherapeutic agents routinely used in treatment of t-AML, hence providing a possible explanation for the typically chemoresistant nature of the disease.

Specifically, the experimental aims were as follows:

- Treat myeloid cell lines with escalating doses of MNU, 6-TG or Ara-C over an extended time period to determine if stable drug-resistant sub-cultures could be generated.
- Determine DNA MMR status of resulting drug-resistant sub-cultures via assessment of cytotoxicity in response to MNU and 6-TG, and via western immunoblotting for expression of DNA MMR proteins.
- Assess cytotoxicity of drug-resistant sub-cultures in response to treatment with therapeutic nucleoside analogues (Ara-C, clofarabine and fludarabine).

5.2. Results

5.2.1. Cell Lines

The myeloid cell lines HL-60, EoL-1 and KG-1 were selected for use in these investigations because they are widely used, well characterised AML cell lines and most likely to represent the postulated *in vivo* target cell population. In addition, the lymphoblastoid cell line TK6 was selected as it had previously been used to generate drug-resistant sub-clones via escalating drug dosage (Matheson et al., 2007).

5.2.2. Characterisation of Cell Lines Treated with MNU

HL-60, EoL-1, KG-1 and TK6 were each treated with escalating doses of MNU as described in Section 2.5. For three of these cell lines (EoL-1, KG-1 and TK6) this resulted in establishment of cell cultures capable of survival in MNU concentrations 10-fold, 20-fold and 50-fold greater than the initial MNU dose (cytotoxic to 70-80% of parental cells), respectively. These were termed EoL-1 MNU^R, KG-1 MNU^R and TK6 MNU^R.

For HL-60, cells recovered from treatment with an MNU dose 10-fold greater than the initial dose (termed HL-60 MNU^R). However treatment with higher doses consistently resulted in death of all cells. Assessment of MNU resistance in HL-60 MNU^R, relative to parental HL-60 cells, demonstrated no acquired MNU-resistance (data not shown), hence this sub-culture was excluded from further investigations.

5.2.2.1. Confirmation of Stable MNU Resistance in TK6, KG-1 and EoL-1

Cytotoxicity assays following passage in drug-free media demonstrated that EoL-1 MNU^R, KG-1 MNU^R and TK6 MNU^R retained resistance to MNU-induced cytotoxicity relative to their parental counterparts, indicating that the mechanisms of resistance were stable (Figure 5.1) and that cells did not require continuous exposure to MNU.

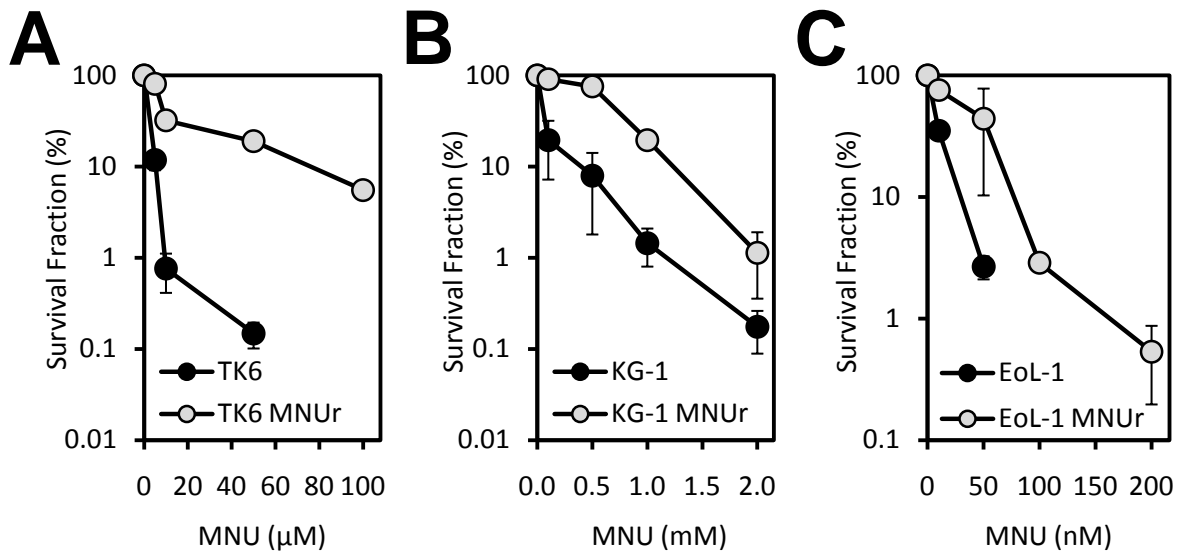


Figure 5.1. Stable acquired resistance to MNU in subcultures derived following escalating MNU exposure.

Cytotoxicity assays were performed to confirm resistance to MNU in TK6 MNU^R (A), KG-1 MNU^R (B) and EoL-1 MNU^R (C) following serial passage in drug-free media. For TK6 and its MNU-resistant subclone, cytotoxicity was compared via clonogenic assay. Data is presented as the number of viable colonies from exposed cell suspensions as a percentage of the number of viable colonies from unexposed control cell suspensions. For KG-1, EoL-1 and their respective MNU-resistant subclones, cytotoxicity was compared via growth inhibition assay. Data are presented as the number of surviving cells from exposed cell suspensions as a percentage of surviving cells from unexposed control cell suspensions. In all cases, data represents the mean and standard error of three independent experiments.

5.2.2.2. Cytotoxicity in MNU-Resistant Cell Lines Following Treatment with 6-TG

To determine whether the observed MNU-resistance in the treated sub-cultures could be the result of a defect in DNA MMR, cellular response to 6-TG was assessed, given that cross-resistance to the cytotoxic effects of this agent is characteristic of MMR-defective cells (Aquilina et al., 1989; Aquilina et al., 1990; Hawn et al., 1995; Shin et al., 1998; Humbert et al., 1999). For TK6 MNU^R (Figure 5.2A) and EoL-1 MNU^R (Figure 5.2C), no differential sensitivity to 6-TG was observed relative to respective parental cell lines. Unexpectedly, and inconsistent with defective DNA MMR, an increase in sensitivity to the cytotoxic effects of 6-TG was observed in KG-1 MNU^R relative to parental KG-1 cells (Figure 5.2B).

5.2.2.3. Expression Levels of MMR Proteins Determined by Western Immunoblotting

Lack of cross-resistance to 6-TG suggests that the mechanism of MNU resistance does not involve significant dysfunction of the DNA MMR pathway in either KG-1 MNU^R, EoL-1 MNU^R or TK6 MNU^R. Nevertheless, western immunoblotting was performed to investigate expression of MutS components (MSH2, MSH3 and MSH6), MutL α components (MLH1 and PMS2) and MGMT in MNU-resistant cells and their normal parental counterparts (Figure 5.3). For TK6 MNU^R, levels of MSH2, MSH3, MSH6, MLH1 and PMS2 were unaffected relative to parental TK6 cells, consistent with retention of functional DNA MMR. The western immunoblot for MGMT however, revealed that re-expression of the protein had occurred in TK6 MNU^R (Figure 5.3). MGMT acts upstream of DNA MMR to remove MNU-induced methyl groups from DNA prior to replication. Re-expression of MGMT has previously been reported to be associated with acquired resistance to methylating agents (Hampson et al., 1997), therefore it is probable that this is the mechanism responsible for the MNU-resistance observed in this cell line.

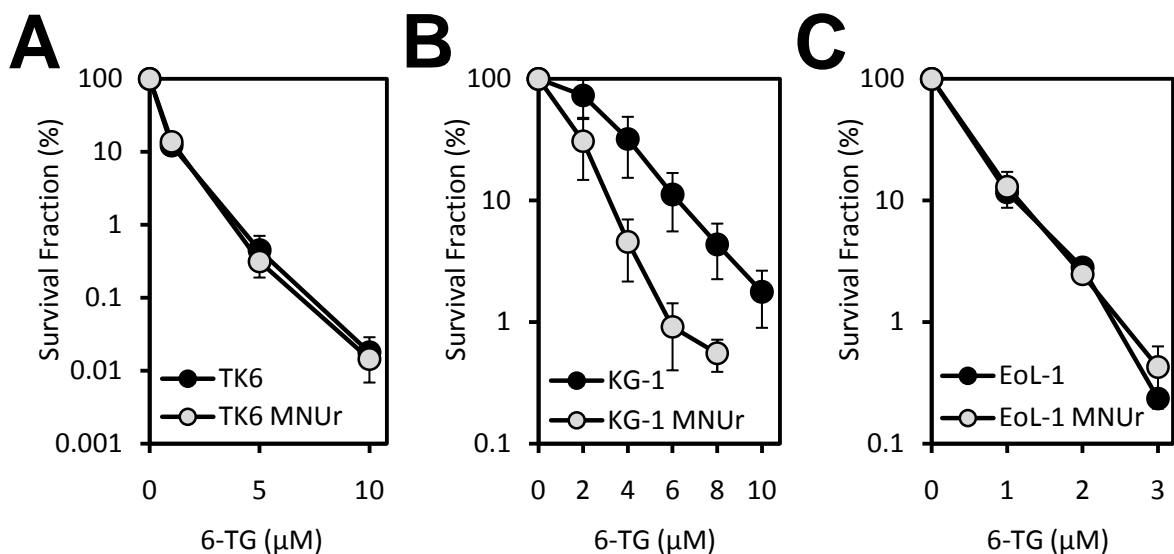


Figure 5.2. Cytotoxicity following treatment with 6-TG in MNU-resistant cell lines.

Cytotoxicity assays were performed to assess resistance to 6-TG in TK6 MNU^R (A), KG-1 MNU^R (B) and EoL-1 MNU^R (C) relative to their respective parental cell lines. For TK6 and its MNU-resistant subclone, cytotoxicity was compared via clonogenic assay. Data is presented as the number of viable colonies from exposed cell suspensions as a percentage of the number of viable colonies from unexposed control cell suspensions. For KG-1, EoL-1 and their respective MNU-resistant subclones, cytotoxicity was compared via growth inhibition assay. Data are presented as the number of surviving cells from exposed cell suspensions as a percentage of surviving cells from unexposed control cell suspensions. In all cases, data represents the mean and standard error of three independent experiments.

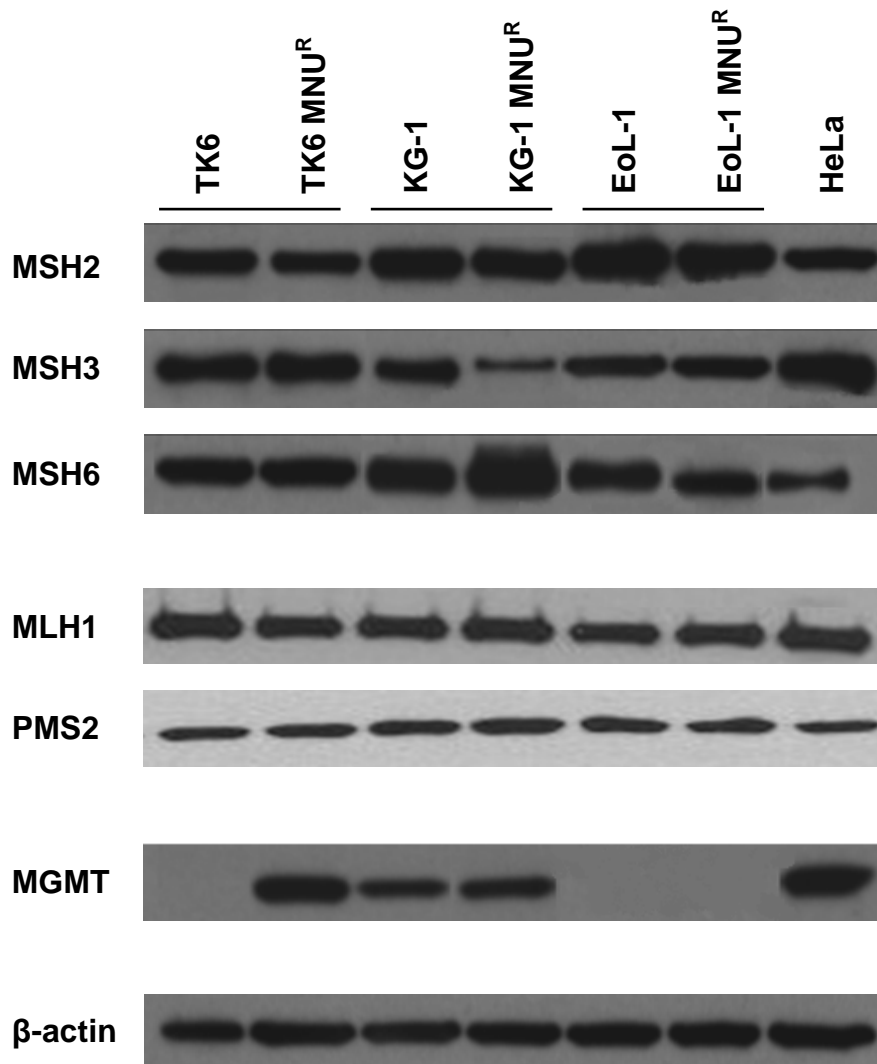


Figure 5.3. MMR protein expression in MNU-resistant cell lines.

Western immunoblotting was performed to determine protein expression of DNA MMR components (MSH2, MSH3, MSH6, MLH1, PMS2 and MGMT) in the MNU-resistant cell lines TK6 MNU^R, KG-1 MNU^R and EoL-1 MNU^R, relative to their respective parental cell lines. The MMR proficient HeLa cell line was included as a positive control. β-actin was used as a loading control. Each blot is representative of three independent experiments.

For KG-1 MNU^R, an increase in the amount of MSH6 protein of approximately 30% was observed, accompanied by an approximate 60% reduction in the amount of MSH3, whereas levels of MSH2, MLH1 and PMS2 were unchanged (Figure 5.3). It could be postulated that increased production of MSH6 protein results in sequestering of more MSH2 into the MutS α complex, leaving a proportion of partnerless MSH3 protein which is subsequently degraded. An increase in the activity of MutS α however, would be expected to confer increased sensitivity to treatment with methylating agents by virtue of an increase in cellular capacity for detection of mispairs. It is therefore unlikely that these observations account for the MNU resistance demonstrated by KG-1 MNU^R, although they could account for the observed increase in sensitivity to 6-TG.

For EoL-1 MNU^R, a slight reduction in MSH6 (approximately 10%) was evident, although this did not appear to affect MSH2 or MSH3 expression (Figure 5.3). Nor was expression of MLH1, PMS2 or MGMT affected relative to parental EoL-1 cells. It is unclear whether a reduction in MSH6 protein of this extent could be responsible for the MNU resistance observed, however this is unlikely given that cross-resistance to 6-TG would also be observed, and it was not.

5.2.2.4. Assessment of Thiopurine Methyltransferase Status in KG-1 MNU^R via Western Immunoblotting

Thiopurine methyltransferase (TPMT) mediates intracellular 6-TG concentration by methylating 6-TG and its derivative, 6-TG monophosphate, resulting in inactive metabolites (see Figure 1.3). Intracellular levels of TPMT vary between individuals due to constitutional genetic polymorphisms that affect gene expression. TPMT activity is correlated with sensitivity to thiopurine drugs *in vivo* (Coulthard and Hogarth, 2005), and *in vitro* studies have demonstrated that lower levels of TPMT are associated with increased sensitivity to 6-TG (Coulthard et al., 2002). To determine whether reduction in TPMT activity could provide an explanation for the 6-TG hypersensitivity observed in KG-1 MNU^R, western immunoblotting was performed in KG-1 MNU^R and parental KG-1 cells to assess levels of TPMT protein. Both KG-1 and its MNU-resistant subclone, KG-1 MNU^R were found to express undetectable levels of TPMT protein (Figure 5.4), hence excluding reduction in activity as responsible for 6-TG hypersensitivity in KG-1 MNU^R, relative to parental KG-1 cells.

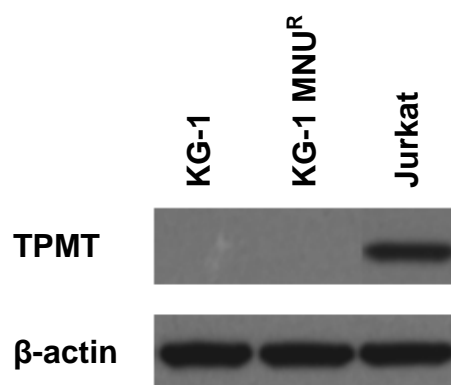


Figure 5.4. TPMT protein expression in KG-1 and KG-1 MNU^R.

Western immunoblotting to determine expression of TPMT protein in KG-1 and its MNU-resistant subclone KG-1 MNU^R and EoL-1 MNU^R. Jurkat cell lysate was included as a positive control. β-actin was used as a loading control. The blot is representative of three independent experiments.

5.2.2.5. Cytotoxicity in MNU-Resistant Cell Lines Following Treatment with Cytarabine

Although it did not appear that MMR-mediated DNA damage signalling was affected in the MNU-resistant subclones, cytotoxicity in response to Ara-C treatment was assessed, given that relative proportions of certain MMR components was perturbed, as evidenced by western immunoblotting (Figure 5.3). For TK6 MNU^R (Figure 5.5A) and EoL-1 MNU^R (Figure 5.5C), there was no difference in response to Ara-C relative to parental cell lines. However, KG-1 MNU^R, which has relative overexpression of MSH6 and underexpression of MSH3 (Figure 5.3), was resistant to cytotoxicity induced by Ara-C relative to parental KG-1 cells (Figure 5.5B). This is consistent with the studies using MMR knockdown cell lines in which MSH3 reduction resulted in resistance to Ara-C (see Figure 3.9), although other mechanisms of action cannot be excluded.

5.2.2.6. Cytotoxicity in KG-1 MNU^R Following Treatment with Clofarabine and Fludarabine

Given that reduction of MSH3 protein in isogenic MMR knockdown cell lines conferred resistance to other therapeutic nucleoside analogues, cytotoxicity in response to clofarabine and fludarabine was also assessed in KG-1 MNU^R. The MNU-resistant subclone demonstrated increased resistance to the cytotoxic effects of both nucleoside analogues relative to the parental cell line (Figure 5.6). These data are therefore consistent with findings from isogenic MMR knockdown cell lines, and provide further evidence that reduction in MSH3 protein confers resistance to nucleoside analogue-induced cytotoxicity.

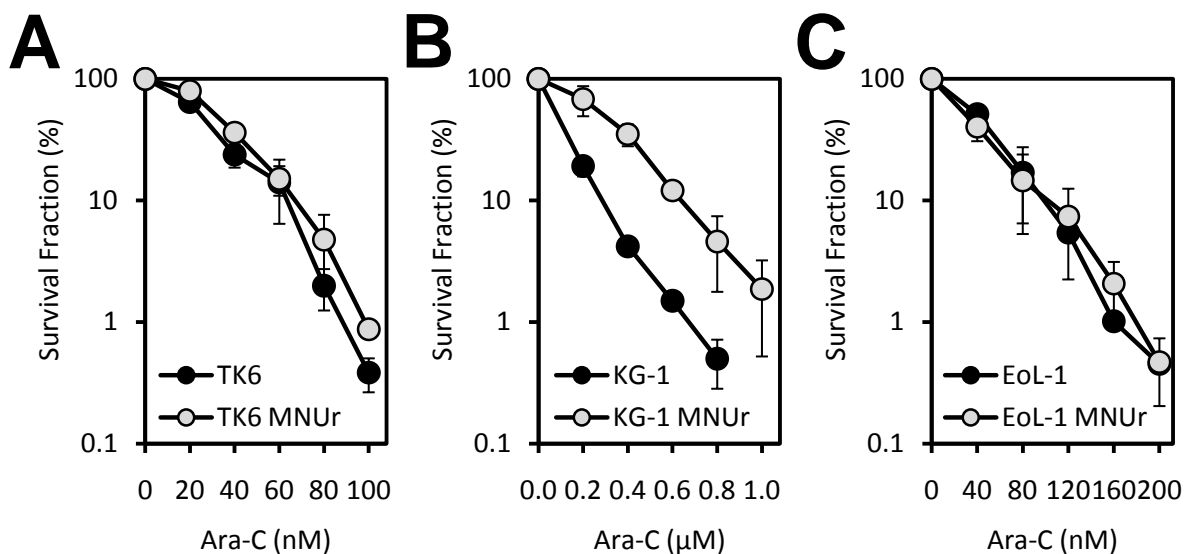


Figure 5.5. Cytotoxicity following treatment with Ara-C in MNU-resistant cell lines.

Cytotoxicity assays were performed to assess resistance to Ara-C in TK6 MNU^R (A), KG-1 MNU^R (B) and EoL-1 MNU^R (C) relative to their respective parental cell lines. For TK6 and its MNU-resistant subclone, cytotoxicity was compared via clonogenic assay. Data is presented as the number of viable colonies from exposed cell suspensions as a percentage of the number of viable colonies from unexposed control cell suspensions. For KG-1, EoL-1 and their respective MNU-resistant subclones, cytotoxicity was compared via growth inhibition assay. Data are presented as the number of surviving cells from exposed cell suspensions as a percentage of surviving cells from unexposed control cell suspensions. In all cases, data represents the mean and standard error of three independent experiments.

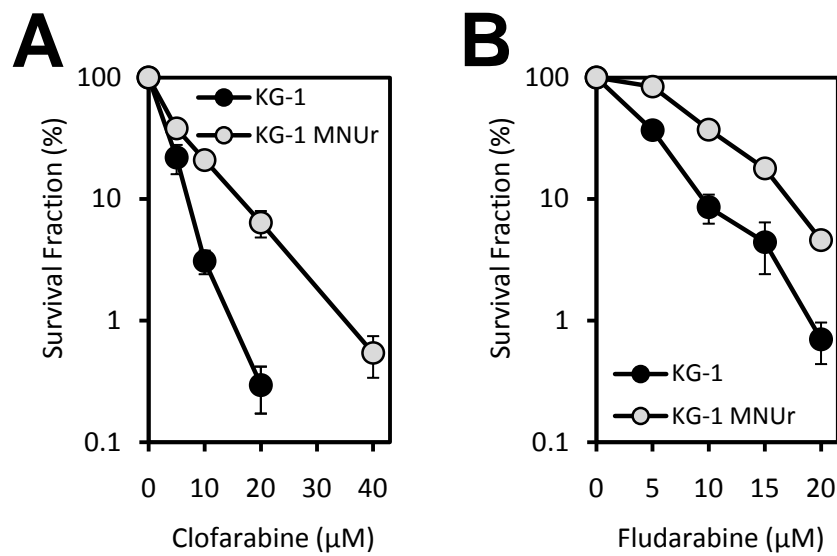


Figure 5.6. Cytotoxicity in KG-1 MNU^R following treatment with clofarabine and fludarabine.

Growth inhibition assays to assess resistance to clofarabine (**A**), and fludarabine (**B**) in KG-1 MNU^R, relative to KG-1. Data are presented as the number of surviving cells from exposed cell suspensions as a percentage of surviving cells from unexposed control cell suspensions. Data represents the mean and standard error of three independent experiments.

5.2.3. Characterisation of Cell Lines Treated with 6-TG

HL-60, EoL-1, KG-1 and TK6 were treated with escalating doses of 6-TG as described in Section 2.5. For both TK6 and HL-60, this resulted in establishment of cell cultures (termed TK6 6-TG^R and HL-60 6-TG^R) that retained viability in 6-TG concentrations 40-fold greater than the initial 6-TG dose.

For EoL-1 and KG-1, cells recovered slowly from a 6-TG concentration which was cytotoxic to 70-80% of cells (0.1µM in both cases), however subsequent increases in dosage resulted in death of all cells and it was not possible to establish 6-TG-resistant sub-clones.

5.2.3.1. Confirmation of 6-TG Resistance in HL-60 and TK6

TK6 6-TG^R and HL-60 6-TG^R retained resistance to 6-TG-induced cytotoxicity relative to their parental counterparts following passage in drug-free media (Figure 5.7). Furthermore, whereas the maximum dose of 6-TG these cells were exposed to during dose escalation was 20µM (see Table 2.2), a dose of 50µM 6-TG induced cell death in less than 50% of cells in both cases (Figure 5.7), demonstrating acquisition of a very high level of stable 6-TG resistance.

5.2.3.2. Cytotoxicity in 6-TG-Resistant Cell Lines Following Treatment with MNU

To determine if the mechanisms responsible for 6-TG resistance in TK6 6-TG^R and HL-60 6-TG^R could involve DNA MMR dysfunction, response of the cell lines to treatment with MNU was assessed via cytotoxicity assay. Neither TK6 6-TG^R nor HL-60 6-TG^R demonstrated differential sensitivity to the cytotoxic effects of MNU relative to their respective parental counterparts (Figure 5.8), suggesting function of the DNA MMR pathway is unperturbed in these 6-TG-resistant subclones.

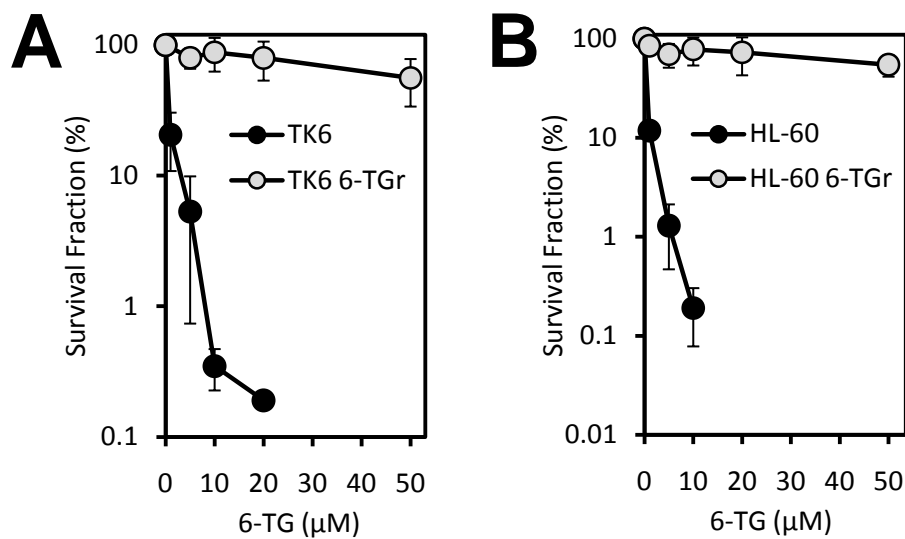


Figure 5.7. Stable acquired resistance to 6-TG following prolonged 6-TG exposure.

Cytotoxicity assays to confirm resistance to 6-TG in TK6 6-TG^R (A) and HL-60 6-TG^R (B) following serial passage in drug-free media. For TK6 and its 6-TG-resistant subclone, cytotoxicity was compared via clonogenic assay. Data is presented as the number of viable colonies from exposed cell suspensions as a percentage of the number of viable colonies from unexposed control cell suspensions. For HL-60 and its 6-TG-resistant subclones, cytotoxicity was compared via growth inhibition assay. Data are presented as the number of surviving cells from exposed cell suspensions as a percentage of surviving cells from unexposed control cell suspensions. In all cases, data represents the mean and standard error of three independent experiments.

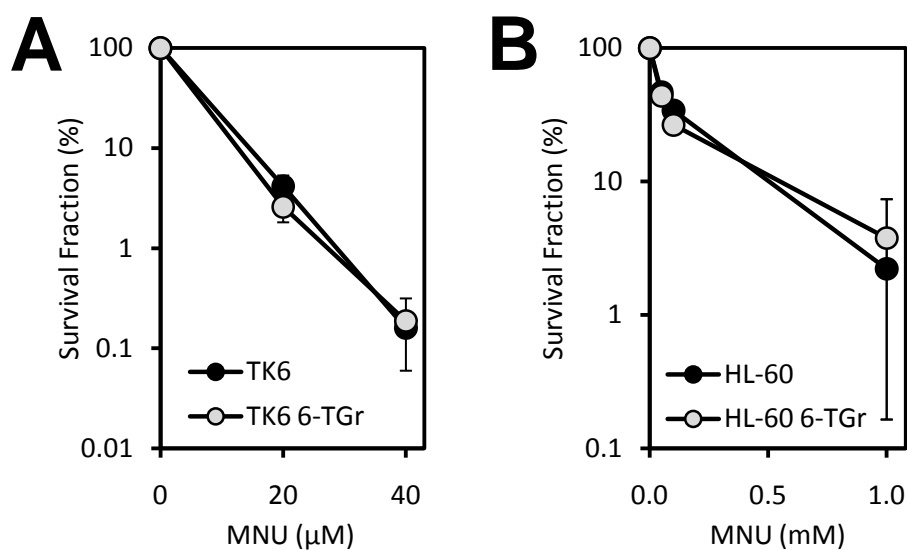


Figure 5.8. Cytotoxicity following treatment with MNU in 6-TG-resistant cell lines.

Cytotoxicity assays to assess resistance to MNU in TK6 6-TG^R (A) and HL-60 6-TG^R (B) relative to their respective parental cell lines. For TK6 and its 6-TG-resistant subclone, cytotoxicity was compared via clonogenic assay. Data is presented as the number of viable colonies from exposed cell suspensions as a percentage of the number of viable colonies from unexposed control cell suspensions. For HL-60 and its 6-TG-resistant subclone, cytotoxicity was compared via growth inhibition assay. Data are presented as the number of surviving cells from exposed cell suspensions as a percentage of surviving cells from unexposed control cell suspensions. In each case, data represents the mean and standard error of three independent experiments.

5.2.3.3. Expression Levels of MMR Proteins Determined by Western Immunoblotting

Western immunoblotting was performed to assess levels of DNA MMR proteins in TK6 6-TG^R and HL-60 6-TG^R, as described above. Neither cell line demonstrated any difference in the levels of DNA MMR components compared to their respective parental counterparts (Figure 5.9), confirming that escalating 6-TG dosage has had no apparent effect on the DNA MMR pathway.

5.2.3.4. Assessment of HPRT Status in 6-TG-Resistant Cell Lines

Loss of function of HPRT (an enzyme involved in intracellular metabolism of 6-TG; see Figure 1.3) through gene mutation represents one well established mechanism by which cells can acquire resistance to 6-TG, due to inability to form active thio-dGTP DNA precursors (van Diggelen et al., 1979). In order to determine whether *HPRT* mutation could be responsible for the high level of 6-TG resistance demonstrated by TK6 6-TG^R and HL-60 6-TG^R, *HPRT* mutational status was assessed in these sub-cultures, as described in Section 2.11.

Genomic multiplex PCR amplification of the *HPRT* locus revealed a deletion of exon 1 in HL-60 6-TG^R and a wild type PCR profile for parental HL-60 cells (Figure 5.10). For TK6 6-TG^R (and parental TK6 cells), a wild type PCR profile was also observed (Figure 5.10). Sequencing of *HPRT* cDNA amplified from TK6 6-TG^R revealed a G:T transversion disrupting the start codon of the *HPRT* coding region (Figure 5.11). Both of these mutations are predicted to result in lack of HPRT protein expression, hence demonstrating the mechanism likely responsible for the high level of 6-TG resistance observed in these sub-cultures.

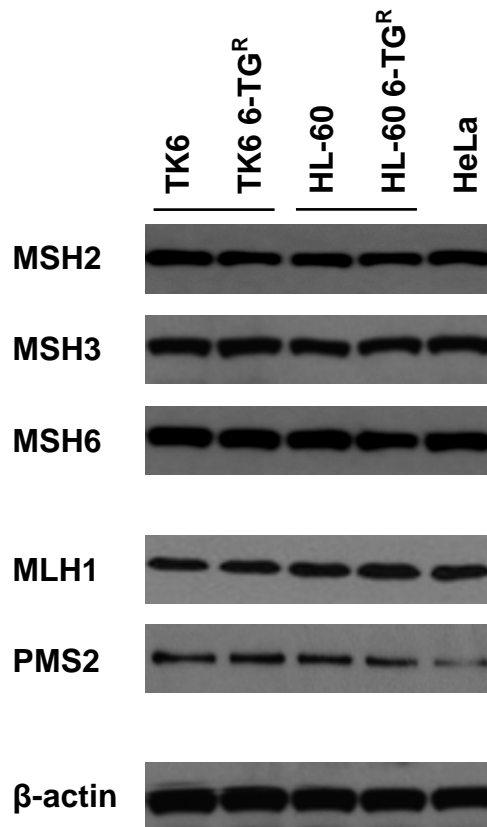


Figure 5.9. MMR protein expression in 6-TG-resistant cell lines.

Western immunoblotting to determine protein expression of DNA MMR components (MSH2, MSH3, MSH6, MLH1 and PMS2) in the 6-TG-resistant cell lines TK6 6-TG^R and HL-60 6-TG^R, relative to their respective parental cell lines. The MMR proficient HeLa cell line was included as a positive control. β-actin was used as a loading control. Each blot is representative of three independent experiments.

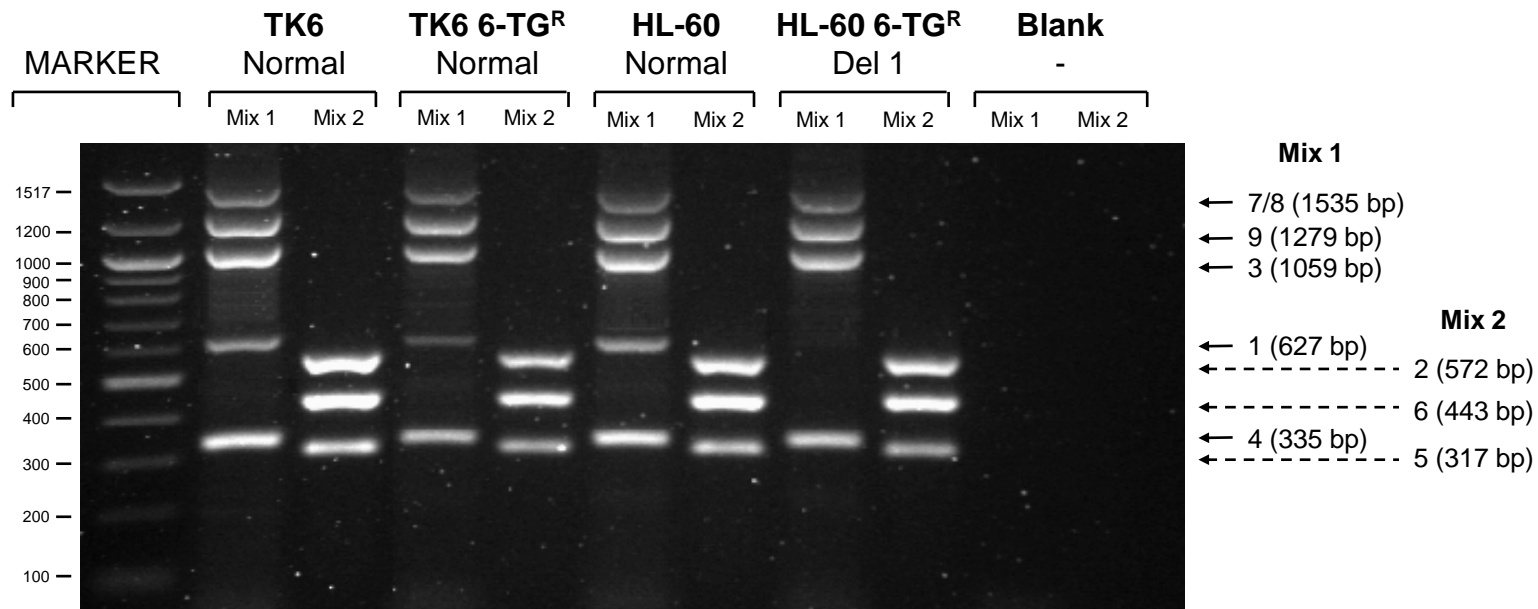


Figure 5.10. Multiplex amplification of the *HPRT* locus in 6-TG-resistant cell lines.

All 9 exons of the human *HPRT* locus were amplified using 8 primer pairs in 2 multiplex PCR reactions. Mix 1 contains primers for exons 1, 3, 4, 7/8 (amplified on a single fragment due to close proximity of exons) and 9. Mix 2 contains primers for exons 2, 5 and 6. For each cell line, the results of the 2 PCR reactions are shown side by side. TK6, TK6 6-TG^R and HL-60 show the normal pattern of 8 bands. HL-60 6-TG^R demonstrates loss of the band corresponding to exon 1. The exons represented by each band, and the size of the amplicons are shown to the right of the gel. A 100 bp marker ladder is shown to the left of the gel. The gel shown is a 1.5% agarose gel loaded with 15µl of the products from each multiplex PCR reaction.

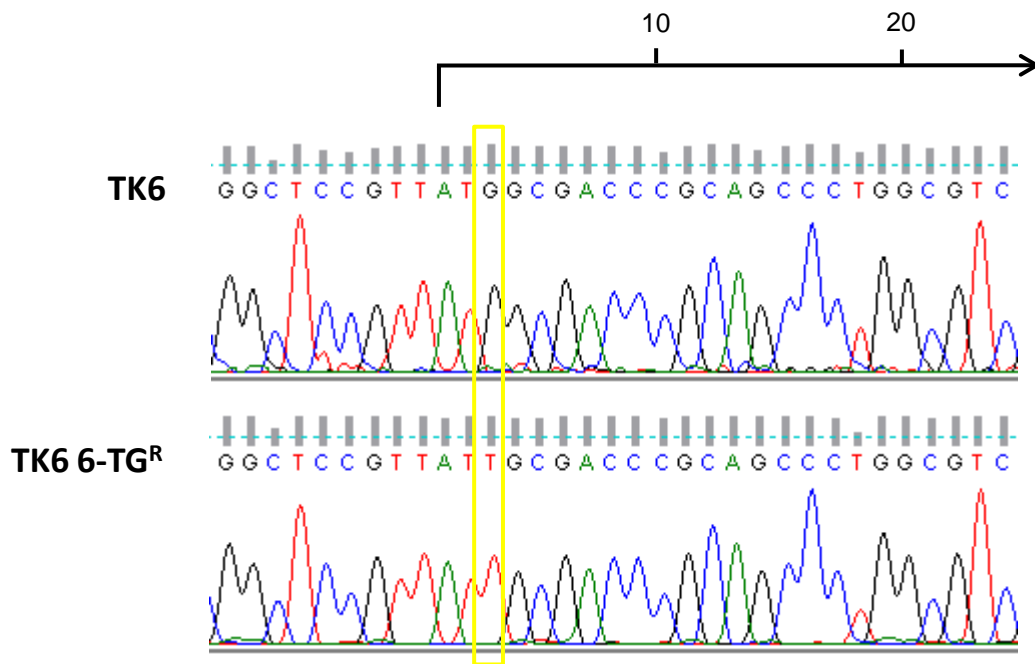


Figure 5.11. Sequencing of the *HPRT* coding region in TK6 6-TG^R.

Sequencing of cDNA from TK6 (upper trace) and its 6-TG-resistant subclone, TK6 6-TG^R (lower trace) revealed a G:T transversion at position 3 of the *HPRT* coding region (highlighted in yellow). The entire *HPRT* coding region was sequenced for each cell line, however only the portion of the positive strand (forward read) containing the mutation is shown. The arrow above the traces shows the origin and direction of the coding region, bases are numbered from the origin.

5.2.4. Characterisation of Cell Lines Treated with Ara-C

HL-60, EoL-1, KG-1 and TK6 were each treated with escalating doses of Ara-C as described in Section 2.5. For both TK6 and HL-60, this resulted in establishment of cell cultures that retained viability in Ara-C concentrations 50-fold and 100-fold greater than the initial Ara-C dose, respectively (termed TK6 Ara-C^R and HL-60 Ara-C^R).

KG-1 cells recovered from exposure to Ara-C concentrations up to 5-fold greater than the initial dose (termed KG-1 Ara-C^R), however treatment with higher doses consistently resulted in death of all cells. Assessment of resistance to Ara-C in KG-1 Ara-C^R, relative to parental KG-1 cells, demonstrated no acquired Ara-C-resistance (data not shown) and this sub-culture was excluded from further investigations.

EoL-1 cells recovered from an initial dose of Ara-C (0.02µM) but consistently failed to recover from any further doses and were excluded from further investigation.

5.2.4.1. Confirmation of Ara-C Resistance in HL-60 and TK6

TK6 Ara-C^R and HL-60 Ara-C^R retained resistance to Ara-C relative to parental TK6 and HL-60 cells following serial passage in drug-free media, indicating stable Ara-C resistance in these sub-cultures (Figure 5.12).

5.2.4.2. Cytotoxicity in Ara-C-Resistant Cell Lines Following Treatment with MNU and 6-TG

Cytotoxicity in response to MNU and 6-TG was investigated in Ara-C-resistant sub-cultures and their respective parental counterparts. Sensitivity of TK6 Ara-C^R (Figure 5.13A) and HL-60 Ara-C^R (Figure 5.13B) to MNU or 6-TG was not significantly different to parental cells, suggesting that MMR function remains unaffected in these cell lines.

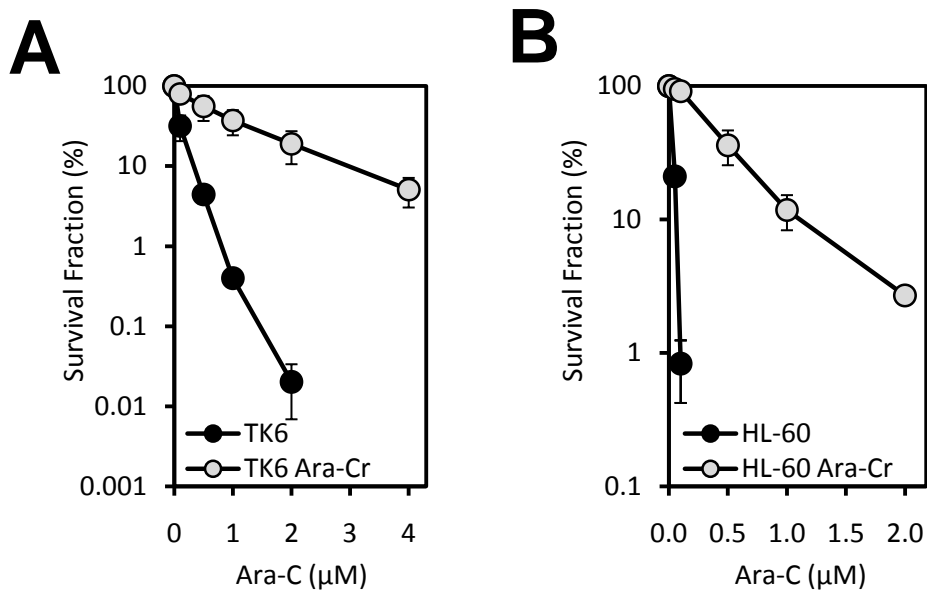


Figure 5.12. Stable acquired resistance to Ara-C following prolonged Ara-C exposure.

Cytotoxicity assays were to confirm resistance to Ara-C in TK6 Ara-C^R (A) and HL-60 Ara-C^R (B) following serial passage in drug-free media. For TK6 and its Ara-C-resistant subclone, cytotoxicity was compared via clonogenic assay. Data is presented as the number of viable colonies from exposed cell suspensions as a percentage of the number of viable colonies from unexposed control cell suspensions. For HL-60 and its Ara-C-resistant subclones, cytotoxicity was compared via growth inhibition assay. Data are presented as the number of surviving cells from exposed cell suspensions as a percentage of surviving cells from unexposed control cell suspensions. In all cases, data represents the mean and standard error of three independent experiments.

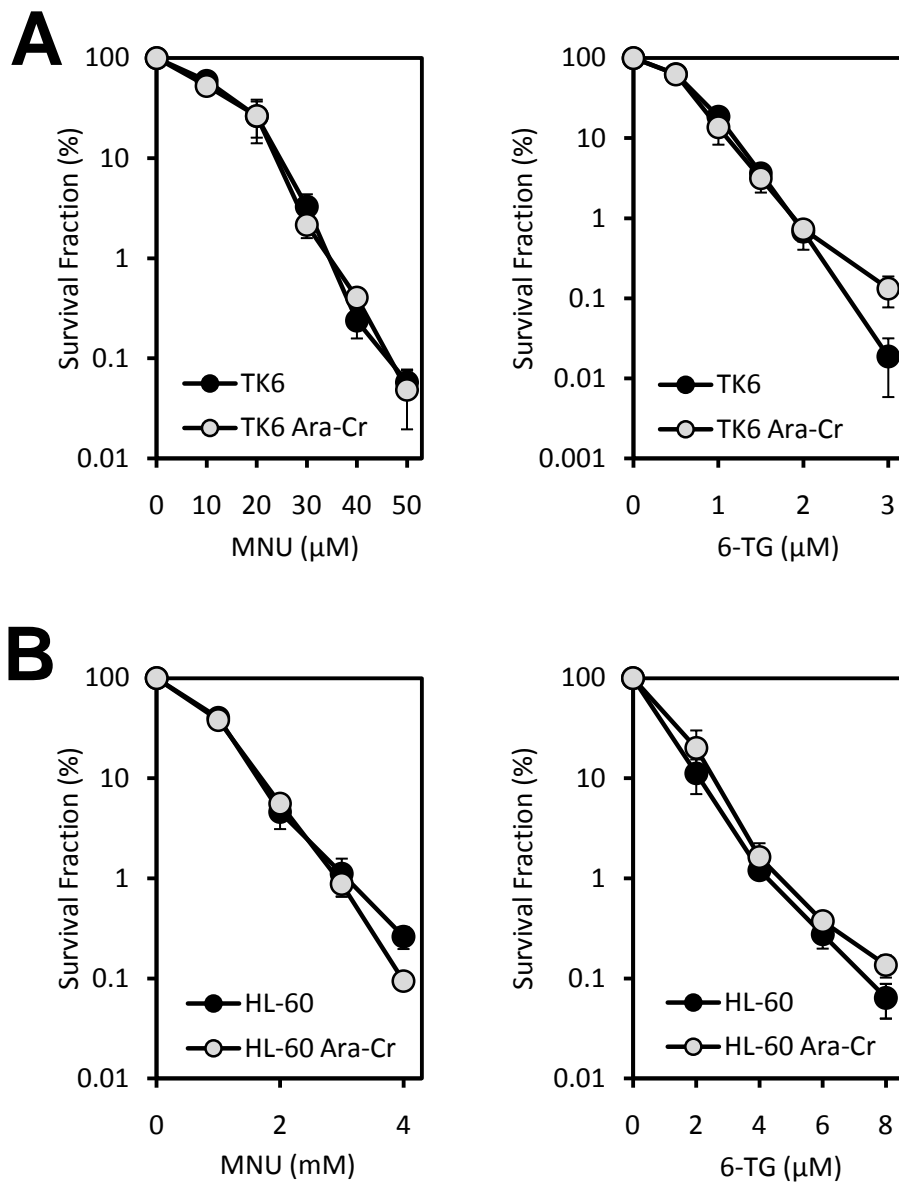


Figure 5.13. Cytotoxicity following treatment with MNU and 6-TG in Ara-C-resistant cell lines.

Cytotoxicity assays to assess response to MNU (left) and 6-TG (right) in TK6 Ara-C^R (**A**) and HL-60 Ara-C^R (**B**) relative to their respective parental cell lines. For TK6 and its Ara-C-resistant subclone, cytotoxicity was compared via clonogenic assay. Data is presented as the number of viable colonies from exposed cell suspensions as a percentage of the number of viable colonies from unexposed control cell suspensions. For HL-60 and its Ara-C-resistant subclone, cytotoxicity was compared via growth inhibition assay. Data are presented as the number of surviving cells from exposed cell suspensions as a percentage of surviving cells from unexposed control cell suspensions. In all cases, data represent the mean and standard error of three independent experiments.

5.2.4.3. Expression Levels of MMR Proteins Determined by Western Immunoblotting

Western immunoblotting of DNA MMR proteins in TK6 Ara-C^R and HL-60 Ara-C^R demonstrated no changes in any of the proteins examined (Figure 5.14). Taken together with data demonstrating no differential sensitivity to either MNU or 6-TG in the Ara-C-resistant sub-cultures, there is no evidence that prolonged exposure to Ara-C induces defects in DNA MMR which could potentially contribute to the development of t-AML.

5.2.4.4. Cytotoxicity in Ara-C-Resistant Cell Lines Following Treatment with Clofarabine and Fludarabine

TK6 Ara-C^R, HL-60 Ara-C^R and their respective parental counterparts were treated with clofarabine and fludarabine in order to determine whether resistance to Ara-C-induced cytotoxicity also extended to these agents. In the case of both Ara-C-resistant sub-cultures, no difference in cytotoxicity was observed following treatment with either agent, relative to normal parental cultures (Figure 5.15). Therefore, although the mechanism of Ara-C-resistance is undetermined in these sub-cultures, it does appear to be relatively specific to this analogue and it does not confer cross-resistance to other nucleoside analogues.

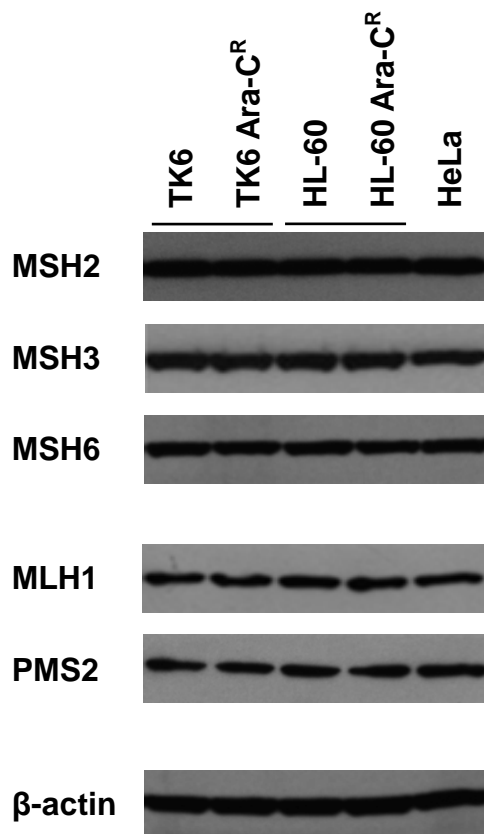


Figure 5.14. MMR protein expression in Ara-C-resistant cell lines.

Western immunoblotting to determine protein expression of DNA MMR components (MSH2, MSH3, MSH6, MLH1 and PMS2) in the Ara-C-resistant cell lines TK6 Ara-C^R and HL-60 Ara-C^R, relative to their respective parental cell lines. The MMR proficient HeLa cell line was included as a positive control. β-actin was used as a loading control. Each blot is representative of three independent experiments.

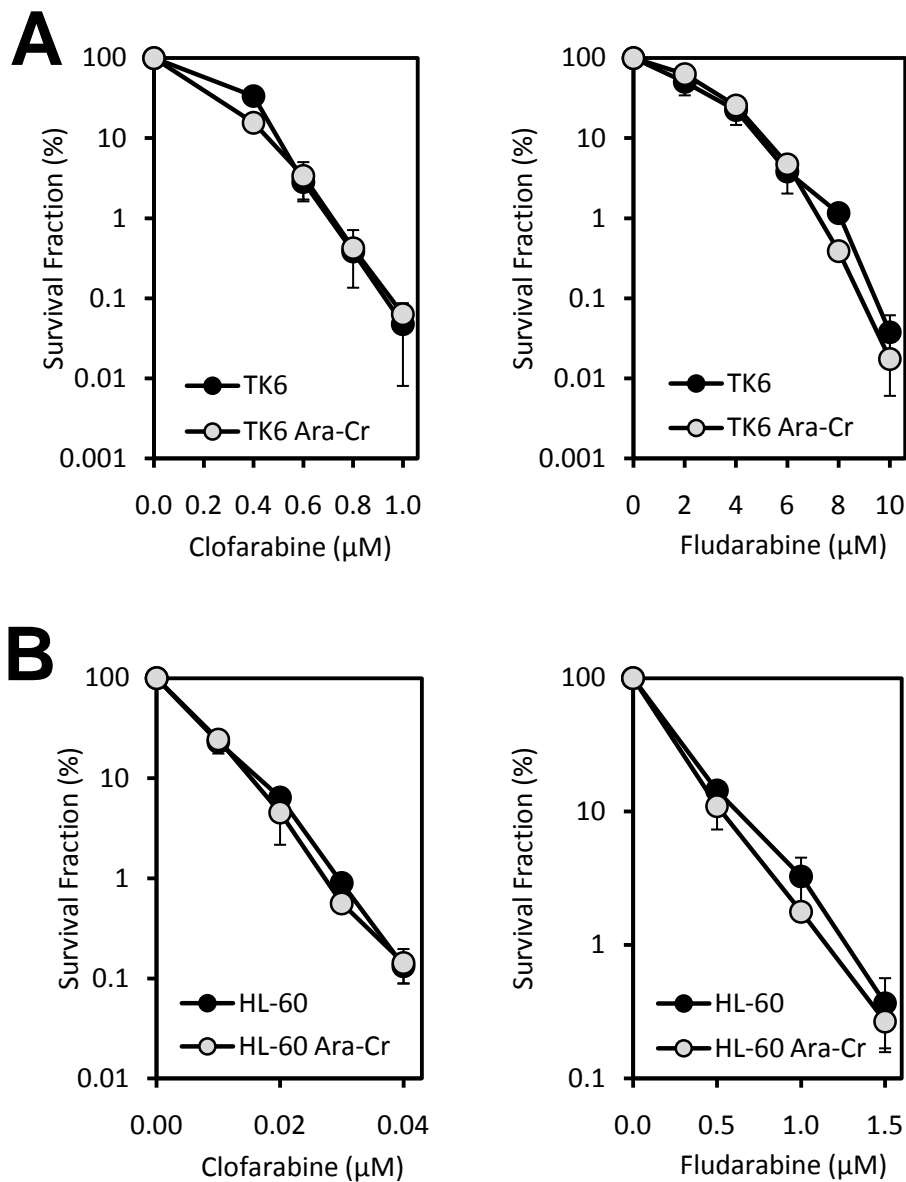


Figure 5.15. Cytotoxicity following treatment with clofarabine and fludarabine in Ara-C-resistant cell lines.

Cytotoxicity assays to assess response to clofarabine (left) and fludarabine (right) in TK6 Ara-C^R (A) and HL-60 Ara-C^R (B) relative to their respective parental cell lines. For TK6 and its Ara-C-resistant subclone, cytotoxicity was compared via clonogenic assay. Data is presented as the number of viable colonies from exposed cell suspensions as a percentage of the number of viable colonies from unexposed control cell suspensions. For HL-60 and its Ara-C-resistant subclone, cytotoxicity was compared via growth inhibition assay. Data are presented as the number of surviving cells from exposed cell suspensions as a percentage of surviving cells from unexposed control cell suspensions. In all cases, data represent the mean and standard error of three independent experiments.

5.3. Discussion

The major focus of these investigations was to determine, using cell line models, whether prolonged exposure to a methylating agent, 6-TG or Ara-C could induce or select for cells defective in DNA MMR, and whether such defects affect cellular response to nucleoside analogues used routinely to treat AML.

Using escalating doses of the methylating agent, MNU, three resistant subclones were generated (TK6 MNU^R, KG-1 MNU^R and EoL-1 MNU^R). In TK6 MNU^R, western immunoblotting demonstrated re-expression of MGMT which, in the absence of any apparent effects on DNA MMR components, represents the likely mechanism of MNU resistance. Using a similar experimental approach in which MGMT-deficient colorectal carcinoma cell lines were treated with MNU, Hampson and colleagues demonstrated that 3 out of 7 MNU-resistant sub-clones had re-expression of MGMT (Hampson et al., 1997). Similarly, a single high dose of the methylating agent MNNG can also induce expression of MGMT in previously-deficient rat hepatoma cells (Fritz et al., 1991). The parental TK6 cells described in the current study exhibit silencing of MGMT through hypermethylation of CpG islands within the promoter region (Danam et al., 2005), and it seems probable that reactivation of the silenced gene due to demethylation is responsible for acquired MNU resistance. The mechanism by which this occurs is unknown but it could involve down-regulation of a DNA methyltransferase responsible for maintaining promoter methylation. *In vivo*, a correlation has been identified between extent of MGMT promoter methylation and response to temozolomide in glioma patients (Hegi et al., 2005). Patients with increased MGMT activity, due to a reduction in promoter methylation respond less well to temozolomide, leading to the suggestion that MGMT up-regulation could represent a mechanism associated with chemoresistance in cancers treated with methylating agents (Hegi et al., 2008). A study using human melanoma cells has suggested that increased expression of MGMT might also be associated with an increase in resistance to 6-TG (Gefen et al., 2010). In the current study however, re-expression of MGMT in TK6 MNU^R resulted in resistance to MNU but not in cross-resistance to 6-TG, arguing against a role for MGMT in 6-TG resistance. Similarly, cross-resistance to Ara-C in TK6 MNU^R was not observed, suggesting that if treatment-induced effects on MGMT expression were to occur in t-AML, they likely would not impact therapeutic response.

In both EoL-1 MNU^R and KG-1 MNU^R, western immunoblotting revealed changes in the levels of DNA MMR proteins relative to respective parental counterparts. Despite this, neither of these MNU-resistant subclones demonstrated cross-resistance to 6-TG, suggesting that the function of the DNA MMR pathway (or at least of MutS α) was not significantly perturbed. A modest reduction (approximately 10%) in MSH6 expression was observed in EoL-1 MNU^R as a sole abnormality. Although reduction in MSH6 activity has previously been associated with MNU resistance (Hampson et al., 1997), it is unlikely to be the mechanism responsible for MNU resistance in EoL-1 MNU^R, given that other DNA MMR components were unaffected and cross-resistance to 6-TG was not observed. It is possible that increased repair of MNU-induced lesions by a mechanism independent of MGMT could also account for the observed MNU resistance in EoL-1 MNU^R, however this remains undetermined. Whatever the mechanism of MNU resistance may be, it did not confer cross-resistance to the nucleoside analogue, Ara-C.

The mechanism of MNU resistance also remains undetermined in KG-1 MNU^R. Western immunoblotting revealed significant over-expression of MSH6, a reduction in MSH3 expression, but no change in MSH2 relative to parental KG-1 cells. Based on the partnerless protein instability theory (Drummond et al., 1995; Drummond et al., 1997), over-production of MSH6 would result in sequestration of the majority of cellular MSH2 into the MutS α complex, leaving partnerless MSH3 subject to degradation. An increase in cellular levels of MutS α activity is expected to confer increased sensitivity to the cytotoxic effects of methylating agents and 6-TG, as has previously been demonstrated in the case of methylating agents (Dosch et al., 1998). Consistent with this model, KG-1 MNU^R cells were hypersensitive to 6-TG relative to the parental KG-1 cell line, suggesting an increase in MutS α -mediated detection of 6-TG-induced DNA damage. It is possible therefore, that MutS α -mediated recognition of O⁶-meG lesions is also elevated in KG-1 MNU^R. If true however, the predicted increase in sensitivity to MNU is clearly masked by a different mechanism by which the cells have acquired resistance to MNU. Repair of a number of other cytotoxic MNU-induced methylated lesions, for instance methylation of the N3 atom of adenine, is mediated primarily by components of the BER pathway (Plosky et al., 2002). It is possible therefore that an increase in cellular capacity for BER may account for the observed MNU resistance in KG-1 MNU^R. Indeed this model could equally apply to EoL-1 MNU^R discussed above.

KG-1 MNU^R demonstrated cross-resistance to the nucleoside analogues Ara-C, clofarabine and fludarabine relative to parental KG-1 cells. It is probable that this is due to reduction in cellular MSH3, and hence the MutS β complex, as a consequence of increased MutS α activity. This model is consistent with the findings in MT-1 and isogenic MMR knockdown cell lines (described in Chapter 3), and adds weight to the suggestion that MutS β is involved in mediating cellular response to nucleoside analogues. Furthermore, these data demonstrate that resistance to nucleoside analogues can be induced in myeloid cells *in vitro* by exposure to MNU and could confer chemoresistance in MMR-defective t-AML.

Exposure of cells *in vitro* to escalating doses of 6-TG can induce 6-TG resistance by virtue of loss of DNA MMR function (Offman et al., 2004). Defects observed were limited to loss of MLH1, and hence MutL α activity, although not all drug resistant clones were characterised (Offman et al., 2004). In the current study, two sub-clones with a very high level of 6-TG resistance were generated (TK6 6-TG^R and HL-60 6-TG^R), however neither developed an apparent defect in DNA MMR as evidenced by western immunoblotting and lack of cross-resistance to MNU. Rather, both sub-clones were deficient in HPRT, a well characterised 6-TG resistance mechanism (which is exploited in mutation assays (see Chapter 6)). A possible explanation for the failure to generate MMR-defective sub-clones, aside from small study size, could be due to the concentration of 6-TG used. Offman and colleagues used a maximum 6-TG concentration of 6 μ M to generate DNA MMR-defective clones (Offman et al., 2004). In the current study however, a maximum 6-TG dose of 20 μ M was used. It is possible therefore that MMR-defective sub-clones were induced at lower concentrations of 6-TG, however as the concentration was increased, these were unable to tolerate extensive DNA damage and were selected against. It cannot be ruled out therefore, that 6-TG exposure *in vivo* could result in generation of DNA MMR defective cell populations.

Whilst trying to identify a possible mechanism accounting for 6-TG hypersensitivity in KG-1 MNU^R, western immunoblotting revealed that neither KG-1 MNU^R nor parental KG-1 cells expressed detectable levels of TPMT protein. Although this could not account for the 6-TG hypersensitivity observed in the MNU-resistant subculture, it could provide a plausible explanation for the unsuccessful attempts to

generate a 6-TG-resistant KG-1 sub-culture. Reduced levels of TPMT activity are associated with increased sensitivity to 6-TG *in vitro*, thought to be due to increased 6-TG nucleotide incorporation into DNA (Coulthard et al., 2002). Lack of detectable TPMT protein in KG-1 cells would therefore presumably result in extensive 6-TG nucleotide incorporation and subsequent cytotoxicity, as observed. Similar failure to generate a 6-TG-resistant subclone was also demonstrated in the case of EoL-1, hence it is possible that this cell line also expresses little or no TPMT protein, although this was not investigated. The generation of Ara-C-resistant EoL-1 and KG-1 sub-cultures was also not successful, although possible explanations were not investigated.

Ara-C and fludarabine have both been implicated in development of t-AML (Coso et al., 1999; Morrison et al., 2002; McLaughlin et al., 2005; Arana-Yi et al., 2008; Carney et al., 2010), although these data are limited and mechanisms have not yet been investigated. In the current study, exposure to escalating doses of Ara-C resulted in the generation of two cell lines (HL-60 Ara-C^R and TK6 Ara-C^R) with a high level of resistance. DNA MMR components were unaffected in both HL-60 Ara-C^R and TK6 Ara-C^R and neither line was cross-resistant to MNU, 6-TG or the purine nucleoside analogues clofarabine and fludarabine. These data therefore do not provide any evidence that prolonged Ara-C exposure can induce defects of the DNA MMR pathway. However this was a limited investigation using only a very small sample set, hence it cannot be completely excluded that such a mechanism could operate. Other mechanisms which could contribute to t-AML development have not been investigated. For instance, balanced translocations affecting haematopoietic genes, arising due to generation of DSBs, are purported to be key in t-AML aetiology following exposure to chemotherapeutic topoisomerase inhibitors (see Section 1.4.2). Ara-C and fludarabine could potentially contribute to t-AML development by a similar mechanism. Consistently, cases of t-AML with translocations affecting the *MLL* locus (11q23) have been reported following treatment of lymphoma patients with fludarabine (Martin-Salces et al., 2007). Furthermore, Ara-C is reported to affect the function of topoisomerase enzymes *in vitro* (Cline and Osheroff, 1999; Chrencik et al., 2003).

Further investigation of potential mechanisms responsible for Ara-C resistance in HL-60 Ara-C^R and TK6 Ara-C^R was not performed given that the primary focus of the

current study was DNA MMR. Mechanisms of resistance to Ara-C have been well characterised *in vitro* and *in vivo* (see Section 1.5.3) and any could feasibly be responsible for Ara-C resistance in HL-60 Ara-C^R and TK6 Ara-C^R. In both cases, the mechanism may be unique to Ara-C, as cross-resistance to clofarabine and fludarabine was not observed. It cannot be ruled out however, that resistance to other nucleoside analogues, for instance other deoxycytidine analogues, could occur.

5.3.1. Summary of Chapter

In conclusion, the current study has demonstrated the following:

- Treatment of myeloid and lymphoid cell lines with escalating doses of MNU resulted in generation of MNU-resistant cell lines, although not as a result of dysfunction of the DNA MMR pathway.
- Despite no apparent effects on MMR-mediated damage signalling, a reduction in the amount of MSH3 protein following MNU exposure (in KG-1 MNU^R) conferred moderate resistance to the nucleoside analogues Ara-C, clofarabine and fludarabine (clinical implications will be discussed in Chapter 8).
- No evidence was found that prolonged exposure to 6-TG or Ara-C could cause defects of the DNA MMR pathway.
- Resistance to Ara-C (via undetermined mechanisms) did not confer cross-resistance to other nucleoside analogues routinely used in AML treatment.

**Chapter 6. *In vitro* Mutagenicity of Cytarabine in Mismatch
Repair Proficient and Deficient Cell Lines**

6.1. Introduction

Any agent which can damage DNA either directly or indirectly has the potential to be mutagenic to DNA if the damage is not detected and repaired, or if apoptosis is not initiated when repair cannot successfully occur. Mutagenic agents are often carcinogenic due to their potential to cause and/or contribute to genomic instability, which is implicated in the aetiology of several malignancies, in particular therapy-related cancer (see Section 1.4.1.1).

The O⁶-meG lesion which forms in DNA as a result of exposure to methylating agents is highly pro-mutagenic. Studies using *E. coli* and mammalian cell lines demonstrate a high frequency of G:C to A:T transitions in particular (Horsfall et al., 1990), which result due to mispairing of O⁶-meG with thymine by DNA polymerases during replication (Abbott and Saffhill, 1979; Toorchen and Topal, 1983; Snow et al., 1984). The role of the DNA MMR pathway is to detect and repair polymerase-mediated base misinsertions before they can be converted to mutations. However, in the case of O⁶-meG mispairs (and certain other drug-induced mispairs), MMR-mediated detection does not result in repair, but rather initiation of apoptosis, as described in Section 1.2.1.2. Consistently, the frequency of methylating agent-induced mutations is increased in cells defective in DNA MMR (Andrew et al., 1998). This is also observed in cells defective in MGMT (Yang et al., 1994), another important cellular line of defence against the cytotoxicity and mutagenicity of the O⁶-meG lesion.

Nucleoside analogues such as Ara-C, which are routinely used in the treatment of AML and other leukaemias, exert their cytotoxic effects primarily by incorporation at the 3'-terminus of replicating DNA, leading to chain termination and subsequent replication fork stalling and collapse. Despite this, there is evidence to suggest that chain termination is not absolute, resulting in the incorporation of nucleoside analogues at internal positions within DNA (see Section 3.1). Such internucleotide lesions have the potential to be mutagenic if polymerase enzymes cannot efficiently replicate these lesions. Indeed, *in vitro* translesion synthesis experiments have demonstrated incorporation of an extra base in the daughter strand following replication of an oligonucleotide containing an internal Ara-C (see Figure 3.11), suggesting replicative polymerases fail to replicate past Ara-C lesions accurately.

Studies of the mutagenic potential of nucleoside analogues have focussed on a particular class of nucleoside analogues, termed nucleoside reverse transcriptase inhibitors (NRTIs), which are used in the treatment of viral infections such as HIV. NRTIs exert their effects mainly through incorporation into viral DNA by viral reverse transcriptase, although they can also be incorporated into host cell genomic DNA (Sussman et al., 1999; Meng et al., 2000). *In vitro* mutagenicity studies of clinically relevant NRTIs have demonstrated the mutagenic potency of several of these agents, leading them to be classified as carcinogens (Sussman et al., 1999; Meng et al., 2000; Meng et al., 2002; Carter et al., 2007). Despite similar mechanisms of action (i.e. the ability to be incorporated into genomic DNA), there have been no published studies to date investigating the mutagenic potential of chemotherapeutic nucleoside analogues such as Ara-C and fludarabine. Investigating the mutagenic potency of these agents might have clinical implications in terms of understanding mechanisms which could contribute to acquisition of drug resistance, or risks associated with development of therapy-related malignancy and/or relapsed disease, for example.

The mutagenic potential of DNA damaging agents can be assessed by a number of *in vitro* and *in vivo* assays. The most commonly utilised *in vitro* mutation assay is the HPRT assay. The product of the X-linked *HPRT* gene is an enzyme involved in the purine salvage pathway. In addition to its role in purine metabolism, the HPRT enzyme is a necessary requirement for conversion of 6-TG to its active DNA precursor (see Figure 1.3). Cells in which *HPRT* gene mutation causes loss of enzymatic function are viable, but resistant to the cytotoxic effects of 6-TG. The HPRT assay works by treating cells (commonly TK6 cells given that they possess only one X chromosome, and hence one functional *HPRT* allele) with the agent in question, following which cells are exposed to 6-TG, allowing selection of mutants based on their acquired 6-TG resistance. The frequency of induced mutants, relative to control untreated cells, can be used as a measure of the mutagenicity of the agent under investigation. A second *in vitro* mutation assay, the TK assay, works on the same principles. Whereas the *HPRT* gene is X-linked, the *TK* locus is located on chromosome 17 in humans. Although the TK assay requires cells to be heterozygous for the *TK* gene (conveniently, TK6 cells are also TK heterozygotes), it has the advantage of being able to pick up larger mutations, such as multi-locus deletions, which would likely be lethal in the HPRT assay (Liber and Thilly, 1982). In addition, for both the *TK* and *HPRT* genes, individual mutants can be

subjected to molecular analysis to determine the nature of the mutation type, enabling generation of an induced (or spontaneously-occurring) mutational spectrum.

6.1.1. Aims of Chapter 6

The main objective of this chapter was to investigate the mutagenicity of Ara-C, in terms of frequency and type of drug-induced mutations, using *in vitro* mutation assays. An additional aim was to determine whether Ara-C is more mutagenic to cells defective in DNA MMR in order to further investigate whether MMR components are involved in cellular response to Ara-C.

Specifically, the experimental aims were as follows:

- Perform *TK* and *HPRT* mutation assays to determine whether exposure to Ara-C is mutagenic at these loci, and whether mutation is increased in MMR-defective cells.
- Determine the spectrum of mutations at the *HPRT* locus following exposure to Ara-C.

6.2. Results

6.2.1. Effect of MNU Exposure on Mutation Frequency at TK and HPRT Loci in MMR-Proficient TK6 and MMR-Deficient TK6 MSH2i Cells

The methylating agent MNU is a potent DNA mutagen, and its mutagenicity is enhanced in cells lacking a functional DNA MMR pathway (Andrew et al., 1998). Initial investigations were performed using MNU to determine whether TK and HPRT mutation assays could be successfully performed in DNA MMR-defective cells, and whether this would result in an increase in the MNU-induced mutation frequency (MF) relative to the MMR-proficient TK6 cells. The TK6 *MSH2i* cell line, which is a subclone of TK6 generated using shRNA-mediated knockdown of the *MSH2* gene (Section 2.4), was used as it lacks MutS α and MutS β components and is deficient in DNA MMR-mediated cell death signalling in response to MNU and 6-TG (see Section 3.2.5).

TK6 and TK6 *MSH2i* were first purged of any pre-existing spontaneous *TK* or *HPRT* mutants by culture in CHAT (cytidine, hypoxanthine, aminopterin, thymidine) medium, as described in Section 2.10.1. Components in CHAT medium (aminopterin) result in cellular inhibition of purine nucleotide biosynthesis, forcing cells to rely on purine salvage pathways. This is therefore cytotoxic to *TK* and *HPRT* mutants because they lack key components of these pathways. Subsequently, TK6 and TK6 *MSH2i* cells were exposed to increasingly cytotoxic doses of MNU for 16 hours (each dose was performed in triplicate using three independent cell populations), following which MF was assessed at *TK* and *HPRT* loci as described in Section 2.10.6.

Exposure of TK6 and TK6 *MSH2i* to MNU caused a significant dose-dependent increase in MF at both *TK* and *HPRT* loci (Table 6.1 and Figure 6.1), confirming the mutagenic potency of this agent. Furthermore, at both loci the MFs observed in MMR-deficient TK6 *MSH2i* cells were higher than those observed in parental TK6 cells at each individual MNU concentration (Figure 6.1). This was also observed in the undosed control populations, demonstrating a higher spontaneous MF in MMR-deficient TK6 *MSH2i* cells, relative to proficient TK6 cells. Two-way analysis of variance (ANOVA) testing demonstrated a significant interaction between drug dose and cell line on induced MF at both loci (Table 6.1), confirming that the enhanced mutability of MNU, presumably due to loss of DNA MMR function, is reflected at *TK* and *HPRT* loci.

MNU (μ M)	TK MF ($\times 10^{-6}$) ^a		HPRT MF ($\times 10^{-6}$) ^a	
	TK6	TK6 MSH2i	TK6	TK6 MSH2i
0	4.8 (0.2)	15.0 (0.9)	4.4 (0.3)	12.5 (0.7)
10	27.8 (6.0)	60.9 (9.5)	23.7 (1.4)	52.9 (4.7)
20	37.8 (6.1)	103.5 (9.2)	36.7 (6.8)	92.6 (10.4)
30	60.4 (6.4)	142.1 (23.0)	49.9 (4.1)	128.3 (16.1)
1-way ANOVA ^b	<0.001	<0.001	<0.001	<0.001
2-way ANOVA ^c	0.004		<0.001	

Table 6.1. Effect of MNU exposure on mutation frequency at TK and HPRT loci.

^a Figures represent the observed MF at each drug concentration. Data represents the mean and standard error (in parentheses) of three independently treated cell populations. These figures are displayed graphically in Figure 6.1.

^b Figures represent the P value determined using a 1-way analysis of variance (ANOVA) test for effect of dose on MF.

^c Figures represent the P value determined using a 2-way ANOVA test for interaction of dose and cell line on induced MF.

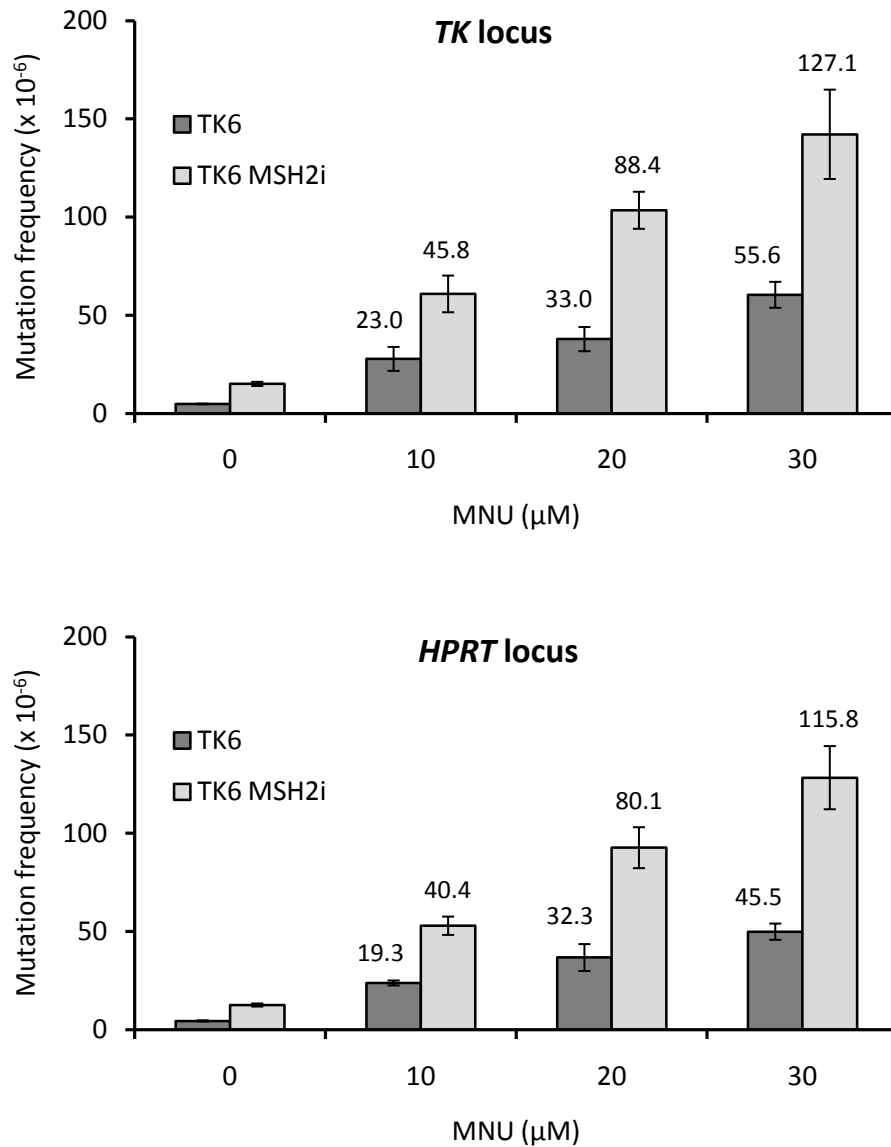


Figure 6.1. Mutagenicity of MNU at *TK* and *HPRT* loci.

Mutation frequency (MF) at *TK* and *HPRT* loci was assessed in MMR-proficient TK6 cells (dark grey bars) and MMR-deficient TK6 *MSH2i* cells (pale grey bars) following 16 hour exposure to MNU. Data represents the mean and standard error of three independently treated cell populations. Numbers above bars represent the induced MF ($\times 10^{-6}$) at each dose, calculated by subtraction of the spontaneous MF ($0\mu\text{M}$ MNU). For cytotoxicity at each MNU concentration, see Figure 6.3B.

6.2.2. Effect of Ara-C Exposure on Mutation Frequency at TK and HPRT Loci in MMR-Proficient TK6 and MMR-Deficient TK6 MSH2i Cell Lines

To assess the mutagenicity of Ara-C, cultures of MMR-proficient TK6 and its MMR-deficient derivative cell line, TK6 *MSH2i* were first purged of any pre-existing spontaneous mutants as described above, then exposed to increasingly cytotoxic doses of Ara-C for 16 hours. MF was subsequently determined at *TK* and *HPRT* loci.

Exposure of TK6 and TK6 *MSH2i* to Ara-C caused a significant dose-dependent increase in MF at both *TK* and *HPRT* loci (Table 6.2 and Figure 6.2), the effect of which was more pronounced at the *TK* locus. Furthermore, similar to the response observed for MNU, *TK* and *HPRT* MF was higher in TK6 *MSH2i* cells compared to parental TK6 cells at equivalent Ara-C concentrations (Figure 6.2). Two-way ANOVA analysis demonstrated a significant interaction between Ara-C dose and cell line on induced MF (Table 6.2).

Although a strict statistical comparison was not possible between two different agents, a comparison of the drug-induced MFs at doses giving a near equivalent cytotoxicity was performed to give an indication of the mutagenic potency of Ara-C relative to MNU. At doses giving 70% cytotoxicity in MMR-proficient TK6, Ara-C was approximately 2.3-fold and 3.5-fold less mutagenic at *TK* and *HPRT* loci, respectively, compared to MNU (Figure 6.3). Furthermore, in MMR-deficient TK6 *MSH2i* cells, the difference increased to approximately 3.1-fold and 7.6-fold (Figure 6.3), demonstrating that loss of DNA MMR activity has a greater influence on the mutagenicity of MNU than Ara-C, particularly at the *HPRT* locus. This was similar at doses which result in approximately 95% cytotoxicity (data not shown).

Taken together, these *in vitro* data provide evidence that exposure to Ara-C is weakly, but significantly, mutagenic to DNA, particularly at the *TK* locus. Furthermore, the mutagenic effect of Ara-C is enhanced in cells lacking a functional DNA MMR pathway.

Ara-C (nM)	TK MF ($\times 10^{-6}$) ^a		HPRT MF ($\times 10^{-6}$) ^a	
	TK6	TK6 <i>MSH2i</i>	TK6	TK6 <i>MSH2i</i>
0.0	4.4 (0.3)	13.7 (0.9)	4.4 (0.6)	12.8 (1.0)
5	10.6 (0.5)	42.6 (3.4)	6.4 (0.4)	23.3 (4.7)
10	14.3 (1.4)	65.5 (1.4)	9.9 (0.4)	31.5 (2.6)
20	21.9 (1.4)	88.5 (10.8)	12.6 (1.4)	47.0 (3.0)
30	29.7 (0.5)		14.4 (1.5)	
1-way ANOVA ^b	<0.001	<0.001	<0.001	<0.001
2-way ANOVA ^c	<0.001		0.001	

Table 6.2. Effect of Ara-C exposure on mutation frequency at TK and HPRT loci.

^a Figures represent the observed MF at each drug concentration. Data represents the mean and standard error (in parentheses) of three independently treated cell populations. These figures are displayed graphically in Figure 6.2.

^b Figures represent the P value determined using a 1-way analysis of variance (ANOVA) test for effect of dose on MF.

^c Figures represent the P value determined using a 2-way ANOVA test for interaction of dose and cell line on induced MF.

Note: No results were obtained for TK6 *MSH2i* at 30nM Ara-C due to insufficient cell growth (attributed to the particular Ara-C hypersensitivity of this cell line).

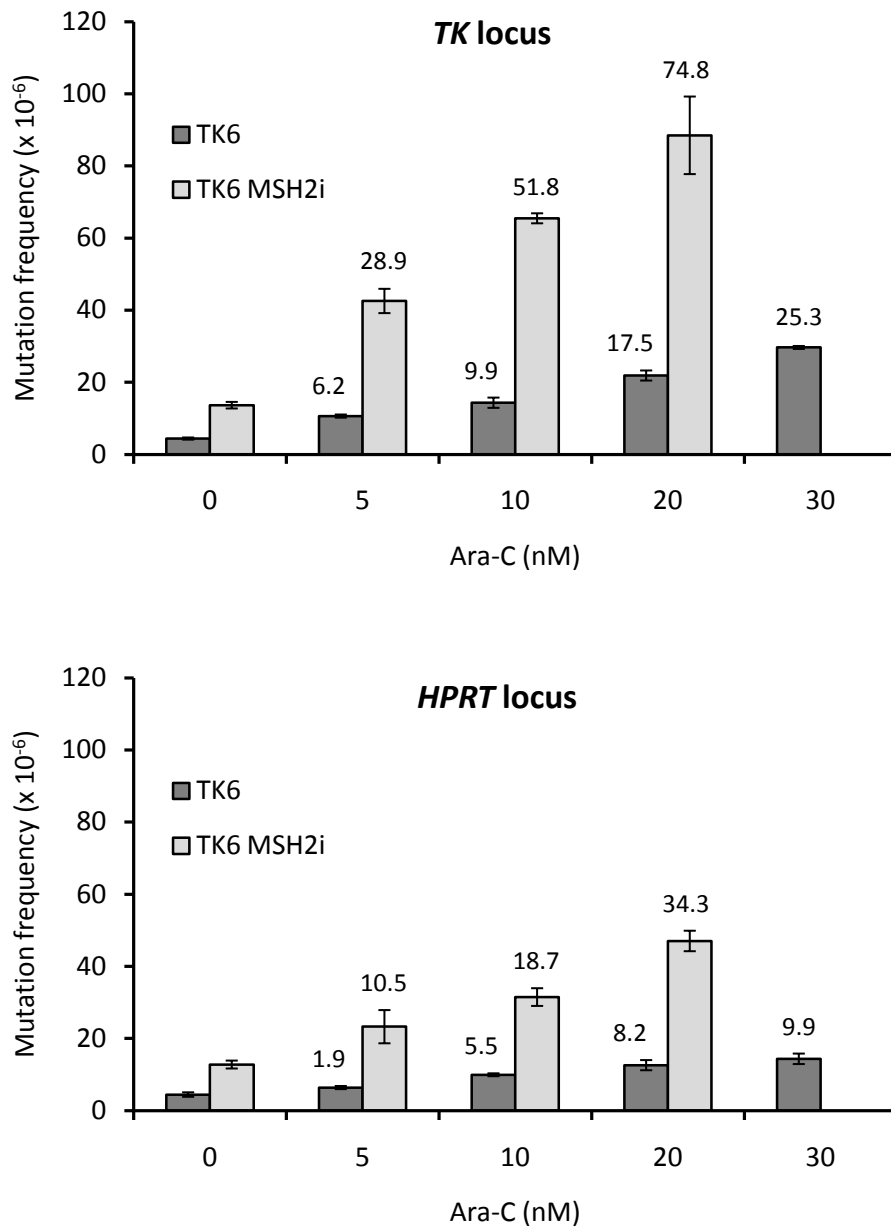


Figure 6.2. Mutagenicity of Ara-C at *TK* and *HPRT* loci.

Mutation frequency (MF) at *TK* and *HPRT* loci was assessed in MMR-proficient TK6 cells (dark grey bars) and MMR-deficient TK6 *MSH2i* cells (pale grey bars) following 16 hour exposure to Ara-C. Data represents the mean and standard error of three independently treated cell populations. Numbers above bars represent the induced MF (x 10⁻⁶) at each dose, calculated by subtraction of the spontaneous MF (0nM Ara-C). For cytotoxicity at each Ara-C concentration, see Figure 6.3B.

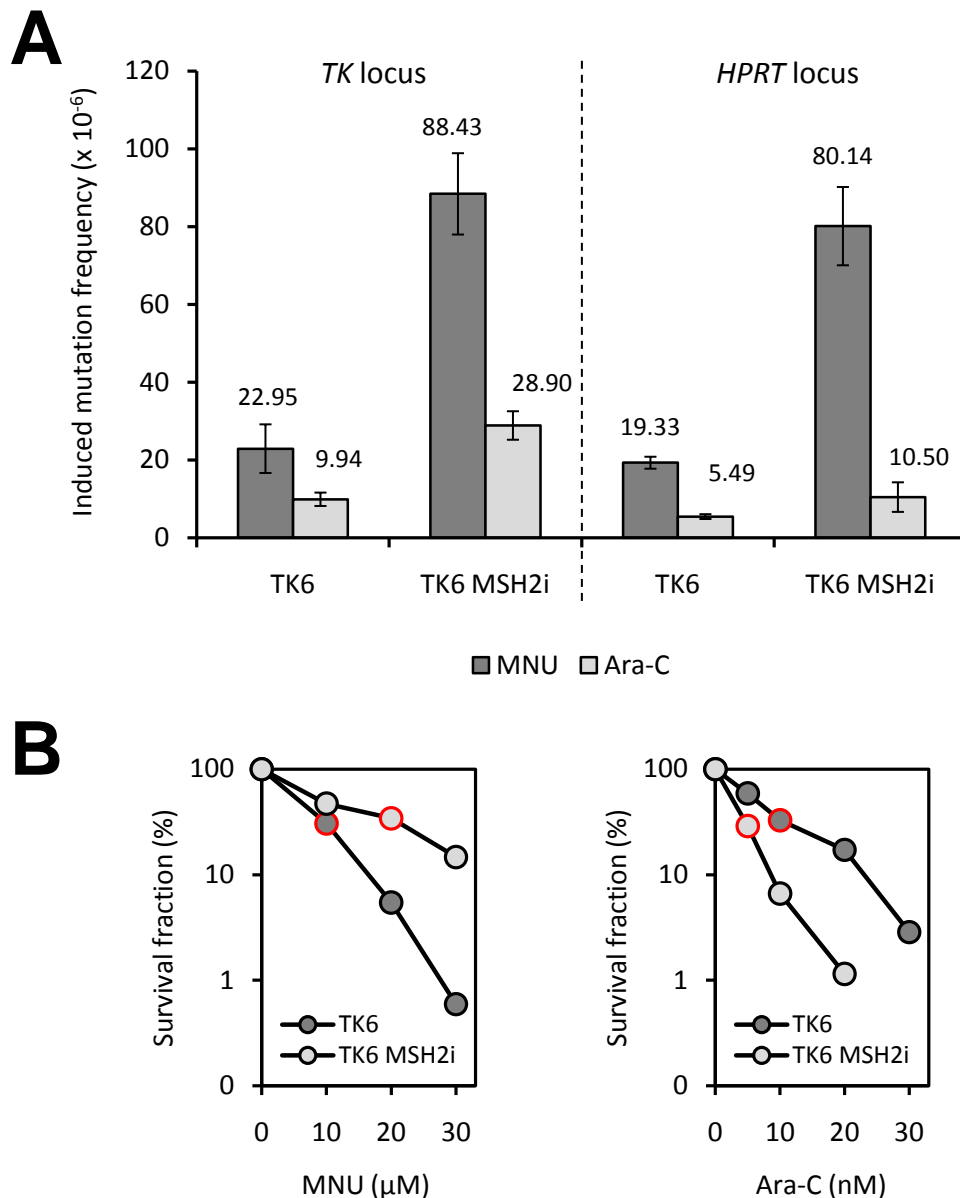


Figure 6.3. Comparison of the mutagenicity of MNU and Ara-C at equivalent cytotoxicity.

A. Induced mutation frequency (MF) at MNU (dark grey bars) and Ara-C (pale grey bars) concentrations cytotoxic to approximately 70% of cells were compared in DNA MMR-proficient TK6 cells and in MMR-deficient TK6 *MSH2i* cells at *TK* and *HPRT* loci. Induced MFs (numbers shown above bars) were calculated by subtraction of the spontaneous MFs (see Figures 6.1 and 6.2) and represent the mean and standard error of three independently treated cell populations. **B.** Cytotoxicity of MNU (left) and Ara-C (right). Data is presented as the the number of viable colonies from dosed cell suspensions as a percentage of the number of viable colonies from vehicle-only treated cell suspensions. The doses at which MFs were compared are highlighted in red.

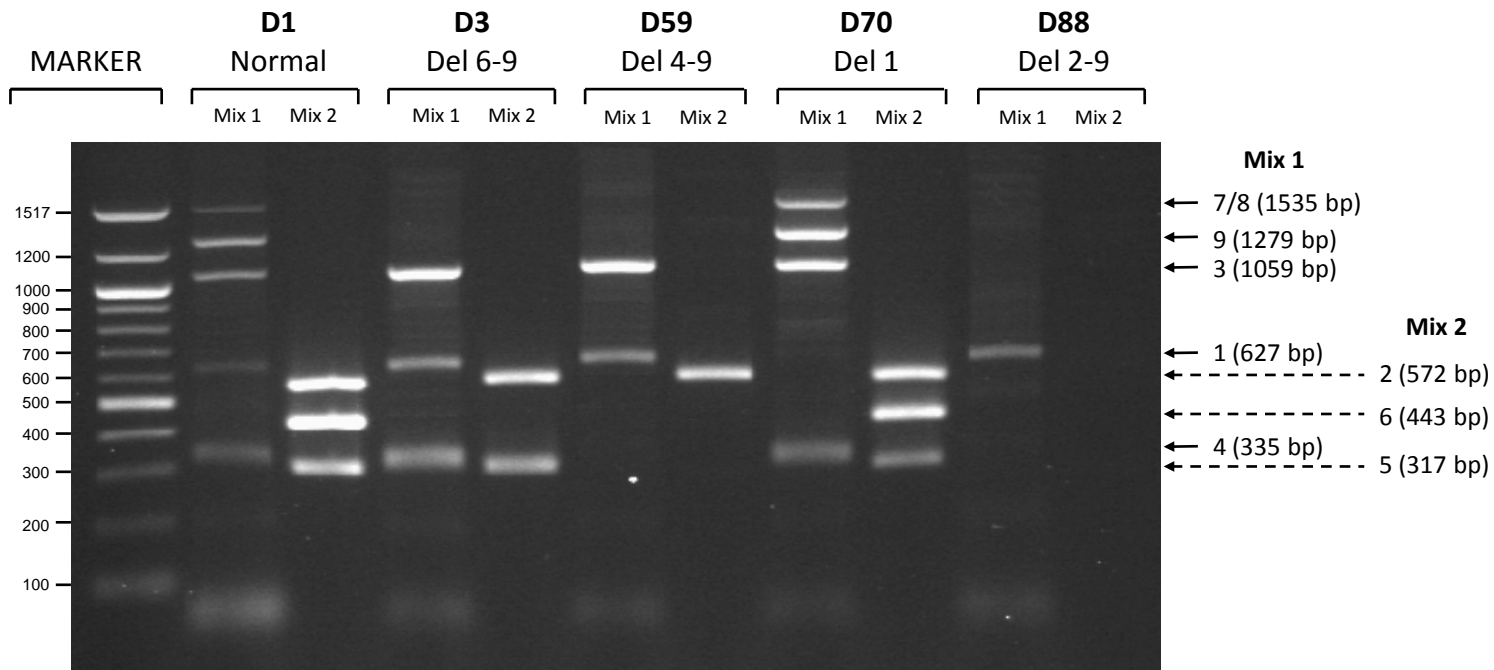
6.2.3. Molecular Analysis of Mutations at the *HPRT* Locus in TK6 Cells

To further investigate the mutagenicity of Ara-C, in terms of the types and frequencies of induced aberrations, a number of the individual mutants generated from the TK6 cell line were subject to molecular analysis in order to produce an Ara-C-induced mutational spectrum. Of particular interest was whether an increase in mutation arising from potential DNA MMR substrates (single base substitutions and frameshift mutations) would be observed. Specific *TK* and *HPRT* mutants can be discerned using molecular analysis, however this is significantly more straight-forward for *HPRT* given the X-linked nature of the gene. As the focus of this investigation was on detection of point mutations it was deemed suitable to perform molecular analysis only on *HPRT* mutants given that they should be equally likely to occur at both loci.

A total of 120 colonies (40 each from three independently treated cell populations) were selected at random from the TK6 *HPRT* mutants that arose following exposure to 30nM Ara-C. These single-cell cloned mutants were expanded in media containing the selective agent 6-TG as described in Section 2.11.1. During expansion, a plate containing 12 colonies had to be abandoned due to fungal infection. A further 4 colonies were lost as they failed to grow in the selective media, giving a total of 104 mutants for molecular analysis. Although the spectrum of mutations occurring spontaneously at the *HPRT* locus has been well characterised (Cariello and Skopek, 1993; Giver et al., 1993), as a control, 60 mutant TK6 colonies (20 each from three independent cell populations) which had not been exposed to Ara-C were also randomly selected and expanded. A plate containing 12 colonies was also lost to further analysis, resulting in a total of 48 spontaneous mutants available for analysis.

6.2.3.1. Analysis of large deletions

The initial step in analysis of the *HPRT* mutants involved the use of genomic *HPRT* multiplex PCR to identify large deletions, as described in Section 2.11.2. Large deletions are operationally defined as deletions encompassing one or more *HPRT* exons, as evidenced by absence of the corresponding multiplex PCR fragment(s); Figure 6.4 shows representative multiplex PCR profiles observed in some of the *HPRT* mutants.

B**Ara-C-treated *HPRT* mutants****Figure 6.4. Multiplex PCR amplification of the *HPRT* locus (continued from previous page).**

The gels show examples of multiplex PCR profiles representing partial *HPRT* deletions which occurred either spontaneously (**A**) or following exposure to Ara-C (**B**). For each mutant, the results of the 2 multiplex PCR reactions are shown side by side, with the mutant identification number (S, spontaneous; D, drug-exposed) and deleted region stated above. Mutants S5 and D1 both show the normal pattern of 8 bands. These mutants contain point mutations which do not perturb the normal amplification pattern. The exons represented by each band, and the size of the amplicons are shown to the right of the gels. A 100 bp marker ladder is shown to the left of each gel. The gels shown are 1.5% agarose gels loaded with 15 μ l of the products from each PCR reaction.

A total of 96 Ara-C-treated mutants, as well as 38 spontaneously-occurring mutants were found to harbour large deletions affecting the *HPRT* locus. After correction for identical mutations arising from the same original cell population, which possibly represent clonal expansion of a single mutant, a total of 13 independent large deletions were observed in Ara-C treated *HPRT* mutants, as well as 8 independent large deletions in the spontaneously-occurring mutants. Table 6.3 lists the specific deletions observed, and Figure 6.5 graphically illustrates the extent of the deleted regions. Interestingly, no common mutation was observed in both the Ara-C-treated and spontaneous mutant populations. Complete deletion of the *HPRT* locus was observed solely in the Ara-C-treated mutant population, as were 3' partial gene deletions (affecting exons 2 – 9 or 6 – 9). 5' partial gene deletions were observed in both spontaneous and Ara-C-treated mutant populations, although the extent of the deleted region differed (exons 1 – 3 or 1 – 7/8 in the spontaneous mutant population, exon 1 only in the Ara-C-treated population). Internal deletions of single exons were observed only in spontaneous *HPRT* mutants. A deletion of exons 2 – 3 was also observed solely in the spontaneous mutant cell population. A larger internal deletion encompassing exons 4 – 8 was observed in Ara-C-treated *HPRT* mutants. Together, this demonstrates that the spectrum of Ara-C-induced large *HPRT* deletions is clearly distinct from the spontaneously-occurring large deletion spectrum.

Deleted Region	Spontaneous	Ara-C Treated
	Number observed ^a	Number observed ^a
Complete gene deletion		2 (2)
5' partial gene deletions		
1		3 (44)
1 – 3	2 (26)	
1 – 7/8 ^c	1 (1)	
Total	3 (27)	3 (44)
3' partial gene deletions		
2 – 9		3 (6)
6 – 9		3 (20)
Total		6 (26)
Internal exon deletions		
4	1 (1)	
5	1 (4)	
7	1 (1)	
2 – 3	1 (4)	
4 – 8 ^b		2 (24)
Total	4 (10)	2 (24)
Other		
1 and 7/8 ^d	1 (1)	
Total	1 (1)	
Total Large Deletions	8 (38)	13 (96)

Table 6.3. Large deletions observed in spontaneous and Ara-C-treated *HPRT* mutants.

^a Figures represent the number of independent mutations after correction for duplicate mutations which likely represent clonal expansions. Actual number observed is shown in parentheses.

^b For these mutants, deletion of exon 9 was observed on multiplex analysis, however cDNA sequencing demonstrated an internal deletion of exons 4-8. The 3' terminus of the deletion must therefore lie within intron 8 and result in deletion of the forward primer binding site for exon 9 amplification.

^c As exons 7 and 8 are amplified on a single PCR fragment, and no cDNA was generated for this mutant, it is not possible to determine the exact 3' terminus of this deletion.

^d As exons 7 and 8 are amplified on a single PCR fragment, and no cDNA was generated for this mutant, it is not possible to determine whether exon 7 or exon 8 or both are deleted.

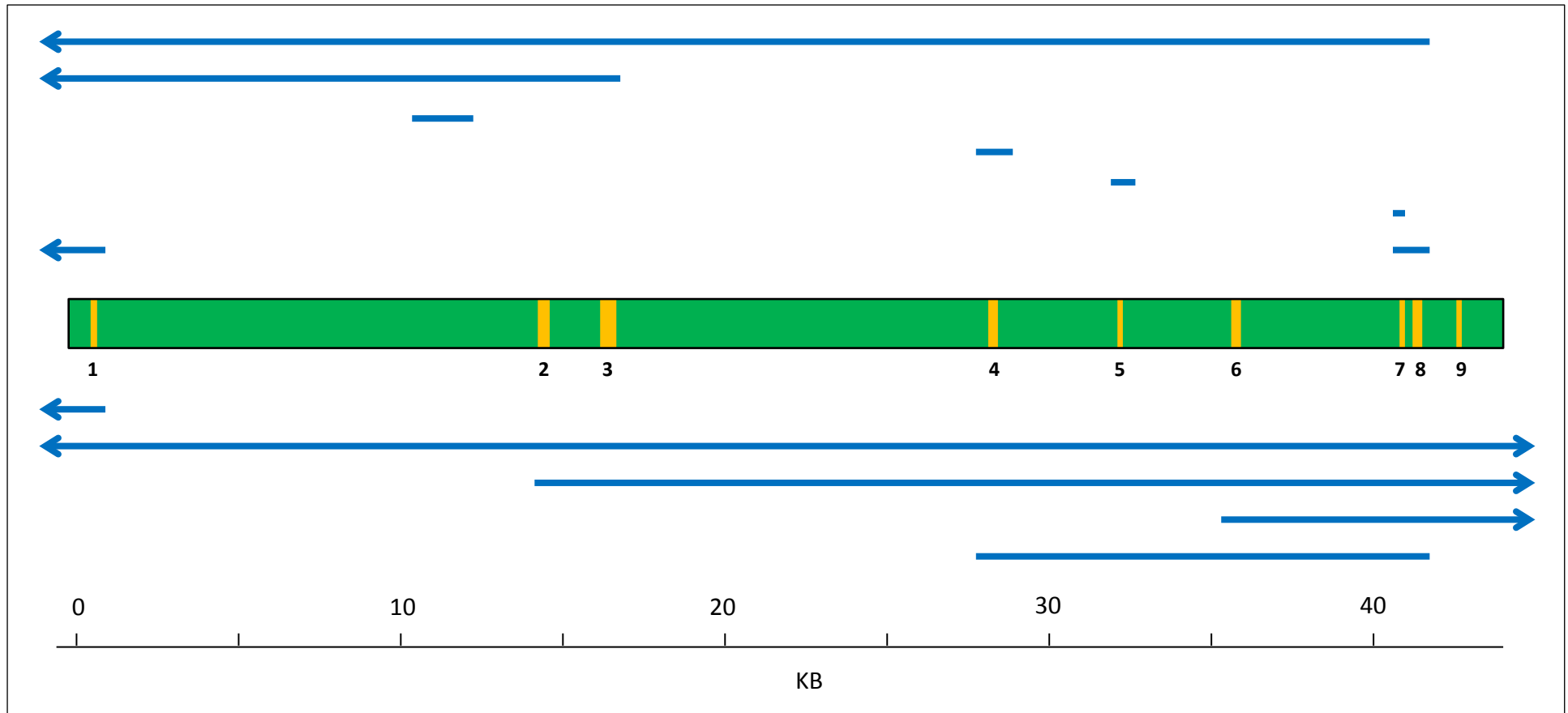


Figure 6.5. Extent of genomic deletions observed in spontaneous and Ara-C-treated *HPRT* mutants.

The *HPRT* locus is displayed to scale with exons shown in yellow. Blue bars demonstrate the deleted regions observed in *HPRT* mutants as determined by multiplex PCR and analysis of *HPRT* cDNA. Those displayed above the gene were observed in spontaneously occurring mutants and those below were in Ara-C-treated mutants. Note that deletions including terminal exons extend for undetermined distances outside of the locus (indicated by arrowheads).

6.2.3.2. Analysis of Point Mutations in *HPRT* Coding Region

For mutants with a normal *HPRT* multiplex PCR result, reverse transcriptase-mediated production of *HPRT* cDNA, PCR amplification, and cDNA sequencing were employed to identify small alterations, as described in Section 2.11.3.

In total, 7 point mutations (3 independent) were observed in the spontaneous *HPRT* mutant population. All were base substitutions, comprising two transition mutations and one transversion mutation. In the Ara-C-treated mutant population, 7 mutants were all found to have the same transversion mutation, which had occurred independently in all three of the treated cell populations. For each mutation, the target sequence and resulting amino acid change is shown in Table 6.4, and the distribution of the mutations within the *HPRT* coding sequence is shown in Figure 6.6.

6.2.3.3. Analysis of Splice Site Mutations

HPRT cDNA from 1 remaining Ara-C-treated *HPRT* mutant demonstrated a deletion of 77 base pairs corresponding to exon 8, although exon 8 appeared to be present based on multiplex PCR analysis. As this was potentially due to aberrant processing of the *HPRT* transcript, leading to exon skipping, genomic sequencing of the intronic regions flanking exon 8 was performed to identify possible mutations affecting splice donor and acceptor sites. This was achieved through sequencing of the PCR product amplified using the exon 7/8 primer pair from the multiplex (as the primer binding sites lie within intronic regions, meaning the exons and flanking sequences are amplified) as described in Section 2.11.4. Sequencing of the region distal to exon 8 revealed a G:A transversion within the donor splice site (Figure 6.7A). The exon 8 5' donor splice site is susceptible to mutation at each position, with all reported mutations (including the G:A mutation detected herein) causing loss of exon 8, without the use of a cryptic donor splice site (O'Neill et al., 1998).

Position ^a	cDNA Alteration	Amino Acid Change	Target Sequence ^b	Spontaneous	Ara-C Treated
				Number Observed ^c	Number Observed ^c
Transitions					
E5:395	T:C	Ile > Thr	TTGATT GT G	1 (2)	
E2:118	G:A	Gly > Arg	TCAT GG ACT	1 (1)	
Transversions					
E6:409	A:T	Ile > Phe	TATA ATT GA	1 (4)	
E6:412	G:T	Asp > Tyr	AAT TG ACAC		3 (7)
Total Point Mutations				3 (7)	3 (7)

Table 6.4. Point mutations observed in spontaneous and Ara-C-treated *HPRT* mutants.

^a Mutated position is identified by the exon in which it occurs and numbered according to the cDNA position.

^b Within the target sequence, the affected base is shown in bold.

^c Figures represent the number of independent mutations after correction for duplicate mutations which likely represent clonal expansions. Actual number observed (ie. uncorrected) is shown in parentheses.

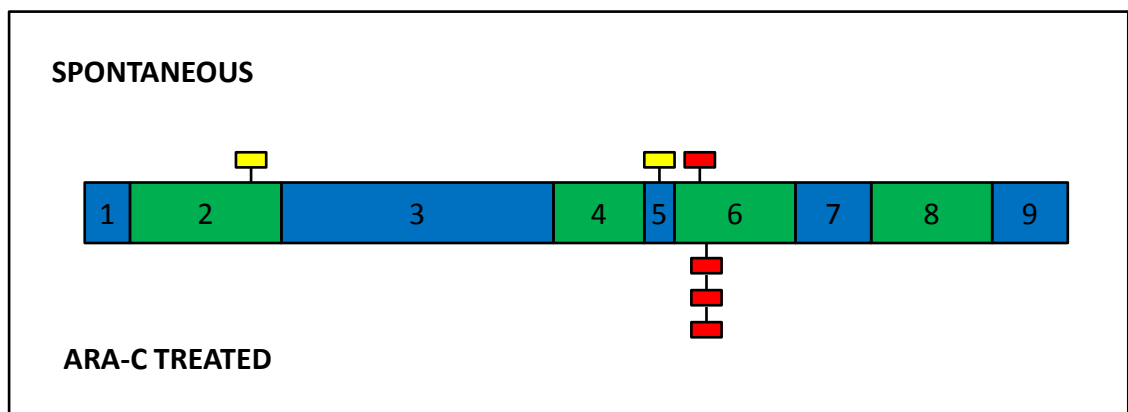


Figure 6.6. Distribution of point mutations within the *HPRT* coding region.

HPRT exons are drawn to scale relative to each other. The rectangles represent point mutations, all of which were single base substitutions, observed within the *HPRT* coding region. Spontaneously occurring mutations are shown above the transcript, those observed in Ara-C-treated mutants are shown below. Transitions are shown in yellow, transversions are shown in red. Sites at which multiple independent mutations were observed are indicated as stacked symbols.

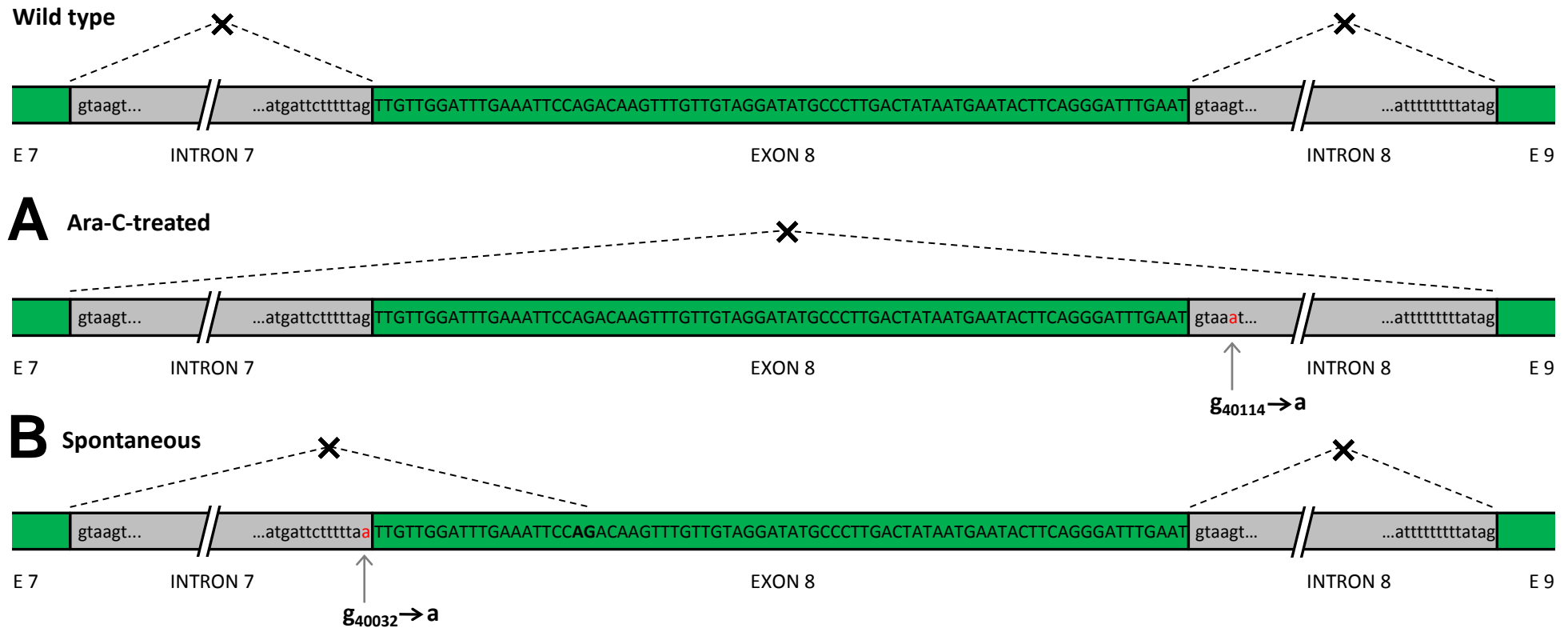


Figure 6.7. Splice site mutations in the *HPRT* gene, causing splicing of exon 8.

The wild type splicing pattern of introns 7 and 8 of the *HPRT* gene is displayed in the top image. Sequences of the intronic splice sites are shown in lower case (intervening intronic sequence is not shown), exon 8 sequence is shown in uppercase. Spliced regions are indicated by dashed lines. Note that exons and introns are not displayed to scale. **A.** Point mutation of the 5' splice donor sequence in intron 8 resulted in exon 8 skipping in one Ara-C-treated *HPRT* mutant. **B.** In one independent spontaneously-occurring mutation event, point mutation of the 3' splice acceptor sequence in intron 7 resulted in splicing of the first 21 bases of exon 8 due to the use of a cryptic splice acceptor site (shown in bold type). Mutated sites (shown in red type) are numbered according to their position in genomic DNA.

Similarly, 3 (2 independent) spontaneously-occurring mutants which demonstrated a normal multiplex PCR profile were found to have a 21 base pair deletion corresponding to the beginning of exon 8. Sequencing of the flanking intronic regions, as described above, revealed a G:A transversion within the acceptor splice site in all three mutants (Figure 6.7B). This mutation has also been previously reported and causes loss of the first 21 bases of exon 8 due to the use of a cryptic acceptor splice site within exon 8 (Figure 6.7B) (O'Neill et al., 1998).

6.2.3.4. Comparison of Spontaneous and Ara-C-Induced *HPRT* Mutational Spectra

A summary of the mutations observed in spontaneous and Ara-C-treated *HPRT* mutant populations, after correction for duplicate mutations that represent presumptive clonal expansions, is shown in Table 6.5. Although large deletions affecting the *HPRT* locus are classified as complete gene deletion, partial gene deletions (3' or 5') or internal exon deletions, given that these deletions would be expected to arise by the same mechanism (discussed below), these deletions were combined for the purposes of statistical analysis of mutational spectra. A Chi-squared test of the homogeneity of spontaneous and Ara-C treated mutant populations (in terms of large deletions and point mutations) demonstrated that the change in the spectrum of mutations due to Ara-C was not significant ($P = 0.44$).

Despite this, the frequency of each class of mutation was used to estimate the Ara-C-specific mutational burden at the *HPRT* locus (Table 6.5 and Figure 6.8), as described in Section 2.11.5. The drug-induced *HPRT* mutation spectrum (Figure 6.8) demonstrates that Ara-C induces all classes of mutation. Furthermore the increase in mutation frequency over background can be mostly accounted for by large deletions affecting the *HPRT* locus, in particular 3' partial deletions. Consistently, a Fisher's exact test demonstrated the occurrence of 3' partial gene deletions in the Ara-C mutant population to be significantly increased over background ($P = 0.02$). Similar testing performed for other classes of mutation did not reach statistical significance (data not shown).

Mutation Type	Spontaneous			Ara-C Treated			
	Number Observed ^a	% Total Mutants (independent)	Absolute Mutant Fraction ^b (x 10 ⁻⁶)	Number Observed ^a	% Total Mutants (independent)	Absolute Mutant Fraction ^b (x 10 ⁻⁶)	Induced Mutant Fraction ^c (x 10 ⁻⁶)
Complete gene deletion	0			2 (2)	11.76	1.69	1.69
5' partial gene deletion	4 (28) ^d	30.77	1.37	3 (44)	17.65	2.53	1.17
3' partial gene deletion	0			6 (26)	35.29	5.06	5.06
Internal exon deletions	4 (10)	30.77	1.37	2 (24)	11.76	1.69	0.32
Point mutations ^e	5 (10)	38.46	1.71	4 (8)	23.53	3.38	1.67
Total	13 (48)	100.00	4.44	17 (104)	100.00	14.35	9.91

Table 6.5. Summary of spontaneous and Ara-C-treated *HPRT* mutants.

^a Figures represent the number of independent mutations after correction for duplicate mutations which might represent clonal expansions. Actual numbers observed (i.e. uncorrected) are shown in parentheses.

^b Calculated by multiplying the mean mutation frequency (from Table 6.2) by the percentage of total mutants represented by each class of mutation.

^c Calculated by subtraction of the spontaneous (absolute) mutant fraction from the Ara-C-treated (absolute) mutant fraction.

^d The single mutant with deletion of exon 1 and exon 7/8 is included here.

^e Includes base substitutions within coding regions and those affecting splice sites.

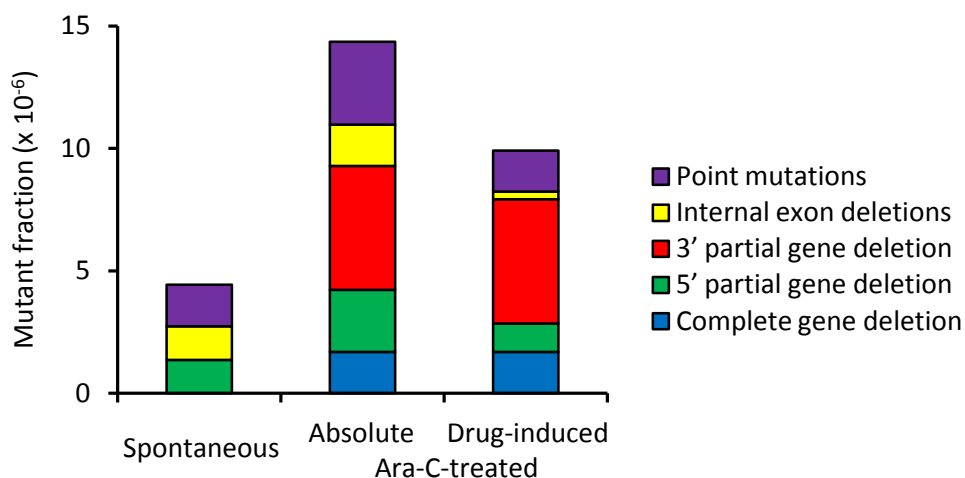


Figure 6.8. Spectra of spontaneous and Ara-C-induced *HPRT* mutations in TK6 cells.

Coloured bars demonstrate the estimated fraction of the total *HPRT* mutants represented by each type of mutation, determined as described in Section 2.11.5.

6.3. Discussion

Despite widespread use in the treatment of AML, as well as other malignancies, there is a paucity of data investigating the mutagenicity of anti-leukaemic nucleoside analogues. The initial aim of this study therefore, was to determine whether the nucleoside analogue Ara-C is mutagenic using *in vitro* mutation assays. In two well established independent mutation assays, a statistically significant dose-dependent increase in MF was observed following 16 hour exposure to the drug, suggesting that Ara-C is capable of acting as a DNA mutagen at the doses investigated. Relative to the potent mutagen MNU, the mutagenic effect of Ara-C in both assays was appreciably weak, however this is expected given the difference in the major mechanistic actions of these agents and the expectation that the majority of Ara-C lesions in DNA would result in chain termination hence would inhibit further rounds of DNA replication required for mutation fixation.

TK6 cells are heterozygous at the *TK* locus and hemizygous at the *HPRT* locus. Many mutagenic mechanisms that involve homologous interaction, such as gene conversion, therefore cannot occur at the X-linked *HPRT* locus. In addition, large multi-locus deletions are likely to be lethal in the *HPRT* assay, because gross deletions may span adjacent genes essential for cell survival. Therefore, if the primary mechanism of mutation induction by a particular agent implicates either homologous interaction or large deletion, the mutagenicity of that agent will be significantly underestimated by the *HPRT* mutation assay. In this investigation, Ara-C-induced MF at the *TK* locus was greater than that induced at the *HPRT* locus, suggesting that the primary mechanism of Ara-C-induced mutation is through one (or both) of these mechanisms. Nucleoside analogue-induced chain termination gives rise to stalled replication forks, which can in turn be converted to DSBs (Arnaudeau et al., 2000; Arnaudeau et al., 2001). Two DSBs in relatively close proximity could therefore give rise to loss of the intervening sequence, resulting in a large deletion. In addition, evidence suggests that HRR is the primary mechanism recruited to repair DSBs at stalled replication forks (Arnaudeau et al., 2001; Lundin et al., 2002; Rothkamm et al., 2003), hence it is possible Ara-C could also induce gene conversion type mutations. Indeed, chain termination could give rise to LOH-type mutations, which can occur by either gene conversion or large deletion events, among others, which would be consistent with a higher Ara-C-induced *TK* MF

relative to *HPRT* MF. Also consistent with these data, studies of the mutagenicity of Zidovudine (3'-Azido-2',3'-dideoxythymidine), an NRTI which can cause DNA chain termination, have demonstrated a greater increase (2.2 fold) in MF at the *TK* locus than at the *HPRT* locus (Sussman et al., 1999; Meng et al., 2000).

MMR-deficient TK6 *MSH2i* cells (generated from TK6 using shRNA-mediated gene knockdown, see Section 2.4) were used to investigate whether the mutagenic potency of Ara-C could be further affected by loss of DNA MMR. As expected, Ara-C was more mutagenic to TK6 *MSH2i* than to parental MMR-proficient TK6 cells, although the influence of DNA MMR loss was relatively modest in comparison to its effect on the mutagenicity of MNU. The mutator phenotype is a hallmark of cells lacking functional DNA MMR (Karran, 2001), consistently, the spontaneous mutation frequencies observed at *TK* and *HPRT* loci were around 3-fold and 4-fold higher respectively in TK6 *MSH2i* cells than parental TK6 cells (see Figure 6.1 and Figure 6.2). The increase in Ara-C-induced mutation frequency observed in TK6 *MSH2i* is therefore likely due, in part, to the hypermutability of this cell line. Two-way ANOVA testing however, demonstrated a statistically significant influence of both Ara-C concentration and cell line on *TK* and *HPRT* mutation frequency, suggesting an interaction between DNA MMR and Ara-C. In other words, these findings suggest that Ara-C-induced mutation is suppressed by DNA MMR, providing further weight to the evidence that this pathway is somehow implicated in cellular response to Ara-C.

The influence of DNA MMR dysfunction on Ara-C mutagenicity appeared to be greater at the *TK* locus than the *HPRT* locus (Figure 6.2) (although this was not assessed statistically), which would indicate a greater increase in structural mutations better detected at this locus, including those arising via multi-locus deletion or gene conversion. Given the purported role of DNA MMR components in suppression of recombination between imperfectly matched sequences (see Section 1.1.2), as well as evidence that gene conversion type mutations occur in cells lacking *MSH2* (Elliott and Jasin, 2001; Villemure et al., 2003; Smith et al., 2007), it is feasible that MMR dysfunction in TK6 *MSH2i* would give rise to an increase in this class of mutation at the *TK* locus. A role for DNA MMR dysfunction in induction of large deletions is harder to envisage, but nevertheless may occur due to loss of an as yet uncharacterised function of DNA MMR components at the replication fork.

As far as can be determined, this work represents one of a limited number of reports of the use of *in vitro* TK and HPRT mutation assays in DNA MMR-compromised cell lines. Given the consistent results observed with MNU, well characterised as hypermutable in DNA MMR-deficient cells (Andrew et al., 1998), these data demonstrate that *in vitro* mutation assays can be routinely performed in MMR-compromised cells and may represent a useful resource for investigating the influence of DNA MMR status on the mutagenicity of particular agents, as this study has demonstrated for Ara-C.

The Ara-C mutational spectrum is predominated by mutants originating from DNA strand breakage events (i.e. Large deletions; 76%), consistent with chain termination as a major mechanism of this agent. Additionally, the inhibitory effects of Ara-C on topoisomerase enzymes (Cline and Osheroff, 1999; Chrencik et al., 2003) could also feasibly give rise to this class of mutation. Although a greater number of large deletions were observed in the Ara-C mutant population compared to the spontaneous population (see Table 6.5), after correction for presumptive clonal expansions, this was not statistically significant. It is probable however that some of the identical deletion events detected within the same dosed cell population were in fact true independent mutation events and not clonal siblings, given that certain deletions (for instance Ara-C induced deletion of *HPRT* exons 2-9) occurred in independently dosed cell populations. Also it is important to note that some apparently identical deletion events may have different breakpoints, although this was not investigated experimentally. Given that the majority of Ara-C-induced mutants are partial gene deletions which extend for undetermined distances outside of the *HPRT* coding sequence it was not possible to sequence breakpoints. The corrected frequencies of each class of mutation are therefore likely to be an underestimation of the true frequencies due to an inability to reliably determine which mutation events arising in the same cell population are independent and which represent clonal siblings. This highlights a caveat of this particular investigation in that only 3 independent Ara-C-dosed cell populations were investigated at each dose. It was not anticipated that such a degree of apparent clonal expansion would be observed, which could potentially be masking independent mutation events. It is therefore planned to extend this investigation to generate a greater number of independently-dosed *HPRT* mutants for molecular analysis.

Although it is likely that each class of large deletion would arise by the same mechanism, there was a statistically significant increase in the occurrence of 3' partial *HPRT* gene deletions in the Ara-C mutant population ($P = 0.02$). Furthermore, this was estimated to account for a large proportion of the Ara-C-induced *HPRT* mutation frequency (Figure 6.8), which could reflect the possible existence of a site (or sites) in the 3' region of the *HPRT* gene at which Ara-C-mediated chain termination is more likely to be converted to a strand break. Similarly, prior to correction for possible clonal siblings, a large proportion of Ara-C-induced mutants were deletions of exon 1 which extend for undetermined lengths 5' of the *HPRT* gene (see Table 6.3), suggesting the possible existence of preferential sites of Ara-C-induced breakage also in this region. In both cases however, it cannot be determined whether all of these mutants share the same breakpoints or whether they represent individual mutational events.

One of the assumptions prior to molecular analysis of Ara-C-induced *HPRT* mutants was that mutations arising from fixation of potential DNA MMR substrates, such as base substitutions and frameshift mutations, would be increased relative to the spontaneously-occurring mutant population. On the contrary, a lower number of independent point mutations was observed in the Ara-C-treated mutant population relative to the spontaneous population. Furthermore, all point mutations observed were single base substitutions, with no frameshift-type mutations observed in either *HPRT* mutant population. Single base substitutions (including those affecting mRNA splicing) are reported to account for around 31% of spontaneously-occurring *HPRT* mutations (Giver et al., 1993), which is consistent with the percentage of independent point mutations analysed in this investigation (38%). The slightly lower number of this class of mutation detected in the Ara-C-induced *HPRT* mutant population (24%) suggests that Ara-C does not readily induce point mutations in DNA (although estimation of the proportion of total *HPRT* mutants represented by point mutations argues that Ara-C is a weak point mutagen (see Figure 6.8)). It cannot be ruled out that these mutations do occur more readily as a result of base misincorporation (or polymerase slippage in the case of frameshift mutations) but the cells possess an efficient mechanism for their reversal prior to fixation to mutation, for instance the DNA MMR pathway. Consistently, the mutagenic potency of Ara-C is significantly increased in MMR-deficient TK6 *MSH2i* cells, which could reflect a reduction in cellular capacity for repair of Ara-C-induced lesions prior to mutation fixation. It is important to

note however, that the mutagenicity of MNU is also significantly increased in MMR-defective cells, although this is not due to a lack of MMR-mediated repair, but rather a failure to initiate death in cells carrying pro-mutagenic mispairs. In this circumstance cells persist and mispairs become fixed as mutation. Insight into whether the DNA MMR pathway is capable of detection and/or repair of Ara-C-induced lesions could be provided by an analysis of the Ara-C-induced mutational spectrum in MMR-deficient TK6 *MSH2i* cells. For instance, if Ara-C can induce base insertion mutations, as suggested by translesion synthesis experiments (see Figure 3.11), which could represent a potential substrate for DNA MMR components, an increase of this class of mutation would be expected in MMR-defective cells.

An analysis of the Ara-C-induced mutation spectrum in TK6 *MSH2i* cells is one of the anticipated follow-up investigations to this work. It may also be interesting to determine the spectrum of Ara-C-induced mutations in TK6 *MSH3i* cells. As these cells are apparently solely dysfunctional in the MutS β complex (see Section 3.2.5), such an investigation may be helpful in further delineating the influence of this complex on cellular response to Ara-C. Given the possibility that DNA MMR status may influence the induction of LOH-type mutations, such as gene conversion (or possibly multi-locus deletion) as suggested above, it may be more pertinent to perform analysis of Ara-C-induced mutations occurring at the *TK* locus, although this type of analysis is significantly more labour intensive.

With the exception of a single mutant which was mutated in the exon 8 donor splice site (see Figure 6.7A), all Ara-C-induced point mutants demonstrated the same transversion mutation (E6:412 G:T; see Table 6.4). The mutability of any particular base pair is affected by several parameters including initial lesion incorporation, ability to remove/repair the lesion and the efficiency of insertion of an incorrect base opposite the lesion by a DNA polymerase. Although speculative, the most likely scenario which would give rise to this particular mutation is that an Ara-C nucleotide was incorporated in place of dCTP in the non-transcribed strand of the *HPRT* gene, and dTTP was misincorporated (instead of dGTP) opposite the lesion at the next round of DNA replication. Given that this mutation occurred independently in all 3 dosed cell populations suggests that this site represents a 'hotspot' for Ara-C-induced point mutation, although this would require extensive further investigation. Why

incorporation of Ara-C would be favoured at this particular site, and also why the mispair appears able to escape repair, is unknown. Such a finding, if substantiated, could have potential implications for the therapeutic use of Ara-C if preferential sites of incorporation at risk of mutation were identified in genes associated with drug resistance, for example. Although observed in independently exposed populations, strongly suggesting independent Ara-C-induced mutational events, the possibility that these mutants originated from a single spontaneous mutant clone cannot be completely excluded. For instance, a mutation could arise subsequent to elimination of pre-existing *HPRT* mutants but prior to drug exposure and hence would be present in independent cell populations, although this seems unlikely.

In conclusion, *in vitro* evidence suggests that Ara-C is mutagenic to DNA, although a more extensive molecular analysis of independent mutants is required to fully delineate the types of mutation this agent can induce, and to further investigate whether mutability is influenced by DNA MMR status. At the time these investigations were underway, another member of the laboratory performed a TK assay in TK6 cells to assess the mutagenicity of the nucleoside analogue fludarabine. A similar result to that described here in response to Ara-C was observed, specifically fludarabine was able to induce a dose-responsive increase in MF at the *TK* locus (V. Forster, unpublished data), adding further weight to the evidence that nucleoside analogues have the potential to be mutagenic to DNA. Given the widespread chemotherapeutic use of these agents, often in patients which may exhibit compromised DNA MMR, *in vivo* investigation of the mutability of these agents would seem warranted (see Chapter 8).

6.3.1. Summary of Chapter

In summary, these investigations have demonstrated that:

- Exposure to Ara-C results in a dose-dependent increase in mutation frequency at both *TK* and *HPRT* loci in TK6 cells, suggesting Ara-C is mutagenic to DNA *in vitro*.
- Ara-C-induced MF is significantly increased in DNA MMR dysfunctional cells at both loci, suggesting MMR components have a role in suppression of Ara-C-induced mutation.
- Large deletions account for the majority of Ara-C-induced mutations, consistent with the chain terminating nature of the drug.
- Ara-C can induce point mutations in DNA (although not statistically significantly). Such mutations arise via fixation of mispairs in DNA, which could potentially represent substrates for DNA MMR.

**Chapter 7. The Clonal Origins of Relapse in Acute Myeloid
Leukaemia**

7.1. Introduction

Despite the ability of standard chemotherapeutic regimes to induce remission in 50 – 85% of *de novo* AML patients, the majority of patients will relapse within 2 years of achieving remission (Larson, 2007; Shipley and Butera, 2009). Furthermore, relapsed AML, in patients who are unsuitable for bone marrow transplant, is almost always fatal (Shipley and Butera, 2009), regardless of whether patients are treated with standard re-induction chemotherapy or alternative regimes using different chemotherapeutic agents. A similarly poor outcome is also observed in patients treated for t-AML that develops following therapy for a previous unrelated malignancy (Larson, 2007).

Important genetic differences have been identified between *de novo* and relapsed AML, including the acquisition of new chromosomal abnormalities (Estey et al., 1995; Kern et al., 2002), gene mutations (Kottaridis et al., 2002) and UPD (Raghavan et al., 2008). Additionally, MSI is observed in some patients with relapsed AML (see Figure 1.9). This, combined with the similarly poor treatment response observed in t-AML patients, suggests that at least some of the mechanisms by which relapsed AML and t-AML evolve are likely to be similar. However, many uncertainties still remain about the molecular abnormalities responsible for relapse in AML, as well as the cellular and genetic relationship between presentation and relapsed disease in individual patients.

The clonal evolution of *de novo* leukaemia, as well as the majority of cancers, is now well characterised (Figure 7.1). Furthermore, in the case of ALL, a recent genome wide SNP analysis in matched samples at diagnosis and relapse from individual patients has provided valuable insights into the clonal origins of relapsed disease (Mullighan et al., 2008). This study demonstrated that, rather than being identical to or evolved from the major clone present at initial disease presentation, the majority of relapsed ALL cases represent clonal evolution from ancestral, pre-diagnosis leukaemic clones (Figure 7.1). Additionally, in a small subset of cases, the clone identified at relapse was genetically distinct from the clone at initial presentation, suggesting the occurrence of either a second *de novo* leukaemia, or possibly a therapy-related malignancy which was misinterpreted as relapsed disease.

Similar studies aimed to delineate the clonal nature of relapsed AML are clearly warranted, but have yet to be published. Understanding the origins of relapsed AML,

as well as t-AML, will prove crucial to the development of novel therapeutic approaches which are targeted towards minimising the risk of their occurrence.

7.1.1. Aims of Chapter 7

The objective of this work was to perform a small pilot study to compare molecular lesions present at initial AML diagnosis to those present at relapse in individual patients in order to investigate the clonal origins of relapsed AML.

Specifically, the experimental aims were to:

- Isolate leukaemic blasts from matched presentation and relapsed AML samples, and prepare DNA for array analysis using the Affymetrix SNP 6.0 platform.
- Use genotyping software to identify CNAs and cn-LOH in the presentation and relapsed AML samples.
- Compare abnormalities detected at presentation and relapse in order to map the clonal evolution of relapsed disease in each patient.
- Determine if any genes involved in DNA MMR, or other DNA repair pathways, are affected by CNA or cn-LOH in each patient.

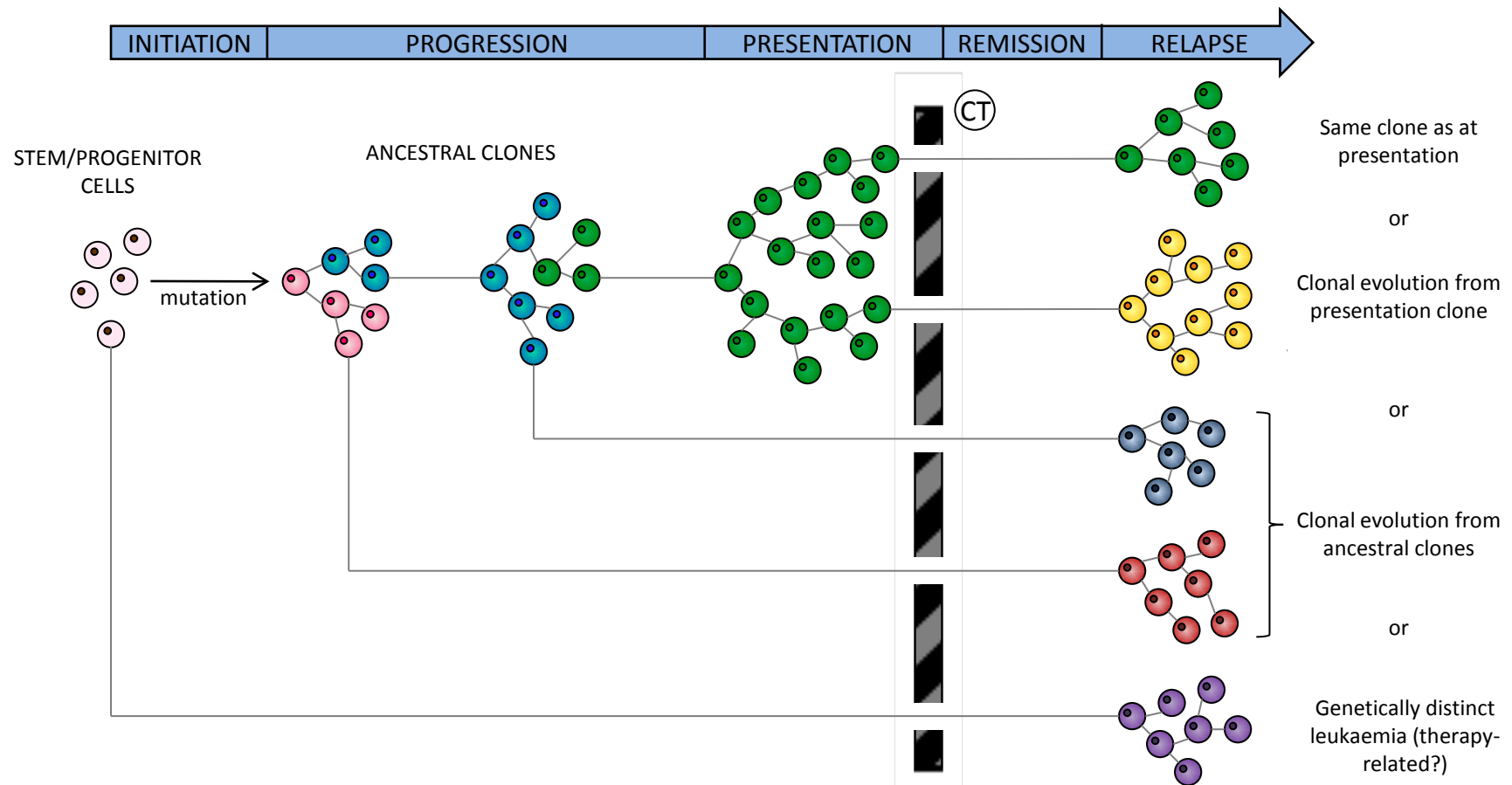


Fig 7.1. Clonal evolution of leukaemia.

Leukaemia, like all cancers, occurs due to the sequential accumulation of genetic abnormalities (termed clonal evolution) which eventually results in transformation to overt leukaemia (presentation). Chemotherapy (CT) can induce remission in the majority of cases, however relapse is likely. Relapsed leukaemia may occur due to re-population of the dominant presentation clone (green), or as a result of subsequent clonal evolution from either the presentation clone (yellow) or from an ancestral clone (dark blue/red). An alternative possibility is that the leukaemic clone observed at relapse is entirely genetically distinct from the original disease (purple), and may represent a second *de novo* leukaemia or a therapy-related leukaemia. Note that at disease presentation, only the dominant clone is depicted, although other minor clones might be present. Similar clonal heterogeneity probably also exists at relapse (see Section 7.3).

7.2. Results

7.2.1. Patients

Matched presentation and relapsed material (mononuclear cells purified from peripheral blood) from 6 adult AML patients was obtained from the Newcastle Haematology Biobank (Newcastle University) (Table 7.1). Median age at initial diagnosis (where information was available) was 37 years (range 32 – 44). Median latency period (from date of initial diagnosis to date of diagnosis of relapsed disease) was 335 days (range 235 – 719). In the case of patient 3, a second relapse occurred a further 1761 days (4.8 years) after the initial relapse, subsequent to bone marrow transplant. Karyotypes, where available, are also included in Table 7.1. In the case of patients 1, 3 and 6, there was evidence of a cytogenetically abnormal clone at presentation. For patient 3, the abnormal clone was not detected at first relapse, and at second relapse, karyotype was not determined (relapse karyotype was also not determined in the case of patient 1). Similarly in patient 6, the abnormal clone was not detected at relapse. All patients were alive at the point of last follow up, with the exception of patient 6, although cause of death is unknown.

7.2.2. Immunophenotypes of Leukaemic Blasts

In order to estimate the percentage of leukaemic blasts in each mononuclear cell sample, flow cytometry was performed to assess expression of CD33 and CD34 (and CD45 for exclusion of any residual red blood cells present in the samples) as described in Section 2.12.1. Blast cells expressing these surface markers are detected in the blood of approximately 90% and 75% of AML patients, respectively (Scolnik et al., 2002; Linenberger, 2005), but are significantly rarer in normal peripheral blood (see Figure 7.2).

Blast immunophenotypes and blast percentages of the samples are included in Table 7.1. All samples consisted of blasts which were positive for CD33 expression. With the exception of patient 3 (described below) all blasts were negative for CD34. For samples where the blast percentage was lower than 85%, blasts were isolated using CD33 MACS[®] microbeads as described in Section 2.12.2, to ensure sufficient purity of leukaemic blast cells for SNP array analysis.

Patient ID	Status ^a	Date of Diagnosis	Age at Diagnosis	Latency (days)	Karyotype ^b	Blast Immunophenotype	Blast % ^c
1	P	21/07/93			46,XY,+21c/46,XY ^d	CD33+ CD34-	83.2
	R	10/07/95		719	ND	CD33+ CD34-	95.0
2	P	22/10/93			46,XX	CD33+ CD34-	93.3
	R	30/08/94		312	ND	CD33+ CD34-	91.8
3	P	08/04/94	32		46,XX,del(7)(q33q36),del(16)(q22q22)	CD33+ CD34+ / CD33+ CD34-	26.1 / 39.1
	R	09/01/95	33	276	46,XX	CD33+ CD34-	38.0
	2nd R	05/11/99	38	2037	ND	CD33+ CD34+	41.5
4	P	09/06/94			46,XX	CD33+ CD34-	89.5
	R	01/06/95		357	ND	CD33+ CD34-	94.2
5	P	09/04/98	37		46,XY[20]	CD33+ CD34-	96.5
	R	10/12/99	38	610	46,XY[20]	CD33+ CD34-	91.8
6	P	17/01/94	44		46,XX,del(3)(p1?p2?)/46,XX	CD33+ CD34-	98.3
	R	09/09/94	45	235	46,XX	CD33+ CD34-	50.6

Table 7.1. Selected features of matched presentation and relapsed AML patient samples included in this study.

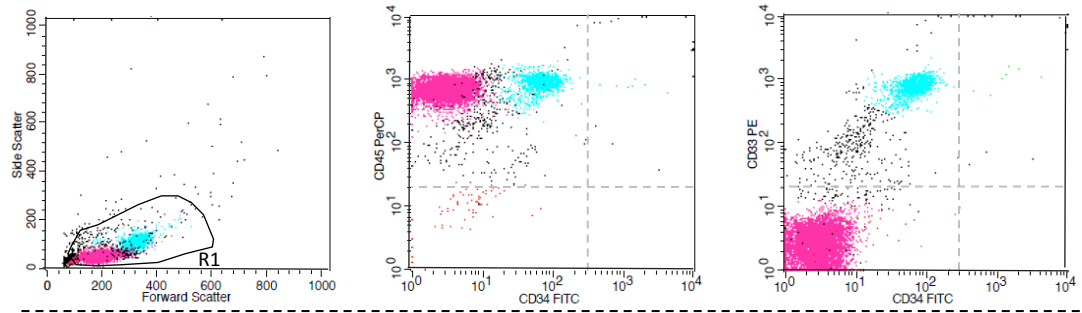
^a P, Initial disease presentation; R, relapsed disease.

^b ND, not determined.

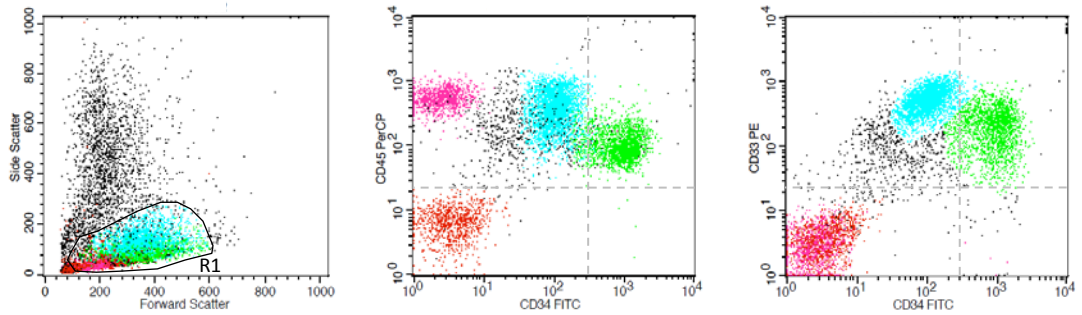
^c Expressed as a percentage of viable cells, determined by flow cytometry.

^d +21c in the karyotype of this patient refers to constitutional trisomy 21 (Down syndrome).

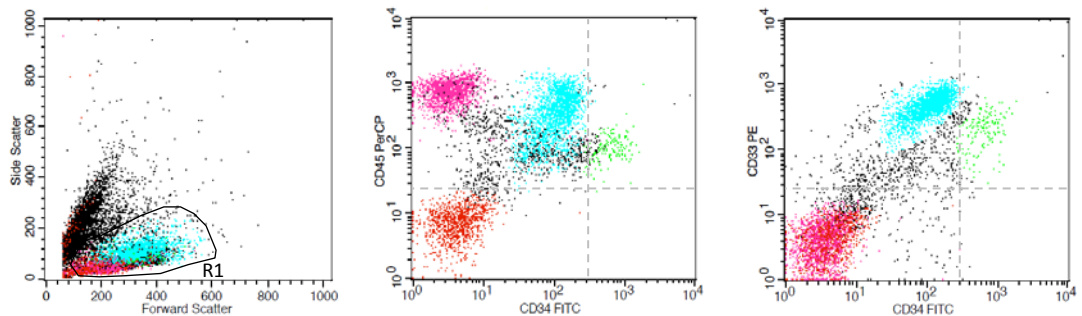
NORMAL PERIPHERAL BLOOD



PRESENTATION



1ST RELAPSE



2ND RELAPSE

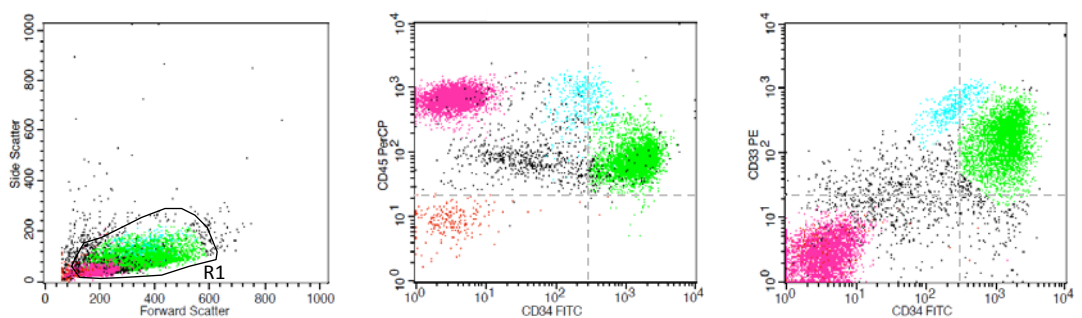


Figure 7.2. Immunophenotyping of leukaemic blasts in peripheral blood at presentation and relapse in AML patient 3.

In each case, 10,000 cells were assessed for expression of CD33, CD34 and CD45 via flow cytometry. Viable cells were identified based on forward scatter and side scatter properties (left plots; R1 gate). Negative CD45 expression (centre plots) was used to identify any contaminating red blood cells (red). Normal blood leukocytes were positive for CD45 expression but negative for both CD33 and CD34 (pink). Leukaemic blasts were identified based on positive expression of CD33 and/or CD34 (right plots). Blast percentages are shown in Table 7.1 and described in the text. Dashed lines indicate cutoff for positive expression of each marker, determined based on analysis of fluorochrome-conjugated isotype controls (data not shown).

Two apparent blast populations were identified at presentation in patient 3 (Figure 7.2) and SNP array analysis was performed independently on each cell population. CD33+CD34+ blast cells were isolated initially using CD34 microbeads, following which the CD33+CD34- cells were isolated from the remaining population using CD33 microbeads. At first relapse, all blasts were CD33+CD34-, whereas at second relapse, all blasts were CD33+CD34+ (Figure 7.2), providing preliminary evidence that the two observed relapses in this patient were due to emergence of different cell clones. In both cases, initial blast percentages were below 85% (see Table 7.1) and so were subsequently isolated using CD33 microbeads.

7.2.3. Copy Number Abnormalities

After exclusion of changes in copy number which likely represent constitutional genetic variation (see Section 2.13.2), a small number of apparently somatic CNAs were detected in 4 of the 6 AML patients (Table 7.2). The majority of CNAs were trisomies of the detected region (copy number 3), ranging in size from 103.1kb (13q32.1; patient 1) and affecting a single gene, to 74.5Mb, representing the majority of a whole chromosome and affecting approximately 430 genes (Chr14; patient 3). The remainder, with the exception of a complex abnormality of chromosome 17p in patient 3 (see below), were monosomies of the detected region (copy number 1), and ranged in size from 1.1Mb (16q22.1, containing 48 genes; patient 3) to 15.5Mb (3p14.1-p12.1, 15 genes; patient 6). Several alterations were common to both presentation and matched relapse, although there were also examples of alterations unique to presentation or relapse (Table 7.2).

In the case of patient 1, the CNA affecting chromosome 21 (copy number 3) correlated with the reported karyotype (constitutional trisomy 21). The same CNA was detected in the relapse sample, consistent with constitutional trisomy 21 in this patient, although karyotype had not been formally determined. All other CNAs detected in this patient using SNP arrays were too small to be detected cytogenetically (also the case for the CNA detected at presentation in patient 2).

Patient ID	Chromosome	PRESENTATION				RELAPSE			
		Band	Copy Number	Length (Mb)	No. Genes ^a	Band	Copy Number	Length (Mb)	No. Genes ^a
1	6	<i>ND^b</i>				q25.3	3	0.3	0 ^c
	12	q13.3	3	0.1	6	<i>As presentation</i>			
	13	q32.1	3	0.1	1	<i>As presentation</i>			
	21	pter-qter	3	46.9	~220	<i>As presentation</i>			
2	15	q25.3	3	0.4	3	<i>As presentation</i>			
3	7	q33 – q36.1 ^d	1	14.9	139	<i>ND</i>			
	14	<i>ND</i>				q12 – q32.33 ^e	3	74.5	~430
	16	q22.1 ^d	1	1.1	48	q22.1 ^f	1	1.1	48
	17	<i>ND</i>				pter – p13.1 ^e	1	8.1	196
	17	<i>ND</i>				p13.1 ^e	4	1.1	15
	17	<i>ND</i>				p13.1 – p12 ^e	3	3.0	19
6	3	p14.1 – p12.1	1	15.5	15	<i>As presentation</i>			

Table 7.2. Regions of detected copy number abnormality in AML patients at presentation and relapse.

^a Estimated based on current RefSeq collection.

^b ND, not detected.

^c This region was also searched for known micro RNA genes and was found not to contain any.

^d Detected in both blast populations at presentation.

^e Detected at second relapse only.

^f This CNA was detected at 2nd relapse (but not 1st relapse), however reported breakpoints were slightly different to those at presentation, suggesting it might be an independent CNA (see text).

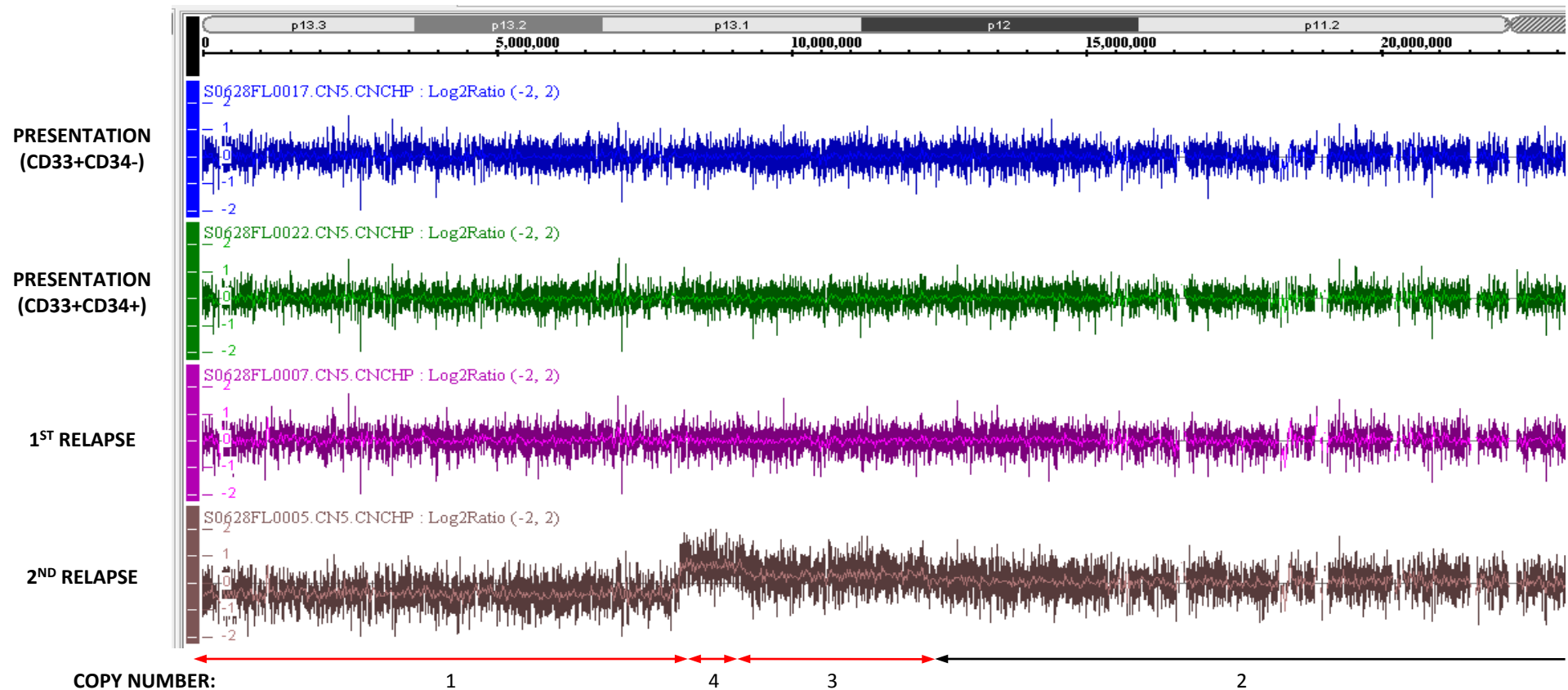


Figure 7.3. Complex copy number abnormality of chromosome 17 (pter – p12) at second relapse in AML patient 3.

Shown is a screen print taken from Genotyping Console software, demonstrating copy number analysis of chromosome 17p in presentation and relapse samples from AML patient 3. Displayed is the copy number profile of chromosome 17p (see ideogram at top of screen print) for each sample in the form of log₂ ratio at each marker. This is calculated by the software for every marker (SNP or copy number probe) as log₂ of the signal intensity in the sample divided by the mean signal intensity of all normal samples at that particular marker. Regions of copy number variation are determined from the log₂ ratios using segmentation algorithms. Regions of copy number abnormality reported at second relapse are represented by the annotation below the screen print.

CNA of chromosome 3 at presentation and relapse in patient 6 correlated with the reported karyotype at AML presentation (del(3)(p1?p2?)), although at relapse, a normal karyotype was reported. In the case of the relapse sample, the blast percentage determined by immunophenotyping was 50.6% (see Table 7.1), furthermore the blast population at relapse might have been heterogeneous (as reported at presentation), suggesting that cells with the deletion could have been missed during karyotypic analysis which only analyses 20 cells.

For patient 3, CNA of chromosome 7q (copy number 1) detected at presentation was consistent with the reported karyotype (del(7)(q33q36)). Additionally, a region of monosomy was detected at 16q22.1 in both blast populations at presentation (consistent with karyotype, del(16)(q22q22)) and also at second relapse (karyotype not determined). In both presentation clones, the breakpoints discerned for this region were identical, however at second relapse the breakpoints differed slightly from those at presentation, resulting in a shorter reported region (approximately 28kb shorter). It is possible therefore, that the 16q22.1 abnormality at second relapse is distinct from that detected at presentation, as discussed below. The complex 17p abnormality detected in patient 3 at second relapse involved a region of monosomy, as well as regions of trisomy and tetrasomy (copy number 4) (Figure 7.3). It is likely that this is the result of a complex chromosomal rearrangement, although this could not be confirmed without the karyotype. Alternatively this may also represent clonal heterogeneity within the blast population, as suggested above. Copy number gain was also reported for the majority of chromosome 14 at second relapse, suggesting a cytogenetically-detectable abnormality of this chromosome was also present.

Although the primary focus of this pilot study was investigation of clonal evolution, a brief search of the genes in regions affected by CNA was performed in order to identify any potential candidate genes involved in AML pathogenesis. Of particular interest given the focus of this research project was whether any DNA MMR genes were affected by CNA or cn-LOH. However, no DNA MMR genes, nor any genes which have been previously associated with AML were identified in regions of CNA at either presentation or relapse, with the exception of heterozygous loss affecting the *TP53* gene (17p13.1) in patient 3 at second relapse. Interestingly, a number of genes involved in other DNA repair pathways were also found within CNA regions in patient 3

at second relapse. These were heterozygous gain affecting *ATXN3* (nucleotide excision repair), *RAD51L1* and *XRCC3* (both DSB repair), and heterozygous loss affecting *RPA1* (involved in several DNA repair pathways). It is possible therefore, that defects in DNA repair which could affect response to DNA-damaging cytotoxic therapies may have contributed to the development of the second relapse in this patient.

Abnormalities affecting genes involved in drug transport and/or metabolism may represent one factor contributing to the development of relapsed AML through acquisition of chemoresistance. Therefore, regions of CNA were also interrogated for genes implicated in drug resistance (genes encoding multidrug transporters and drug metabolising enzymes) as well as those specifically associated with intracellular metabolism of Ara-C (see Section 1.5.3 for details of these pathways), but none were found in any of the patients studied.

7.2.3.1. Putative Focal CNAs

In addition to the abnormalities listed in Table 7.2, which were identified automatically using Affymetrix Genotyping Console software, a more detailed manual interrogation of the raw data was performed to identify any CNAs which might affect key genes involved in either leukaemogenesis or drug resistance. A small number of putative focal abnormalities were observed; the most significant in terms of this project being a region of monosomy incorporating the *MSH3* gene (5q14.1) at relapse in patient 6. This region was approximately 9.5kb in length and spanned exons 2 and 3 of *MSH3*. In addition, a small (0.3kb) region of tetrasomy was detected within exon 6 of the *BRCA1* gene (17q21.2) at second relapse in patient 3, again potentially implicating defective DNA repair in development of the late relapse in this patient. It is important to note in both cases that these abnormalities affected only a small number of markers and therefore escape detection by the algorithms used by the Genotyping Console software. Confirmation of their presence in individual patients by another method, such as fluorescence in situ hybridisation (FISH), is therefore required.

7.2.4. Copy-Neutral Loss of Heterozygosity

In addition to defining CNAs, an analysis of regions of cn-LOH was also performed by comparison of the SNP genotypes of individual samples to pooled reference samples from the International HapMap project. Using this method of analysis, regions of cn-LOH were frequently observed in AML patients, with a mean of 71.1 and 70.7 cn-LOH regions detected throughout the genome at presentation and relapse, respectively. Given that LOH analysis was performed using pooled reference samples as opposed to matched reference material from the individual patients, it was not possible to confidently determine which of the detected regions were constitutional and which were specific to the leukaemic blasts. For this reason, only regions of cn-LOH which were unique to either the presentation or relapse samples were further analysed.

Regions of cn-LOH which were unique to either the presentation or relapse sample in individual patients are listed in Table 7.3. Size of detected cn-LOH regions ranged from 0.1Mb to 95.3Mb (median 1Mb); the largest region representing cn-LOH of the majority of chromosome 13. In combination with the detected regions of CNA, these regions can be used to estimate the possible clonal origins of relapse in each patient. In addition, regions of cn-LOH acquired at relapse might contain mutated duplicated genes or unmask recessive mutations that could contribute to the development of relapsed AML. For instance, acquisition of cn-LOH of chromosome 13, which was observed in 2 patients in this study, has previously been associated with the generation of homozygous *FLT3* (13q12) mutations via recombination-mediated gene duplication of a single copy (Raghavan et al., 2008). Candidate genes in regions of acquired cn-LOH which may warrant further investigation for mutational status include *FLT3* (patients 2 and 4), and the DNA repair genes *BRCA2* (13q12.3; patients 2 and 4), *ERCC5* (13q33.1; patients 2 and 4) and *LIG4* (13q33.3; patients 2 and 4).

Patient ID	Chromosome	PRESENTATION			RELAPSE		
		Band	Length (Mb)	No. Genes ^a	Band	Length (Mb)	No. Genes ^a
1	1	p35.2 - p35.1	1	22		<i>ND</i> ^b	
	1	p34.3	0.6	11		<i>ND</i>	
	1	p12	0.2	3		<i>ND</i>	
	2	q22.3	1.5	6		<i>ND</i>	
	3	q11.2	0.7	1		<i>ND</i>	
	3		<i>ND</i>		q13.13	1	1
	4	q12	1	0		<i>ND</i>	
	4		<i>ND</i>		q13.2	0.3	5
	4	q13.2	0.7	5		<i>ND</i>	
	4	q26	1.1	3		<i>ND</i>	
	4	q31.21	1.6	7		<i>ND</i>	
	5	p15.1	1.2	2		<i>ND</i>	
	5	q13.3	1	5		<i>ND</i>	
	6	p21.33	0.9	31		<i>ND</i>	
	6	q12	1.2	1		<i>ND</i>	
	6		<i>ND</i>		q12	1.2	2
	6	q22.31	1.2	5		<i>ND</i>	
	7		<i>ND</i>		q22.1	1	20
	8		<i>ND</i>		q24.3	0.1	6
	10		<i>ND</i>		q22.3	1	9
12	q21.31	1.1	0		<i>ND</i>		
13	q21.1	1.1	0		<i>ND</i>		
16		<i>ND</i>		p12.2	1	8	
16		<i>ND</i>		p11.2	1.1	0	
17		<i>ND</i>		q25.1	1	33	
18	q11.2	1.2	6		<i>ND</i>		
2	13		<i>ND</i>		q12.11 - qter	9.4	~280
	17	q21.2	1.3	62		<i>ND</i>	
3	1		<i>ND</i>		q43 ^f	1	3
	2		<i>ND</i>		p12 ^g	1	0
	2		<i>ND</i>		p12 ^h	1	0
	2		<i>ND</i>		q11.2 ^g	0.3	8
	5		<i>ND</i>		p14.2 ^g	1.2	1
	6		<i>ND</i>		q13 ^g	1.2	7
	7		<i>ND</i>		q11.23 ^f	1.9	19
	7	q34 ^c	1.4	13		<i>ND</i>	
	8	p11.21 ^d	0.4	5		<i>ND</i>	
	8	q21.2 ^e	1	9		<i>ND</i>	
	10		<i>ND</i>		q11.22 ^f	1.6	8
	12		<i>ND</i>		q12 ^f	1	5
	14		<i>ND</i>		q32.33 ^h	0.4	8
	16		<i>ND</i>		p12.2 ^g	1	8
	19		<i>ND</i>		p12 ^g	2	9
	X		<i>ND</i>		p11.3 ^f	1	12
	X		<i>ND</i>		p11.23 ^g	1.2	42
X		<i>ND</i>		q13.1 ^g	2.1	11	

Table 7.3. Regions of detected copy-neutral LOH in AML patients at presentation and relapse (continued on next page).

Patient ID	Chromosome	PRESENTATION			RELAPSE		
		Band	Length (Mb)	No. Genes	Band	Length (Mb)	No. Genes
4	1	p12	0.1	1	ND		
	2	p15	0.8	4	ND		
	7	p11.2	1	11	ND		
	7		ND		q11.23	0.9	15
	13		ND		q12.11-qter	95.2	~300
	15		ND		pter-q11.2	20.3	6
	X	p21.1	1.1	7	ND		
5	1		ND		q25.3	1.1	5
	2		ND		q33.1	1.1	9
6	10		ND		q11.23	1	11
	16		ND		p11.2	0.1	0

Table 7.3. Regions of detected copy-neutral LOH in AML patients at presentation and relapse (continued from previous page).

^a Estimated based on current RefSeq collection

^b ND, not detected.

^c Detected only in CD33+CD34+ blast population at presentation

^d Detected in both blast populations at presentation

^e Detected only in CD33+CD34- blast population at presentation

^f Detected at both first and second relapse

^g Detected at first relapse only

^h Detected at second relapse only

7.3. Discussion

Despite being of limited size, this study demonstrates that the pattern of clonal evolution of relapsed AML likely shares some similarities with ALL, with respect to the origins of clones responsible for relapsed disease. In all patients studied there was clear evidence of a relationship between the presentation and relapse AML samples. In two cases (patients 5 and 6), relapse appeared to represent clonal evolution of the major presentation leukaemic clone. This is illustrated in the case of patient 6 (Figure 7.4A) in which all abnormalities detected at presentation were also present at relapse, but were accompanied by the acquisition of further regions of cn-LOH unique to the relapse clone.

In three cases (patients 1, 2 and 4), the presence of abnormalities at diagnosis but not at relapse suggests that, rather than evolving directly from the major presentation clone, the relapse clone was derived from an ancestral, pre-leukaemic clone which also gave rise to the major clone at presentation. This is illustrated in the case of patient 1 in Figure 7.4B. In this case, the acquisition of a large number of regions of cn-LOH unique to the relapse clone (as well as a unique region of CNA; see Table 7.3 and Table 7.2, respectively) could suggest evolution from a particularly early ancestral clone. Alternatively, it is possible that relapse evolved from a minor leukaemic clone at presentation that was not detected using SNP arrays, which are limited in their scope to identify such low frequency clones.

For the remaining patient (patient 3), in which first relapse was followed 4.8 years later by a second relapse, the available evidence suggests that at least one of the relapses is in fact independent from the initial presentation disease. Based on immunophenotypic and cytogenetic data (Table 7.1) in combination with detected CNAs (Table 7.2), it appears that the second relapse in this patient was derived from an ancestral clone which also gave rise to both presentation clones (Figure 7.4C i). Given that the clone detected at first relapse does not demonstrate any cytogenetic or CN abnormalities, this suggests it to be an independent AML (or it could be derived from a very early clone prior to acquisition of any numerical abnormalities). Addition of the cn-LOH data (Table 7.3) however suggests a different model. The observation of a number of regions of cn-LOH which are common to both relapses, but not observed in

either presentation clone, suggests that both relapse clones in fact share a common ancestor and are both semi-independent of the initial presentation AML (Figure 7.4C ii). In this case, the 16q CNA detected at second relapse must have occurred completely independently in initial presentation disease and second relapse. Consistently, independent acquisition of the same abnormality in two or more clones has been demonstrated in ALL (Anderson et al., 2011). Also consistent with this model, the breakpoints of the 16q CNA at second relapse in patient 3 were slightly different to those reported at presentation (which were identical in both presentation clones), suggesting it to be derived from an independent event. Sequencing of the breakpoints is required to confirm whether the presentation and relapse 16q CNAs are in fact unique.

It is not clear from this analysis whether the abnormalities specific to relapse in these patients were already present in a minor clone at AML presentation and selected for at relapse, or whether they were acquired as new genomic alterations subsequent to initial therapy. This again highlights a caveat of the use of SNP arrays in the study of CNAs in that the results reflect predominant cell populations and fail to detect alterations in minor, less abundant clones, as suggested above. Approaches designed to detect alterations at low frequency, or even in single cells, could be used to further determine the temporal acquisition of specific lesions, and whether they developed as a consequence of cytotoxic therapy. In the aforementioned study performed in ALL (Mullighan et al., 2008), lesion-specific PCR assays provided evidence for the existence of the relapse clone at diagnosis in the majority of samples, suggesting presence of this clone as a minor subpopulation at initial disease presentation. Further extension of this work, in which the presence of multiple CNAs was investigated in single cells (using FISH), demonstrated considerable genetic heterogeneity of clones at ALL presentation (Anderson et al., 2011), therefore providing a rich, genetically diverse population from which disease can progress. It is possible that a similar scenario exists in AML, although currently this is more difficult to establish given that relatively few CNAs are identified in AML (Radtke et al., 2009; Walter et al., 2009). Clonal heterogeneity, if confirmed in AML, will likely have therapeutic implications, in particular in the use of targeted therapies, as will be described in Chapter 8.

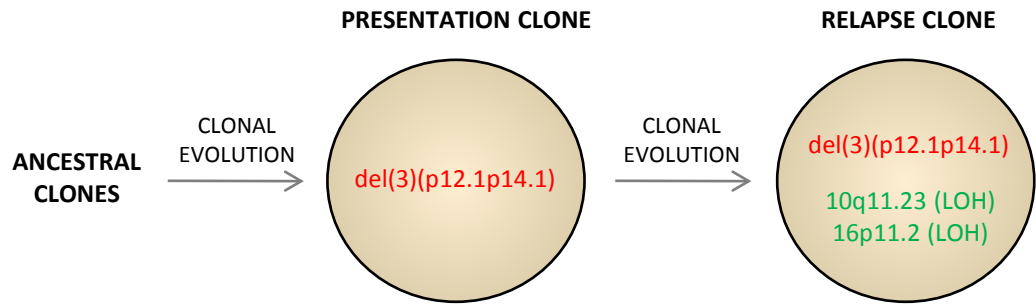
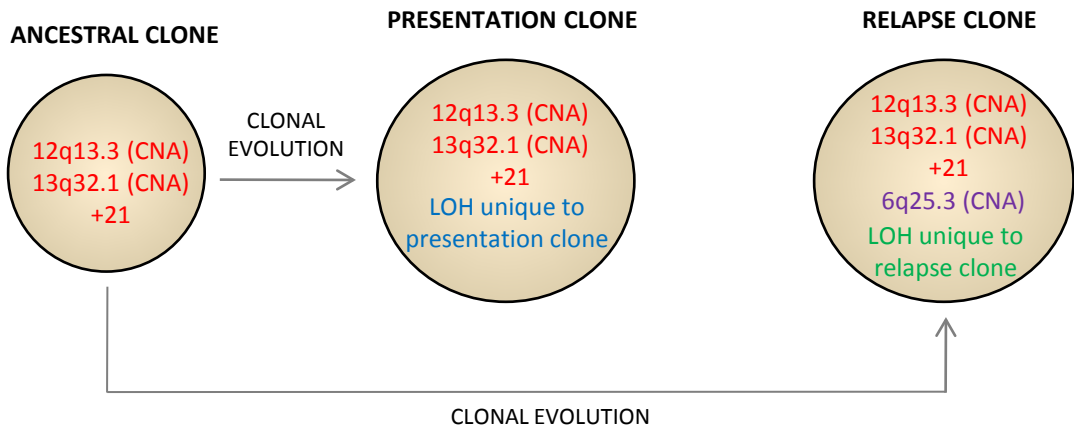
A**B**

Figure 7.4. Clonal evolution of relapse in AML patients (continued on next page).

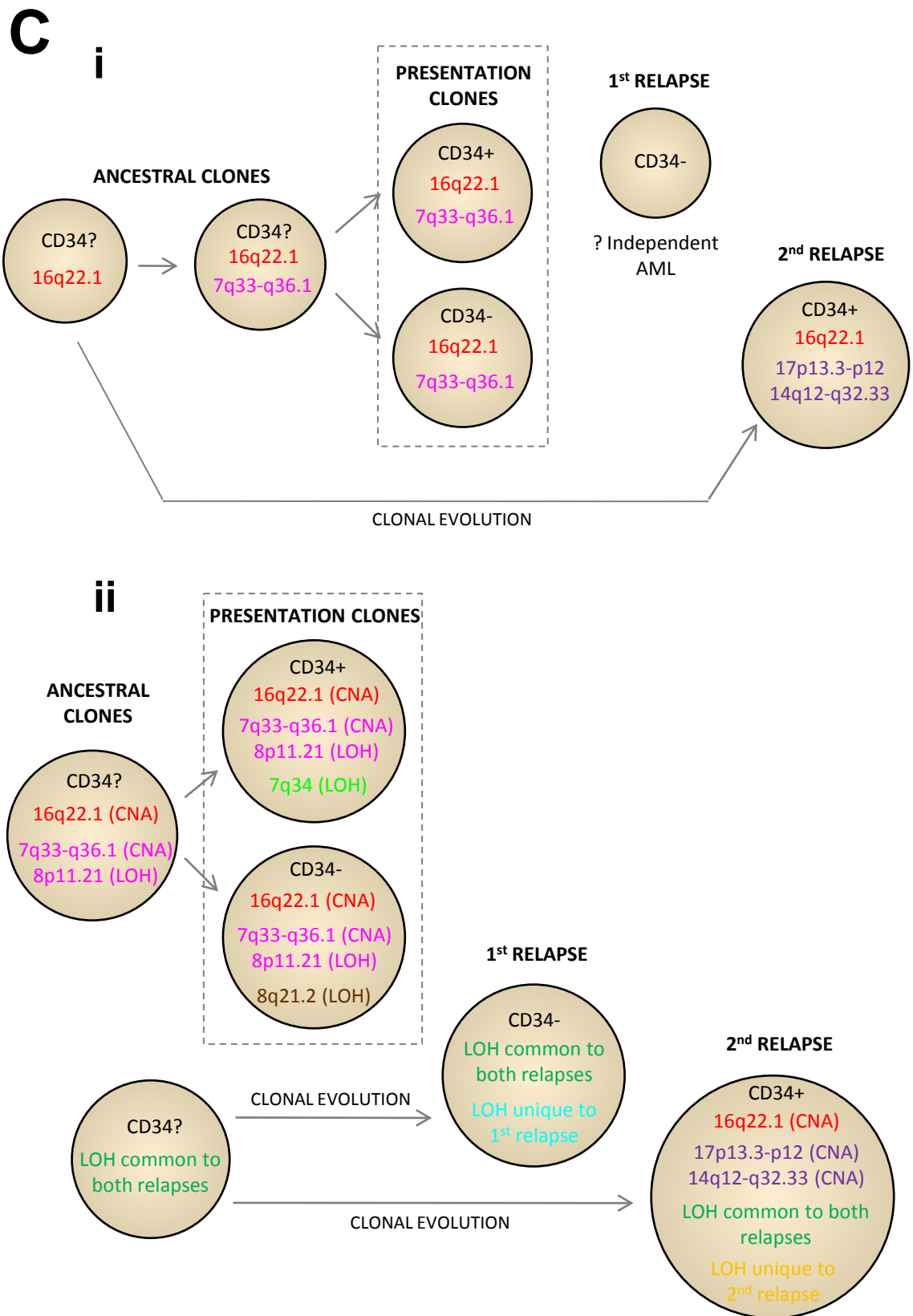


Figure 7.4. Clonal evolution of relapse in AML patients (continued from previous page).

A. Evolution from the major clone detected at presentation (patient 6).

B. Evolution from an ancestral clone not detectable at disease presentation (patient 1).

C. Evolution from an independent clone (patient 3). Pathways are described in the text.

Delineating the clonal origins of relapsed AML only represents one part of the complete picture of how and why relapse occurs. Understanding mechanisms which promote clonal expansion is an equally important goal. For example, mutagenic therapy can initiate leukaemogenesis leading to t-AML (see Section 1.4.1.1), but also probably plays a role in promoting relapse following treatment for *de novo* disease. For some malignancies, relapse can be attributed in large part to the acquisition of generalised drug resistance mechanisms, such as overexpression of membrane efflux pumps (drug transporters) resulting in reduced intracellular levels of multiple chemotherapeutic agents (Choi, 2005). Likewise, in AML, reduced intracellular levels of Ara-CTP are associated with clinical resistance to Ara-C (Galmarini et al., 2002; Cros et al., 2004), demonstrating that the Ara-C metabolic pathway is closely related to Ara-C resistance. Furthermore, in freshly isolated blast samples from AML patients, a low cellular content of membrane-bound nucleoside transporters is correlated with Ara-C resistance (Gati et al., 1997). Taken together, these data suggest that AML relapse could be due, at least for some patients, to acquired resistance to Ara-C through genetic aberrations affecting genes associated with intracellular transport and/or metabolism. Larger studies will be required to identify all mechanisms responsible for promoting disease relapse. Furthermore, it is also important to consider that aberrations detected in this study (CNAs) represent only one type of genetic alteration; genome sequencing analysis (see below) coupled with analysis of gene expression and epigenetic changes will also be important requirements for understanding mechanisms contributing to development of relapsed as well as therapy-related AML.

Although only a small number of patients were analysed in the current study, the findings suggest that the occurrence of CNAs is not a prominent feature of AML. This is in agreement with previous studies in which CNAs were identified in only 50-60% of patients at presentation, with a mean of 2.3 CNAs per genome (Radtke et al., 2009; Walter et al., 2009). The observation of MSI in a subset of relapsed AML patients (Ohyashiki et al., 1996; Tasaka et al., 1997) suggests that acquisition of a genomic instability phenotype, possibly induced by the effects of chemotherapy (similar to methylating agent-related t-AML), could be one of the mechanisms promoting clonal expansion leading to relapsed disease. If this was the case, AML clones at relapse might be expected to demonstrate an increase in CNAs relative to genomically stable

clones at presentation. In this study, a similar number of CNAs were observed at relapse relative to initial disease presentation, which would argue against this form of genomic instability as a major contributing mechanism. Furthermore, no confirmed abnormalities affecting DNA MMR genes were identified in these patients, which would confer a mutator phenotype. However, it should be noted that the SNP array approach cannot detect copy-neutral DNA mutations which may also affect gene function, such as base substitutions, hence a mutator phenotype cannot be excluded in these patients. Indeed, base substitution and gene silencing are the primary mechanisms of DNA mismatch repair gene inactivation. It remains possible that MSI+ relapsed AML are incorrectly classified as relapsed disease, and are in fact cases of t-AML arising from a completely independent cell of origin, similar to the scenario suggested in ALL (Mullighan et al., 2008). Further interrogation of the clonal origins of apparent MSI+ relapsed AML would provide valuable clues as to whether such cases are *bona fide* relapse, and whether genomic instability represents a mechanism contributing to relapse in AML.

Data from this pilot study suggest that larger and more extensive investigations of the clonal origins of relapse in AML are warranted. Indeed, it is now planned to extend this study to include more patients and to perform 'ultra deep' exomic sequencing using high-throughput pyrosequencing to further delineate the clonal relationships of presentation and relapse in AML. This so-called 'next generation' approach will be employed to sequence the entire exome of the leukaemic blast population at presentation and relapse in each patient, enabling detection of DNA point mutations and small insertions/deletions acquired at relapse. However, rather than sequencing pools of DNA templates, as is the case in conventional sequencing approaches, 'ultra deep' sequencing allows simultaneous sequencing of individual molecules of DNA (termed massively parallel sequencing), meaning abnormalities present at very low levels (in as few as 1% of cells, depending on level of coverage achieved) can be detected. The proof of principle of this approach has been demonstrated by the publication of the sequences of two AML genomes at presentation, which enabled identification of novel mutations which might contribute to AML pathogenesis (Ley et al., 2008; Mardis et al., 2009). The planned exomic sequencing of matched presentation and relapsed AML samples will permit extension of these findings, enabling identification of mutations potentially responsible for

development of relapse in individual patients. Additionally, this approach will allow investigation of the genetic heterogeneity of AML at both presentation and relapse (which is not possible using SNP array, as discussed above), providing further insights into the origins of relapse-initiating clones.

7.3.1. Summary of Chapter

In conclusion, this pilot study has demonstrated the following:

- Clonal evolution leading to relapse in AML shares similarities with ALL in that, for the majority of cases, relapse represents evolution from ancestral pre-diagnosis clones, and does not often evolve directly from the dominant clone at disease presentation.
- Although yet to be formally confirmed, the presence of low numbers of relapse-initiating clones at initial presentation has implications for the use of targeted therapeutic approaches in AML.
- Larger studies and alternative approaches (e.g. deep sequencing) are required to fully delineate the heterogeneity of AML and disease evolution from diagnosis to relapse.

Chapter 8. Concluding Discussion

8.1. DNA MMR Dysfunction and Chemoresistance in t-AML

The poor survival of patients with t-AML is a function of multiple competing risks, including persistence of the primary malignancy, organ dysfunction from prior therapies, prolonged immunocompromised status, patient age, and lack of uniform treatment (Smith et al., 2003; Godley and Larson, 2008). Chemoresistance is also likely to be a significant contributing factor, particularly in the case of methylating agent-related t-AML, given the probable origin of the condition, in many cases, from a population of DNA MMR-defective, genomically unstable cells selected (or initiated) due to tolerance to cytotoxic therapy (see Section 1.4.1.1). Furthermore, associations between DNA MMR dysfunction and adverse treatment response have been highlighted in other malignancies in which MMR defects are commonplace. For instance, defective DNA MMR has been associated with poor response to 5-FU therapy in colorectal cancer patients (Ribic et al., 2003; Carethers et al., 2004; Jover et al., 2006), although the contribution of other repair pathways is not clear. Despite the possibility that DNA MMR-mediated chemoresistance may be operating in t-AML, there have yet to be any *in vitro* or *in vivo* investigations aimed at elucidating an association between DNA MMR status and response to routine chemotherapeutic regimens used in t-AML treatment, of which nucleoside analogues form the backbone.

Through the use of MMR-proficient and MMR-dysfunctional cell line models (widely available, extensively studied cell line pairs, as well as others generated specifically for use in this project using gene knockdown), this study has provided the first evidence that DNA MMR status affects response to nucleoside analogues in routine use for the treatment of t-AML, including Ara-C, clofarabine and fludarabine. Notably, the investigations herein (Chapters 3 and 4) demonstrate that apparent defects of MSH3, and hence the MutS β complex, confer tolerance to the cytotoxic effects of these nucleoside analogues, suggesting that chemoresistance due to MSH3 defects could represent a potential factor contributing to poor outcome in t-AML patients.

The detailed mechanisms underlying the observed phenotypes remain to be fully elucidated, and the postulated roles for DNA MMR components in cellular response to nucleoside analogues (described in Section 3.3) should be formally investigated. One thing which remains particularly unclear is how two apparently opposing defects in

MMR (i.e. loss of MSH3 due to gene knockdown, or overproduction of MSH3 due to genetic amplification; Sections 3.2.6 and 4.2.2 respectively) give rise to the same drug tolerant phenotype, but only when the function of the MutS α complex is unperturbed (see below). This particular finding suggests multiple roles for DNA MMR components in mediating response to chemotherapy-induced DNA damage, and possible effects on other cellular functions, including other DNA repair activities. Further work will be required to delineate these mechanisms.

8.2. Exploitation of DNA MMR Dysfunction to Improve Therapeutic Outcome

Given the identification of DNA MMR defects as a possible causative factor in an increasing repertoire of malignancies, an important goal is the identification of current chemotherapeutic agents (or indeed the development of novel agents) which are selectively toxic to MMR-defective cells. Some examples have already been highlighted, of particular note the cytidine nucleoside analogue gemcitabine, which is differentially cytotoxic to MSH2 or MLH1-deficient colorectal carcinoma cells relative to wild type counterparts *in vitro* (Takahashi et al., 2005).

In the present study, defects of the MutS α complex resulted in a moderate increase in sensitivity to nucleoside analogues, relative to MMR-proficient parental counterparts (Chapter 3). Furthermore, this response appeared to override any effects of MutS β dysfunction in cells in which the formation of both MutS α and MutS β complexes were perturbed. A number of nucleoside analogues are currently being trialled in AML treatment, many with favourable results in t-AML patients and other historically poor prognosis patient groups (see Section 1.3.2.2). The findings herein could help to explain the favourable responses observed in these patients. Notably, clofarabine is being used successfully in the treatment of elderly AML, a subgroup also associated with increased incidence of MSI and putative DNA MMR dysfunction (Das-Gupta et al., 2001). This investigation suggests the generally favourable response observed in these patients might be due, in part, to DNA MMR status, although increased tolerance of the drug due to its favourable toxicity profile is also likely a contributory factor (see Section 1.5.4).

Defects in DNA MMR components could also impact on other cellular functions and other DNA repair pathways, some of which could be exploited for patient benefit.

For example, DNA MMR dysfunction can affect HRR (Worrillow and Allan, 2006), although the precise role of specific MMR components has yet to be fully determined. Defects in DNA repair function suggests the possibility of using a so-called 'synthetic lethality' approach in treatment of MMR deficient t-AML patients, in which inhibitors of other DNA repair pathways are used to potentiate the effects of DNA damaging agents. This approach has already been used successfully in the treatment of solid cancers, such as breast cancer (Calvert and Azzariti, 2011). PARP-1 is an enzyme involved in the BER pathway, the activity of which can be blocked using various small molecule inhibitors. Inhibition of PARP-1 *in vitro* has previously been shown to be selectively toxic to MMR deficient cells when used in combination with the chemotherapeutic methylating agent, temozolomide (Curtin et al., 2004). In MMR proficient AML patients, the possibility exists of developing small molecule inhibitors of DNA MMR components which could be used in combination with inhibitors of other DNA repair components, such as PARP-1, to increase the efficacy of established genotoxic DNA damaging chemotherapeutic agents. Therapeutic approaches aimed at disrupting DNA MMR components however, will need to be used with caution due to their potential to increase mutation frequency. Such an effect in either leukaemic or non-leukaemic cells could promote the development of relapsed or t-AML, respectively, particularly if mutagenic nucleoside analogues are also included in treatment (see Section 8.4, below). Evidence suggests that exposure to agents that interact with DNA MMR (notably methylating agents and 6-TG), although highly effective at eradicating malignant cells, can promote emergence of genomically unstable DNA MMR defective sub-clones with a mutator phenotype (described in Section 1.4.1.1). The use of agents which specifically disrupt DNA MMR function could have a similar effect and should therefore be used with caution.

8.3. Detection of DNA MMR Defects in t-AML Patients

Given the potential for DNA MMR defects to influence outcome and/or direct therapeutic choice, retrospective or prospective studies aimed at detection of specific DNA MMR defects and their potential association with treatment response in t-AML patients are warranted. A small number of studies have previously demonstrated mutations in *MSH2* in t-AML patients (Horiike et al., 1999; Zhu et al., 1999). Similarly there have been some reports of aberrations affecting *MLH1* expression (Casorelli et

al., 2003). A putative deletion within the *MSH3* gene was observed at AML relapse in this study (Chapter 7), although whether aberrations affecting other MMR components, in particular *MSH3*, occur in t-AML remains to be determined. Importantly, such studies would also determine whether specific DNA MMR abnormalities affect leukaemic blast cell response to clinically relevant concentrations of nucleoside analogues *in vivo*, as suggested by the *in vitro* findings herein.

Translation of these findings into routine clinical practice would require an appropriate method for screening MMR defects at disease presentation. Observation of MSI at certain microsatellite markers is used as a biomarker of defective MMR in HNPCC (Umar et al., 2004), however the results herein suggest this would not be suitable in AML patients, given that it does not discriminate between different abnormalities which might be associated with different treatment responses. Gene expression profiling of DNA MMR genes is a second possibility, although this will fail to identify mutations which affect translation or protein function, but not gene expression. For example, bi-allelic mutation of *MSH6* in MT-1 results in lack of *MSH6* protein, but this is not detected using quantitative RT-PCR, as gene expression is unaffected (see Figure 3.2). Techniques which assess cellular levels of DNA MMR proteins, such as western immunoblotting, are also a possibility, although this approach is rarely used clinically given that a large amount of cellular material is required. Immunohistochemical staining has been demonstrated as a straight-forward and cost effective method of assessment of DNA MMR protein expression in colorectal cancer (Newton and Hill, 2010). A similar approach could be used for t-AML, especially since suitable material (bone marrow or peripheral blood smears) is already routinely prepared for assessment of cellular morphology at disease presentation. In the case of both techniques however, mutations which produce a non-functional protein might still be missed. Furthermore, protein expression levels may vary between individuals, requiring appropriate controls to be established. Next generation targeted DNA sequencing is currently being assessed in myeloid leukaemia patients as a means of mutation detection (Grossmann et al., 2011b; Grossmann et al., 2011a). Although this approach is in its infancy, it is possible that DNA MMR genes could form part of a panel of prognostically relevant genes routinely sequenced for mutations at disease presentation (if of course, recurrent mutations associated with treatment response are identified).

8.4. Chemotherapy Involving Nucleoside Analogues and Risk of t-AML Development

Several lines of evidence provided in this study suggest that nucleoside analogues used either alone, or in combination with agents known to interact with DNA MMR components, could result in risk of therapy-associated complications such as adverse treatment response and risk of relapse or t-AML development.

Data reported herein provide the first evidence that exposure to Ara-C is mutagenic to DNA (Chapter 6), demonstrating the potential genotoxicity of this agent and implicating Ara-C itself as a risk factor for the development of t-AML. A similar conclusion can also be drawn regarding fludarabine (see Section 6.3), which might partly explain why risk of developing t-AML is increasingly being associated with prior use of this drug (Coso et al., 1999; Morrison et al., 2002; McLaughlin et al., 2005; Carney et al., 2010). *In vivo*, if Ara-C-induced mutation occurred in a gene involved in haematopoietic regulation, it could contribute to the development of t-AML. Similarly, if a mutation occurred in a gene implicated in Ara-C resistance, such as one involved in cellular uptake or metabolism of the drug, this could increase the likelihood of relapse or development of treatment-refractory disease. Such a mutation might be responsible for the Ara-C-resistant cell lines generated in this project (Chapter 5), although this was not determined. Given the *in vitro* mutagenicity of Ara-C demonstrated in this study, an *in vivo* investigation into the genetic consequences of Ara-C chemotherapy is warranted and would provide important insight into the potential involvement of this and other nucleoside analogues in development of t-AML, as well as relapsed and/or refractory disease. Human T-cells containing mutations at the *HPRT* locus can be cloned directly from peripheral blood and investigations have demonstrated the *HPRT* locus as an efficient biomarker reflective of genome-wide somatic mutational events occurring in non-malignant cells (Albertini et al., 1993). Indeed, this approach has been used to investigate the *in vivo* mutagenicity of chemotherapeutic regimes for the treatment of ALL (Finette et al., 2000; Kendall et al., 2006), and could easily be recapitulated in AML patients receiving Ara-C chemotherapy.

As a result of treating myeloid cells with escalating doses of a methylating agent (Chapter 5), a cell line with reduced expression of MSH3 protein (and over-expression of MSH6) was generated, which demonstrated moderate tolerance to the cytotoxic effects of nucleoside analogues. Furthermore, *in vitro* mutation assay (Chapter 6)

demonstrated that mutability of Ara-C was enhanced in cells with defective DNA MMR. If a similar mechanism were operating *in vivo*, the therapeutic combination of a methylating agent with a nucleoside analogue could potentially result in an adverse treatment response and increased risk of relapse or t-AML development due to increased mutability. A similar phenotype might be expected in the case of simultaneous use of a thiopurine and a nucleoside analogue, given that these agents can also select for DNA MMR defects (Offman et al., 2004), although in the investigation herein, this was not observed. 6-Mercaptopurine, a 6-TG analogue with similar cytotoxic mechanisms, is used in combination with Ara-C in the treatment of children with ALL (Pui et al., 2011). Reports suggest that t-AML is a significant risk in survivors of ALL (Barnard and Woods, 2005), which might be a consequence of the combined use of a mutagenic agent with another agent that contributes strongly to genomic instability. Consistently, *HPRT* mutations are observed at an increased level in ALL patients (Kendall et al., 2006), although which particular agent(s) are responsible is presently unclear.

The use of agents which do not directly interact with DNA MMR components, but which could affect MMR function through a coincidental mechanism should also be used with caution if combined with agents that do specifically interact with the MMR pathway. A notable example of this is MTX, where exposure can lead to co-amplification of *DHFR* and *MSH3* loci (as described in Section 4.1). Children with ALL are routinely treated with MTX, in combination with 6-mercaptopurine and Ara-C, during the maintenance phase of chemotherapy (Pui et al., 2011). Concerns have previously been raised about using MTX and thiopurines in combination chemotherapy, given that co-resistance to both agents could be acquired due to gene amplification. The observation herein that *MSH3* overexpression (in HL-60R; Chapter 4) confers tolerance to the cytotoxic effects of Ara-C *in vitro*, suggests that Ara-C resistance *in vivo* should be considered as a potential risk of using this nucleoside analogue in combination with MTX in ALL treatment. However, the observation that TK6 MTX^R and PreB697 MTX^R, which were generated using clinically relevant concentrations of MTX (Matheson et al., 2007), were not differentially sensitive to Ara-C, relative to respective parental cell lines, argues against this being a significant clinical risk. Nevertheless, it is possible that additional selective pressure during long-term drug exposure could result in further amplification of these loci to an extent

where DNA MMR function is perturbed. Ara-C and MTX are also used in combination in the treatment of primary central nervous system lymphomas (Ferreri et al., 2009), and co-resistance to these agents through acquired gene amplification should also be considered a risk in this malignancy.

Genetic susceptibility determined by polymorphic variation can also affect risk of adverse therapeutic responses, and/or the risk of developing relapsed or therapy related malignancy. Of particular relevance to this work are studies which have identified polymorphisms in DNA MMR genes which may confer increased risk of t-AML development (described in Section 1.4.6). Susceptible individuals, at diagnosis of a primary malignancy, are particularly unlikely to be suitable for treatment with agents known to be mutagenic to DNA, including Ara-C. This highlights the importance of developing evidence-based personalised medicine, the goal of which is to prospectively identify patients more or less likely to respond favourably to particular therapies, in order to tailor therapeutic regimes appropriately. The aim of such an approach is to both improve initial treatment outcome, as well as minimise risk of therapy-related complications. Screening for common DNA MMR polymorphisms associated with increased risk of t-AML development may be warranted at diagnosis of a *de novo* malignancy, particularly in cases where frontline treatment involves the use of agents known to interact with the DNA MMR pathway.

8.5. Clonal Evolution and Clonal Heterogeneity in AML

A key recent investigation performed by Anderson et al., (2011) demonstrated for the first time that genetically distinct populations of leukaemia propagating cells are present at low levels at the time of leukaemia diagnosis that can survive chemotherapy and provide a reservoir for clonal expansion leading to relapse. The pilot study performed during this project (Chapter 7) provides evidence that similar clonal heterogeneity exists in the case of AML. Furthermore, these data also shed light on the evolution of relapsed AML, implicating transformation of an ancestral pre-leukaemic clone not part of the major clone at diagnosis. The planned extension of this study (as described in Section 7.3) will provide more detailed evidence for the clonal origins of these malignant complications. The demonstration of clonal heterogeneity of leukaemia, with the potential existence of relapse-initiating cell clones at disease presentation, could represent a significant roadblock to effective chemotherapy. For

instance, the use of an agent targeted towards a mutation present in a dominant clone could allow enrichment of minor (ancestral) clones which lack the mutation, and subsequently acquire further mutation leading to relapse. Advances in technology which allow cost effective and rapid whole genome analysis at the single cell level will be required to identify the full complexity of AML in individual patients at diagnosis in order to enable selection of the appropriate therapeutic agents to induce complete remission with minimal risk of subsequent relapse or therapy-related complications.

8.6. Summary of Findings

In summary, this project has demonstrated that cellular DNA MMR status mediates response to therapeutic nucleoside analogues routinely used in treatment of t-AML. *Ex vivo* studies are now warranted to investigate the occurrence of particular MMR defects in t-AML patients and whether they are associated with treatment response. For instance, in the case of t-AML, patients demonstrating loss of MSH2 in the leukaemic clone would be expected to respond favourably to therapeutic regimes containing nucleoside analogues. Similar treatment of patients with defects of MSH3 however could potentially result in an adverse treatment response. This will potentially assist development of personalised medicine, with the aim of improving treatment response in patient subgroups which currently do not respond favourably to conventional therapies. Additionally, the potential genotoxicity of Ara-C has been demonstrated, which highlights the possibility of an association with t-AML development, suggesting use of this agent in combination with other drugs known to select for DNA MMR dysfunction should be avoided. Finally, the likely clonal heterogeneity of AML at diagnosis, as well as clonal evolution of relapsed disease has been demonstrated. This not only has implications for selection and success of chemotherapy, but also suggests another factor which might contribute to poor therapeutic response in certain AML subgroups.

8.7. Future Directions

A number of further investigations are anticipated subsequent to the completion of this project:

8.7.1. MSH3 overexpression and tolerance to nucleoside analogues

The investigations detailed in Chapter 4 demonstrate that gross overexpression of *MSH3* in the HL-60R cell line confers tolerance to the cytotoxic effects of Ara-C and other therapeutic nucleoside analogues. As a follow up to this work, a further investigation is planned in which *MSH3*-stably overexpressing cells will be generated (from both HL-60 and TK6 cell lines) using a commercially available expression vector system. Cytotoxic response to nucleoside analogues will then be assessed relative to isogenic parental cells. It is predicted that this will recapitulate the Ara-C-tolerant phenotype of HL-60R cells and hence provide evidence that this response is a direct consequence of *MSH3* over-expression.

8.7.2. Ara-C-induced mutation spectrum in TK6 (MMR proficient) and TK6 MSH2i (MMR deficient) cell lines

Mutation screening in TK6 cells revealed that Ara-C can induce a spectrum of *HPRT* mutations which are unique compared to the spontaneous background mutation spectrum (see Chapter 6). Due to small numbers of independent mutations remaining after correction for possible clonal expansion, it is planned to generate a much larger number (n=50) of independently induced Ara-C mutants for inclusion in the drug-induced mutation spectrum. Additionally, it is anticipated that a similar investigation will be performed using the MMR-deficient TK6 *MSH2i* (or TK6 *MSH3i*) cell line generated herein, in order to determine whether DNA MMR status can influence the mutagenicity of Ara-C in terms of types of mutations induced.

8.7.3. Clonal evolution in relapsed and therapy-related AML

Chapter 7 describes the results of a pilot study in which patterns of clonal evolution were investigated (via SNP array analysis) in matched presentation and relapsed samples from a small number of AML patients. Based on the results of this study, it is now planned to extend the study and perform similar SNP 6.0 arrays on

further matched presentation and relapsed samples (14 patients in total). In addition to SNP array analysis, another study is planned in which high-throughput pyrosequencing will be performed on the matched samples, as well as on some t-AML patient samples which have been collected. Sequencing of the entire exome of the leukaemic blasts will enable identification of mutations potentially responsible for development of relapse (or t-AML) in individual patients. Additionally, this approach will allow investigation of the genetic heterogeneity of AML at both presentation and relapse, providing further insights into the origins of relapse-initiating clones.

8.7.4. Effect of varying levels of knockdown of DNA MMR components on drug response

Knockdown of DNA MMR components using shRNA was performed as part of the studies described in Chapter 3. In these studies, cell clones in which 95-100% knockdown of the target gene (MSH2, MSH3 or MSH6) was achieved were used in cytotoxicity assays to assess effect of loss of key MMR components on drug response. Although not described herein, cell clones in which different levels of knockdown (20-80%) of the target genes were also generated from TK6 and HL-60 cells. Another possible line of investigation therefore may involve assessment of whether different levels of reduction of MMR components can affect response to therapeutic nucleoside analogues.

References

- Abbott PJ and Saffhill R. (1979) 'DNA synthesis with methylated poly(dC-dG) templates. Evidence for a competitive nature to miscoding by O(6)-methylguanine'. *Biochim Biophys Acta*, **562** (1): 51-61.
- Abe S, Funato T, Takahashi S, Yokoyama H, Yamamoto J, Tomiya Y, et al. (2006) 'Increased expression of insulin-like growth factor i is associated with Ara-C resistance in leukemia'. *Tohoku J Exp Med*, **209** (3): 217-28.
- Abuin A, Zhang H and Bradley A. (2000) 'Genetic analysis of mouse embryonic stem cells bearing Msh3 and Msh2 single and compound mutations'. *Mol Cell Biol*, **20** (1): 149-57.
- Acharya S, Wilson T, Gradia S, Kane MF, Guerrette S, Marsischky GT, et al. (1996) 'hMSH2 forms specific mispair-binding complexes with hMSH3 and hMSH6'. *Proc Natl Acad Sci U S A*, **93** (24): 13629-34.
- Adamson AW, Beardsley DI, Kim WJ, Gao Y, Baskaran R and Brown KD. (2005) 'Methylator-induced, mismatch repair-dependent G2 arrest is activated through Chk1 and Chk2'. *Mol Biol Cell*, **16** (3): 1513-26.
- Aebi S, Kurdi-Haidar B, Gordon R, Cenni B, Zheng H, Fink D, et al. (1996) 'Loss of DNA mismatch repair in acquired resistance to cisplatin'. *Cancer Res*, **56** (13): 3087-90.
- Alani E, Lee S, Kane MF, Griffith J and Kolodner RD. (1997) 'Saccharomyces cerevisiae MSH2, a mispaired base recognition protein, also recognizes Holliday junctions in DNA'. *J Mol Biol*, **265** (3): 289-301.
- Albertini RJ, Nicklas JA and O'Neill JP. (1993) 'Somatic cell gene mutations in humans: biomarkers for genotoxicity'. *Environ Health Perspect*, **101 Suppl 3** 193-201.
- Allan JM, Wild CP, Rollinson S, Willett EV, Moorman AV, Dovey GJ, et al. (2001) 'Polymorphism in glutathione S-transferase P1 is associated with susceptibility to chemotherapy-induced leukemia'. *Proc Natl Acad Sci U S A*, **98** (20): 11592-7.
- Allan JM, Smith AG, Wheatley K, Hills RK, Travis LB, Hill DA, et al. (2004) 'Genetic variation in XPD predicts treatment outcome and risk of acute myeloid leukemia following chemotherapy'. *Blood*, **104** (13): 3872-7.
- Allan JM and Travis LB. (2005) 'Mechanisms of therapy-related carcinogenesis'. *Nat Rev Cancer*, **5** (12): 943-55.

- Allen DJ, Makhov A, Grilley M, Taylor J, Thresher R, Modrich P, et al. (1997) 'MutS mediates heteroduplex loop formation by a translocation mechanism'. *Embo J*, **16** (14): 4467-76.
- Ambros V. (2004) 'The functions of animal microRNAs'. *Nature*, **431** (7006): 350-5.
- Anderson K, Lutz C, van Delft FW, Bateman CM, Guo Y, Colman SM, et al. (2011) 'Genetic variegation of clonal architecture and propagating cells in leukaemia'. *Nature*, **469** (7330): 356-61.
- Andrew SE, McKinnon M, Cheng BS, Francis A, Penney J, Reitmair AH, et al. (1998) 'Tissues of MSH2-deficient mice demonstrate hypermutability on exposure to a DNA methylating agent'. *Proc Natl Acad Sci U S A*, **95** (3): 1126-30.
- Aquilina G, Zijno A, Moscufo N, Dogliotti E and Bignami M. (1989) 'Tolerance to methylnitrosourea-induced DNA damage is associated with 6-thioguanine resistance in CHO cells'. *Carcinogenesis*, **10** (7): 1219-23.
- Aquilina G, Giammarioli AM, Zijno A, Di Muccio A, Dogliotti E and Bignami M. (1990) 'Tolerance to O6-methylguanine and 6-thioguanine cytotoxic effects: a cross-resistant phenotype in N-methylnitrosourea-resistant Chinese hamster ovary cells'. *Cancer Res*, **50** (14): 4248-53.
- Aquilina G, Ceccotti S, Martinelli S, Hampson R and Bignami M. (1998) 'N-(2-chloroethyl)-N'-cyclohexyl-N-nitrosourea sensitivity in mismatch repair-defective human cells'. *Cancer Res*, **58** (1): 135-41.
- Aquilina G, Crescenzi M and Bignami M. (1999) 'Mismatch repair, G(2)/M cell cycle arrest and lethality after DNA damage'. *Carcinogenesis*, **20** (12): 2317-26.
- Aquilina G, Ceccotti S, Martinelli S, Soddu S, Crescenzi M, Branch P, et al. (2000) 'Mismatch repair and p53 independently affect sensitivity to N-(2-chloroethyl)-N'-cyclohexyl-N-nitrosourea'. *Clin Cancer Res*, **6** (2): 671-80.
- Arana-Yi C, Block AW, Sait SN, Ford LA, Barcos M and Baer MR. (2008) 'Therapy-related myelodysplastic syndrome and acute myeloid leukemia following treatment of acute myeloid leukemia: possible role of cytarabine'. *Leuk Res*, **32** (7): 1043-8.

- Armitage JO, Carbone PP, Connors JM, Levine A, Bennett JM and Kroll S. (2003) 'Treatment-related myelodysplasia and acute leukemia in non-Hodgkin's lymphoma patients'. *J Clin Oncol*, **21** (5): 897-906.
- Armstrong MJ and Galloway SM. (1997) 'Mismatch repair provokes chromosome aberrations in hamster cells treated with methylating agents or 6-thioguanine, but not with ethylating agents'. *Mutat Res*, **373** (2): 167-78.
- Arnaudeau C, Tenorio Miranda E, Janssen D and Helleday T. (2000) 'Inhibition of DNA synthesis is a potent mechanism by which cytostatic drugs induce homologous recombination in mammalian cells'. *Mutat Res*, **461** (3): 221-8.
- Arnaudeau C, Lundin C and Helleday T. (2001) 'DNA double-strand breaks associated with replication forks are predominantly repaired by homologous recombination involving an exchange mechanism in mammalian cells'. *J Mol Biol*, **307** (5): 1235-45.
- Arnold JA, Ranson SA and Abdalla SH. (1999) 'Azathioprine-associated acute myeloid leukaemia with trilineage dysplasia and complex karyotype: a case report and review of the literature'. *Clin Lab Haematol*, **21** (4): 289-92.
- Ayton PM and Cleary ML. (2001) 'Molecular mechanisms of leukemogenesis mediated by MLL fusion proteins'. *Oncogene*, **20** (40): 5695-707.
- Bacher U, Haferlach T, Kern W, Haferlach C and Schnittger S. (2007) 'A comparative study of molecular mutations in 381 patients with myelodysplastic syndrome and in 4130 patients with acute myeloid leukemia'. *Haematologica*, **92** (6): 744-52.
- Bacher U, Haferlach C, Kern W, Haferlach T and Schnittger S. (2008) 'Prognostic relevance of FLT3-TKD mutations in AML: the combination matters--an analysis of 3082 patients'. *Blood*, **111** (5): 2527-37.
- Baker SM, Bronner CE, Zhang L, Plug AW, Robatzek M, Warren G, et al. (1995) 'Male mice defective in the DNA mismatch repair gene PMS2 exhibit abnormal chromosome synapsis in meiosis'. *Cell*, **82** (2): 309-19.
- Baker SM, Plug AW, Prolla TA, Bronner CE, Harris AC, Yao X, et al. (1996) 'Involvement of mouse Mlh1 in DNA mismatch repair and meiotic crossing over'. *Nat Genet*, **13** (3): 336-42.

- Baldus CD, Mrozek K, Marcucci G and Bloomfield CD. (2007) 'Clinical outcome of de novo acute myeloid leukaemia patients with normal cytogenetics is affected by molecular genetic alterations: a concise review'. *Br J Haematol*, **137** (5): 387-400.
- Banerjee D, Mayer-Kuckuk P, Capiiaux G, Budak-Alpdogan T, Gorlick R and Bertino JR. (2002) 'Novel aspects of resistance to drugs targeted to dihydrofolate reductase and thymidylate synthase'. *Biochim Biophys Acta*, **1587** (2-3): 164-73.
- Bannister LA, Waldman BC and Waldman AS. (2004) 'Modulation of error-prone double-strand break repair in mammalian chromosomes by DNA mismatch repair protein Mlh1'. *DNA Repair (Amst)*, **3** (5): 465-74.
- Barjesteh van Waalwijk van Doorn-Khosrovani S, Erpelinck C, van Putten WL, Valk PJ, van der Poel-van de Luytgaarde S, Hack R, et al. (2003) 'High EVI1 expression predicts poor survival in acute myeloid leukemia: a study of 319 de novo AML patients'. *Blood*, **101** (3): 837-45.
- Barnard DR and Woods WG. (2005) 'Treatment-related myelodysplastic syndrome/acute myeloid leukemia in survivors of childhood cancer--an update'. *Leuk Lymphoma*, **46** (5): 651-63.
- Bartek J and Lukas J. (2003) 'Chk1 and Chk2 kinases in checkpoint control and cancer'. *Cancer Cell*, **3** (5): 421-9.
- Barwell J, Pangon L, Hodgson S, Georgiou A, Kesterton I, Slade T, et al. (2007) 'Biallelic mutation of MSH2 in primary human cells is associated with sensitivity to irradiation and altered RAD51 foci kinetics'. *J Med Genet*, **44** (8): 516-20.
- Baskaran R, Wood LD, Whitaker LL, Canman CE, Morgan SE, Xu Y, et al. (1997) 'Ataxia telangiectasia mutant protein activates c-Abl tyrosine kinase in response to ionizing radiation'. *Nature*, **387** (6632): 516-9.
- Beaupre DM and Kurzrock R. (1999) 'RAS and leukemia: from basic mechanisms to gene-directed therapy'. *J Clin Oncol*, **17** (3): 1071-9.
- Ben-Yehuda D, Krichevsky S, Caspi O, Rund D, Polliack A, Abeliovich D, et al. (1996) 'Microsatellite instability and p53 mutations in therapy-related leukemia suggest mutator phenotype'. *Blood*, **88** (11): 4296-303.

- Bennett JM, Catovsky D, Daniel MT, Flandrin G, Galton DA, Gralnick HR, et al. (1976) 'Proposals for the classification of the acute leukaemias. French-American-British (FAB) co-operative group'. *Br J Haematol*, **33** (4): 451-8.
- Beranek DT. (1990) 'Distribution of methyl and ethyl adducts following alkylation with monofunctional alkylating agents'. *Mutat Res*, **231** (1): 11-30.
- Berardini M, Mazurek A and Fishel R. (2000) 'The effect of O6-methylguanine DNA adducts on the adenosine nucleotide switch functions of hMSH2-hMSH6 and hMSH2-hMSH3'. *J Biol Chem*, **275** (36): 27851-7.
- Blackwell LJ, Bjornson KP and Modrich P. (1998) 'DNA-dependent activation of the hMutSalpha ATPase'. *J Biol Chem*, **273** (48): 32049-54.
- Blum W, Klisovic RB, Hackanson B, Liu Z, Liu S, Devine H, et al. (2007) 'Phase I study of decitabine alone or in combination with valproic acid in acute myeloid leukemia'. *J Clin Oncol*, **25** (25): 3884-91.
- Boiteux S and Radicella JP. (2000) 'The human OGG1 gene: structure, functions, and its implication in the process of carcinogenesis'. *Arch Biochem Biophys*, **377** (1): 1-8.
- Bonnet D and Dick JE. (1997) 'Human acute myeloid leukemia is organized as a hierarchy that originates from a primitive hematopoietic cell'. *Nat Med*, **3** (7): 730-7.
- Boyer JC, Umar A, Risinger JI, Lipford JR, Kane M, Yin S, et al. (1995) 'Microsatellite instability, mismatch repair deficiency, and genetic defects in human cancer cell lines'. *Cancer Res*, **55** (24): 6063-70.
- Boyer JC, Risinger JI and Farber RA. (1998) 'Stability of microsatellites in myeloid neoplasias'. *Cancer Genet Cytogenet*, **106** (1): 54-61.
- Branch P, Aquilina G, Bignami M and Karran P. (1993) 'Defective mismatch binding and a mutator phenotype in cells tolerant to DNA damage'. *Nature*, **362** (6421): 652-4.
- Branch P, Hampson R and Karran P. (1995) 'DNA mismatch binding defects, DNA damage tolerance, and mutator phenotypes in human colorectal carcinoma cell lines'. *Cancer Res*, **55** (11): 2304-9.

- Breems DA, Van Putten WL, De Greef GE, Van Zelderren-Bhola SL, Gerssen-Schoorl KB, Mellink CH, et al. (2008) 'Monosomal karyotype in acute myeloid leukemia: a better indicator of poor prognosis than a complex karyotype'. *J Clin Oncol*, **26** (29): 4791-7.
- Brown KD, Rathi A, Kamath R, Beardsley DI, Zhan Q, Mannino JL, et al. (2003) 'The mismatch repair system is required for S-phase checkpoint activation'. *Nat Genet*, **33** (1): 80-4.
- Bulgar AD, Snell M, Donze JR, Kirkland EB, Li L, Yang S, et al. (2010) 'Targeting base excision repair suggests a new therapeutic strategy of fludarabine for the treatment of chronic lymphocytic leukemia'. *Leukemia*, **24** (10): 1795-9.
- Bullock G, Ray S, Reed J, Miyashita T, Maria Ibrado A, Huang Y, et al. (1995) 'Evidence against a direct role for the induction of c-jun expression in the mediation of drug-induced apoptosis in human acute leukemia cells'. *Clin Cancer Res*, **1** (5): 559-64.
- Burriss HA, 3rd, Moore MJ, Andersen J, Green MR, Rothenberg ML, Modiano MR, et al. (1997) 'Improvements in survival and clinical benefit with gemcitabine as first-line therapy for patients with advanced pancreas cancer: a randomized trial'. *J Clin Oncol*, **15** (6): 2403-13.
- Cai J, Damaraju VL, Groulx N, Mowles D, Peng Y, Robins MJ, et al. (2008) 'Two distinct molecular mechanisms underlying cytarabine resistance in human leukemic cells'. *Cancer Res*, **68** (7): 2349-57.
- Calvert H and Azzariti A. (2011) 'The clinical development of inhibitors of poly(ADP-ribose) polymerase'. *Ann Oncol*, **22 Suppl 1** i53-9.
- Caporali S, Falcinelli S, Starace G, Russo MT, Bonmassar E, Jiricny J, et al. (2004) 'DNA damage induced by temozolomide signals to both ATM and ATR: role of the mismatch repair system'. *Mol Pharmacol*, **66** (3): 478-91.
- Carethers JM, Hawn MT, Chauhan DP, Luce MC, Marra G, Koi M, et al. (1996) 'Competency in mismatch repair prohibits clonal expansion of cancer cells treated with N-methyl-N'-nitro-N-nitrosoguanidine'. *J Clin Invest*, **98** (1): 199-206.

- Carethers JM, Chauhan DP, Fink D, Nebel S, Bresalier RS, Howell SB, et al. (1999) 'Mismatch repair proficiency and in vitro response to 5-fluorouracil'. *Gastroenterology*, **117** (1): 123-31.
- Carethers JM, Smith EJ, Behling CA, Nguyen L, Tajima A, Doctolero RT, et al. (2004) 'Use of 5-fluorouracil and survival in patients with microsatellite-unstable colorectal cancer'. *Gastroenterology*, **126** (2): 394-401.
- Cariello NF and Skopek TR. (1993) 'Analysis of mutations occurring at the human hprt locus'. *J Mol Biol*, **231** (1): 41-57.
- Carney DA, Westerman DA, Tam CS, Milner A, Prince HM, Kenealy M, et al. (2010) 'Therapy-related myelodysplastic syndrome and acute myeloid leukemia following fludarabine combination chemotherapy'. *Leukemia*, **24** (12): 2056-62.
- Carter MM, Torres SM, Cook DL, Jr., McCash CL, Yu M, Walker VE, et al. (2007) 'Relative mutagenic potencies of several nucleoside analogs, alone or in drug pairs, at the HPRT and TK loci of human TK6 lymphoblastoid cells'. *Environ Mol Mutagen*, **48** (3-4): 239-47.
- Casorelli I, Offman J, Mele L, Pagano L, Sica S, D'Errico M, et al. (2003) 'Drug treatment in the development of mismatch repair defective acute leukemia and myelodysplastic syndrome'. *DNA Repair (Amst)*, **2** (5): 547-59.
- Casorelli I, Russo MT and Bignami M. (2008) 'Role of mismatch repair and MGMT in response to anticancer therapies'. *Anticancer Agents Med Chem*, **8** (4): 368-80.
- Cejka P, Stojic L, Mojas N, Russell AM, Heinimann K, Cannavo E, et al. (2003) 'Methylation-induced G(2)/M arrest requires a full complement of the mismatch repair protein hMLH1'. *Embo J*, **22** (9): 2245-54.
- Cejka P, Stojic L, Marra G and Jiricny J. (2004) 'Is mismatch repair really required for ionizing radiation-induced DNA damage signaling?'. *Nat Genet*, **36** (5): 432-3; author reply 34.
- Chauhan DP. (2002) 'Chemotherapeutic potential of curcumin for colorectal cancer'. *Curr Pharm Des*, **8** (19): 1695-706.

- Chen YW, Cleaver JE, Hanaoka F, Chang CF and Chou KM. (2006) 'A novel role of DNA polymerase eta in modulating cellular sensitivity to chemotherapeutic agents'. *Mol Cancer Res*, **4** (4): 257-65.
- Cho SH, Toouli CD, Fujii GH, Crain C and Parry D. (2005) 'Chk1 is essential for tumor cell viability following activation of the replication checkpoint'. *Cell Cycle*, **4** (1): 131-9.
- Choi CH. (2005) 'ABC transporters as multidrug resistance mechanisms and the development of chemosensitizers for their reversal'. *Cancer Cell Int*, **5** 30.
- Choi JY, Chowdhury G, Zang H, Angel KC, Vu CC, Peterson LA, et al. (2006) 'Translesion synthesis across O6-alkylguanine DNA adducts by recombinant human DNA polymerases'. *J Biol Chem*, **281** (50): 38244-56.
- Chou KM, Kukhanova M and Cheng YC. (2000) 'A novel action of human apurinic/aprimidinic endonuclease: excision of L-configuration deoxyribonucleoside analogs from the 3' termini of DNA'. *J Biol Chem*, **275** (40): 31009-15.
- Chrencik JE, Burgin AB, Pommier Y, Stewart L and Redinbo MR. (2003) 'Structural impact of the leukemia drug 1-beta-D-arabinofuranosylcytosine (Ara-C) on the covalent human topoisomerase I-DNA complex'. *J Biol Chem*, **278** (14): 12461-6.
- Christiansen DH, Andersen MK and Pedersen-Bjergaard J. (2001) 'Mutations with loss of heterozygosity of p53 are common in therapy-related myelodysplasia and acute myeloid leukemia after exposure to alkylating agents and significantly associated with deletion or loss of 5q, a complex karyotype, and a poor prognosis'. *J Clin Oncol*, **19** (5): 1405-13.
- Christiansen DH, Andersen MK and Pedersen-Bjergaard J. (2004) 'Mutations of AML1 are common in therapy-related myelodysplasia following therapy with alkylating agents and are significantly associated with deletion or loss of chromosome arm 7q and with subsequent leukemic transformation'. *Blood*, **104** (5): 1474-81.
- Christiansen DH, Andersen MK, Desta F and Pedersen-Bjergaard J. (2005) 'Mutations of genes in the receptor tyrosine kinase (RTK)/RAS-BRAF signal transduction pathway in therapy-related myelodysplasia and acute myeloid leukemia'. *Leukemia*, **19** (12): 2232-40.

- Cimino GD, Gamper HB, Isaacs ST and Hearst JE. (1985) 'Psoralens as photoactive probes of nucleic acid structure and function: organic chemistry, photochemistry, and biochemistry'. *Annu Rev Biochem*, **54** 1151-93.
- Ciotta C, Ceccotti S, Aquilina G, Humbert O, Palombo F, Jiricny J, et al. (1998) 'Increased somatic recombination in methylation tolerant human cells with defective DNA mismatch repair'. *J Mol Biol*, **276** (4): 705-19.
- Claij N and Te Riele H. (2002) 'Methylation tolerance in mismatch repair proficient cells with low MSH2 protein level'. *Oncoqene*, **21** (18): 2873-9.
- Clark AB, Valle F, Drotschmann K, Gary RK and Kunkel TA. (2000) 'Functional interaction of proliferating cell nuclear antigen with MSH2-MSH6 and MSH2-MSH3 complexes'. *J Biol Chem*, **275** (47): 36498-501.
- Cline SD and Osheroff N. (1999) 'Cytosine arabinoside lesions are position-specific topoisomerase II poisons and stimulate DNA cleavage mediated by the human type II enzymes'. *J Biol Chem*, **274** (42): 29740-3.
- Colussi C, Parlanti E, Degan P, Aquilina G, Barnes D, Macpherson P, et al. (2002) 'The mammalian mismatch repair pathway removes DNA 8-oxodGMP incorporated from the oxidized dNTP pool'. *Curr Biol*, **12** (11): 912-8.
- Cooke MS, Evans MD, Dizdaroglu M and Lunec J. (2003) 'Oxidative DNA damage: mechanisms, mutation, and disease'. *FASEB J*, **17** (10): 1195-214.
- Coso D, Costello R, Cohen-Valensi R, Sainty D, Nezri M, Gastaut JA, et al. (1999) 'Acute myeloid leukemia and myelodysplasia in patients with chronic lymphocytic leukemia receiving fludarabine as initial therapy'. *Ann Oncol*, **10** (3): 362-3.
- Coulthard S and Hogarth L. (2005) 'The thiopurines: an update'. *Invest New Drugs*, **23** (6): 523-32.
- Coulthard SA, Hogarth LA, Little M, Matheson EC, Redfern CP, Minto L, et al. (2002) 'The effect of thiopurine methyltransferase expression on sensitivity to thiopurine drugs'. *Mol Pharmacol*, **62** (1): 102-9.
- Cros E, Jordheim L, Dumontet C and Galmarini CM. (2004) 'Problems related to resistance to cytarabine in acute myeloid leukemia'. *Leuk Lymphoma*, **45** (6): 1123-32.

- Curtin NJ, Wang LZ, Yiakouvaki A, Kyle S, Arris CA, Canan-Koch S, et al. (2004) 'Novel poly(ADP-ribose) polymerase-1 inhibitor, AG14361, restores sensitivity to temozolomide in mismatch repair-deficient cells'. *Clin Cancer Res*, **10** (3): 881-9.
- Danam RP, Howell SR, Brent TP and Harris LC. (2005) 'Epigenetic regulation of O6-methylguanine-DNA methyltransferase gene expression by histone acetylation and methyl-CpG binding proteins'. *Mol Cancer Ther*, **4** (1): 61-9.
- Das-Gupta EP, Seedhouse CH and Russell NH. (2001) 'Microsatellite instability occurs in defined subsets of patients with acute myeloblastic leukaemia'. *Br J Haematol*, **114** (2): 307-12.
- Davis JN, McGhee L and Meyers S. (2003) 'The ETO (MTG8) gene family'. *Gene*, **303** 1-10.
- Davis TW, Wilson-Van Patten C, Meyers M, Kunugi KA, Cuthill S, Reznikoff C, et al. (1998) 'Defective expression of the DNA mismatch repair protein, MLH1, alters G2-M cell cycle checkpoint arrest following ionizing radiation'. *Cancer Res*, **58** (4): 767-78.
- de Campos-Nebel M, Larripa I and Gonzalez-Cid M. (2008) 'Non-homologous end joining is the responsible pathway for the repair of fludarabine-induced DNA double strand breaks in mammalian cells'. *Mutat Res*, **646** (1-2): 8-16.
- De Silva IU, McHugh PJ, Clingen PH and Hartley JA. (2000) 'Defining the roles of nucleotide excision repair and recombination in the repair of DNA interstrand cross-links in mammalian cells'. *Mol Cell Biol*, **20** (21): 7980-90.
- de The H, Chomienne C, Lanotte M, Degos L and Dejean A. (1990) 'The t(15;17) translocation of acute promyelocytic leukaemia fuses the retinoic acid receptor alpha gene to a novel transcribed locus'. *Nature*, **347** (6293): 558-61.
- de Wind N, Dekker M, Berns A, Radman M and te Riele H. (1995) 'Inactivation of the mouse Msh2 gene results in mismatch repair deficiency, methylation tolerance, hyperrecombination, and predisposition to cancer'. *Cell*, **82** (2): 321-30.
- Decker RH, Levin J, Kramer LB, Dai Y and Grant S. (2003) 'Enforced expression of the tumor suppressor p53 renders human leukemia cells (U937) more sensitive to 1-[beta-D-arabinofuranosyl]cytosine (ara-C)-induced apoptosis'. *Biochem Pharmacol*, **65** (12): 1997-2008.

- Deguchi K and Gilliland DG. (2002) 'Cooperativity between mutations in tyrosine kinases and in hematopoietic transcription factors in AML'. *Leukemia*, **16** (4): 740-4.
- DeWeese TL, Shipman JM, Larrier NA, Buckley NM, Kidd LR, Groopman JD, et al. (1998) 'Mouse embryonic stem cells carrying one or two defective Msh2 alleles respond abnormally to oxidative stress inflicted by low-level radiation'. *Proc Natl Acad Sci U S A*, **95** (20): 11915-20.
- di Pietro M, Marra G, Cejka P, Stojic L, Menigatti M, Cattaruzza MS, et al. (2003) 'Mismatch repair-dependent transcriptome changes in human cells treated with the methylating agent N-methyl-n'-nitro-N-nitrosoguanidine'. *Cancer Res*, **63** (23): 8158-66.
- Dixon-McIver A, East P, Mein CA, Cazier JB, Molloy G, Chaplin T, et al. (2008) 'Distinctive patterns of microRNA expression associated with karyotype in acute myeloid leukaemia'. *PLoS One*, **3** (5): e2141.
- Dosch J, Christmann M and Kaina B. (1998) 'Mismatch G-T binding activity and MSH2 expression is quantitatively related to sensitivity of cells to methylating agents'. *Carcinogenesis*, **19** (4): 567-73.
- Drummond JT, Li GM, Longley MJ and Modrich P. (1995) 'Isolation of an hMSH2-p160 heterodimer that restores DNA mismatch repair to tumor cells'. *Science*, **268** (5219): 1909-12.
- Drummond JT, Genschel J, Wolf E and Modrich P. (1997) 'DHFR/MSH3 amplification in methotrexate-resistant cells alters the hMutSalpha/hMutSbeta ratio and reduces the efficiency of base-base mismatch repair'. *Proc Natl Acad Sci U S A*, **94** (19): 10144-9.
- Duckett DR, Drummond JT, Murchie AI, Reardon JT, Sancar A, Lilley DM, et al. (1996) 'Human MutSalpha recognizes damaged DNA base pairs containing O6-methylguanine, O4-methylthymine, or the cisplatin-d(GpG) adduct'. *Proc Natl Acad Sci U S A*, **93** (13): 6443-7.
- Duckett DR, Bronstein SM, Taya Y and Modrich P. (1999) 'hMutSalpha- and hMutLalpha-dependent phosphorylation of p53 in response to DNA methylator damage'. *Proc Natl Acad Sci U S A*, **96** (22): 12384-8.

- Dumontet C, Fabianowska-Majewska K, Mantincic D, Callet Bauchu E, Tigaud I, Gandhi V, et al. (1999) 'Common resistance mechanisms to deoxynucleoside analogues in variants of the human erythroleukaemic line K562'. *Br J Haematol*, **106** (1): 78-85.
- Dzantiev L, Constantin N, Genschel J, Iyer RR, Burgers PM and Modrich P. (2004) 'A defined human system that supports bidirectional mismatch-provoked excision'. *Mol Cell*, **15** (1): 31-41.
- Edelmann W, Cohen PE, Kane M, Lau K, Morrow B, Bennett S, et al. (1996) 'Meiotic pachytene arrest in MLH1-deficient mice'. *Cell*, **85** (7): 1125-34.
- Elliott B and Jasin M. (2001) 'Repair of double-strand breaks by homologous recombination in mismatch repair-defective mammalian cells'. *Mol Cell Biol*, **21** (8): 2671-82.
- Ellis L, Atadja PW and Johnstone RW. (2009) 'Epigenetics in cancer: targeting chromatin modifications'. *Mol Cancer Ther*, **8** (6): 1409-20.
- Estey E, Keating MJ, Pierce S and Stass S. (1995) 'Change in karyotype between diagnosis and first relapse in acute myelogenous leukemia'. *Leukemia*, **9** (6): 972-6.
- Estey EH, Giles FJ, Beran M, O'Brien S, Pierce SA, Faderl SH, et al. (2002) 'Experience with gemtuzumab ozogamycin ("mylotarg") and all-trans retinoic acid in untreated acute promyelocytic leukemia'. *Blood*, **99** (11): 4222-4.
- Evans E, Sugawara N, Haber JE and Alani E. (2000) 'The *Saccharomyces cerevisiae* Msh2 mismatch repair protein localizes to recombination intermediates in vivo'. *Mol Cell*, **5** (5): 789-99.
- Ewald B, Sampath D and Plunkett W. (2007) 'H2AX phosphorylation marks gemcitabine-induced stalled replication forks and their collapse upon S-phase checkpoint abrogation'. *Mol Cancer Ther*, **6** (4): 1239-48.
- Ewald B, Sampath D and Plunkett W. (2008a) 'ATM and the Mre11-Rad50-Nbs1 complex respond to nucleoside analogue-induced stalled replication forks and contribute to drug resistance'. *Cancer Res*, **68** (19): 7947-55.

- Ewald B, Sampath D and Plunkett W. (2008b) 'Nucleoside analogs: molecular mechanisms signaling cell death'. *Oncogene*, **27** (50): 6522-37.
- Faderl S, Gandhi V, O'Brien S, Bonate P, Cortes J, Estey E, et al. (2005) 'Results of a phase 1-2 study of clofarabine in combination with cytarabine (ara-C) in relapsed and refractory acute leukemias'. *Blood*, **105** (3): 940-7.
- Faderl S, Ravandi F, Huang X, Garcia-Manero G, Ferrajoli A, Estrov Z, et al. (2008) 'A randomized study of clofarabine versus clofarabine plus low-dose cytarabine as front-line therapy for patients aged 60 years and older with acute myeloid leukemia and high-risk myelodysplastic syndrome'. *Blood*, **112** (5): 1638-45.
- Falck J, Mailand N, Syljuasen RG, Bartek J and Lukas J. (2001) 'The ATM-Chk2-Cdc25A checkpoint pathway guards against radioresistant DNA synthesis'. *Nature*, **410** (6830): 842-7.
- Feijoo C, Hall-Jackson C, Wu R, Jenkins D, Leitch J, Gilbert DM, et al. (2001) 'Activation of mammalian Chk1 during DNA replication arrest: a role for Chk1 in the intra-S phase checkpoint monitoring replication origin firing'. *J Cell Biol*, **154** (5): 913-23.
- Feldman EJ, Lancet JE, Kolitz JE, Ritchie EK, Roboz GJ, List AF, et al. (2011) 'First-In-Man Study of CPX-351: A Liposomal Carrier Containing Cytarabine and Daunorubicin in a Fixed 5:1 Molar Ratio for the Treatment of Relapsed and Refractory Acute Myeloid Leukemia'. *J Clin Oncol*, **29** (8): 979-85.
- Felix CA, Walker AH, Lange BJ, Williams TM, Winick NJ, Cheung NK, et al. (1998) 'Association of CYP3A4 genotype with treatment-related leukemia'. *Proc Natl Acad Sci U S A*, **95** (22): 13176-81.
- Fern L, Pallis M, Ian Carter G, Seedhouse C, Russell N and Byrne J. (2004) 'Clonal haemopoiesis may occur after conventional chemotherapy and is associated with accelerated telomere shortening and defects in the NQO1 pathway; possible mechanisms leading to an increased risk of t-AML/MDS'. *Br J Haematol*, **126** (1): 63-71.
- Fernandez-Capetillo O, Lee A, Nussenzweig M and Nussenzweig A. (2004) 'H2AX: the histone guardian of the genome'. *DNA Repair (Amst)*, **3** (8-9): 959-67.

- Ferreri AJ, Reni M, Foppoli M, Martelli M, Pangalis GA, Frezzato M, et al. (2009) 'High-dose cytarabine plus high-dose methotrexate versus high-dose methotrexate alone in patients with primary CNS lymphoma: a randomised phase 2 trial'. *Lancet*, **374** (9700): 1512-20.
- Finette BA, Homans AC and Albertini RJ. (2000) 'Emergence of genetic instability in children treated for leukemia'. *Science*, **288** (5465): 514-7.
- Fink D, Nebel S, Aebi S, Zheng H, Cenni B, Nehme A, et al. (1996) 'The role of DNA mismatch repair in platinum drug resistance'. *Cancer Res*, **56** (21): 4881-6.
- Fink D, Zheng H, Nebel S, Norris PS, Aebi S, Lin TP, et al. (1997) 'In vitro and in vivo resistance to cisplatin in cells that have lost DNA mismatch repair'. *Cancer Res*, **57** (10): 1841-5.
- Fink D, Nebel S, Norris PS, Baergen RN, Wilczynski SP, Costa MJ, et al. (1998) 'Enrichment for DNA mismatch repair-deficient cells during treatment with cisplatin'. *Int J Cancer*, **77** (5): 741-6.
- Fischer F, Baerenfaller K and Jiricny J. (2007) '5-Fluorouracil is efficiently removed from DNA by the base excision and mismatch repair systems'. *Gastroenterology*, **133** (6): 1858-68.
- Fishel R. (2001) 'The selection for mismatch repair defects in hereditary nonpolyposis colorectal cancer: revising the mutator hypothesis'. *Cancer Res*, **61** (20): 7369-74.
- Fiumicino S, Martinelli S, Colussi C, Aquilina G, Leonetti C, Crescenzi M, et al. (2000) 'Sensitivity to DNA cross-linking chemotherapeutic agents in mismatch repair-defective cells in vitro and in xenografts'. *Int J Cancer*, **85** (4): 590-6.
- Foray N, Marot D, Randrianarison V, Venezia ND, Picard D, Perricaudet M, et al. (2002) 'Constitutive association of BRCA1 and c-Abl and its ATM-dependent disruption after irradiation'. *Mol Cell Biol*, **22** (12): 4020-32.
- Forster A, Pannell R, Drynan LF, McCormack M, Collins EC, Daser A, et al. (2003) 'Engineering de novo reciprocal chromosomal translocations associated with Mll to replicate primary events of human cancer'. *Cancer Cell*, **3** (5): 449-58.

- Franchitto A, Pichierri P, Piergentili R, Crescenzi M, Bignami M and Palitti F. (2003) 'The mammalian mismatch repair protein MSH2 is required for correct MRE11 and RAD51 relocalization and for efficient cell cycle arrest induced by ionizing radiation in G2 phase'. *Oncogene*, **22** (14): 2110-20.
- Fritz G, Tano K, Mitra S and Kaina B. (1991) 'Inducibility of the DNA repair gene encoding O6-methylguanine-DNA methyltransferase in mammalian cells by DNA-damaging treatments'. *Mol Cell Biol*, **11** (9): 4660-8.
- Fritzell JA, Narayanan L, Baker SM, Bronner CE, Andrew SE, Prolla TA, et al. (1997) 'Role of DNA mismatch repair in the cytotoxicity of ionizing radiation'. *Cancer Res*, **57** (22): 5143-7.
- Fujii H and Shimada T. (1989) 'Isolation and characterization of cDNA clones derived from the divergently transcribed gene in the region upstream from the human dihydrofolate reductase gene'. *J Biol Chem*, **264** (17): 10057-64.
- Furth EE, Thilly WG, Penman BW, Liber HL and Rand WM. (1981) 'Quantitative assay for mutation in diploid human lymphoblasts using microtiter plates'. *Anal Biochem*, **110** (1): 1-8.
- Galmarini CM, Thomas X, Calvo F, Rousselot P, Rabilloud M, El Jaffari A, et al. (2002) 'In vivo mechanisms of resistance to cytarabine in acute myeloid leukaemia'. *Br J Haematol*, **117** (4): 860-8.
- Gandhi V, Huang P, Chapman AJ, Chen F and Plunkett W. (1997) 'Incorporation of fludarabine and 1-beta-D-arabinofuranosylcytosine 5'-triphosphates by DNA polymerase alpha: affinity, interaction, and consequences'. *Clin Cancer Res*, **3** (8): 1347-55.
- Gao YG, van der Marel GA, van Boom JH and Wang AH. (1991) 'Molecular structure of a DNA decamer containing an anticancer nucleoside arabinosylcytosine: conformational perturbation by arabinosylcytosine in B-DNA'. *Biochemistry*, **30** (41): 9922-31.
- Garcia-Diaz M, Murray MS, Kunkel TA and Chou KM. (2010) 'Interaction between DNA Polymerase lambda and anticancer nucleoside analogs'. *J Biol Chem*, **285** (22): 16874-9.

- Garzon R, Volinia S, Liu CG, Fernandez-Cymering C, Palumbo T, Pichiorri F, et al. (2008) 'MicroRNA signatures associated with cytogenetics and prognosis in acute myeloid leukemia'. *Blood*, **111** (6): 3183-9.
- Gati WP, Paterson AR, Larratt LM, Turner AR and Belch AR. (1997) 'Sensitivity of acute leukemia cells to cytarabine is a correlate of cellular es nucleoside transporter site content measured by flow cytometry with SAENTA-fluorescein'. *Blood*, **90** (1): 346-53.
- Gefen N, Brkic G, Galron D, Priel E, Ozer J, Benharroch D, et al. (2010) 'Acquired resistance to 6-thioguanine in melanoma cells involves the repair enzyme O6-methylguanine-DNA methyltransferase (MGMT)'. *Cancer Biol Ther*, **9** (1): 49-55.
- Genschel J, Littman SJ, Drummond JT and Modrich P. (1998) 'Isolation of MutSbeta from human cells and comparison of the mismatch repair specificities of MutSbeta and MutSalpha'. *J Biol Chem*, **273** (31): 19895-901.
- Genschel J, Bazemore LR and Modrich P. (2002) 'Human exonuclease I is required for 5' and 3' mismatch repair'. *J Biol Chem*, **277** (15): 13302-11.
- Giannini G, Ristori E, Cerignoli F, Rinaldi C, Zani M, Viel A, et al. (2002) 'Human MRE11 is inactivated in mismatch repair-deficient cancers'. *EMBO Rep*, **3** (3): 248-54.
- Giannini G, Rinaldi C, Ristori E, Ambrosini MI, Cerignoli F, Viel A, et al. (2004) 'Mutations of an intronic repeat induce impaired MRE11 expression in primary human cancer with microsatellite instability'. *Oncogene*, **23** (15): 2640-7.
- Gibbs RA, Nguyen PN, Edwards A, Civitello AB and Caskey CT. (1990) 'Multiplex DNA deletion detection and exon sequencing of the hypoxanthine phosphoribosyltransferase gene in Lesch-Nyhan families'. *Genomics*, **7** (2): 235-44.
- Gibson SL, Narayanan L, Hegan DC, Buermeier AB, Liskay RM and Glazer PM. (2006) 'Overexpression of the DNA mismatch repair factor, PMS2, confers hypermutability and DNA damage tolerance'. *Cancer Lett*, **244** (2): 195-202.
- Gilliland DG and Griffin JD. (2002) 'The roles of FLT3 in hematopoiesis and leukemia'. *Blood*, **100** (5): 1532-42.

- Giver CR, Nelson SL and Grosovsky AJ. (1993) 'Spectrum of spontaneous HPRT-mutations in TK6 human lymphoblasts'. *Environ Mol Mutagen*, **22** (3): 138-46.
- Godley LA and Larson RA. (2008) 'Therapy-related myeloid leukemia'. *Semin Oncol*, **35** (4): 418-29.
- Goldfarb T and Alani E. (2005) 'Distinct roles for the *Saccharomyces cerevisiae* mismatch repair proteins in heteroduplex rejection, mismatch repair and nonhomologous tail removal'. *Genetics*, **169** (2): 563-74.
- Goldmacher VS, Cuzick RA, Jr. and Thilly WG. (1986) 'Isolation and partial characterization of human cell mutants differing in sensitivity to killing and mutation by methylnitrosourea and N-methyl-N'-nitro-N-nitrosoguanidine'. *J Biol Chem*, **261** (27): 12462-71.
- Gong JG, Costanzo A, Yang HQ, Melino G, Kaelin WG, Jr., Levrero M, et al. (1999) 'The tyrosine kinase c-Abl regulates p73 in apoptotic response to cisplatin-induced DNA damage'. *Nature*, **399** (6738): 806-9.
- Goth-Goldstein R. (1980) 'Inability of Chinese hamster ovary cells to excise O6-alkylguanine'. *Cancer Res*, **40** (7): 2623-4.
- Goz B and Bastow KF. (1997) 'A possible role for topoisomerase II in cell death and N-phosphonoacetyl-L-aspartate-resistance frequency and its enhancement by 1-beta-D-arabinofuranosyl cytosine and 5-fluoro-2'-deoxyuridine'. *Mutat Res*, **384** (2): 89-106.
- Gradia S, Acharya S and Fishel R. (1997) 'The human mismatch recognition complex hMSH2-hMSH6 functions as a novel molecular switch'. *Cell*, **91** (7): 995-1005.
- Gradia S, Subramanian D, Wilson T, Acharya S, Makhov A, Griffith J, et al. (1999) 'hMSH2-hMSH6 forms a hydrolysis-independent sliding clamp on mismatched DNA'. *Mol Cell*, **3** (2): 255-61.
- Grisendi S, Mecucci C, Falini B and Pandolfi PP. (2006) 'Nucleophosmin and cancer'. *Nat Rev Cancer*, **6** (7): 493-505.

- Grossmann V, Schnittger S, Schindela S, Klein HU, Eder C, Dugas M, et al. (2011a) 'Strategy for robust detection of insertions, deletions, and point mutations in CEBPA, a GC-rich content gene, using 454 next-generation deep-sequencing technology'. *J Mol Diagn*, **13** (2): 129-36.
- Grossmann V, Kohlmann A, Klein HU, Schindela S, Schnittger S, Dicker F, et al. (2011b) 'Targeted next-generation sequencing detects point mutations, insertions, deletions and balanced chromosomal rearrangements as well as identifies novel leukemia-specific fusion genes in a single procedure'. *Leukemia*, **25** (4): 671-80.
- Gu L, Hong Y, McCulloch S, Watanabe H and Li GM. (1998) 'ATP-dependent interaction of human mismatch repair proteins and dual role of PCNA in mismatch repair'. *Nucleic Acids Res*, **26** (5): 1173-8.
- Guarne A, Ramon-Maiques S, Wolff EM, Ghirlando R, Hu X, Miller JH, et al. (2004) 'Structure of the MutL C-terminal domain: a model of intact MutL and its roles in mismatch repair'. *Embo J*, **23** (21): 4134-45.
- Gudmundsdottir K and Ashworth A. (2006) 'The roles of BRCA1 and BRCA2 and associated proteins in the maintenance of genomic stability'. *Oncogene*, **25** (43): 5864-74.
- Guillem VM, Collado M, Terol MJ, Calasanz MJ, Esteve J, Gonzalez M, et al. (2007) 'Role of MTHFR (677, 1298) haplotype in the risk of developing secondary leukemia after treatment of breast cancer and hematological malignancies'. *Leukemia*, **21** (7): 1413-22.
- Gunji H, Kharbanda S and Kufe D. (1991) 'Induction of internucleosomal DNA fragmentation in human myeloid leukemia cells by 1-beta-D-arabinofuranosylcytosine'. *Cancer Res*, **51** (2): 741-3.
- Hake CR, Graubert TA and Fenske TS. (2007) 'Does autologous transplantation directly increase the risk of secondary leukemia in lymphoma patients?'. *Bone Marrow Transplant*, **39** (2): 59-70.
- Ham MF, Takakuwa T, Luo WJ, Liu A, Horii A and Aozasa K. (2006) 'Impairment of double-strand breaks repair and aberrant splicing of ATM and MRE11 in leukemia-lymphoma cell lines with microsatellite instability'. *Cancer Sci*, **97** (3): 226-34.

- Hampson R, Humbert O, Macpherson P, Aquilina G and Karran P. (1997) 'Mismatch repair defects and O6-methylguanine-DNA methyltransferase expression in acquired resistance to methylating agents in human cells'. *J Biol Chem*, **272** (45): 28596-606.
- Han S, Hickey RJ, Tom TD, Wills PW, Syvaioja JE and Malkas LH. (2000) 'Differential inhibition of the human cell DNA replication complex-associated DNA polymerases by the antimetabolite 1-beta-D-arabinofuranosylcytosine triphosphate (ara-CTP)'. *Biochem Pharmacol*, **60** (3): 403-11.
- Harada H, Harada Y, Tanaka H, Kimura A and Inaba T. (2003) 'Implications of somatic mutations in the AML1 gene in radiation-associated and therapy-related myelodysplastic syndrome/acute myeloid leukemia'. *Blood*, **101** (2): 673-80.
- Harada Y and Harada H. (2009) 'Molecular pathways mediating MDS/AML with focus on AML1/RUNX1 point mutations'. *J Cell Physiol*, **220** (1): 16-20.
- Hasselbach L, Haase S, Fischer D, Kolberg HC and Sturzbecher HW. (2005) 'Characterisation of the promoter region of the human DNA-repair gene Rad51'. *Eur J Gynaecol Oncol*, **26** (6): 589-98.
- Hawn MT, Umar A, Carethers JM, Marra G, Kunkel TA, Boland CR, et al. (1995) 'Evidence for a connection between the mismatch repair system and the G2 cell cycle checkpoint'. *Cancer Res*, **55** (17): 3721-5.
- Hegi ME, Diserens AC, Gorlia T, Hamou MF, de Tribolet N, Weller M, et al. (2005) 'MGMT gene silencing and benefit from temozolomide in glioblastoma'. *N Engl J Med*, **352** (10): 997-1003.
- Hegi ME, Liu L, Herman JG, Stupp R, Wick W, Weller M, et al. (2008) 'Correlation of O6-methylguanine methyltransferase (MGMT) promoter methylation with clinical outcomes in glioblastoma and clinical strategies to modulate MGMT activity'. *J Clin Oncol*, **26** (25): 4189-99.
- Heinemann V, Xu YZ, Chubb S, Sen A, Hertel LW, Grindey GB, et al. (1992) 'Cellular elimination of 2',2'-difluorodeoxycytidine 5'-triphosphate: a mechanism of self-potentialiation'. *Cancer Res*, **52** (3): 533-9.

- Hemminki A, Mecklin JP, Jarvinen H, Aaltonen LA and Joensuu H. (2000) 'Microsatellite instability is a favorable prognostic indicator in patients with colorectal cancer receiving chemotherapy'. *Gastroenterology*, **119** (4): 921-8.
- Hentosh P, Koob R and Blakley RL. (1990) 'Incorporation of 2-halogeno-2'-deoxyadenosine 5-triphosphates into DNA during replication by human polymerases alpha and beta'. *J Biol Chem*, **265** (7): 4033-40.
- Herzog G, Lu-Hesselmann J, Zimmermann Y, Haferlach T, Hiddemann W and Dreyling M. (2005) 'Microsatellite instability and p53 mutations are characteristic of subgroups of acute myeloid leukemia but independent events'. *Haematologica*, **90** (5): 693-5.
- Hess JL, Yu BD, Li B, Hanson R and Korsmeyer SJ. (1997) 'Defects in yolk sac hematopoiesis in Mll-null embryos'. *Blood*, **90** (5): 1799-806.
- Hickman MJ and Samson LD. (1999) 'Role of DNA mismatch repair and p53 in signaling induction of apoptosis by alkylating agents'. *Proc Natl Acad Sci U S A*, **96** (19): 10764-9.
- Hirose Y, Katayama M, Stokoe D, Haas-Kogan DA, Berger MS and Pieper RO. (2003) 'The p38 mitogen-activated protein kinase pathway links the DNA mismatch repair system to the G2 checkpoint and to resistance to chemotherapeutic DNA-methylating agents'. *Mol Cell Biol*, **23** (22): 8306-15.
- Hoeijmakers JH. (2001) 'Genome maintenance mechanisms for preventing cancer'. *Nature*, **411** (6835): 366-74.
- Horiike S, Misawa S, Kaneko H, Sasai Y, Kobayashi M, Fujii H, et al. (1999) 'Distinct genetic involvement of the TP53 gene in therapy-related leukemia and myelodysplasia with chromosomal losses of Nos 5 and/or 7 and its possible relationship to replication error phenotype'. *Leukemia*, **13** (8): 1235-42.
- Horsfall MJ, Gordon AJ, Burns PA, Zielenska M, van der Vliet GM and Glickman BW. (1990) 'Mutational specificity of alkylating agents and the influence of DNA repair'. *Environ Mol Mutagen*, **15** (2): 107-22.
- Hsiang YH, Lihou MG and Liu LF. (1989) 'Arrest of replication forks by drug-stabilized topoisomerase I-DNA cleavable complexes as a mechanism of cell killing by camptothecin'. *Cancer Res*, **49** (18): 5077-82.

- Hu B, Mitra J, van den Heuvel S and Enders GH. (2001) 'S and G2 phase roles for Cdk2 revealed by inducible expression of a dominant-negative mutant in human cells'. *Mol Cell Biol*, **21** (8): 2755-66.
- Hu J, Liu YF, Wu CF, Xu F, Shen ZX, Zhu YM, et al. (2009) 'Long-term efficacy and safety of all-trans retinoic acid/arsenic trioxide-based therapy in newly diagnosed acute promyelocytic leukemia'. *Proc Natl Acad Sci U S A*, **106** (9): 3342-7.
- Huang P, Chubb S and Plunkett W. (1990) 'Termination of DNA synthesis by 9-beta-D-arabinofuranosyl-2-fluoroadenine. A mechanism for cytotoxicity'. *J Biol Chem*, **265** (27): 16617-25.
- Huang P, Chubb S, Hertel LW, Grindey GB and Plunkett W. (1991) 'Action of 2',2'-difluorodeoxycytidine on DNA synthesis'. *Cancer Res*, **51** (22): 6110-7.
- Huang Y, Yuan ZM, Ishiko T, Nakada S, Utsugisawa T, Kato T, et al. (1997) 'Pro-apoptotic effect of the c-Abl tyrosine kinase in the cellular response to 1-beta-D-arabinofuranosylcytosine'. *Oncogene*, **15** (16): 1947-52.
- Hubeek I, Stam RW, Peters GJ, Broekhuizen R, Meijerink JP, van Wering ER, et al. (2005) 'The human equilibrative nucleoside transporter 1 mediates in vitro cytarabine sensitivity in childhood acute myeloid leukaemia'. *Br J Cancer*, **93** (12): 1388-94.
- Humbert O, Fiumicino S, Aquilina G, Branch P, Oda S, Zijno A, et al. (1999) 'Mismatch repair and differential sensitivity of mouse and human cells to methylating agents'. *Carcinogenesis*, **20** (2): 205-14.
- Illmer T, Thiede C, Fredersdorf A, Stadler S, Neubauer A, Ehninger G, et al. (2005) 'Activation of the RAS pathway is predictive for a chemosensitive phenotype of acute myelogenous leukemia blasts'. *Clin Cancer Res*, **11** (9): 3217-24.
- Indraccolo S, Minuzzo S, Nicoletti L, Cretella E, Simon M, Papakonstantinou G, et al. (1999) 'Mutator phenotype in human hematopoietic neoplasms and its association with deletions disabling DNA repair genes and bcl-2 rearrangements'. *Blood*, **94** (7): 2424-32.
- Irving JA and Hall AG. (2001) 'Mismatch repair defects as a cause of resistance to cytotoxic drugs'. *Expert Rev Anticancer Ther*, **1** (1): 149-58.

- Issaeva N, Thomas HD, Djureinovic T, Jaspers JE, Stoimenov I, Kyle S, et al. (2010) '6-thioguanine selectively kills BRCA2-defective tumors and overcomes PARP inhibitor resistance'. *Cancer Res*, **70** (15): 6268-76.
- Iwasaki H, Huang P, Keating MJ and Plunkett W. (1997) 'Differential incorporation of ara-C, gemcitabine, and fludarabine into replicating and repairing DNA in proliferating human leukemia cells'. *Blood*, **90** (1): 270-8.
- Jackson GH. (2004) 'Use of fludarabine in the treatment of acute myeloid leukemia'. *Hematol J*, **5 Suppl 1** S62-7.
- Jeong C, Cho WK, Song KM, Cook C, Yoon TY, Ban C, et al. (2011) 'MutS switches between two fundamentally distinct clamps during mismatch repair'. *Nat Struct Mol Biol*, **18** (3): 379-85.
- Jiang HY, Hickey RJ, Abdel-Aziz W and Malkas LH. (2000) 'Effects of gemcitabine and araC on in vitro DNA synthesis mediated by the human breast cell DNA synthesome'. *Cancer Chemother Pharmacol*, **45** (4): 320-8.
- Jiang Z, Jin S, Yalowich JC, Brown KD and Rajasekaran B. (2010) 'The mismatch repair system modulates curcumin sensitivity through induction of DNA strand breaks and activation of G2-M checkpoint'. *Mol Cancer Ther*, **9** (3): 558-68.
- Jones PA, Baker MS and Benedict WF. (1976) 'The effect of 1-beta-D-arabinofuranosylcytosine on cell viability, DNA synthesis, and chromatid breakage in synchronized hamster fibrosarcoma cells'. *Cancer Res*, **36** (10): 3789-97.
- Jongen-Lavrencic M, Sun SM, Dijkstra MK, Valk PJ and Lowenberg B. (2008) 'MicroRNA expression profiling in relation to the genetic heterogeneity of acute myeloid leukemia'. *Blood*, **111** (10): 5078-85.
- Joslin JM, Fernald AA, Tennant TR, Davis EM, Kogan SC, Anastasi J, et al. (2007) 'Haploinsufficiency of EGR1, a candidate gene in the del(5q), leads to the development of myeloid disorders'. *Blood*, **110** (2): 719-26.
- Josting A, Wiedenmann S, Franklin J, May M, Sieber M, Wolf J, et al. (2003) 'Secondary myeloid leukemia and myelodysplastic syndromes in patients treated for Hodgkin's disease: a report from the German Hodgkin's Lymphoma Study Group'. *J Clin Oncol*, **21** (18): 3440-6.

- Jover R, Zapater P, Castells A, Llor X, Andreu M, Cubiella J, et al. (2006) 'Mismatch repair status in the prediction of benefit from adjuvant fluorouracil chemotherapy in colorectal cancer'. *Gut*, **55** (6): 848-55.
- Kadyrov FA, Dzantiev L, Constantin N and Modrich P. (2006) 'Endonucleolytic function of MutL α in human mismatch repair'. *Cell*, **126** (2): 297-308.
- Kaina B, Fritz G, Mitra S and Coquerelle T. (1991) 'Transfection and expression of human O6-methylguanine-DNA methyltransferase (MGMT) cDNA in Chinese hamster cells: the role of MGMT in protection against the genotoxic effects of alkylating agents'. *Carcinogenesis*, **12** (10): 1857-67.
- Kaina B, Ziouta A, Ochs K and Coquerelle T. (1997) 'Chromosomal instability, reproductive cell death and apoptosis induced by O6-methylguanine in Mex-, Mex+ and methylation-tolerant mismatch repair compromised cells: facts and models'. *Mutat Res*, **381** (2): 227-41.
- Kakizuka A, Miller WH, Jr., Umesono K, Warrell RP, Jr., Frankel SR, Murty VV, et al. (1991) 'Chromosomal translocation t(15;17) in human acute promyelocytic leukemia fuses RAR alpha with a novel putative transcription factor, PML'. *Cell*, **66** (4): 663-74.
- Kanno S, Higurashi A, Watanabe Y, Shouji A, Asou K and Ishikawa M. (2004) 'Susceptibility to cytosine arabinoside (Ara-C)-induced cytotoxicity in human leukemia cell lines'. *Toxicol Lett*, **152** (2): 149-58.
- Kanno S, Hiura T, Ohtake T, Koiwai K, Suzuki H, Ujibe M, et al. (2007) 'Characterization of resistance to cytosine arabinoside (Ara-C) in NALM-6 human B leukemia cells'. *Clin Chim Acta*, **377** (1-2): 144-9.
- Kantarjian HM, Keating MJ, Walters RS, Smith TL, Cork A, McCredie KB, et al. (1986) 'Therapy-related leukemia and myelodysplastic syndrome: clinical, cytogenetic, and prognostic features'. *J Clin Oncol*, **4** (12): 1748-57.
- Karnitz LM, Flatten KS, Wagner JM, Loegering D, Hackbarth JS, Arlander SJ, et al. (2005) 'Gemcitabine-induced activation of checkpoint signaling pathways that affect tumor cell survival'. *Mol Pharmacol*, **68** (6): 1636-44.
- Karran P and Bignami M. (1994) 'DNA damage tolerance, mismatch repair and genome instability'. *Bioessays*, **16** (11): 833-9.

- Karran P. (2001) 'Mechanisms of tolerance to DNA damaging therapeutic drugs'. *Carcinogenesis*, **22** (12): 1931-7.
- Karran P, Offman J and Bignami M. (2003) 'Human mismatch repair, drug-induced DNA damage, and secondary cancer'. *Biochimie*, **85** (11): 1149-60.
- Karran P and Attard N. (2008) 'Thiopurines in current medical practice: molecular mechanisms and contributions to therapy-related cancer'. *Nat Rev Cancer*, **8** (1): 24-36.
- Kastan MB and Bartek J. (2004) 'Cell-cycle checkpoints and cancer'. *Nature*, **432** (7015): 316-23.
- Kat A, Thilly WG, Fang WH, Longley MJ, Li GM and Modrich P. (1993) 'An alkylation-tolerant, mutator human cell line is deficient in strand-specific mismatch repair'. *Proc Natl Acad Sci U S A*, **90** (14): 6424-8.
- Kayser S, Dohner K, Krauter J, Kohne CH, Horst HA, Held G, et al. (2011) 'The impact of therapy-related acute myeloid leukemia (AML) on outcome in 2853 adult patients with newly diagnosed AML'. *Blood*, **117** (7): 2137-45.
- Kelly LM and Gilliland DG. (2002) 'Genetics of myeloid leukemias'. *Annu Rev Genomics Hum Genet*, **3** 179-98.
- Kendall HE, Vacek PM, Rivers JL, Rice SC, Messier TL and Finette BA. (2006) 'Analysis of genetic alterations and clonal proliferation in children treated for acute lymphocytic leukemia'. *Cancer Res*, **66** (17): 8455-61.
- Kern W, Haferlach T, Schnittger S, Ludwig WD, Hiddemann W and Schoch C. (2002) 'Karyotype instability between diagnosis and relapse in 117 patients with acute myeloid leukemia: implications for resistance against therapy'. *Leukemia*, **16** (10): 2084-91.
- Kim WJ, Rajasekaran B and Brown KD. (2007) 'MLH1- and ATM-dependent MAPK signaling is activated through c-Abl in response to the alkylator N-methyl-N'-nitro-N'-nitrosoguanidine'. *J Biol Chem*, **282** (44): 32021-31.
- Klapacz J, Meira LB, Luchetti DG, Calvo JA, Bronson RT, Edelman W, et al. (2009) 'O6-methylguanine-induced cell death involves exonuclease 1 as well as DNA mismatch recognition in vivo'. *Proc Natl Acad Sci U S A*, **106** (2): 576-81.

- Kleczkowska HE, Marra G, Lettieri T and Jiricny J. (2001) 'hMSH3 and hMSH6 interact with PCNA and colocalize with it to replication foci'. *Genes Dev*, **15** (6): 724-36.
- Koi M, Umar A, Chauhan DP, Cherian SP, Carethers JM, Kunkel TA, et al. (1994) 'Human chromosome 3 corrects mismatch repair deficiency and microsatellite instability and reduces N-methyl-N'-nitro-N-nitrosoguanidine tolerance in colon tumor cells with homozygous hMLH1 mutation'. *Cancer Res*, **54** (16): 4308-12.
- Kolas NK and Cohen PE. (2004) 'Novel and diverse functions of the DNA mismatch repair family in mammalian meiosis and recombination'. *Cytogenet Genome Res*, **107** (3-4): 216-31.
- Koo HM, McWilliams MJ, Alvord WG and Vande Woude GF. (1999) 'Ras oncogene-induced sensitization to 1-beta-D-arabinofuranosylcytosine'. *Cancer Res*, **59** (24): 6057-62.
- Kottaridis PD, Gale RE, Langabeer SE, Frew ME, Bowen DT and Linch DC. (2002) 'Studies of FLT3 mutations in paired presentation and relapse samples from patients with acute myeloid leukemia: implications for the role of FLT3 mutations in leukemogenesis, minimal residual disease detection, and possible therapy with FLT3 inhibitors'. *Blood*, **100** (7): 2393-8.
- Krishnan A, Bhatia S, Slovak ML, Arber DA, Niland JC, Nademanee A, et al. (2000) 'Predictors of therapy-related leukemia and myelodysplasia following autologous transplantation for lymphoma: an assessment of risk factors'. *Blood*, **95** (5): 1588-93.
- Kufe DW, Major PP, Egan EM and Beardsley GP. (1980) 'Correlation of cytotoxicity with incorporation of ara-C into DNA'. *J Biol Chem*, **255** (19): 8997-900.
- Kufe DW, Weichselbaum R, Egan EM, Dahlberg W and Fram RJ. (1984) 'Lethal effects of 1-beta-D-arabinofuranosylcytosine incorporation into deoxyribonucleic acid during ultraviolet repair'. *Mol Pharmacol*, **25** (2): 322-6.
- Lahue RS, Au KG and Modrich P. (1989) 'DNA mismatch correction in a defined system'. *Science*, **245** (4914): 160-4.
- Lamarche BJ, Orazio NI and Weitzman MD. (2010) 'The MRN complex in double-strand break repair and telomere maintenance'. *FEBS Lett*, **584** (17): 3682-95.

- Lamberti C, Lundin S, Bogdanow M, Pagenstecher C, Friedrichs N, Buttner R, et al. (2007) 'Microsatellite instability did not predict individual survival of unselected patients with colorectal cancer'. *Int J Colorectal Dis*, **22** (2): 145-52.
- Lan L, Hayashi T, Rabeya RM, Nakajima S, Kanno S, Takao M, et al. (2004) 'Functional and physical interactions between ERCC1 and MSH2 complexes for resistance to cis-diamminedichloroplatinum(II) in mammalian cells'. *DNA Repair (Amst)*, **3** (2): 135-43.
- Larson ED, Iams K and Drummond JT. (2003) 'Strand-specific processing of 8-oxoguanine by the human mismatch repair pathway: inefficient removal of 8-oxoguanine paired with adenine or cytosine'. *DNA Repair (Amst)*, **2** (11): 1199-210.
- Larson RA, Sievers EL, Stadtmauer EA, Lowenberg B, Estey EH, Dombret H, et al. (2005) 'Final report of the efficacy and safety of gemtuzumab ozogamicin (Mylotarg) in patients with CD33-positive acute myeloid leukemia in first recurrence'. *Cancer*, **104** (7): 1442-52.
- Larson RA. (2007) 'Etiology and management of therapy-related myeloid leukemia'. *Hematology Am Soc Hematol Educ Program*, 453-9.
- Lau PJ and Kolodner RD. (2003) 'Transfer of the MSH2.MSH6 complex from proliferating cell nuclear antigen to mispaired bases in DNA'. *J Biol Chem*, **278** (1): 14-7.
- Le Beau MM, Larson RA, Bitter MA, Vardiman JW, Golomb HM and Rowley JD. (1983) 'Association of an inversion of chromosome 16 with abnormal marrow eosinophils in acute myelomonocytic leukemia. A unique cytogenetic-clinicopathological association'. *N Engl J Med*, **309** (11): 630-6.
- Le Beau MM, Espinosa R, 3rd, Davis EM, Eisenbart JD, Larson RA and Green ED. (1996) 'Cytogenetic and molecular delineation of a region of chromosome 7 commonly deleted in malignant myeloid diseases'. *Blood*, **88** (6): 1930-5.
- Ley TJ, Mardis ER, Ding L, Fulton B, McLellan MD, Chen K, et al. (2008) 'DNA sequencing of a cytogenetically normal acute myeloid leukaemia genome'. *Nature*, **456** (7218): 66-72.

- Li F, Liu Q, Chen YY, Yu ZN, Zhang ZP, Zhou YF, et al. (2008a) 'Escherichia coli mismatch repair protein MutL interacts with the clamp loader subunits of DNA polymerase III'. *Mutat Res*, **637** (1-2): 101-10.
- Li GM and Modrich P. (1995) 'Restoration of mismatch repair to nuclear extracts of H6 colorectal tumor cells by a heterodimer of human MutL homologs'. *Proc Natl Acad Sci U S A*, **92** (6): 1950-4.
- Li GM. (2008) 'Mechanisms and functions of DNA mismatch repair'. *Cell Res*, **18** (1): 85-98.
- Li LS, Morales JC, Hwang A, Wagner MW and Boothman DA. (2008b) 'DNA mismatch repair-dependent activation of c-Abl/p73alpha/GADD45alpha-mediated apoptosis'. *J Biol Chem*, **283** (31): 21394-403.
- Li Z, Lu J, Sun M, Mi S, Zhang H, Luo RT, et al. (2008c) 'Distinct microRNA expression profiles in acute myeloid leukemia with common translocations'. *Proc Natl Acad Sci U S A*, **105** (40): 15535-40.
- Liber HL and Thilly WG. (1982) 'Mutation assay at the thymidine kinase locus in diploid human lymphoblasts'. *Mutat Res*, **94** (2): 467-85.
- Libura J, Slater DJ, Felix CA and Richardson C. (2005) 'Therapy-related acute myeloid leukemia-like MLL rearrangements are induced by etoposide in primary human CD34+ cells and remain stable after clonal expansion'. *Blood*, **105** (5): 2124-31.
- Lin DP, Wang Y, Scherer SJ, Clark AB, Yang K, Avdievich E, et al. (2004) 'An Msh2 point mutation uncouples DNA mismatch repair and apoptosis'. *Cancer Res*, **64** (2): 517-22.
- Linenberger ML. (2005) 'CD33-directed therapy with gemtuzumab ozogamicin in acute myeloid leukemia: progress in understanding cytotoxicity and potential mechanisms of drug resistance'. *Leukemia*, **19** (2): 176-82.
- Ling YH, Nelson JA, Cheng YC, Anderson RS and Beattie KL. (1991) '2'-Deoxy-6-thioguanosine 5'-triphosphate as a substrate for purified human DNA polymerases and calf thymus terminal deoxynucleotidyltransferase in vitro'. *Mol Pharmacol*, **40** (4): 508-14.

- Liu A, Yoshioka K, Salerno V and Hsieh P. (2008) 'The mismatch repair-mediated cell cycle checkpoint response to fluorodeoxyuridine'. *J Cell Biochem*, **105** (1): 245-54.
- Liu P, Tarle SA, Hajra A, Claxton DF, Marlton P, Freedman M, et al. (1993) 'Fusion between transcription factor CBF beta/PEBP2 beta and a myosin heavy chain in acute myeloid leukemia'. *Science*, **261** (5124): 1041-4.
- Liu TX, Becker MW, Jelinek J, Wu WS, Deng M, Mikhalkevich N, et al. (2007) 'Chromosome 5q deletion and epigenetic suppression of the gene encoding alpha-catenin (CTNNA1) in myeloid cell transformation'. *Nat Med*, **13** (1): 78-83.
- Liu Y, Nairn RS and Vasquez KM. (2009) 'Targeted gene conversion induced by triplex-directed psoralen interstrand crosslinks in mammalian cells'. *Nucleic Acids Res*, **37** (19): 6378-88.
- Livak KJ and Schmittgen TD. (2001) 'Analysis of relative gene expression data using real-time quantitative PCR and the 2^{-Delta Delta C(T)} Method'. *Methods*, **25** (4): 402-8.
- Lo-Coco F, Cimino G, Breccia M, Noguera NI, Diverio D, Finolezzi E, et al. (2004) 'Gemtuzumab ozogamicin (Mylotarg) as a single agent for molecularly relapsed acute promyelocytic leukemia'. *Blood*, **104** (7): 1995-9.
- Loegering D, Arlander SJ, Hackbarth J, Vroman BT, Roos-Mattjus P, Hopkins KM, et al. (2004) 'Rad9 protects cells from topoisomerase poison-induced cell death'. *J Biol Chem*, **279** (18): 18641-7.
- Longley DB, Harkin DP and Johnston PG. (2003) '5-fluorouracil: mechanisms of action and clinical strategies'. *Nat Rev Cancer*, **3** (5): 330-8.
- Longley MJ, Pierce AJ and Modrich P. (1997) 'DNA polymerase delta is required for human mismatch repair in vitro'. *J Biol Chem*, **272** (16): 10917-21.
- Lundin C, Erixon K, Arnaudeau C, Schultz N, Jessen D, Meuth M, et al. (2002) 'Different roles for nonhomologous end joining and homologous recombination following replication arrest in mammalian cells'. *Mol Cell Biol*, **22** (16): 5869-78.
- Lyndaker AM and Alani E. (2009) 'A tale of tails: insights into the coordination of 3' end processing during homologous recombination'. *Bioessays*, **31** (3): 315-21.

- Macpherson P, Barone F, Maga G, Mazzei F, Karran P and Bignami M. (2005) '8-oxoguanine incorporation into DNA repeats in vitro and mismatch recognition by MutSalpha'. *Nucleic Acids Res*, **33** (16): 5094-105.
- Major PP, Egan EM, Beardsley GP, Minden MD and Kufe DW. (1981) 'Lethality of human myeloblasts correlates with the incorporation of arabinofuranosylcytosine into DNA'. *Proc Natl Acad Sci U S A*, **78** (5): 3235-9.
- Marcucci G, Radmacher MD, Maharry K, Mrozek K, Ruppert AS, Paschka P, et al. (2008a) 'MicroRNA expression in cytogenetically normal acute myeloid leukemia'. *N Engl J Med*, **358** (18): 1919-28.
- Marcucci G, Maharry K, Radmacher MD, Mrozek K, Vukosavljevic T, Paschka P, et al. (2008b) 'Prognostic significance of, and gene and microRNA expression signatures associated with, CEBPA mutations in cytogenetically normal acute myeloid leukemia with high-risk molecular features: a Cancer and Leukemia Group B Study'. *J Clin Oncol*, **26** (31): 5078-87.
- Marcucci G, Radmacher MD, Mrozek K and Bloomfield CD. (2009) 'MicroRNA expression in acute myeloid leukemia'. *Curr Hematol Malig Rep*, **4** (2): 83-8.
- Mardis ER, Ding L, Dooling DJ, Larson DE, McLellan MD, Chen K, et al. (2009) 'Recurring mutations found by sequencing an acute myeloid leukemia genome'. *N Engl J Med*, **361** (11): 1058-66.
- Margison GP and Santibanez-Koref MF. (2002) 'O6-alkylguanine-DNA alkyltransferase: role in carcinogenesis and chemotherapy'. *Bioessays*, **24** (3): 255-66.
- Mariano AR, Colombo E, Luzi L, Martinelli P, Volorio S, Bernard L, et al. (2006) 'Cytoplasmic localization of NPM in myeloid leukemias is dictated by gain-of-function mutations that create a functional nuclear export signal'. *Oncogene*, **25** (31): 4376-80.
- Marquez N, Chappell SC, Sansom OJ, Clarke AR, Court J, Errington RJ, et al. (2003) 'Single cell tracking reveals that Msh2 is a key component of an early-acting DNA damage-activated G2 checkpoint'. *Oncogene*, **22** (48): 7642-8.
- Marra G, Iaccarino I, Lettieri T, Roscilli G, Delmastro P and Jiricny J. (1998) 'Mismatch repair deficiency associated with overexpression of the MSH3 gene'. *Proc Natl Acad Sci U S A*, **95** (15): 8568-73.

- Martin-Salces M, Canales MA, de Paz R and Hernandez-Navarro F. (2007) 'Treatment-related acute myeloid leukemia with 11q23 translocation following treatment with fludarabine, cyclophosphamide and rituximab'. *Leuk Res*,
- Martin LM, Marples B, Coffey M, Lawler M, Lynch TH, Hollywood D, et al. (2010) 'DNA mismatch repair and the DNA damage response to ionizing radiation: making sense of apparently conflicting data'. *Cancer Treat Rev*, **36** (7): 518-27.
- Martin SA, Lord CJ and Ashworth A. (2008) 'DNA repair deficiency as a therapeutic target in cancer'. *Curr Opin Genet Dev*, **18** (1): 80-6.
- Martin SA, McCarthy A, Barber LJ, Burgess DJ, Parry S, Lord CJ, et al. (2009) 'Methotrexate induces oxidative DNA damage and is selectively lethal to tumour cells with defects in the DNA mismatch repair gene MSH2'. *EMBO Mol Med*, **1** (6-7): 323-37.
- Maruta H and Burgess AW. (1994) 'Regulation of the Ras signalling network'. *Bioessays*, **16** (7): 489-96.
- Matheson EC, Hogarth LA, Case MC, Irving JA and Hall AG. (2007) 'DHFR and MSH3 co-amplification in childhood acute lymphoblastic leukaemia, in vitro and in vivo'. *Carcinogenesis*, **28** (6): 1341-6.
- Matsuda A and Sasaki T. (2004) 'Antitumor activity of sugar-modified cytosine nucleosides'. *Cancer Sci*, **95** (2): 105-11.
- Matsumoto M, Yaginuma K, Igarashi A, Imura M, Hasegawa M, Iwabuchi K, et al. (2007) 'Perturbed gap-filling synthesis in nucleotide excision repair causes histone H2AX phosphorylation in human quiescent cells'. *J Cell Sci*, **120** (Pt 6): 1104-12.
- Mazurek A, Berardini M and Fishel R. (2002) 'Activation of human MutS homologs by 8-oxo-guanine DNA damage'. *J Biol Chem*, **277** (10): 8260-6.
- McLaughlin P, Estey E, Glassman A, Romaguera J, Samaniego F, Ayala A, et al. (2005) 'Myelodysplasia and acute myeloid leukemia following therapy for indolent lymphoma with fludarabine, mitoxantrone, and dexamethasone (FND) plus rituximab and interferon alpha'. *Blood*, **105** (12): 4573-5.
- Meikrantz W, Bergom MA, Memisoglu A and Samson L. (1998) 'O6-alkylguanine DNA lesions trigger apoptosis'. *Carcinogenesis*, **19** (2): 369-72.

- Meloche S and Pouyssegur J. (2007) 'The ERK1/2 mitogen-activated protein kinase pathway as a master regulator of the G1- to S-phase transition'. *Oncogene*, **26** (22): 3227-39.
- Meng Q, Su T, Olivero OA, Poirier MC, Shi X, Ding X, et al. (2000) 'Relationships between DNA incorporation, mutant frequency, and loss of heterozygosity at the TK locus in human lymphoblastoid cells exposed to 3'-azido-3'-deoxythymidine'. *Toxicol Sci*, **54** (2): 322-9.
- Meng Q, Su T, O'Neill JP and Walker VE. (2002) 'Molecular analysis of mutations at the HPRT and TK loci of human lymphoblastoid cells after combined treatments with 3'-azido-3'-deoxythymidine and 2',3'-dideoxyinosine'. *Environ Mol Mutagen*, **39** (4): 282-95.
- Mesa RA, Loegering D, Powell HL, Flatten K, Arlander SJ, Dai NT, et al. (2005) 'Heat shock protein 90 inhibition sensitizes acute myelogenous leukemia cells to cytarabine'. *Blood*, **106** (1): 318-27.
- Meyer M, Rubsamen D, Slany R, Illmer T, Stabla K, Roth P, et al. (2009) 'Oncogenic RAS enables DNA damage- and p53-dependent differentiation of acute myeloid leukemia cells in response to chemotherapy'. *PLoS One*, **4** (11): e7768.
- Meyers M, Wagner MW, Hwang HS, Kinsella TJ and Boothman DA. (2001) 'Role of the hMLH1 DNA mismatch repair protein in fluoropyrimidine-mediated cell death and cell cycle responses'. *Cancer Res*, **61** (13): 5193-201.
- Meyers M, Wagner MW, Mazurek A, Schmutte C, Fishel R and Boothman DA. (2005) 'DNA mismatch repair-dependent response to fluoropyrimidine-generated damage'. *J Biol Chem*, **280** (7): 5516-26.
- Mirzayans R, Dietrich K and Paterson MC. (1993) 'Aphidicolin and 1-beta-D-arabinofuranosylcytosine strongly inhibit transcriptionally active DNA repair in normal human fibroblasts'. *Carcinogenesis*, **14** (12): 2621-6.
- Miyamoto T, Weissman IL and Akashi K. (2000) 'AML1/ETO-expressing nonleukemic stem cells in acute myelogenous leukemia with 8;21 chromosomal translocation'. *Proc Natl Acad Sci U S A*, **97** (13): 7521-6.

- Mo JY, Maki H and Sekiguchi M. (1992) 'Hydrolytic elimination of a mutagenic nucleotide, 8-oxodGTP, by human 18-kilodalton protein: sanitization of nucleotide pool'. *Proc Natl Acad Sci U S A*, **89** (22): 11021-5.
- Mojas N, Lopes M and Jiricny J. (2007) 'Mismatch repair-dependent processing of methylation damage gives rise to persistent single-stranded gaps in newly replicated DNA'. *Genes Dev*, **21** (24): 3342-55.
- Morrison C, Sonoda E, Takao N, Shinohara A, Yamamoto K and Takeda S. (2000) 'The controlling role of ATM in homologous recombinational repair of DNA damage'. *Embo J*, **19** (3): 463-71.
- Morrison VA, Rai KR, Peterson BL, Kolitz JE, Elias L, Appelbaum FR, et al. (2002) 'Therapy-related myeloid leukemias are observed in patients with chronic lymphocytic leukemia after treatment with fludarabine and chlorambucil: results of an intergroup study, cancer and leukemia group B 9011'. *J Clin Oncol*, **20** (18): 3878-84.
- Mrozek K, Heerema NA and Bloomfield CD. (2004) 'Cytogenetics in acute leukemia'. *Blood Rev*, **18** (2): 115-36.
- Mullighan CG, Phillips LA, Su X, Ma J, Miller CB, Shurtleff SA, et al. (2008) 'Genomic analysis of the clonal origins of relapsed acute lymphoblastic leukemia'. *Science*, **322** (5906): 1377-80.
- Naoe T, Takeyama K, Yokozawa T, Kiyoi H, Seto M, Uike N, et al. (2000) 'Analysis of genetic polymorphism in NQO1, GST-M1, GST-T1, and CYP3A4 in 469 Japanese patients with therapy-related leukemia/ myelodysplastic syndrome and de novo acute myeloid leukemia'. *Clin Cancer Res*, **6** (10): 4091-5.
- Neff T and Blau CA. (1996) 'Forced expression of cytidine deaminase confers resistance to cytosine arabinoside and gemcitabine'. *Exp Hematol*, **24** (11): 1340-6.
- Nehme A, Baskaran R, Aebi S, Fink D, Nebel S, Cenni B, et al. (1997) 'Differential induction of c-Jun NH2-terminal kinase and c-Abl kinase in DNA mismatch repair-proficient and -deficient cells exposed to cisplatin'. *Cancer Res*, **57** (15): 3253-7.
- Nehme A, Baskaran R, Nebel S, Fink D, Howell SB, Wang JY, et al. (1999) 'Induction of JNK and c-Abl signalling by cisplatin and oxaliplatin in mismatch repair-proficient and -deficient cells'. *Br J Cancer*, **79** (7-8): 1104-10.

- Neubauer A, Maharry K, Mrozek K, Thiede C, Marcucci G, Paschka P, et al. (2008) 'Patients with acute myeloid leukemia and RAS mutations benefit most from postremission high-dose cytarabine: a Cancer and Leukemia Group B study'. *J Clin Oncol*, **26** (28): 4603-9.
- Newton K and Hill J. (2010) '5-FU and mismatch repair deficient colorectal cancer: is it time to consider a change in practice?'. *Colorectal Dis*, **12** (7): 706-7.
- Nomdedeu JF, Perea G, Estivill C, Lasa A, Carnicer MJ, Brunet S, et al. (2005) 'Microsatellite instability is not an uncommon finding in adult de novo acute myeloid leukemia'. *Ann Hematol*, **84** (6): 368-75.
- O'Neill JP, Rogan PK, Cariello N and Nicklas JA. (1998) 'Mutations that alter RNA splicing of the human HPRT gene: a review of the spectrum'. *Mutat Res*, **411** (3): 179-214.
- Offman J, Opelz G, Doehler B, Cummins D, Halil O, Banner NR, et al. (2004) 'Defective DNA mismatch repair in acute myeloid leukemia/myelodysplastic syndrome after organ transplantation'. *Blood*, **104** (3): 822-8.
- Offman J, Gascoigne K, Bristow F, Macpherson P, Bignami M, Casorelli I, et al. (2005) 'Repeated sequences in CASPASE-5 and FANCD2 but not NF1 are targets for mutation in microsatellite-unstable acute leukemia/myelodysplastic syndrome'. *Mol Cancer Res*, **3** (5): 251-60.
- Ohno Y, Spriggs D, Matsukage A, Ohno T and Kufe D. (1988) 'Effects of 1-beta-D-arabinofuranosylcytosine incorporation on elongation of specific DNA sequences by DNA polymerase beta'. *Cancer Res*, **48** (6): 1494-8.
- Ohyashiki JH, Ohyashiki K, Aizawa S, Kawakubo K, Shimamoto T, Iwama H, et al. (1996) 'Replication errors in hematological neoplasias: genomic instability in progression of disease is different among different types of leukemia'. *Clin Cancer Res*, **2** (9): 1583-9.
- Okuda T, van Deursen J, Hiebert SW, Grosveld G and Downing JR. (1996) 'AML1, the target of multiple chromosomal translocations in human leukemia, is essential for normal fetal liver hematopoiesis'. *Cell*, **84** (2): 321-30.

- Olipitz W, Hopfinger G, Aguiar RC, Gunsilius E, Girschikofsky M, Bodner C, et al. (2002) 'Defective DNA-mismatch repair: a potential mediator of leukemogenic susceptibility in therapy-related myelodysplasia and leukemia'. *Genes Chromosomes Cancer*, **34** (2): 243-8.
- Ottini L, Falchetti M, Saieva C, De Marco M, Masala G, Zanna I, et al. (2004) 'MRE11 expression is impaired in gastric cancer with microsatellite instability'. *Carcinogenesis*, **25** (12): 2337-43.
- Pabla N, Ma Z, McIlhatton MA, Fishel R and Dong Z. (2011) 'hMSH2 Recruits ATR to DNA Damage Sites for Activation during DNA Damage-induced Apoptosis'. *J Biol Chem*, **286** (12): 10411-8.
- Pabst T, Schwaller J, Bellomo MJ, Oestreicher M, Muhlematter D, Tichelli A, et al. (1996) 'Frequent clonal loss of heterozygosity but scarcity of microsatellite instability at chromosomal breakpoint cluster regions in adult leukemias'. *Blood*, **88** (3): 1026-34.
- Pabst T, Mueller BU, Zhang P, Radomska HS, Narravula S, Schnittger S, et al. (2001) 'Dominant-negative mutations of CEBPA, encoding CCAAT/enhancer binding protein-alpha (C/EBPalpha), in acute myeloid leukemia'. *Nat Genet*, **27** (3): 263-70.
- Pabst T and Mueller BU. (2007) 'Transcriptional dysregulation during myeloid transformation in AML'. *Oncogene*, **26** (47): 6829-37.
- Pabst T and Mueller BU. (2009) 'Complexity of CEBPA dysregulation in human acute myeloid leukemia'. *Clin Cancer Res*, **15** (17): 5303-7.
- Palombo F, Iaccarino I, Nakajima E, Ikejima M, Shimada T and Jiricny J. (1996) 'hMutSbeta, a heterodimer of hMSH2 and hMSH3, binds to insertion/deletion loops in DNA'. *Curr Biol*, **6** (9): 1181-4.
- Pandolfi PP. (2001) 'Oncogenes and tumor suppressors in the molecular pathogenesis of acute promyelocytic leukemia'. *Hum Mol Genet*, **10** (7): 769-75.
- Papadopoulos N, Nicolaides NC, Liu B, Parsons R, Lengauer C, Palombo F, et al. (1995) 'Mutations of GTBP in genetically unstable cells'. *Science*, **268** (5219): 1915-7.

- Papouli E, Cejka P and Jiricny J. (2004) 'Dependence of the cytotoxicity of DNA-damaging agents on the mismatch repair status of human cells'. *Cancer Res*, **64** (10): 3391-4.
- Paques F and Haber JE. (1997) 'Two pathways for removal of nonhomologous DNA ends during double-strand break repair in *Saccharomyces cerevisiae*'. *Mol Cell Biol*, **17** (11): 6765-71.
- Parker WB, Bapat AR, Shen JX, Townsend AJ and Cheng YC. (1988) 'Interaction of 2-halogenated dATP analogs (F, Cl, and Br) with human DNA polymerases, DNA primase, and ribonucleotide reductase'. *Mol Pharmacol*, **34** (4): 485-91.
- Parker WB, Shaddix SC, Chang CH, White EL, Rose LM, Brockman RW, et al. (1991) 'Effects of 2-chloro-9-(2-deoxy-2-fluoro-beta-D-arabinofuranosyl)adenine on K562 cellular metabolism and the inhibition of human ribonucleotide reductase and DNA polymerases by its 5'-triphosphate'. *Cancer Res*, **51** (9): 2386-94.
- Paull TT, Rogakou EP, Yamazaki V, Kirchgessner CU, Gellert M and Bonner WM. (2000) 'A critical role for histone H2AX in recruitment of repair factors to nuclear foci after DNA damage'. *Curr Biol*, **10** (15): 886-95.
- Paulsen RD and Cimprich KA. (2007) 'The ATR pathway: fine-tuning the fork'. *DNA Repair (Amst)*, **6** (7): 953-66.
- Pavlov YI and Shcherbakova PV. (2010) 'DNA polymerases at the eukaryotic fork-20 years later'. *Mutat Res*, **685** (1-2): 45-53.
- Pedersen-Bjergaard J, Andersen MK and Christiansen DH. (2000) 'Therapy-related acute myeloid leukemia and myelodysplasia after high-dose chemotherapy and autologous stem cell transplantation'. *Blood*, **95** (11): 3273-9.
- Pedersen-Bjergaard J, Andersen MT and Andersen MK. (2007) 'Genetic pathways in the pathogenesis of therapy-related myelodysplasia and acute myeloid leukemia'. *Hematology Am Soc Hematol Educ Program*, **2007** 392-7.
- Pedersen-Bjergaard J, Andersen MK, Andersen MT and Christiansen DH. (2008) 'Genetics of therapy-related myelodysplasia and acute myeloid leukemia'. *Leukemia*, **22** (2): 240-8.

- Peltomaki P. (2003) 'Role of DNA mismatch repair defects in the pathogenesis of human cancer'. *J Clin Oncol*, **21** (6): 1174-9.
- Pemble S, Schroeder KR, Spencer SR, Meyer DJ, Hallier E, Bolt HM, et al. (1994) 'Human glutathione S-transferase theta (GSTT1): cDNA cloning and the characterization of a genetic polymorphism'. *Biochem J*, **300** (Pt 1) 271-6.
- Pepponi R, Graziani G, Falcinelli S, Vernole P, Levati L, Lacal PM, et al. (2001) 'hMSH3 overexpression and cellular response to cytotoxic anticancer agents'. *Carcinogenesis*, **22** (8): 1131-7.
- Perrino FW and Mekosh HL. (1992) 'Incorporation of cytosine arabinoside monophosphate into DNA at internucleotide linkages by human DNA polymerase alpha'. *J Biol Chem*, **267** (32): 23043-51.
- Perrino FW, Miller H and Ealey KA. (1994) 'Identification of a 3'-->5'-exonuclease that removes cytosine arabinoside monophosphate from 3' termini of DNA'. *J Biol Chem*, **269** (23): 16357-63.
- Perrino FW, Mazur DJ, Ward H and Harvey S. (1999) 'Exonucleases and the incorporation of arnucleotides into DNA'. *Cell Biochem Biophys*, **30** (3): 331-52.
- Perrino FW, Blans P, Harvey S, Gelhaus SL, McGrath C, Akman SA, et al. (2003) 'The N2-ethylguanine and the O6-ethyl- and O6-methylguanine lesions in DNA: contrasting responses from the "bypass" DNA polymerase eta and the replicative DNA polymerase alpha'. *Chem Res Toxicol*, **16** (12): 1616-23.
- Petrie K and Zelent A. (2007) 'AML1/ETO, a promiscuous fusion oncoprotein'. *Blood*, **109** (10): 4109-10.
- Petrini JH. (2000) 'The Mre11 complex and ATM: collaborating to navigate S phase'. *Curr Opin Cell Biol*, **12** (3): 293-6.
- Pichierri P, Franchitto A, Piergentili R, Colussi C and Palitti F. (2001) 'Hypersensitivity to camptothecin in MSH2 deficient cells is correlated with a role for MSH2 protein in recombinational repair'. *Carcinogenesis*, **22** (11): 1781-7.
- Plosky B, Samson L, Engelward BP, Gold B, Schlaen B, Millas T, et al. (2002) 'Base excision repair and nucleotide excision repair contribute to the removal of N-methylpurines from active genes'. *DNA Repair (Amst)*, **1** (8): 683-96.

- Pluciennik A and Modrich P. (2007) 'Protein roadblocks and helix discontinuities are barriers to the initiation of mismatch repair'. *Proc Natl Acad Sci U S A*, **104** (31): 12709-13.
- Popat S, Hubner R and Houlston RS. (2005) 'Systematic review of microsatellite instability and colorectal cancer prognosis'. *J Clin Oncol*, **23** (3): 609-18.
- Pourquier P, Takebayashi Y, Urasaki Y, Gioffre C, Kohlhagen G and Pommier Y. (2000) 'Induction of topoisomerase I cleavage complexes by 1-beta -D-arabinofuranosylcytosine (ara-C) in vitro and in ara-C-treated cells'. *Proc Natl Acad Sci U S A*, **97** (4): 1885-90.
- Prakasha Gowda AS, Polizzi JM, Eckert KA and Spratt TE. (2010) 'Incorporation of gemcitabine and cytarabine into DNA by DNA polymerase beta and ligase III/XRCC1'. *Biochemistry*, **49** (23): 4833-40.
- Pui CH, Carroll WL, Meshinchi S and Arceci RJ. (2011) 'Biology, risk stratification, and therapy of pediatric acute leukemias: an update'. *J Clin Oncol*, **29** (5): 551-65.
- Qian Z, Chen L, Fernald AA, Williams BO and Le Beau MM. (2008) 'A critical role for Apc in hematopoietic stem and progenitor cell survival'. *J Exp Med*, **205** (9): 2163-75.
- Qian Z, Joslin JM, Tennant TR, Reshmi SC, Young DJ, Stoddart A, et al. (2010) 'Cytogenetic and genetic pathways in therapy-related acute myeloid leukemia'. *Chem Biol Interact*, **184** (1-2): 50-7.
- Radtke I, Mullighan CG, Ishii M, Su X, Cheng J, Ma J, et al. (2009) 'Genomic analysis reveals few genetic alterations in pediatric acute myeloid leukemia'. *Proc Natl Acad Sci U S A*, **106** (31): 12944-9.
- Raelson JV, Nervi C, Rosenauer A, Benedetti L, Monczak Y, Pearson M, et al. (1996) 'The PML/RAR alpha oncoprotein is a direct molecular target of retinoic acid in acute promyelocytic leukemia cells'. *Blood*, **88** (8): 2826-32.
- Raghavan M, Smith LL, Lillington DM, Chaplin T, Kakkas I, Molloy G, et al. (2008) 'Segmental uniparental disomy is a commonly acquired genetic event in relapsed acute myeloid leukemia'. *Blood*, **112** (3): 814-21.

- Rajesh C, Gruver AM, Basrur V and Pittman DL. (2009) 'The interaction profile of homologous recombination repair proteins RAD51C, RAD51D and XRCC2 as determined by proteomic analysis'. *Proteomics*, **9** (16): 4071-86.
- Rajesh P, Litvinchuk AV, Pittman DL and Wyatt MD. (2011) 'The homologous recombination protein RAD51D mediates the processing of 6-thioguanine lesions downstream of mismatch repair'. *Mol Cancer Res*, **9** (2): 206-14.
- Ramilo C, Gu L, Guo S, Zhang X, Patrick SM, Turchi JJ, et al. (2002) 'Partial reconstitution of human DNA mismatch repair in vitro: characterization of the role of human replication protein A'. *Mol Cell Biol*, **22** (7): 2037-46.
- Rathe SK and Largaespada DA. (2010) 'Deoxycytidine kinase is downregulated in Ara-C-resistant acute myeloid leukemia murine cell lines'. *Leukemia*, **24** (8): 1513-5.
- Rayssiguier C, Thaler DS and Radman M. (1989) 'The barrier to recombination between *Escherichia coli* and *Salmonella typhimurium* is disrupted in mismatch-repair mutants'. *Nature*, **342** (6248): 396-401.
- Rebbeck TR, Jaffe JM, Walker AH, Wein AJ and Malkowicz SB. (1998) 'Modification of clinical presentation of prostate tumors by a novel genetic variant in CYP3A4'. *J Natl Cancer Inst*, **90** (16): 1225-9.
- Reese JS, Liu L and Gerson SL. (2003) 'Repopulating defect of mismatch repair-deficient hematopoietic stem cells'. *Blood*, **102** (5): 1626-33.
- Reilly JT. (2005) 'Pathogenesis of acute myeloid leukaemia and inv(16)(p13;q22): a paradigm for understanding leukaemogenesis?'. *Br J Haematol*, **128** (1): 18-34.
- Renneville A, Roumier C, Biggio V, Nibourel O, Boissel N, Fenaux P, et al. (2008) 'Cooperating gene mutations in acute myeloid leukemia: a review of the literature'. *Leukemia*, **22** (5): 915-31.
- Ribic CM, Sargent DJ, Moore MJ, Thibodeau SN, French AJ, Goldberg RM, et al. (2003) 'Tumor microsatellite-instability status as a predictor of benefit from fluorouracil-based adjuvant chemotherapy for colon cancer'. *N Engl J Med*, **349** (3): 247-57.
- Richardson C and Jasin M. (2000) 'Frequent chromosomal translocations induced by DNA double-strand breaks'. *Nature*, **405** (6787): 697-700.

- Richardson KA, Vega TP, Richardson FC, Moore CL, Rohloff JC, Tomkinson B, et al. (2004) 'Polymerization of the triphosphates of AraC, 2',2'-difluorodeoxycytidine (dFdC) and OSI-7836 (T-araC) by human DNA polymerase alpha and DNA primase'. *Biochem Pharmacol*, **68** (12): 2337-46.
- Rimsza LM, Kopecky KJ, Ruschulte J, Chen IM, Slovak ML, Karanes C, et al. (2000) 'Microsatellite instability is not a defining genetic feature of acute myeloid leukemogenesis in adults: results of a retrospective study of 132 patients and review of the literature'. *Leukemia*, **14** (6): 1044-51.
- Robak T and Wierzbowska A. (2009) 'Current and emerging therapies for acute myeloid leukemia'. *Clin Ther*, **31 Pt 2** 2349-70.
- Roos W, Baumgartner M and Kaina B. (2004) 'Apoptosis triggered by DNA damage O6-methylguanine in human lymphocytes requires DNA replication and is mediated by p53 and Fas/CD95/Apo-1'. *Oncogene*, **23** (2): 359-67.
- Roos WP and Kaina B. (2006) 'DNA damage-induced cell death by apoptosis'. *Trends Mol Med*, **12** (9): 440-50.
- Rothkamm K, Kruger I, Thompson LH and Lobrich M. (2003) 'Pathways of DNA double-strand break repair during the mammalian cell cycle'. *Mol Cell Biol*, **23** (16): 5706-15.
- Rowley JD and Olney HJ. (2002) 'International workshop on the relationship of prior therapy to balanced chromosome aberrations in therapy-related myelodysplastic syndromes and acute leukemia: overview report'. *Genes Chromosomes Cancer*, **33** (4): 331-45.
- Rund D, Krichevsky S, Bar-Cohen S, Goldschmidt N, Kedmi M, Malik E, et al. (2005) 'Therapy-related leukemia: clinical characteristics and analysis of new molecular risk factors in 96 adult patients'. *Leukemia*, **19** (11): 1919-28.
- Russo MT, Blasi MF, Chiera F, Fortini P, Degan P, Macpherson P, et al. (2004) 'The oxidized deoxynucleoside triphosphate pool is a significant contributor to genetic instability in mismatch repair-deficient cells'. *Mol Cell Biol*, **24** (1): 465-74.
- Russo MT, De Luca G, Degan P and Bignami M. (2007) 'Different DNA repair strategies to combat the threat from 8-oxoguanine'. *Mutat Res*, **614** (1-2): 69-76.

- Samimi G, Fink D, Varki NM, Husain A, Hoskins WJ, Alberts DS, et al. (2000) 'Analysis of MLH1 and MSH2 expression in ovarian cancer before and after platinum drug-based chemotherapy'. *Clin Cancer Res*, **6** (4): 1415-21.
- Sanderson RN, Johnson PR, Moorman AV, Roman E, Willett E, Taylor PR, et al. (2006) 'Population-based demographic study of karyotypes in 1709 patients with adult acute myeloid leukemia'. *Leukemia*, **20** (3): 444-50.
- Sasai Y, Horiike S, Misawa S, Kaneko H, Kobayashi M, Fujii H, et al. (1999) 'Genotype of glutathione S-transferase and other genetic configurations in myelodysplasia'. *Leuk Res*, **23** (11): 975-81.
- Schnell JR, Dyson HJ and Wright PE. (2004) 'Structure, dynamics, and catalytic function of dihydrofolate reductase'. *Annu Rev Biophys Biomol Struct*, **33** 119-40.
- Schoch C, Schnittger S, Klaus M, Kern W, Hiddemann W and Haferlach T. (2003) 'AML with 11q23/MLL abnormalities as defined by the WHO classification: incidence, partner chromosomes, FAB subtype, age distribution, and prognostic impact in an unselected series of 1897 cytogenetically analyzed AML cases'. *Blood*, **102** (7): 2395-402.
- Schonfeld SJ, Gilbert ES, Dores GM, Lynch CF, Hodgson DC, Hall P, et al. (2006) 'Acute myeloid leukemia following Hodgkin lymphoma: a population-based study of 35,511 patients'. *J Natl Cancer Inst*, **98** (3): 215-8.
- Schweitzer BI, Dicker AP and Bertino JR. (1990) 'Dihydrofolate reductase as a therapeutic target'. *FASEB J*, **4** (8): 2441-52.
- Schweitzer BI, Mikita T, Kellogg GW, Gardner KH and Beardsley GP. (1994) 'Solution structure of a DNA dodecamer containing the anti-neoplastic agent arabinosylcytosine: combined use of NMR, restrained molecular dynamics, and full relaxation matrix refinement'. *Biochemistry*, **33** (38): 11460-75.
- Scolnik MP, Morilla R, de Bracco MM, Catovsky D and Matutes E. (2002) 'CD34 and CD117 are overexpressed in AML and may be valuable to detect minimal residual disease'. *Leuk Res*, **26** (7): 615-9.

- Seedhouse C, Bainton R, Lewis M, Harding A, Russell N and Das-Gupta E. (2002) 'The genotype distribution of the XRCC1 gene indicates a role for base excision repair in the development of therapy-related acute myeloblastic leukemia'. *Blood*, **100** (10): 3761-6.
- Seedhouse C, Faulkner R, Ashraf N, Das-Gupta E and Russell N. (2004) 'Polymorphisms in genes involved in homologous recombination repair interact to increase the risk of developing acute myeloid leukemia'. *Clin Cancer Res*, **10** (8): 2675-80.
- Seedhouse C and Russell N. (2007) 'Advances in the understanding of susceptibility to treatment-related acute myeloid leukaemia'. *Br J Haematol*, **137** (6): 513-29.
- Seidegard J, Vorachek WR, Pero RW and Pearson WR. (1988) 'Hereditary differences in the expression of the human glutathione transferase active on trans-stilbene oxide are due to a gene deletion'. *Proc Natl Acad Sci U S A*, **85** (19): 7293-7.
- Sekizawa K, Suzuki T and Kishi K. (2007) 'Cytogenetic study of the induction mechanism of chromosome-type aberrations by 1-beta-D-arabinofuranosylcytosine'. *Mutat Res*, **619** (1-2): 1-8.
- Selva EM, New L, Crouse GF and Lahue RS. (1995) 'Mismatch correction acts as a barrier to homeologous recombination in *Saccharomyces cerevisiae*'. *Genetics*, **139** (3): 1175-88.
- Serrano E, Carnicer MJ, Orantes V, Estivill C, Lasa A, Brunet S, et al. (2008) 'Uniparental disomy may be associated with microsatellite instability in acute myeloid leukemia (AML) with a normal karyotype'. *Leuk Lymphoma*, **49** (6): 1178-83.
- Shafman T, Khanna KK, Kedar P, Spring K, Kozlov S, Yen T, et al. (1997) 'Interaction between ATM protein and c-Abl in response to DNA damage'. *Nature*, **387** (6632): 520-3.
- Shcherbakova PV and Kunkel TA. (1999) 'Mutator phenotypes conferred by MLH1 overexpression and by heterozygosity for mlh1 mutations'. *Mol Cell Biol*, **19** (4): 3177-83.
- Shcherbakova PV, Bebenek K and Kunkel TA. (2003) 'Functions of eukaryotic DNA polymerases'. *Sci Aging Knowledge Environ*, **2003** (8): RE3.

- Sheikhha MH, Tobal K and Liu Yin JA. (2002) 'High level of microsatellite instability but not hypermethylation of mismatch repair genes in therapy-related and secondary acute myeloid leukaemia and myelodysplastic syndrome'. *Br J Haematol*, **117** (2): 359-65.
- Shi Z, Azuma A, Sampath D, Li YX, Huang P and Plunkett W. (2001) 'S-Phase arrest by nucleoside analogues and abrogation of survival without cell cycle progression by 7-hydroxystaurosporine'. *Cancer Res*, **61** (3): 1065-72.
- Shibutani S, Takeshita M and Grollman AP. (1991) 'Insertion of specific bases during DNA synthesis past the oxidation-damaged base 8-oxodG'. *Nature*, **349** (6308): 431-4.
- Shiloh Y. (2006) 'The ATM-mediated DNA-damage response: taking shape'. *Trends Biochem Sci*, **31** (7): 402-10.
- Shimodaira H, Yoshioka-Yamashita A, Kolodner RD and Wang JY. (2003) 'Interaction of mismatch repair protein PMS2 and the p53-related transcription factor p73 in apoptosis response to cisplatin'. *Proc Natl Acad Sci U S A*, **100** (5): 2420-5.
- Shin KH, Yang YM and Park JG. (1998) 'Absence or decreased levels of the hMLH1 protein in human gastric carcinoma cell lines: implication of hMLH1 in alkylation tolerance'. *J Cancer Res Clin Oncol*, **124** (8): 421-6.
- Shibley JL and Butera JN. (2009) 'Acute myelogenous leukemia'. *Exp Hematol*, **37** (6): 649-58.
- Side LE, Curtiss NP, Teel K, Kratz C, Wang PW, Larson RA, et al. (2004) 'RAS, FLT3, and TP53 mutations in therapy-related myeloid malignancies with abnormalities of chromosomes 5 and 7'. *Genes Chromosomes Cancer*, **39** (3): 217-23.
- Siehler SY, Schrauder M, Gerischer U, Cantor S, Marra G and Wiesmuller L. (2009) 'Human MutL-complexes monitor homologous recombination independently of mismatch repair'. *DNA Repair (Amst)*, **8** (2): 242-52.
- Sill H, Goldman JM and Cross NC. (1996) 'Rarity of microsatellite alterations in acute myeloid leukaemia'. *Br J Cancer*, **74** (2): 255-7.

- Skalski V, Brown KR, Choi BY, Lin ZY and Chen S. (2000) 'A 3'-5' exonuclease in human leukemia cells: implications for resistance to 1-beta -D-arabinofuranosylcytosine and 9-beta -D-arabinofuranosyl-2-fluoroadenine 5'-monophosphate'. *J Biol Chem*, **275** (33): 25814-9.
- Slupska MM, Luther WM, Chiang JH, Yang H and Miller JH. (1999) 'Functional expression of hMYH, a human homolog of the Escherichia coli MutY protein'. *J Bacteriol*, **181** (19): 6210-3.
- Smith JA, Waldman BC and Waldman AS. (2005) 'A role for DNA mismatch repair protein Msh2 in error-prone double-strand-break repair in mammalian chromosomes'. *Genetics*, **170** (1): 355-63.
- Smith JA, Bannister LA, Bhattacharjee V, Wang Y, Waldman BC and Waldman AS. (2007) 'Accurate homologous recombination is a prominent double-strand break repair pathway in mammalian chromosomes and is modulated by mismatch repair protein Msh2'. *Mol Cell Biol*, **27** (22): 7816-27.
- Smith SM, Le Beau MM, Huo D, Karrison T, Sobecks RM, Anastasi J, et al. (2003) 'Clinical-cytogenetic associations in 306 patients with therapy-related myelodysplasia and myeloid leukemia: the University of Chicago series'. *Blood*, **102** (1): 43-52.
- Snow ET, Foote RS and Mitra S. (1984) 'Base-pairing Properties of O⁶-Methylguanine in Template DNA during *in Vitro* DNA Replication'. *J Biol Chem*, **259** (13): 8095-100.
- Sonoda E, Sasaki MS, Buerstedde JM, Bezzubova O, Shinohara A, Ogawa H, et al. (1998) 'Rad51-deficient vertebrate cells accumulate chromosomal breaks prior to cell death'. *Embo J*, **17** (2): 598-608.
- Spampinato C and Modrich P. (2000) 'The MutL ATPase is required for mismatch repair'. *J Biol Chem*, **275** (13): 9863-9.
- Stasi R, Evangelista ML, Buccisano F, Venditti A and Amadori S. (2008) 'Gemtuzumab ozogamicin in the treatment of acute myeloid leukemia'. *Cancer Treat Rev*, **34** (1): 49-60.
- Stirewalt DL and Radich JP. (2003) 'The role of FLT3 in haematopoietic malignancies'. *Nat Rev Cancer*, **3** (9): 650-65.

- Stojic L, Mojas N, Cejka P, Di Pietro M, Ferrari S, Marra G, et al. (2004a) 'Mismatch repair-dependent G2 checkpoint induced by low doses of SN1 type methylating agents requires the ATR kinase'. *Genes Dev*, **18** (11): 1331-44.
- Stojic L, Brun R and Jiricny J. (2004b) 'Mismatch repair and DNA damage signalling'. *DNA Repair (Amst)*, **3** (8-9): 1091-101.
- Sudan N, Rossetti JM, Shadduck RK, Latsko J, Lech JA, Kaplan RB, et al. (2006) 'Treatment of acute myelogenous leukemia with outpatient azacitidine'. *Cancer*, **107** (8): 1839-43.
- Sugawara N, Paques F, Colaiacovo M and Haber JE. (1997) 'Role of *Saccharomyces cerevisiae* Msh2 and Msh3 repair proteins in double-strand break-induced recombination'. *Proc Natl Acad Sci U S A*, **94** (17): 9214-9.
- Sugawara N, Goldfarb T, Studamire B, Alani E and Haber JE. (2004) 'Heteroduplex rejection during single-strand annealing requires Sgs1 helicase and mismatch repair proteins Msh2 and Msh6 but not Pms1'. *Proc Natl Acad Sci U S A*, **101** (25): 9315-20.
- Sundaralingam M. (1975) 'Structure and conformation of nucleosides and nucleotides and their analogs as determined by x-ray diffraction'. *Ann N Y Acad Sci*, **255** 3-42.
- Surtees JA and Alani E. (2006) 'Mismatch repair factor MSH2-MSH3 binds and alters the conformation of branched DNA structures predicted to form during genetic recombination'. *J Mol Biol*, **360** (3): 523-36.
- Sussman HE, Olivero OA, Meng Q, Pietras SM, Poirier MC, O'Neill JP, et al. (1999) 'Genotoxicity of 3'-azido-3'-deoxythymidine in the human lymphoblastoid cell line, TK6: relationships between DNA incorporation, mutant frequency, and spectrum of deletion mutations in HPRT'. *Mutat Res*, **429** (2): 249-59.
- Swann PF, Waters TR, Moulton DC, Xu YZ, Zheng Q, Edwards M, et al. (1996) 'Role of postreplicative DNA mismatch repair in the cytotoxic action of thioguanine'. *Science*, **273** (5278): 1109-11.
- Symington LS. (2002) 'Role of RAD52 epistasis group genes in homologous recombination and double-strand break repair'. *Microbiol Mol Biol Rev*, **66** (4): 630-70, table of contents.

- Tajima A, Hess MT, Cabrera BL, Kolodner RD and Carethers JM. (2004) 'The mismatch repair complex hMutS alpha recognizes 5-fluorouracil-modified DNA: implications for chemosensitivity and resistance'. *Gastroenterology*, **127** (6): 1678-84.
- Takagaki K, Katsuma S, Kaminishi Y, Horio T, Nakagawa S, Tanaka T, et al. (2004) 'Gene-expression profiling reveals down-regulation of equilibrative nucleoside transporter 1 (ENT1) in Ara-C-resistant CCRF-CEM-derived cells'. *J Biochem*, **136** (5): 733-40.
- Takahashi M, Koi M, Balaguer F, Boland CR and Goel A. (2011) 'MSH3 Mediates Sensitization of Colorectal Cancer Cells to Cisplatin, Oxaliplatin, and a Poly(ADP-ribose) Polymerase Inhibitor'. *J Biol Chem*, **286** (14): 12157-65.
- Takahashi T, Min Z, Uchida I, Arita M, Watanabe Y, Koi M, et al. (2005) 'Hypersensitivity in DNA mismatch repair-deficient colon carcinoma cells to DNA polymerase reaction inhibitors'. *Cancer Lett*, **220** (1): 85-93.
- Tanaka M, Yoshida S, Saneyoshi M and Yamaguchi T. (1981) 'Utilization of 5-fluoro-2'-deoxyuridine triphosphate and 5-fluoro-2'-deoxycytidine triphosphate in DNA synthesis by DNA polymerases alpha and beta from calf thymus'. *Cancer Res*, **41** (10): 4132-5.
- Taniguchi T, Garcia-Higuera I, Andreassen PR, Gregory RC, Grompe M and D'Andrea AD. (2002) 'S-phase-specific interaction of the Fanconi anemia protein, FANCD2, with BRCA1 and RAD51'. *Blood*, **100** (7): 2414-20.
- Tasaka T, Lee S, Spira S, Takeuchi S, Nagai M, Takahara J, et al. (1997) 'Microsatellite instability during the progression of acute myelocytic leukaemia'. *Br J Haematol*, **98** (1): 219-21.
- Testoni N, Borsaru G, Martinelli G, Carboni C, Ruggeri D, Ottaviani E, et al. (1999) '3q21 and 3q26 cytogenetic abnormalities in acute myeloblastic leukemia: biological and clinical features'. *Haematologica*, **84** (8): 690-4.
- Thiede C, Koch S, Creutzig E, Steudel C, Illmer T, Schaich M, et al. (2006) 'Prevalence and prognostic impact of NPM1 mutations in 1485 adult patients with acute myeloid leukemia (AML)'. *Blood*, **107** (10): 4011-20.

- Thompson LH and Hinz JM. (2009) 'Cellular and molecular consequences of defective Fanconi anemia proteins in replication-coupled DNA repair: mechanistic insights'. *Mutat Res*, **668** (1-2): 54-72.
- Tokunaga E, Oda S, Fukushima M, Maehara Y and Sugimachi K. (2000) 'Differential growth inhibition by 5-fluorouracil in human colorectal carcinoma cell lines'. *Eur J Cancer*, **36** (15): 1998-2006.
- Tominaga Y, Tsuzuki T, Shiraishi A, Kawate H and Sekiguchi M. (1997) 'Alkylation-induced apoptosis of embryonic stem cells in which the gene for DNA-repair, methyltransferase, had been disrupted by gene targeting'. *Carcinogenesis*, **18** (5): 889-96.
- Toorchen D and Topal MD. (1983) 'Mechanisms of chemical mutagenesis and carcinogenesis: effects on DNA replication of methylation at the O6-guanine position of dGTP'. *Carcinogenesis*, **4** (12): 1591-7.
- Traver RD, Horikoshi T, Danenberg KD, Stadlbauer TH, Danenberg PV, Ross D, et al. (1992) 'NAD(P)H:quinone oxidoreductase gene expression in human colon carcinoma cells: characterization of a mutation which modulates DT-diaphorase activity and mitomycin sensitivity'. *Cancer Res*, **52** (4): 797-802.
- Travis LB, Rabkin CS, Brown LM, Allan JM, Alter BP, Ambrosone CB, et al. (2006) 'Cancer survivorship--genetic susceptibility and second primary cancers: research strategies and recommendations'. *J Natl Cancer Inst*, **98** (1): 15-25.
- Umar A, Boyer JC, Thomas DC, Nguyen DC, Risinger JI, Boyd J, et al. (1994) 'Defective mismatch repair in extracts of colorectal and endometrial cancer cell lines exhibiting microsatellite instability'. *J Biol Chem*, **269** (20): 14367-70.
- Umar A, Buermeyer AB, Simon JA, Thomas DC, Clark AB, Liskay RM, et al. (1996) 'Requirement for PCNA in DNA mismatch repair at a step preceding DNA resynthesis'. *Cell*, **87** (1): 65-73.
- Umar A, Koi M, Risinger JI, Glaab WE, Tindall KR, Kolodner RD, et al. (1997) 'Correction of hypermutability, N-methyl-N'-nitro-N-nitrosoguanidine resistance, and defective DNA mismatch repair by introducing chromosome 2 into human tumor cells with mutations in MSH2 and MSH6'. *Cancer Res*, **57** (18): 3949-55.

- Umar A, Boland CR, Terdiman JP, Syngal S, de la Chapelle A, Ruschoff J, et al. (2004) 'Revised Bethesda Guidelines for hereditary nonpolyposis colorectal cancer (Lynch syndrome) and microsatellite instability'. *J Natl Cancer Inst*, **96** (4): 261-8.
- van Diggelen OP, Donahue TF and Shin SI. (1979) 'Basis for differential cellular sensitivity to 8-azaguanine and 6-thioguanine'. *J Cell Physiol*, **98** (1): 59-71.
- Vasquez KM. (2010) 'Targeting and processing of site-specific DNA interstrand crosslinks'. *Environ Mol Mutagen*, **51** (6): 527-39.
- Vernole P, Pepponi R and D'Atri S. (2003) 'Role of mismatch repair in the induction of chromosomal aberrations and sister chromatid exchanges in cells treated with different chemotherapeutic agents'. *Cancer Chemother Pharmacol*, **52** (3): 185-92.
- Veuger MJ, Honders MW, Spoelder HE, Willemze R and Barge RM. (2003) 'Inactivation of deoxycytidine kinase and overexpression of P-glycoprotein in AraC and daunorubicin double resistant leukemic cell lines'. *Leuk Res*, **27** (5): 445-53.
- Villemure JF, Abaji C, Cousineau I and Belmaaza A. (2003) 'MSH2-deficient human cells exhibit a defect in the accurate termination of homology-directed repair of DNA double-strand breaks'. *Cancer Res*, **63** (12): 3334-9.
- von der Maase H. (2000) 'Gemcitabine in locally advanced and/or metastatic bladder cancer'. *Crit Rev Oncol Hematol*, **34** (3): 175-83.
- Wagner MW, Li LS, Morales JC, Galindo CL, Garner HR, Bornmann WG, et al. (2008) 'Role of c-Abl kinase in DNA mismatch repair-dependent G2 cell cycle checkpoint arrest responses'. *J Biol Chem*, **283** (31): 21382-93.
- Walter MJ, Graubert TA, Dipersio JF, Mardis ER, Wilson RK and Ley TJ. (2009) 'Next-generation sequencing of cancer genomes: back to the future'. *Per Med*, **6** (6): 653.
- Wang H and Hays JB. (2004) 'Signaling from DNA mispairs to mismatch-repair excision sites despite intervening blockades'. *Embo J*, **23** (10): 2126-33.
- Wang JC. (2002) 'Cellular roles of DNA topoisomerases: a molecular perspective'. *Nat Rev Mol Cell Biol*, **3** (6): 430-40.

- Wang Q, Ponomareva ON, Lasarev M and Turker MS. (2006) 'High frequency induction of mitotic recombination by ionizing radiation in Mlh1 null mouse cells'. *Mutat Res*, **594** (1-2): 189-98.
- Wang Y, Cortez D, Yazdi P, Neff N, Elledge SJ and Qin J. (2000) 'BASC, a super complex of BRCA1-associated proteins involved in the recognition and repair of aberrant DNA structures'. *Genes Dev*, **14** (8): 927-39.
- Wang Y and Qin J. (2003) 'MSH2 and ATR form a signaling module and regulate two branches of the damage response to DNA methylation'. *Proc Natl Acad Sci U S A*, **100** (26): 15387-92.
- Warren JJ, Forsberg LJ and Beese LS. (2006) 'The structural basis for the mutagenicity of O(6)-methyl-guanine lesions'. *Proc Natl Acad Sci U S A*, **103** (52): 19701-6.
- Waters TR and Swann PF. (1997) 'Cytotoxic mechanism of 6-thioguanine: hMutSalpha, the human mismatch binding heterodimer, binds to DNA containing S6-methylthioguanine'. *Biochemistry*, **36** (9): 2501-6.
- Wattel E, Preudhomme C, Hecquet B, Vanrumbeke M, Quesnel B, Dervite I, et al. (1994) 'p53 mutations are associated with resistance to chemotherapy and short survival in hematologic malignancies'. *Blood*, **84** (9): 3148-57.
- Whitman SP, Liu S, Vukosavljevic T, Rush LJ, Yu L, Liu C, et al. (2005) 'The MLL partial tandem duplication: evidence for recessive gain-of-function in acute myeloid leukemia identifies a novel patient subgroup for molecular-targeted therapy'. *Blood*, **106** (1): 345-52.
- Wiencke JK, Pemble S, Ketterer B and Kelsey KT. (1995) 'Gene deletion of glutathione S-transferase theta: correlation with induced genetic damage and potential role in endogenous mutagenesis'. *Cancer Epidemiol Biomarkers Prev*, **4** (3): 253-9.
- Wiley JS, Taupin J, Jamieson GP, Snook M, Sawyer WH and Finch LR. (1985) 'Cytosine arabinoside transport and metabolism in acute leukemias and T cell lymphoblastic lymphoma'. *J Clin Invest*, **75** (2): 632-42.
- Wilson DM, 3rd and Barsky D. (2001) 'The major human abasic endonuclease: formation, consequences and repair of abasic lesions in DNA'. *Mutat Res*, **485** (4): 283-307.

- Worrillow LJ, Travis LB, Smith AG, Rollinson S, Smith AJ, Wild CP, et al. (2003) 'An intron splice acceptor polymorphism in hMSH2 and risk of leukemia after treatment with chemotherapeutic alkylating agents'. *Clin Cancer Res*, **9** (8): 3012-20.
- Worrillow LJ and Allan JM. (2006) 'Deregulation of homologous recombination DNA repair in alkylating agent-treated stem cell clones: a possible role in the aetiology of chemotherapy-induced leukaemia'. *Oncogene*, **25** (12): 1709-20.
- Worrillow LJ, Smith AG, Scott K, Andersson M, Ashcroft AJ, Dores GM, et al. (2008) 'Polymorphic MLH1 and risk of cancer after methylating chemotherapy for Hodgkin lymphoma'. *J Med Genet*, **45** (3): 142-6.
- Wu L, Davies SL, Levitt NC and Hickson ID. (2001) 'Potential role for the BLM helicase in recombinational repair via a conserved interaction with RAD51'. *J Biol Chem*, **276** (22): 19375-81.
- Wu Q, Christensen LA, Legerski RJ and Vasquez KM. (2005) 'Mismatch repair participates in error-free processing of DNA interstrand crosslinks in human cells'. *EMBO Rep*, **6** (6): 551-7.
- Wu Q and Vasquez KM. (2008) 'Human MLH1 protein participates in genomic damage checkpoint signaling in response to DNA interstrand crosslinks, while MSH2 functions in DNA repair'. *PLoS Genet*, **4** (9): e1000189.
- Xie C and Plunkett W. (1995) 'Metabolism and actions of 2-chloro-9-(2-deoxy-2-fluoro-beta-D- arabinofuranosyl)-adenine in human lymphoblastoid cells'. *Cancer Res*, **55** (13): 2847-52.
- Xie KC and Plunkett W. (1996) 'Deoxynucleotide pool depletion and sustained inhibition of ribonucleotide reductase and DNA synthesis after treatment of human lymphoblastoid cells with 2-chloro-9-(2-deoxy-2-fluoro-beta-D-arabinofuranosyl) adenine'. *Cancer Res*, **56** (13): 3030-7.
- Xu B, Kim ST, Lim DS and Kastan MB. (2002) 'Two molecularly distinct G(2)/M checkpoints are induced by ionizing irradiation'. *Mol Cell Biol*, **22** (4): 1049-59.
- Yamada M, O'Regan E, Brown R and Karran P. (1997) 'Selective recognition of a cisplatin-DNA adduct by human mismatch repair proteins'. *Nucleic Acids Res*, **25** (3): 491-6.

- Yamane K, Taylor K and Kinsella TJ. (2004) 'Mismatch repair-mediated G2/M arrest by 6-thioguanine involves the ATR-Chk1 pathway'. *Biochem Biophys Res Commun*, **318** (1): 297-302.
- Yamane K, Schupp JE and Kinsella TJ. (2007) 'BRCA1 activates a G2-M cell cycle checkpoint following 6-thioguanine-induced DNA mismatch damage'. *Cancer Res*, **67** (13): 6286-92.
- Yan J, Zhang XX, Fetni R and Drouin R. (2001a) 'Trisomy 8 and monosomy 7 detected in bone marrow using primed in situ labeling, fluorescence in situ hybridization, and conventional cytogenetic analyses. A study of 54 cases with hematological disorders'. *Cancer Genet Cytogenet*, **125** (1): 30-40.
- Yan T, Schupp JE, Hwang HS, Wagner MW, Berry SE, Strickfaden S, et al. (2001b) 'Loss of DNA mismatch repair imparts defective cdc2 signaling and G(2) arrest responses without altering survival after ionizing radiation'. *Cancer Res*, **61** (22): 8290-7.
- Yan T, Berry SE, Desai AB and Kinsella TJ. (2003) 'DNA mismatch repair (MMR) mediates 6-thioguanine genotoxicity by introducing single-strand breaks to signal a G2-M arrest in MMR-proficient RKO cells'. *Clin Cancer Res*, **9** (6): 2327-34.
- Yan T, Desai AB, Jacobberger JW, Sramkoski RM, Loh T and Kinsella TJ. (2004) 'CHK1 and CHK2 are differentially involved in mismatch repair-mediated 6-thioguanine-induced cell cycle checkpoint responses'. *Mol Cancer Ther*, **3** (9): 1147-57.
- Yan T, Seo Y and Kinsella TJ. (2009) 'Differential cellular responses to prolonged LDR-IR in MLH1-proficient and MLH1-deficient colorectal cancer HCT116 cells'. *Clin Cancer Res*, **15** (22): 6912-20.
- Yang G, Scherer SJ, Shell SS, Yang K, Kim M, Lipkin M, et al. (2004a) 'Dominant effects of an Msh6 missense mutation on DNA repair and cancer susceptibility'. *Cancer Cell*, **6** (2): 139-50.
- Yang JL, Hsieh FP, Lee PC and Tseng HJ. (1994) 'Strand- and sequence-specific attenuation of N-methyl-N'-nitro-N-nitrosoguanidine-induced G.C to A.T transitions by expression of human 6-methylguanine-DNA methyltransferase in Chinese hamster ovary cells'. *Cancer Res*, **54** (14): 3857-63.

- Yang Q, Zhang R, Wang XW, Linke SP, Sengupta S, Hickson ID, et al. (2004b) 'The mismatch DNA repair heterodimer, hMSH2/6, regulates BLM helicase'. *Oncogene*, **23** (21): 3749-56.
- Yarosh DB, Foote RS, Mitra S and Day RS, 3rd. (1983) 'Repair of O6-methylguanine in DNA by demethylation is lacking in Mer- human tumor cell strains'. *Carcinogenesis*, **4** (2): 199-205.
- Yin B, Morgan K, Hasz DE, Mao Z and Largaespada DA. (2006) 'Nfl gene inactivation in acute myeloid leukemia cells confers cytarabine resistance through MAPK and mTOR pathways'. *Leukemia*, **20** (1): 151-4.
- Yin CC, Medeiros LJ and Bueso-Ramos CE. (2010) 'Recent advances in the diagnosis and classification of myeloid neoplasms--comments on the 2008 WHO classification'. *Int J Lab Hematol*, **32** (5): 461-76.
- York SJ and Modrich P. (2006) 'Mismatch repair-dependent iterative excision at irreparable O6-methylguanine lesions in human nuclear extracts'. *J Biol Chem*, **281** (32): 22674-83.
- Yoshioka K, Yoshioka Y and Hsieh P. (2006) 'ATR kinase activation mediated by MutSalpha and MutLalpha in response to cytotoxic O6-methylguanine adducts'. *Mol Cell*, **22** (4): 501-10.
- Yuan Y, Zhou L, Miyamoto T, Iwasaki H, Harakawa N, Hetherington CJ, et al. (2001) 'AML1-ETO expression is directly involved in the development of acute myeloid leukemia in the presence of additional mutations'. *Proc Natl Acad Sci U S A*, **98** (18): 10398-403.
- Yuan ZM, Shioya H, Ishiko T, Sun X, Gu J, Huang YY, et al. (1999) 'p73 is regulated by tyrosine kinase c-Abl in the apoptotic response to DNA damage'. *Nature*, **399** (6738): 814-7.
- Zhang DE, Zhang P, Wang ND, Hetherington CJ, Darlington GJ and Tenen DG. (1997) 'Absence of granulocyte colony-stimulating factor signaling and neutrophil development in CCAAT enhancer binding protein alpha-deficient mice'. *Proc Natl Acad Sci U S A*, **94** (2): 569-74.

- Zhang H, Tsujimura T, Bhattacharyya NP, Maher VM and McCormick JJ. (1996) 'O6-methylguanine induces intrachromosomal homologous recombination in human cells'. *Carcinogenesis*, **17** (10): 2229-35.
- Zhang H, Marra G, Jiricny J, Maher VM and McCormick JJ. (2000) 'Mismatch repair is required for O(6)-methylguanine-induced homologous recombination in human fibroblasts'. *Carcinogenesis*, **21** (9): 1639-46.
- Zhang N, Lu X, Zhang X, Peterson CA and Legerski RJ. (2002) 'hMutSbeta is required for the recognition and uncoupling of psoralen interstrand cross-links in vitro'. *Mol Cell Biol*, **22** (7): 2388-97.
- Zhang N, Liu X, Li L and Legerski R. (2007) 'Double-strand breaks induce homologous recombinational repair of interstrand cross-links via cooperation of MSH2, ERCC1-XPF, REV3, and the Fanconi anemia pathway'. *DNA Repair (Amst)*, **6** (11): 1670-8.
- Zhang Y, Rohde LH, Emami K, Hammond D, Casey R, Mehta SK, et al. (2008) 'Suppressed expression of non-DSB repair genes inhibits gamma-radiation-induced cytogenetic repair and cell cycle arrest'. *DNA Repair (Amst)*, **7** (11): 1835-45.
- Zhao J, Jain A, Iyer RR, Modrich PL and Vasquez KM. (2009) 'Mismatch repair and nucleotide excision repair proteins cooperate in the recognition of DNA interstrand crosslinks'. *Nucleic Acids Res*, **37** (13): 4420-9.
- Zhenchuk A, Lotfi K, Juliusson G and Albertioni F. (2009) 'Mechanisms of anti-cancer action and pharmacology of clofarabine'. *Biochem Pharmacol*, **78** (11): 1351-9.
- Zhu YM, Das-Gupta EP and Russell NH. (1999) 'Microsatellite instability and p53 mutations are associated with abnormal expression of the MSH2 gene in adult acute leukemia'. *Blood*, **94** (2): 733-40.
- Zhukovskaya N, Branch P, Aquilina G and Karran P. (1994) 'DNA replication arrest and tolerance to DNA methylation damage'. *Carcinogenesis*, **15** (10): 2189-94.
- Zou L and Elledge SJ. (2003) 'Sensing DNA damage through ATRIP recognition of RPA-ssDNA complexes'. *Science*, **300** (5625): 1542-8.